Finite Element Formulation for Large Displacement Analysis

Mario Gomez Botero

Department of Mechanical Engineering
EAFIT University

March 16, 2009

Contents

1 Introduction to the Variational Formulation **9**
- 1.1 Minimum Total Potential Energy Principle 9
- 1.2 Derivation of the Principle of Virtual Displacements 11
- 1.3 Derivation of the equilibrium equations from the principle of virtual displacements 12

2 Displacement Based FEM **15**
- 2.1 Finite Element Equations 16

3 FEA for Large Displacements **21**
- 3.1 Basic Notions 21
  - 3.1.1 The Displacement gradient and the Deformation gradient 23
  - 3.1.2 Green-Lagrange strain tensor 27
  - 3.1.3 Second Piola-Kirchhoff stress tensor 29
- 3.2 Non-linear equations of motion 32
- 3.3 Total Lagrangian Formulation 36

4 Bar or Truss Elements **41**
- 4.1 Bars under the small displacements hypothesis 41
- 4.2 Bars under the large displacements hypothesis 50
  - 4.2.1 A general 2–D expression for ${}_0\widetilde{e_{11}}$ 56
  - 4.2.2 A general 2–D expression for $\delta_0\widetilde{\eta_{11}}$ 58
  - 4.2.3 A general 2–D expression for ${}^t_0\widetilde{\epsilon_{11}}$ 59

5 Beam Elements **61**
- 5.1 Euler-Bernoulli and Timoshenko beams 61
- 5.2 Timoshenko beams fundamentals 62
- 5.3 Displacement-based two-node Timoshenko beam 64
- 5.4 Mixed Formulations 68

6 Plane Stress Elements **75**
6.1 Large displacement plane-stress elements 77
6.1.1 A general expression for ${}^t_0B_L$ 79
6.1.2 A general expression for ${}^t_0B_{NL}$ 82

7 Shell Elements **87**
7.1 A brief introduction to Curvilinear coordinates 88
7.1.1 Minimum Total Potential Energy (MTPE) Principle in Curvilinear Coordinates 91
7.2 Mixed Plate/Shell elements for small displacements 93
7.2.1 Plate Elements 93
7.2.2 Shell Elements 99
7.3 Mixed Shell Elements under LDH 99
7.3.1 Total Lagrangian Formulation 106
7.4 Computer implementation 115
7.4.1 Examples 115

8 Validation Results **119**
8.1 Description of the Experiment 119
8.2 Obtaining the Geometry and the Properties Files 121
8.3 Linear versus non-linear simulations 123
8.4 Numerical Simulations 124
8.4.1 Cantilever with a single force on its free end 125
8.4.2 Cantilever with displacement applied at its free end . . . 125

A Displacement and Deformation Gradient in a 3–D Cartesian coordinate system **131**

B Evaluation of the Jacobian for a truss element **133**

C Calculation of ${}^t_0K_L$, ${}^t_0K_{NL}$, and ${}^t_0\mathbf{F}$ for a bar element **137**

D User's Manual of the C++ Shell Program **145**
D.1 Description of the input files 145
D.1.1 Geometry File 145
D.1.2 Properties File 149
D.2 Compilation Process 152
D.2.1 Windows: 154
D.2.2 Linux: 155
D.3 Result Files: 155

Acknowledgments

To my family for their support and trust, especially to my mother Belen who has always been by my side providing me with love, patience, and all the ongoing teaching required to live according to the correct values and the moral needed in our society. I want to thank Professor Manuel J. Garcia and Professor Pierre Boulanger for their guidance. Their point of view about science and life encouraged me to work on this field. They gave me the opportunity to comprehend the real meaning and the most important values needed in science and engineering. They taugh me that friendship goes together with labor; this fact motivates a good working environment which is fundamental to achieve good results. To all the staff of the Applied Mechanics Lab and the AMMI Lab, their friendship was essential to accomplish this study. All their advices and the help provided was priceless and necessary to keep science fun. To all my friends, and all those persons who somehow helped me with the tasks needed to finish this thesis.

Abstract

In structural engineering, shells are usually curved objects which can support remarkable external forces without fracture or damage. Due to this remarkable stiffness behaviour and the low amount of material used in the fabrication process, nowadays shell structures are getting lots of followers in the engineering world. In consequence, scientists and the industry in general are keen with the idea of developing efficient and accurate models to predict their behaviour.

In the manufacturing industry, inspection procedures are becoming more common every day. This task constists on measuring how much difference exists between the original-ideal object specified by the designer, and the object that just comes out from the manufacturing process. Generally, this goal is achived by placing the manufactured part in the location where it was designed to be, such as the assamblage of a machine. Subsequently, a 3–D scan of the placed part is made. The registered measurments are compared with the CAD geometry of the original-ideal object in order to acept or reject the manufactured part. However, this procedure represents an inefficient and very time consumig process. If instead, the part is scanned when it just comes out from the fabrication process, and the scanned geometry is placed into the assemblage via a Finite Element software; a more efficient procedure could be achieved assuming that the simulation is fast and reliable. The goal of this work is to provide this virtual inspection enviroment.

Given the nature of the manufactured parts, the physics of the problem corresponds to shell structures subjected to large displacements. In consequence, the formulation, implementation, and validation of a shell element based on a large displacement hypothesis have to be fully understood. Nevertheless, before arriving to shell elements, it has been considered as convenient to comprehend the Finite Element formulation proposed in the literature for bars, beams, and plane stress elements.

Although all the topics analysed in this report have been somehow studied by several authors and published in FEM journals and books, the information recopilated into this text does not represent a mere attempt to make a literature review of the Finite Element Method for large displacements. Instead, every single piece of information included in this text has been considered as very valuable because either it introduces a keen and important FEM topic, or because the mathematical treatment accomplished to be able to get to the final results suggested by FEM literature, has not been fully explained or published. In other words, most of the times FEM authors assume that the reader is able

to reach the same results they publish without giving many clues about the right way to get to that point. This text gets into the detail of the mathematics required to deal with finite deformations and large displacements applied to the Finite Element Method; for that purpose, it was necessary to understand several author's point of view and sometimes comprehend very different mathematical notations to explain the same idea. The final products obtained (both the written report and the C++ shell program) represent a big shortcut for those who want to gain good knowledge and understanding of the Finite Element Method under the large displacement hypothesis.

The chapter 1 of this text contains a brief review of the Total Potential Energy principle explained in terms of a variational formulation. This is done because this principle represents the base of the Finite Element method. In chapter 2 the principle of Virtual Displacements is used to deduce the Finite Element method, arriving to the general 3–D Finite Element equations to be used in a small displacement scenario. Next, in chapter 3 a large displacements hypothesis is used, and the Finite Element method is amended for this situation; furthermore, some new stress and strain measures needed for this formulation are introduced. Bars, beams and plane-stress elements are studied in chapters 4, 5, and 6 in order to introduce some concepts required for the shell formulation. The shell formulation explained in chapter 7 was implemented as a C++ program and the displacements results obtained are validated in chapter 8. At the end of the text there are included some appendixes with some material which was considered as important for a better understanding of the Finite Element method. The user's manual of the shell software programmed is included in the Appendix D.

Chapter 1

Introduction to the Variational Formulation

The study of mechanics has always been a branch of interest for scientists. In general, the problems found therein can be expressed through mathematical models which can be written in terms of partial differential equations (PDE). Two main lines of study have been developed to generate these equations: The first one, and the most recognised, is the one based on Newton's laws of motion, which seeks for all the forces acting on every particle within a domain. The differential formulation has its foundations in this trend. *"The second branch of mechanics, usually called analytical mechanics, which bases the entire study of equilibrium and motion on two fundamental scalar quantities, the kinetic energy and the potential energy"*(Lan86), represents the basis of the variational formulation.

1.1 Minimum Total Potential Energy Principle

The Calculus of Variations has come up as an efficient tool that can be applied to a large amount of mathematical problems. Fortunately for engineers, in general it is possible to express the basic principles of mechanics as a mathematical variational problem. In such a way, this physical phenomenom acquires a big mathematical meaning which allows to understand more clearly how nature works. The principle of Minimum Total Potential Energy (MTPE) is a fundamental concept used in structural mechanics. It states that an object will deform into a position where the total potential energy is minimised. In clas-

sical mechanics, this principle can be expressed in terms of the displacement field $\vec{u} = u_i$, and at most, in terms of its first derivative with respect to the spatial coordinates, that is $\frac{\partial u_i}{\partial x_j}$. This aspect will be seen more clearly when defining the energies considered by the MTPE principle.

Mathematically, this principle asserts that the Total Potential Energy Π of the system being analysed, equals to the difference between the strain energy $\mathbf{U}$ stored in the deformed object, and the potential energy of the loads $\mathbf{W}$. That is,

$$\Pi_{(u_i,\partial u_i/\partial x_j)} = \mathbf{U}_{(u_i,\partial u_i/\partial x_j)} - \mathbf{W}_{(u_i,\partial u_i/\partial x_j)}. \tag{1.1}$$

According to what it is expressed above, the functional $\Pi_{(u_i,\partial u_i/\partial x_j)}$ may be understood as a master function whose domain is constituted by the vector functions u_i and $\partial u_i/\partial x_j$. It is also important to remark that Π remains unchanged during motion of the object; therefore $\delta\Pi = 0$. For that reason, when a loss of potential energy occurs, that quantity of energy is gained by the strain energy and vice versa.

Even though the equations for mechanical problems can be generated via a differential formulation, a better way to face the problem and get to the truly core of the concepts involved therein would be the Calculus of Variations. Indeed, for engineering purposes, the MTPE principle can be specialised into the the principle of virtual displacements using the Calculus of Variations. This principle is widely employed in continuum mechanics, mainly because it serves as a basis to state the equilibrium equations in a deformable medium.

In order to see how the the principle of virtual displacements works, it is possible to think of a particle which is located at point P_1 at a time t_1, and has a velocity v_1. The particle will move to point P_2 at a time t_2. An infinity number of paths could be taken by the particle to get from P_1 to P_2. However, a tentative path can be chosen and be gradually corrected by the application of the principle of virtual displacements. *"The mathematical theory shows that the final result can be established without taking into account the infinity of tentatively possible paths. The mathematical experiment can be restricted to such paths which are infinitely near to the actual path. A tentative path which differs from the actual path in an arbitrary but still infinitesimal degree, is called a variation of the actual path; and the calculus of variations deals with this problem"*(Lan86).

1.2 Derivation of the Principle of Virtual Displacements

The variational problem to be solved in structural mechanics consists on finding a function u_i for which the functional $\Pi_{(u_i,\partial u_i/\partial x_j)}$ is a maximum, is a minimum, or has a saddle point. The condition to get to the governing equations is

$$\delta\Pi_{(u_i,\partial u_i/\partial x_j)} = 0,$$

and due to the calculus of variations

$$\delta\Pi_{(u_i,\partial u_i/\partial x_j)} = \frac{\partial\Pi}{\partial u_i}\delta u_i + \frac{\partial\Pi}{\partial(\partial u_i/\partial x)}\delta(\partial u_i/\partial x)$$

"It must be noted that δu_i stands for variations on u_i that are arbitrary except that they must be zero at and corresponding to the state variable boundary conditions. The second derivatives of Π with respect to u_i then decide whether the solution corresponds to a maximum, a minimum, or a saddle point."(Bat96).

In general, the total potential energy of a 3–D structural body, can be expressed as

$$\begin{aligned}\underbrace{\Pi_{(u_i,\partial u_i/\partial x_j)}}_{\text{total potential energy}} &= \underbrace{\int_V \frac{1}{2}\tau_{ij}\, e_{ij}\, dV}_{\text{strain energy}} - \underbrace{\left(\int_V f_i^B u_i\, dV + \int_S f_i^{S_f} u_i^{S_f}\, dS\right)}_{\text{total potential of the loads}} \\ &= \int_V \frac{1}{2} C_{ijmn}\, e_{mn}\, e_{ij}\, dV - \int_V f_i^B u_i\, dV - \int_{S_f} f_i^{S_f} u_i^{S_f}\, dS,\end{aligned}$$

where f_i^B represents the body forces per unit volume, $f_i^{S_f}$ are the surface forces per unit area, and $e_{ij} = \frac{1}{2}(\frac{\partial u_i}{\partial x_j} + \frac{\partial u_j}{\partial x_i}) = \frac{1}{2}(u_{i,j} + u_{j,i})$. As it was stated before, note that the energies considered by MTPE principle can be written at most in terms of $\frac{\partial u_i}{\partial x_j}$. The first variation of Π with respect to the displacement field is

$$\begin{aligned}\delta\Pi_{(u_i,\partial u_i/\partial x_j)} = 0 = &\int_V \frac{1}{2} C_{ijmn}\, e_{mn}\, \delta(e_{ij})\, dV + \int_V \frac{1}{2} C_{ijmn}\, \delta(e_{mn})\, e_{ij}\, dV \\ &- \int_V f_i^B \delta u_i\, dV - \int_{S_f} f_i^{S_f} \delta u_i^{S_f}\, dS.\end{aligned}$$

Now, in light of the symmetry of the constitutive tensor ($C_{ijmn} = C_{mnij}$), the

first variation of Π can be rewritten as

$$0 = \int_V \frac{1}{2}\tau_{ij}\,\delta(e_{ij})\,dV + \int_V \frac{1}{2}C_{mnij}\,e_{ij}\,\delta(e_{mn})\,dV - \int_V f_i^B \delta u_i\,dV - \int_{S_f} f_i^{S_f}\delta u_i^{S_f}\,dS$$
$$= \int_V \frac{1}{2}\tau_{ij}\,\delta(e_{ij})\,dV + \int_V \frac{1}{2}\tau_{mn}\,\delta(e_{mn})\,dV - \int_V f_i^B \delta u_i\,dV - \int_{S_f} f_i^{S_f}\delta u_i^{S_f}\,dS,$$

and taking into account that ij and mn are free indices, the final expression for the first variation of Π is obtained,

$$\underbrace{\int_V \tau_{ij}\,\delta(e_{ij})\,dV}_{\text{internal virtual work}} = \underbrace{\int_V f_i^B \delta u_i\,dV + \int_{S_f} f_i^{S_f}\delta u_i^{S_f}\,dS.}_{\text{external virtual work}} \tag{1.2}$$

The above expression is known as the **principle of virtual displacements**, and constitutes a general expression for the development of equations used by the Finite Element Method applied to structural mechanics.

1.3 Derivation of the equilibrium equations from the principle of virtual displacements

Considering the symmetry of the Cauchy stress tensor ($\tau_{ij} = \tau_{ji}$), it is possible to say that

$$\tau_{ij}\,\delta e_{ij} = \tau_{ij}\,\delta\left[\frac{1}{2}(u_{i,j} + u_{j,i})\right] = \tau_{ij}\,\frac{1}{2}\left[(\delta u_{i,j} + \delta u_{j,i})\right]$$
$$= \frac{1}{2}\tau_{ij}\,\delta u_{i,j} + \frac{1}{2}\tau_{ij}\,\delta u_{j,i}$$
$$= \underbrace{\frac{1}{2}\tau_{ij}\,\delta u_{i,j}}_{\text{term 1}} + \underbrace{\frac{1}{2}\tau_{ji}\,\delta u_{j,i}}_{\text{term 2}},$$

but taking a closer look, it can be seen that term 1 and term 2 are independent. It means that the indices i and j in term 1 are not related to indices i and j in term 2. Hence, they are similar terms, thus

$$\tau_{ij}\,\delta e_{ij} = \tau_{ij}\,\delta u_{i,j}.$$

Therefore, Equation 1.2 can be expressed as

$$\int_V \tau_{ij}\,\delta u_{i,j}\,dV = \int_V f_i^B \delta u_i\,dV + \int_{S_f} f_i^{S_f}\delta u_i^{S_f}\,dS,$$

now if the mathematical identity $\tau_{ij}\,\delta u_{i,j} = (\tau_{ij}\,\delta u_i)_{,j} - \tau_{ij,j}\,\delta u_i$ is used, it yields to

$$\int_V \left[(\tau_{ij}\,\delta u_i)_{,j} - \tau_{ij,j}\,\delta u_i\right]\,dV = \int_V f_i^B \delta u_i\,dV + \int_{S_f} f_i^{S_f}\delta u_i^{S_f}\,dS,$$

and by the divergence theorem

$$\int_S (\tau_{ij}\,\delta u_i) n_j\,dS - \int_V \tau_{ij,j}\,\delta u_i\,dV = \int_V f_i^B \delta u_i\,dV + \int_{S_f} f_i^{S_f}\delta u_i^{S_f}\,dS$$

where $S_f \cup S_u = S$, and $S_f \cap S_u = 0$. S_f corresponds to the surface where the loads are applied, and S_u is the surface where the displacements are prescribed, hence

$$\int_{S_f} (\tau_{ij}\,n_j - f_i^{S_f})\delta u_i^{S_f}\,dS + \int_{S_u} \tau_{ij}\,n_j \delta u_i^{S_u}\,dS = \int_V (\tau_{ij,j} + f_i^B)\delta u_i\,dV. \quad (1.3)$$

Looking for a good interpretation of Equation 1.3, it is essential to remember the fundamental theorem of the calculus of variations:

Theorem 1 *If $f_{(x)}$ is continuous in $[a,b]$ and if*

$$\int_a^b f_{(x)}\alpha_{(x)}\,dx = 0$$

for every continuous function $\alpha_{(x)}$ in $[a,b]$ that vanishes in a and b, hence $f_{(x)} = 0$ for every $x \in [a,b]$.

This theorem can be naturally extended to several variables (TG07). To obtain the differential equation which governs this 3–D structural problem, it is indispensable to check out under what particular conditions Equation 1.3 vanishes for any possible perturbation δu_i. Choosing perturbations δu_i that ara zero at S_u and S_f, the left hand side of 1.3 vanishes. That is $\delta u_i^{S_u} = 0$ and $\delta u_i^{S_f} = 0$. Now, it is time to search under what conditions $\int_V (\tau_{ij,j} + f_i^B)\delta u_i\,dV$ vanishes for any δu_i that satisfies $\delta u_i^{S_u} = 0$ and $\delta u_i^{S_f} = 0$. The fundamental theorem of the calculus of variations guarantees that

$$\tau_{ij,j} + f_i^B = 0. \quad (1.4)$$

In such a way, the partial differential equation which governs this problem has been found. In the same way, choosing perturbations δu_i that ara zero

everywhere except at S_f, and according to the fundamental theorem of the calculus of variations; it is possible to state that the problem is accomplished with the natural boundary condition

$$\tau_{ij}\, n_j - f_i^{S_f} = 0,$$

and the prescribed essential boundary conditions.

When utilising a variational approach, two different kinds of Boundary Conditions can generated: The essential and the natural boundary conditions. Consider that in the functional Π, the highest derivative of the state variable with respect to a space variable is of order m. That problem is known as a C^{m-1} variational problem. The essential boundary conditions correspond to the prescribed displacements and rotations, for that reason are also called geometric boundary conditions. The order of the derivatives in the essential boundary conditions is, in a C^{m-1} problem, at most $m-1$. On the other hand, the natural boundary conditions correspond to the prescribed boundary forces and moments. The highest derivatives are of order m to $2m-1$ (Bat96).

Finally, going back to Equation 1.2, is possible to affirm that to be able to find a displacement function u_i which is a solution of the problem, *"the internal virtual work must be equal to the external virtual work for arbitrary test or virtual displacement functions δu_i that are continuous and satisfy the condition $\delta u_i^{S_u} = 0$ and $\delta u_i^{S_f} = 0$"*(Bat96).

Chapter 2

Displacement Based FEM

In general, when solving an engineering problem, it is necessary to identify and sometimes to develop a mathematical model whose results are close enough to reality. Normally, the mathematical model leads to a set of the mathematical equations that must be solved considering some solution method. In the particular case of structural mechanichs, when using a variational formulation to describe a deformation process, the final system of continuous differential equations generated (see Equation 1.4) establish mathematically the equilibrium requirements, compatibility conditions, and constitutive relations for all the differential elements within the domain of the object to be deformed.

The Finite Element Method (FEM) emerges as the most popular model used by engineers to solve a system of differential equations. However, to be able to get into the world of the Finite Elements, it is necessary to discretise the system of continuous equations. Of course the final result will not coincide with the exact solution of the model; instead, a very good approximation might be achieved.

In order to discretise the system of continuous equations, the domain of the problem has to be divided into a finite number of elements. Then, a system of finite element equilibrium equations which are deduced from the principle of virtual displacements are applied to each element. Finally, the complete system of equations obtained from the whole amount of elements is solved via some numerical method. In general, the elements used to discretise the domain are basic geometries such as pyramids and prisms for the 3–D cases, or triangles and quadrilaterals for 2–D. The state variables of the problem are usually located at the vertices of the elements, but sometimes they are also located inside the element or over its edges. State variables are those that contain enough information about the system being analysed to enable computation

of its behaviour under certain boundary conditions, e.g. the displacements, the strains, etc. The spatial points where the state variables are located are called nodes.

2.1 Finite Element Equations

In this section the general procedure to state the finite element equations for a general 3–D problem will be derived. First, it is appropriate to define the problem that is wanted to be solved: Consider an arbitrary 3–D body which is being deformed because the imposition of some boundary conditions, see Figure 2.1. The body is referred to a Cartesian coordinate system. The displacements are prescribed on surface S_u and it is also subjected to surface forces f^{S_f}. Furthermore, there exists a body force per unit volume f^B acting over the whole domain. The problem is to calculate the displacements u_i of the body and the corresponding strains e_{ij} and stresses τ_{ij}.

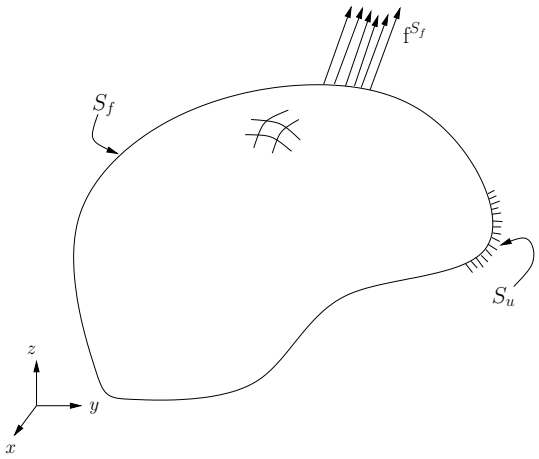

Figure 2.1: Geometry of a general 3-D body. Figure taken from reference (Bat96).

As already was said, in Finite Element Analysis (FEA), the body which is going to be analysed is approximated into an assemblage of finite elements. Those elements are composed by nodal points, which can be located over its boundary or within its interior. The displacements u_i of every element, are assumed to be a function of the displacements at the n finite element nodal

points. Then, for an element m it can be stated that

$$ {}^{(m)}u_i = \sum_{k=1}^{n} h_k \, u_i^k, \qquad i = 1, 2, 3. $$

where ${}^{(m)}u_i$ is measured in a conveniently local coordinate system, h_k are the interpolation base functions, and u_i^k correspond to the state variables of element m. Displacements ${}^{(m)}u_i = {}^{(m)}\mathbf{u}$ can be assembled as the multiplication of a matrix H and a vector $\hat{\mathbf{u}}$. That is,

$$ {}^{(m)}\mathbf{u} = {}^{(m)}H \, \hat{\mathbf{u}}, \tag{2.1} $$

where ${}^{(m)}H$ is called as the displacement interpolation matrix, and $\hat{\mathbf{u}}$ is a vector containing the global displacement components at all nodal points of the assemblage. The size of ${}^{(m)}H$ and $\hat{\mathbf{u}}$ depends on the space where the problem is being simulated (3–D, 2–D, or 1–D), the total amount of nodes n of the system, and the number of degrees of freedom (dof) per node used. In the particular case when the problem analysed is in 3–D, with only displacements used as state variables, the size of ${}^{(m)}H$ would be $3 \times 3n$, and $\hat{\mathbf{u}}$ would be of size $3n$, thus

$$ \hat{\mathbf{u}} = [u_1^1, u_2^1, u_3^1, u_1^2, u_2^2, u_3^2, \ldots, u_1^{n-1}, u_2^{n-1}, u_3^{n-1}, u_1^n, u_2^n, u_3^n]. $$

The Cauchy stress tensor τ_{ij} and the small strain tensor e_{ij} can be written in vector form, e.g. in the 3–D case $e_{ij} = \mathbf{e} = [e_{11}, e_{22}, e_{33}, 2\,e_{12}, 2\,e_{13}, 2\,e_{23}]$, where the fact that $e_{ij} = e_{ji}$ has been considered. Hence, the corresponding element strains can be calculated by differentiating Equation 2.1 as

$$ {}^{(m)}\mathbf{e} = {}^{(m)}B\hat{\mathbf{u}}, \tag{2.2} $$

where ${}^{(m)}B$ is the strain-displacement matrix[1]. The size of ${}^{(m)}B$ depends on the problem being analysed, for example a 3–D element with only displacement degrees of freedom would have a size of $6 \times 3n$.

Virtual displacements and virtual strains are calculated similarly; hence

$$ {}^{(m)}\delta\mathbf{u} = {}^{(m)}H \, \delta\hat{\mathbf{u}} \tag{2.3} $$

$$ {}^{(m)}\delta\mathbf{e} = {}^{(m)}B \, \delta\hat{\mathbf{u}}, \tag{2.4} $$

and the stresses are related to the strains via the material constitutive relation

$$ {}^{(m)}\tau_{ij} = {}^{(m)}C_{ijmn}{}^{(m)}e_{mn}, \tag{2.5} $$

[1] see reference (Bat96, pag. 161-163), for an enhancement of this concept

or written in matrix notation

$$ {}^{(m)}\tau = {}^{(m)}C\,{}^{(m)}\mathbf{e}. \tag{2.6} $$

where ${}^{(m)}C$ is the material constitutive matrix. In the 3–D case, ${}^{(m)}C$ is a 6×6 square matrix. Now, if tensors τ_{ij} and e_{ij} are expressed in vector form, Equation 1.2 (principle of virtual displacements) can be rewritten as

$$ \int_V \tau\, \delta\mathbf{e}\, dV = \int_V \mathbf{f^B} \delta\mathbf{u}\, dV + \int_{S_f} \mathbf{f^{S_f}} \delta\mathbf{u^{S_f}}\, dS. $$

Next, substitution of equations 2.1 to 2.6 into the above expression, and considering the whole assemblage of elements, yields to

$$ \sum_{m=1}^{\text{n-ele}} \int_{(m)V} \underbrace{\delta\hat{\mathbf{u}}^T\, {}^{(m)}B^T}_{{}^{(m)}\delta\mathbf{e}}\, \underbrace{{}^{(m)}C\, {}^{(m)}B\, {}^{(m)}\hat{\mathbf{u}}}_{{}^{(m)}\tau}\, {}^{(m)}dV = $$

$$ \sum_{m=1}^{\text{n-ele}} \int_{(m)V} {}^{(m)}\mathbf{f^B}\, {}^{(m)}H^T\, {}^{(m)}\delta\hat{\mathbf{u}}^T\, {}^{(m)}dV + $$

$$ \sum_{m=1}^{\text{n-ele}} \int_{(m)S_f} {}^{(m)}\mathbf{f^{S_f}} \left[{}^{(m)}H^{S_f}\right]^T \delta\hat{\mathbf{u}}^T\, {}^{(m)}dS, $$

and rearranging terms

$$ \delta\hat{\mathbf{u}}^T \Big[\sum_{m=1}^{\text{n-ele}} \int_{(m)V} {}^{(m)}B^T\, {}^{(m)}C\, {}^{(m)}B\, {}^{(m)}dV \Big] \hat{\mathbf{u}} = $$

$$ \delta\hat{\mathbf{u}}^T \Big[\sum_{m=1}^{\text{n-ele}} \int_{(m)V} {}^{(m)}H^T\, {}^{(m)}\mathbf{f^B}\, {}^{(m)}dV + \tag{2.7} $$

$$ \sum_{m=1}^{\text{n-ele}} \int_{(m)S_f} \left[{}^{(m)}H^{S_f}\right]^{T(m)}\mathbf{f^{S_f}}\, {}^{(m)}dS \Big]. $$

"To obtain from 2.7 the equations for the unknown nodal point displacements, the principle of virtual displacements is applied n times by imposing virtual displacements in turn for all components of $\delta\hat{\mathbf{u}}$*. In the first application* $\delta\hat{\mathbf{u}} = \boldsymbol{e}_1$*, in the second application* $\delta\hat{\mathbf{u}} = \boldsymbol{e}_2$*, and so on, until in the nth application* $\delta\hat{\mathbf{u}} = \boldsymbol{e}_n$*"*(Bat96). In this way, Equation 2.7 can be expressed as

$$ K\,\hat{\mathbf{u}} = \mathbf{R} \tag{2.8} $$

where

$$\mathbf{R} = \sum_{m=1}^{\text{n-ele}} \int_{(m)V} {}^{(m)}H^{T\ (m)}\mathbf{f}^{\mathbf{B}\ (m)}dV + \sum_{m=1}^{\text{n-ele}} \int_{(m)S_f} \left[{}^{(m)}H^{S_f}\right]^{T\ (m)}\mathbf{f}^{\mathbf{S_f}\ (m)}dS.$$

K is known as the stiffness matrix of the element, and is given by

$$K = \sum_{m=1}^{\text{n-ele}} \int_{(m)V} {}^{(m)}B^{T\ (m)}\ C\ {}^{(m)}B\ {}^{(m)}dV. \tag{2.9}$$

In case that concentrated loads are going to be considered, they are written directly in vector $\mathbf{R}$ in the posicion corresponding to the discrete displacement variable $\hat{\mathbf{u}}$ where the concentrated load is applied. This kind of loads were not considered in the functional $\Pi_{(u_i,\partial u_i/\partial x_j)}$ because in real world, punctual forces does not exist; instead, forces over a very small area do exist.

Chapter 3

Large Displacement-based Nonlinear FEA

In the previous chapter, only small displacements were considered. *"The fact that the displacements must be small has entered into evaluation of matrix K and load vector $\mathbf{R}$ because all integrations have been performed over the original volume of the finite elements, and the strain-displacement matrix ${}^{(m)}B$ of each element was assumed to be constant and independent of the element displacements"*(Bat96). Therefore, the formulation described therein, applies only to a certain kind of problems with many engineering restrictive characteristics. Hence, a more general formulation considering large displacements represents a better approach to the real conditions of some problems. This fact will be discussed in this chapter; first some basic concepts will be explained, followed by the mathematical formulation of the problem which must be solved. Finally, the formulation for the incremental Total Lagrangian equations will be described, which leads to the Finite Element equations.

3.1 Basic Notions

In large deformation analysis, the domain V of the body is changing continuously, as well as its boundary conditions and the external loads. Therefore, if the coordinate system chosen remains stationary and the body is moving in this coordinate frame, the stress and strain measures (τ_{ij}, e_{ij}) used in small displacement analysis, become useless because they vary under rigid body rotations, which is not allowed by the Principle of Frame Indifference[1]. Fur-

[1] see (Mal69) for an explanation

thermore, the small strain tensor e_{ij} by definition does not take into account higher order terms which are necessary in a large deformation analysis. Thus, corresponding stress and strain measures which are invariant under rigid body rotations and with no omission of higher order terms must be defined.

Several different kinds of strain, stress, and some other related quantities have been proposed. This quantities might be defined in terms of the undeformed configuration (Lagrangian formulation), or in terms of the deformed configuration (Eulerian formulation). The coordinates of the undeformed original object are known as material coordinates, and therefore are used by the Lagrangian formulation. Instead, Eulerian formulation uses spatial coordinates which are those of the deformed configuration.

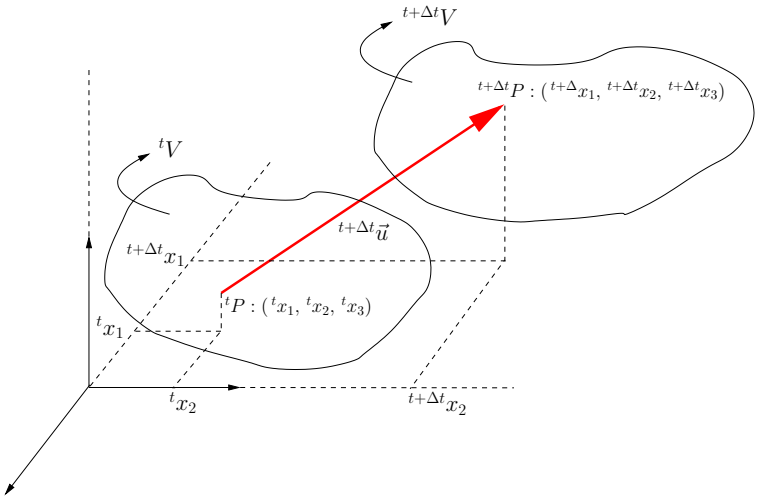

Figure 3.1: Movement of a point in large displacement analysis.

For this kind of problems it is necessary to employ an incremental formulation. A time variable t describes the loading and the motion of the body. The aim is to evaluate the equilibrium positions of the complete body at the discrete time points $0, \Delta t, 2\Delta t, 3\Delta t, \ldots$, where Δt is an increment in time. Towards the solution of the problem, assume that the static and kinematic variables for all time steps from time 0 to time t, inclusive, have been obtained already. Hence, the location of the body for the next equilibrium position corresponding to the discrete time $t + \Delta t$ needs to be reached. This process is applied repetitively until the complete solution path has been solved for (Bat96).

Figure 3.1 shows how a point $^{t}P \in {}^{t}V$ (the superscript t means that these

quantities are referred to the configuration at time t) in a large deformation analysis can lie very far away from its initial position after deformation ${}^{t+\Delta t}\mathbf{u}$.

In the classical linear theory of elasticity, the displacements experimented by a deformable body are assumed to be very small. Hence, the final position ${}^{t+\Delta t}P$ of a point in a body lies very close to its initial position ${}^{t}P$. Approximations based on the idea of infinitesimal displacement lead to a complete linearisation of the theory of deformation. However, in a more general formulation, it is necessary to abandon this restriction (BC99).

Before new stress and strain quantities are defined, some kinematic measures of motion for a body must be outlined:

3.1.1 The Displacement gradient and the Deformation gradient

The deformation suffered by any particle within a body from time t to time $t+\Delta t$, is commonly represented by a 3–D vector (see Figure 3.2) with components

$$ {}^{t+\Delta t}\mathbf{u} = {}^{t+\Delta t}u_1\,\hat{\mathrm{i}} + {}^{t+\Delta t}u_2\,\hat{\mathrm{j}} + {}^{t+\Delta t}u_3\,\hat{\mathrm{k}}, $$

where

$$ {}^{t+\Delta t}u_1 = {}^{t+\Delta t}x_1 - {}^{t}x_1, \quad {}^{t+\Delta t}u_2 = {}^{t+\Delta t}x_2 - {}^{t}x_2, \quad {}^{t+\Delta t}u_3 = {}^{t+\Delta t}x_3 - {}^{t}x_3. \quad (3.1) $$

Hereafter this point, the amount of deformation ${}^{t+\Delta t}\mathbf{u}$ will be denoted by $\mathbf{u}$, or in indicial notation ${}^{t+\Delta t}u_i = u_i$.

In Figure 3.2, it is implicitly assumed that the object with domain ${}^{t}V$ has already been deformed from its initial state at time 0 to the state at time t. Of course, at time 0 the original domain of the object was ${}^{0}V$. Therefore, the amount of deformation which takes place between time 0 and t is denoted by ${}^{t}\mathbf{u} = {}^{t}u_i$, and its vectorial components are:

$$ {}^{t}u_1 = {}^{t}x_1 - {}^{0}x_1, \quad {}^{t}u_2 = {}^{t}x_2 - {}^{0}x_2, \quad {}^{t}u_3 = {}^{t}x_3 - {}^{0}x_3. $$

In a Cartesian coordinate system, when analysing the deformation of a body, a particle initially located at a point ${}^{t}P : ({}^{t}x_1, {}^{t}x_2, {}^{t}x_3)$ passes to a point ${}^{t+\Delta t}P : ({}^{t+\Delta t}x_1, {}^{t+\Delta t}x_2, {}^{t+\Delta t}x_3)$. Likewise, a particle ${}^{t}Q : ({}^{t}x_1 + d\,{}^{t}x_1, {}^{t}x_2 + d\,{}^{t}x_2, {}^{t}x_3 + d\,{}^{t}x_3)$ passes to a point ${}^{t+\Delta t}Q : ({}^{t+\Delta t}x_1 + d\,{}^{t+\Delta t}x_1, {}^{t+\Delta t}x_2 + d\,{}^{t+\Delta t}x_2, {}^{t+\Delta t}x_3 + d\,{}^{t+\Delta t}x_3)$, see Figure 3.2. The infinitesimal line ${}^{t}\overline{PQ}$ is ordinarily elongated or contracted when it passes to be line ${}^{t+\Delta t}\overline{PQ}$. The differential

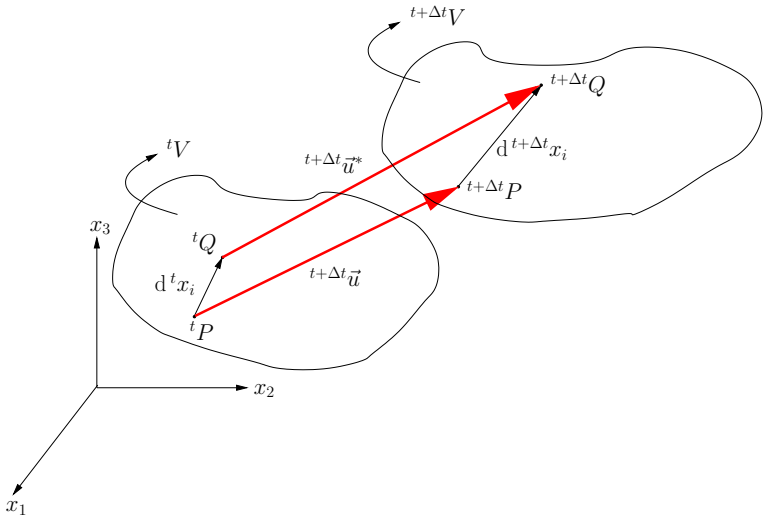

Figure 3.2: Infinitesimal vectors $d\,^{t}x_i$ and $d\,^{t+\Delta t}x_i$.

vector $^{t}\overline{PQ}$ is denoted by $d\,^{t}x_i$, and $^{t+\Delta t}\overline{PQ}$ is denoted by $d\,^{t+\Delta t}x_i$. After deformation, vector $d\,^{t}x_i$ transforms into $d\,^{t+\Delta t}x_i$ where

$$d\,^{t}x_i = d\,^{t}x_1\,\hat{\mathrm{i}} + d\,^{t}x_2\,\hat{\mathrm{j}} + d\,^{t}x_3\,\hat{\mathrm{k}}$$
$$d\,^{t+\Delta t}x_i = d\,^{t+\Delta t}x_1\,\hat{\mathrm{i}} + d\,^{t+\Delta t}x_2\,\hat{\mathrm{j}} + d\,^{t+\Delta t}x_3\,\hat{\mathrm{k}}.$$

$d\,^{t+\Delta t}x_i$ must be interpreted as the position occupied by the deformed material vector which at its original configuration was $d\,^{t}x_i$. Therefore, there must be a set of three functions which transform any point ^{t}P into a point $^{t+\Delta t}P$ and vice versa. Hence

$$^{t+\Delta t}x_i = {}^{t+\Delta t}x_{i(^{t}x_1,\,^{t}x_2,\,^{t}x_3)}. \tag{3.2}$$

This concept can be understood in a more clear way, imaging that every particle within the domain ^{t}V will be moved towards a new location $^{t+\Delta t}V$ after deformation. The new location of every particle in configuration $t+\Delta t$ will differ from the rest of the other particles. It means, that there must exist a vector function which transforms the initial coordinates of every particle into its final position.

The displacement gradient and deformation gradient arise as tensor quantities that measure the deformation of an object. To be able to define these tensors, it is necessary to remember the definition of the total differential of a scalar function: Looking at Figure 3.3a and using a first order Taylor's approximation, it can be stated that

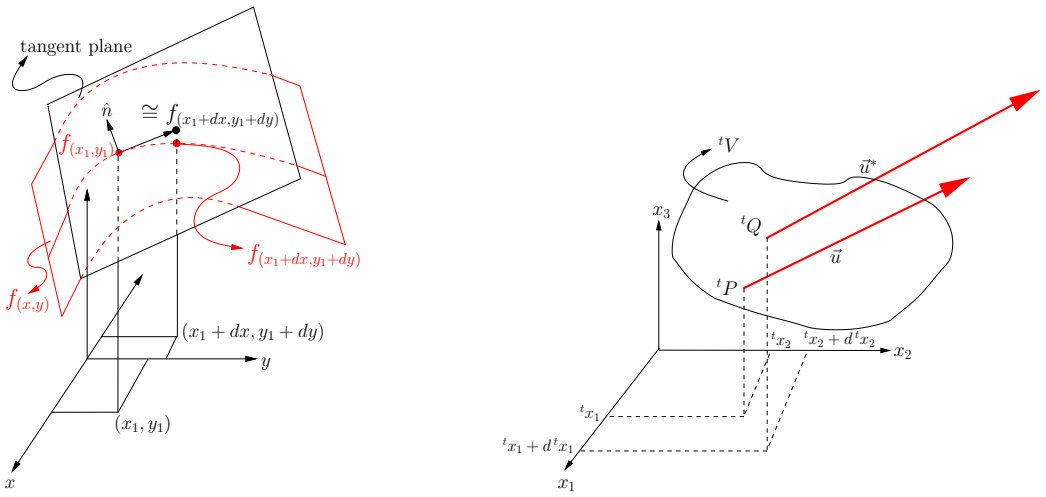

(a) Scalar function in 2–D. (b) vector function in 3–D.

Figure 3.3: Total differential of a function.

$$f_{(x_1+dx,y_1+dy)} \cong f_{(x_1,y_1)} + \frac{\partial f_{(x,y)}}{\partial x}\Big|_{x_1,y_1} dx + \frac{\partial f_{(x,y)}}{\partial y}\Big|_{x_1,y_1} dy.$$

This concept can be extrapolated to a 3–D vector function as (see Figure 3.3b)

$$\begin{aligned} u_i^* &= u_i + \frac{\partial u_i}{\partial\, {}^t x_1} d\,{}^t x_1 + \frac{\partial u_i}{\partial\, {}^t x_2} d\,{}^t x_2 + \frac{\partial u_i}{\partial\, {}^t x_3} d\,{}^t x_3 \\ u_i^* - u_i &= \frac{\partial u_i}{\partial {}^t x_j} d\,{}^t x_j \end{aligned} \tag{3.3}$$

where $\frac{\partial u_i}{\partial {}^t x_j} = {}_t u_{i,j}$ is known as the displacement gradient. This tensor can be written as a 3×3 matrix, that is

$${}_t u_{i,j} = \begin{bmatrix} \frac{\partial u_1}{\partial {}^t x_1} & \frac{\partial u_1}{\partial {}^t x_2} & \frac{\partial u_1}{\partial {}^t x_3} \\ \frac{\partial u_2}{\partial {}^t x_1} & \frac{\partial u_2}{\partial {}^t x_2} & \frac{\partial u_2}{\partial {}^t x_3} \\ \frac{\partial u_3}{\partial {}^t x_1} & \frac{\partial u_3}{\partial {}^t x_2} & \frac{\partial u_3}{\partial {}^t x_3} \end{bmatrix}.$$

However, in order to get a general expression which relates $d\,{}^{t+\Delta t} x_i$ with $d\,{}^t x_i$,

the expressions stated in 3.1 are replaced into 3.3, which yields to

$$\begin{aligned}
u_i^* - u_i &= \frac{\partial u_i}{\partial {}^t x_j} d\,{}^t x_j \\
du_i &= \frac{\partial u_i}{\partial {}^t x_j} d\,{}^t x_j \\
d({}^{t+\Delta t}x_i - {}^t x_i) &= \frac{\partial ({}^{t+\Delta t}x_i - {}^t x_i)}{\partial {}^t x_j} d\,{}^t x_j \\
d\,{}^{t+\Delta t}x_i - d\,{}^t x_i &= \frac{\partial {}^{t+\Delta t}x_i}{\partial {}^t x_j} d\,{}^t x_j - \frac{\partial {}^t x_i}{\partial {}^t x_j} d\,{}^t x_j \\
d\,{}^{t+\Delta t}x_i - d\,{}^t x_i &= \frac{\partial {}^{t+\Delta t}x_i}{\partial {}^t x_j} d\,{}^t x_j - \delta_{ij} d\,{}^t x_j \\
d\,{}^{t+\Delta t}x_i - d\,{}^t x_i &= \frac{\partial {}^{t+\Delta t}x_i}{\partial {}^t x_j} d\,{}^t x_j - d\,{}^t x_i \\
d\,{}^{t+\Delta t}x_i &= \frac{\partial {}^{t+\Delta t}x_i}{\partial {}^t x_j} d\,{}^t x_j;
\end{aligned}$$

hence,

$$d\,{}^{t+\Delta t}x_i = {}^{t+\Delta t}_{t}x_{i,j}\, d\,{}^t x_j. \tag{3.4}$$

The expression ${}^{t+\Delta t}_{t}x_{ij}$ is a second order tensor named in structural mechanics as the deformation gradient. ${}^{t+\Delta t}_{t}x_{i,j}$ can be written in matrix form as

$${}^{t+\Delta t}_{t}x_{i,j} = \begin{bmatrix} \frac{\partial {}^{t+\Delta t}x_1}{\partial {}^t x_1} & \frac{\partial {}^{t+\Delta t}x_1}{\partial {}^t x_2} & \frac{\partial {}^{t+\Delta t}x_1}{\partial {}^t x_3} \\ \frac{\partial {}^{t+\Delta t}x_2}{\partial {}^t x_1} & \frac{\partial {}^{t+\Delta t}x_2}{\partial {}^t x_2} & \frac{\partial {}^{t+\Delta t}x_2}{\partial {}^t x_3} \\ \frac{\partial {}^{t+\Delta t}x_3}{\partial {}^t x_1} & \frac{\partial {}^{t+\Delta t}x_3}{\partial {}^t x_2} & \frac{\partial {}^{t+\Delta t}x_3}{\partial {}^t x_3} \end{bmatrix}.$$

Both, the displacement gradient ${}_t u_{i,j}$ and the deformation gradient ${}^{t+\Delta t}_{t}x_{i,j}$ are taking place in configuration $t + \Delta t$; however, they are measured in configuration t.

"${}^{t+\Delta t}_{t}x_{i,j}$ tensor includes rotation plus stretch effects which represents a disadvantage. Because constitutive equations employing it will have to be so constructed that they will not predict a stress due to rigid body rotation"(Mal69)[2].

[2]For an enhancement of the displacement gradient concept consult references (Mal69), (Bat96), (BC99)

Appendix A deduces in matrix form how the expressions for the displacement gradient and the deformation gradient are obtained for a 3–D Cartesian system.

3.1.2 Green-Lagrange strain tensor

The mathematical definition of the Green-Lagrange strain tensor comes from the idea of measuring how much the length of a piece of material of differential size has changed when going from its initial configuration to its deformed configuration. Therefore, the measure obtained from the subtraction of the final and the initial length of vectors $d^{t+\Delta t}x_i$ and $d^{t}x_i$ constitutes the basis to define the Green-Lagrange strain.

The magnitudes of vectors $d^{t+\Delta t}x_i$ and $d^{t}x_i$ can be quantified by their Euclidean norm, that is

$$(\parallel d^{t+\Delta t}x_i \parallel)^2 = d^{t+\Delta t}x_i\, d^{t+\Delta t}x_i \qquad \text{and} \qquad (\parallel d^{t}x_i \parallel)^2 = d^{t}x_i\, d^{t}x_i.$$

Next, using the Equation 3.4, the subtraction operation: length of $d^{t+\Delta t}x_i$ minus length of $d^{t}x_i$ can be developed as:

$$\begin{aligned}(\parallel d^{t+\Delta t}x_i \parallel)^2 - (\parallel d^{t}x_i \parallel)^2 &= d^{t+\Delta t}x_i\, d^{t+\Delta t}x_i - d^{t}x_i\, d^{t}x_i \\ &= \frac{\partial^{t+\Delta t}x_i}{\partial^{t}x_j} d^{t}x_j \frac{\partial^{t+\Delta t}x_i}{\partial^{t}x_k} d^{t}x_k - d^{t}x_i\, d^{t}x_i,\end{aligned}$$

and using the expressions stated in 3.1, the following is obtained

$$\begin{aligned}d^{t+\Delta t}x_i\, d^{t+\Delta t}x_i - d^{t}x_i\, d^{t}x_i =& \frac{\partial(u_i + {}^{t}x_i)}{\partial^{t}x_j} d^{t}x_j \frac{\partial(u_i + {}^{t}x_i)}{\partial^{t}x_k} d^{t}x_k - d^{t}x_i\, d^{t}x_i \\ =& \Big[\frac{\partial u_i}{\partial^{t}x_j}\frac{\partial u_i}{\partial^{t}x_k} d^{t}x_j\, d^{t}x_k + \frac{\partial u_i}{\partial^{t}x_j}\frac{\partial^{t}x_i}{\partial^{t}x_k} d^{t}x_j\, d^{t}x_k + \\ & \frac{\partial^{t}x_i}{\partial^{t}x_j}\frac{\partial u_i}{\partial^{t}x_k} d^{t}x_j\, d^{t}x_k + \frac{\partial^{t}x_i}{\partial^{t}x_j}\frac{\partial^{t}x_i}{\partial^{t}x_k} d^{t}x_j\, d^{t}x_k - \\ & d^{t}x_i\, d^{t}x_i\Big].\end{aligned}$$

Now, multiplying by $\frac{1}{2}$ in both sides of the equation

$$\begin{aligned}\frac{1}{2}\Big[d^{\,t+\Delta t}x_i\, d^{\,t+\Delta t}x_i - d^{\,t}x_i\, d^{\,t}x_i\Big] =& \frac{1}{2}\Big[\frac{\partial u_i}{\partial^t x_j}\frac{\partial u_i}{\partial^t x_k} d^{\,t}x_j\, d^{\,t}x_k + \frac{\partial u_i}{\partial^t x_j}\delta_{ik}\, d^{\,t}x_j\, d^{\,t}x_k + \\ & \frac{\partial u_i}{\partial^t x_k}\delta_{ij}\, d^{\,t}x_j\, d^{\,t}x_k + \delta_{ij}\delta_{ik}\, d^{\,t}x_j\, d^{\,t}x_k - \\ & d^{\,t}x_i\, d^{\,t}x_i\Big] \\ =& \frac{1}{2}\Big[\frac{\partial u_i}{\partial^t x_j}\frac{\partial u_i}{\partial^t x_k} d^{\,t}x_j\, d^{\,t}x_k + \frac{\partial u_k}{\partial^t x_j} d^{\,t}x_j\, d^{\,t}x_k + \\ & \frac{\partial u_j}{\partial^t x_k} d^{\,t}x_j\, d^{\,t}x_k + d^{\,t}x_i\, d^{\,t}x_i - d^{\,t}x_i\, d^{\,t}x_i\Big] \\ =& \underbrace{\frac{1}{2}\Big[\frac{\partial u_k}{\partial^t x_j} + \frac{\partial u_j}{\partial^t x_k} + \frac{\partial u_i}{\partial^t x_j}\frac{\partial u_i}{\partial^t x_k}\Big]}_{{}^{t+\Delta t}_{t}\epsilon_{jk}} d^{\,t}x_j\, d^{\,t}x_k.\end{aligned}$$

Hence,

$$\frac{1}{2}\Big[d^{\,t+\Delta t}x_i\, d^{\,t+\Delta t}x_i - d^{\,t}x_i\, d^{\,t}x_i\Big] = d^{\,t}x_j\ {}^{t+\Delta t}_{t}\epsilon_{jk}\ d^{\,t}x_k,$$

where ${}^{t+\Delta t}_{t}\epsilon_{jk}$ is the Green-Lagrange strain tensor taking place in configuration $t+\Delta t$ but measured in configuration t.

It can also be easily deduced that

$${}^{t+\Delta t}_{t}\epsilon_{jk} = \frac{1}{2}\Big[{}^{t+\Delta t}_{t}x_{i,j}\ {}^{t+\Delta t}_{t}x_{i,k} - \delta_{jk}\Big] = \frac{1}{2}\Big[\frac{\partial u_k}{\partial^t x_j} + \frac{\partial u_j}{\partial^t x_k} + \frac{\partial u_i}{\partial^t x_j}\frac{\partial u_i}{\partial^t x_k}\Big]. \qquad (3.5)$$

If the expression defined above is developed for a 3-D system, $j = 1, 2, 3$, and $k = 1, 2, 3$, each one of the terms of the Green-Lagrange tensor are obtained:

$$\begin{aligned}{}^{t+\Delta t}_{t}\epsilon_{11} &= \frac{\partial\, u_1}{\partial\, {}^t x_1} + \frac{1}{2}\left[\left(\frac{\partial\, u_1}{\partial\, {}^t x_1}\right)^2 + \left(\frac{\partial\, u_2}{\partial\, {}^t x_1}\right)^2 + \left(\frac{\partial\, u_3}{\partial\, {}^t x_1}\right)^2\right] \\ {}^{t+\Delta t}_{t}\epsilon_{22} &= \frac{\partial\, u_2}{\partial\, {}^t x_2} + \frac{1}{2}\left[\left(\frac{\partial\, u_1}{\partial\, {}^t x_2}\right)^2 + \left(\frac{\partial\, u_2}{\partial\, {}^t x_2}\right)^2 + \left(\frac{\partial\, u_3}{\partial\, {}^t x_2}\right)^2\right] \\ {}^{t+\Delta t}_{t}\epsilon_{33} &= \frac{\partial\, u_3}{\partial\, {}^t x_3} + \frac{1}{2}\left[\left(\frac{\partial\, u_1}{\partial\, {}^t x_3}\right)^2 + \left(\frac{\partial\, u_2}{\partial\, {}^t x_3}\right)^2 + \left(\frac{\partial\, u_3}{\partial\, {}^t x_3}\right)^2\right]\end{aligned}$$

$$
\begin{aligned}
{}^{t+\Delta t}_{t}\epsilon_{12} &= \frac{1}{2}\left[\frac{\partial\, u_2}{\partial\, {}^t x_1} + \frac{\partial\, u_1}{\partial\, {}^t x_2} + \frac{\partial\, u_1}{\partial\, {}^t x_1}\frac{\partial\, u_1}{\partial\, {}^t x_2} + \frac{\partial\, u_2}{\partial\, {}^t x_1}\frac{\partial\, u_2}{\partial\, {}^t x_2} + \frac{\partial\, u_3}{\partial\, {}^t x_1}\frac{\partial\, u_3}{\partial\, {}^t x_2}\right] \\
{}^{t+\Delta t}_{t}\epsilon_{13} &= \frac{1}{2}\left[\frac{\partial\, u_3}{\partial\, {}^t x_1} + \frac{\partial\, u_1}{\partial\, {}^t x_3} + \frac{\partial\, u_1}{\partial\, {}^t x_1}\frac{\partial\, u_1}{\partial\, {}^t x_3} + \frac{\partial\, u_2}{\partial\, {}^t x_1}\frac{\partial\, u_2}{\partial\, {}^t x_3} + \frac{\partial\, u_3}{\partial\, {}^t x_1}\frac{\partial\, u_3}{\partial\, {}^t x_3}\right] \\
{}^{t+\Delta t}_{t}\epsilon_{23} &= \frac{1}{2}\left[\frac{\partial\, u_3}{\partial\, {}^t x_2} + \frac{\partial\, u_2}{\partial\, {}^t x_3} + \frac{\partial\, u_1}{\partial\, {}^t x_2}\frac{\partial\, u_1}{\partial\, {}^t x_3} + \frac{\partial\, u_2}{\partial\, {}^t x_2}\frac{\partial\, u_2}{\partial\, {}^t x_3} + \frac{\partial\, u_3}{\partial\, {}^t x_2}\frac{\partial\, u_3}{\partial\, {}^t x_3}\right].
\end{aligned}
$$

This strain measure ${}^{t+\Delta t}_{t}\epsilon_{jk}$ does not change under rigid-body rotations[3], and represents a complete finite strain tensor and not merely an approximation to it.

There is also an important deformation measure named **right Cauchy-Green deformation tensor** which is defined as

$$
{}^{t+\Delta t}_{t}C_{ij} = {}^{t+\Delta t}_{t}x_{i,k}\ {}^{t+\Delta t}_{t}x_{k,j}, \tag{3.6}
$$

" ${}^{t+\Delta t}_{t}C_{ij}$ is used to measure the stretch of a material fibber and the change in angle between adjacent material fibres due to deformation"(Bat96). Indeed, the strain tensor ${}^{t+\Delta t}_{t}\epsilon_{ij}$ can be written in terms of ${}^{t+\Delta t}_{t}C_{ij}$ as[4]

$$
2\,{}^{t+\Delta t}_{t}\epsilon_{ij} = {}^{t+\Delta t}_{t}C_{ij} - \delta_{ij}.
$$

Both, ${}^{t+\Delta t}_{t}\epsilon_{ij}$ and ${}^{t+\Delta t}_{t}C_{ij}$ are positive-definite matrices, because they come from the the evaluation of $(\parallel d\,{}^{t+\Delta t}x_i \parallel)^2$ and $(\parallel d\,{}^{t}x_i \parallel)^2$ which are always positive.

When the displacement gradient is finite, which means that it is not small compared to unity, it can also be demonstrated that[5]

$$
\begin{aligned}
{}^{t+\Delta t}_{t}x_{k,p} &= {}^{t+\Delta t}_{t}R_{kq}\ {}^{t+\Delta t}_{t}U_{qp} \\
&= {}^{t+\Delta t}_{t}V_{kq}\ {}^{t+\Delta t}_{t}R_{qp},
\end{aligned} \tag{3.7}
$$

therefore, *"a multiplicative decomposition into two tensors can be always achieved. One of which represents a rigid-body rotation ${}^{t+\Delta t}_{t}R_{kq}$, while the other is a symmetric positive-definite tensor ${}^{t+\Delta t}_{t}U_{qp}$ or ${}^{t+\Delta t}_{t}V_{kq}$"*(Mal69).

3.1.3 Second Piola-Kirchhoff stress tensor

Looking back into chapter 1, and paying special attention in the way how the general equation of equilibrium for a 3–D structural object was deduced

[3] see (Bat96, pag. 518)

[4] see references (Mal69) and (Bat96) for an explanation

[5] see (Mal69, pag. 172-181)

(see Equation 1.4). It can be seen that the domain V represents the space of integration over which Expression 1.4 applies. Indeed, it was implicitly assumed that V stands for the current deformed configuration of the object, which means that $V = {}^{t+\Delta t}V$.

In fact, *"the stress tensor field τ_{ij} is defined as function of the spatial coordinates (Eulerian formulation). Therefore, a suitable strain measure to use with the Cauchy stress tensor would be one of the strain or deformation tensors of the Eulerian formulation in terms of the spatial position in the deformed configuration"*(Mal69). But the Green-Lagrange strain recently defined with the intention of being used in a large displacement analysis, has been expressed in terms of the material points of the body (Lagrangian formulation). Hence, it becomes important to specify a stress measure as a function of the material coordinates, as well as a redefinition of the equilibrium equation of motion.

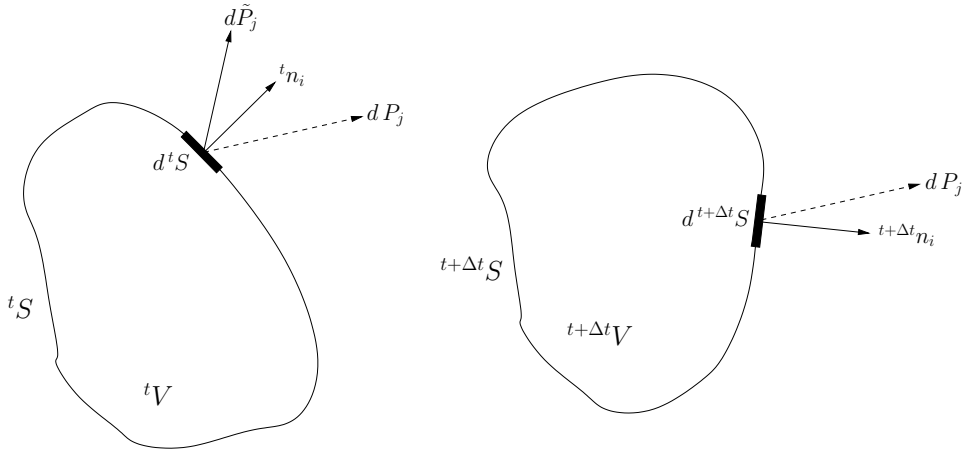

Figure 3.4: Force vectors for Piola-Kirchhoff stress definitions. Figure taken from (Mal69, pag. 221)

The Lagrangian stress tensor ${}^{t+\Delta t}_{t}T_{ij}$ or better called as the First Piola-Kirchhoff stress tensor is defined through the expression

$$d\,P_j = ({}^{t+\Delta t}n_i \; {}^{t+\Delta t}\tau_{ij}) d\,{}^{t+\Delta t}S = ({}^{t}n_i \; {}^{t+\Delta t}_{t}T_{ij}) d\,{}^{t}S,$$

where τ_{ij} is the Cauchy stress tensor, and $d\,P_j$ is the real force vector acting over $d\,{}^{t+\Delta t}S$ on the deformed configuration ${}^{t+\Delta t}V$, see Figure 3.4. With the above expression, a new stress tensor measure ${}^{t+\Delta t}_{t}T_{ij}$ has been defined. This tensor is related to the actual force vector and the Cauchy stress tensor (both defined in terms of the spatial position), but actually ${}^{t+\Delta t}_{t}T_{ij}$ acts over the

non-deformed configuration; hence, it is defined in a material configuration scheme. But even ${}^{t+\Delta t}_{t}T_{ij}$ is very simple to define and leads to a simple form of the equations of motion (equilibrium), it has the disadvantage of being not symmetric; in consequence, it cannot be used in constitutive equations with a symmetric strain tensor (Mal69).

The second Piola-Kirchhoff ${}^{t+\Delta t}_{t}S_{ij}$ comes up as a symmetric stress tensor that can be used with the Green-Lagrange strain tensor through appropriate constitutive relation. *"${}^{t+\Delta t}_{t}S_{ij}$ is formulated somewhat differently. Instead of the actual force $d\,P_j$ on $d\,{}^{t+\Delta t}S$ it gives a force $d\,\tilde{P}_j$ related to the force $d\,P_j$ in the same way that a material vector $d\,{}^{t}x_i$ at ${}^{t}V$ is related by the deformation to the corresponding spatial vector $d\,{}^{t+\Delta t}x_i$ at ${}^{t+\Delta t}V$. That is*

$$d\,\tilde{P}_i = \left[{}^{t+\Delta t}_{t}x_{i,j}\right]^{-1} d\,P_j \qquad \text{just as} \qquad d\,{}^{t}x_i = \left[{}^{t+\Delta t}_{t}x_{i,j}\right]^{-1} d\,{}^{t+\Delta t}x_j$$

where $d\,\tilde{P}_i$ and $d\,{}^{t}S$ have been stretched and rotated the same amount relative to the final positions $d\,P_i$ and $d\,{}^{t+\Delta t}S$ respectively"(Mal69), then

$$d\,\tilde{P}_j = \left[{}^{t+\Delta t}_{t}x_{j,q}\right]^{-1} \underbrace{\left({}^{t+\Delta t}n_i\ {}^{t+\Delta t}\tau_{iq}\right) d\,{}^{t+\Delta t}S}_{d\,P_q} = \left({}^{t}n_i\ {}^{t+\Delta t}_{t}S_{ij}\right) d\,{}^{t}S. \tag{3.8}$$

Now, in order to obtain an expression for the second Piola-Kirchhoff stress in terms of the Cauchy stress, it is necessary to use the Nanson's formula[6] which says that,

$${}^{t+\Delta t}\rho\,{}^{t+\Delta t}n_j\,d\,{}^{t+\Delta t}S = {}^{t}\rho\,{}^{t}n_i\left[{}^{t+\Delta t}_{t}x_{i,j}\right]^{-1} d\,{}^{t}S.$$

Replacing this formula into 3.8 yields to

$$\left({}^{t}n_i\ {}^{t+\Delta t}_{t}S_{ij}\right)\ d\,{}^{t}S = \left[{}^{t+\Delta t}_{t}x_{j,q}\right]^{-1}\left({}^{t+\Delta t}n_p\ {}^{t+\Delta t}\tau_{pq}\right)\ d\,{}^{t+\Delta t}S$$

$$\left({}^{t}n_i\ {}^{t+\Delta t}_{t}S_{ij}\right)\ d\,{}^{t}S = \left[{}^{t+\Delta t}_{t}x_{j,q}\right]^{-1}\left(\frac{{}^{t}\rho}{{}^{t+\Delta t}\rho}\,{}^{t}n_k\left[{}^{t+\Delta t}_{t}x_{k,p}\right]^{-1}\frac{d\,{}^{t}S}{d\,{}^{t+\Delta t}S}\right)\ {}^{t+\Delta t}\tau_{pq}\,d\,{}^{t+\Delta t}S$$

$$\left({}^{t}n_i\ {}^{t+\Delta t}_{t}S_{ij}\right) = \frac{{}^{t}\rho}{{}^{t+\Delta t}\rho}\,{}^{t}n_k\ {}^{t}_{t+\Delta t}x_{k,p}\ {}^{t+\Delta t}\tau_{pq}\ {}^{t}_{t+\Delta t}x_{j,q}.$$

Finally, *"for arbitrary unit vector ${}^{t}\hat{n}$, because this relationship must hold for any surface area and also any interior surface area that could be created by a cut in the body. Hence ${}^{t}n_i$ is arbitrary and can be chosen to be in succession equal to the unit coordinate vectors"*(Mal69), then

$${}^{t+\Delta t}_{t}S_{ij} = \frac{{}^{t}\rho}{{}^{t+\Delta t}\rho}\ {}^{t}_{t+\Delta t}x_{i,p}\ {}^{t+\Delta t}\tau_{pq}\ {}^{t}_{t+\Delta t}x_{j,q}. \tag{3.9}$$

[6] a demonstration of this formula is deduced in (Mal69, pag. 169)

This is the expression usually used in large displacement structural mechanics to relate Cauchy stresses with the second Piola-Kirchoff stress tensor.

3.2 Non-linear equations of motion

The principle of virtual displacements (Equation 1.2) deduced in chapter 1 is expressed in terms of the spatial coordinates (Eulerian formulation) at time $t + \Delta t$. In other words, it is applicable to the current deformed configuration of the object. Therefore, Equation 1.2 can be rewritten as

$$\int_{t+\Delta t V} {}^{t+\Delta t}\tau_{ij}\, \delta\left({}_{t+\Delta t}e_{ij}\right)\, d\,{}^{t+\Delta t}V = \int_{t+\Delta t V} {}^{t+\Delta t}f_i^B\, \delta\left({}^{t+\Delta t}u_i\right)\, d\,{}^{t+\Delta t}V + \int_{t+\Delta t S_f} {}^{t+\Delta t}f_i^{S_f}\, \delta\left({}^{t+\Delta t}u_i^{S_f}\right)\, d\,{}^{t+\Delta t}S \tag{3.10}$$

In structural mechanics, a Lagrangian formulation is usually preferred instead of the Eulerian formulation. This happens because the volume of the object being analysed is not known at time $t + \Delta t$, and also because it is assumed that the body would return to its natural state when it is unloaded (Mal69).

It is then necessary to rewrite Equation 3.10 using a Lagrangian formulation. In section 3.1.3 it was shown that the Cauchy stress tensor ${}^{t+\Delta t}\tau_{ij}$ can be expressed in terms of the second Piola-Kirchhoff stress tensor ${}_{t}^{t+\Delta t}S_{ij}$, which is already written in terms of the material coordinates. However, it is still indispensable to transform the term $\delta_{t+\Delta t}e_{ij}$ to be able to express the left hand side of Equation 3.10 in Lagrangian form.

For this purpose, it is precise to consider both a body in its deformed configuration (time $t + \Delta t$), and in its previous known configuration at time t (time t can be a deformed previous calculated configuration ${}^{t}V$ or the original undeformed configuration ${}^{0}V$), see Figure 3.5. A virtual displacement field $\delta^{t+2\Delta t}u_i$ is applied. This field is a function of the spatial coordinates $t+\Delta t$ (see Figure 3.5), and can also be thought as a variation on the displacement field ${}^{t+\Delta t}u_i$. Hence, it is conceivable to assume that $\delta^{t+2\Delta t}u_i \cong \delta^{t+\Delta t}u_i$. Moreover, a variation field ${}^{t+\Delta t}u_i$ will cause a variation on the small stress tensor $\delta_{t+\Delta t}e_{ij}$, where

$${}_{t+\Delta t}e_{ij} = \frac{1}{2}\left(\frac{\partial^{t+2\Delta t}u_i}{\partial^{t+\Delta t}x_j} + \frac{\partial^{t+2\Delta t}u_j}{\partial^{t+\Delta t}x_i}\right) = \frac{1}{2}\left({}_{t+\Delta t}^{t+2\Delta t}u_{i,j} + {}_{t+\Delta t}^{t+2\Delta t}u_{j,i}\right), \tag{3.11}$$

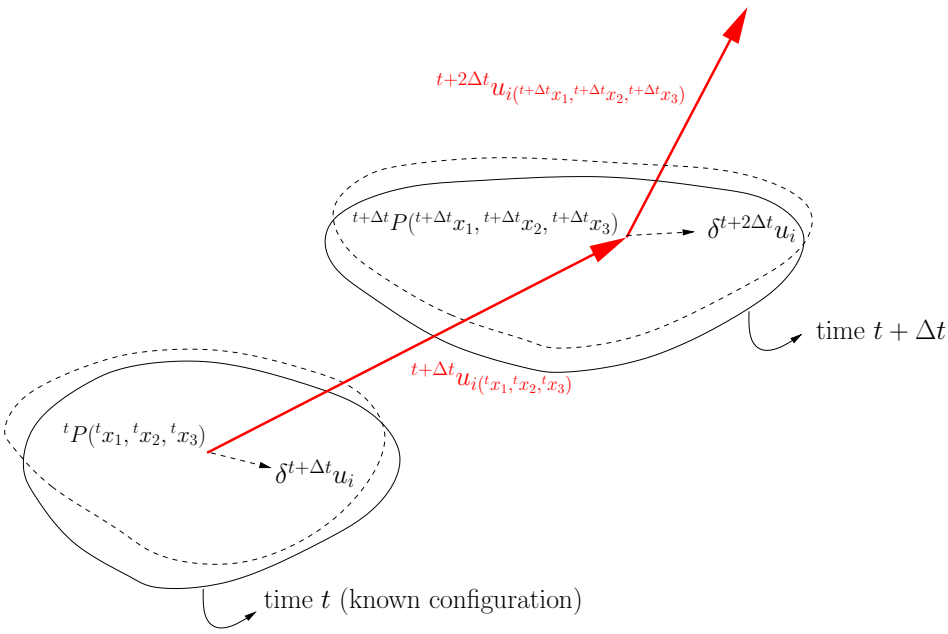

Figure 3.5: Body at time $t+\Delta t$ subjected to virtual displacement field given by $\delta^{t+\Delta t}u_i$. Figure taken from (Bat96, pag. 514)

and ${}^{t+2\Delta t}u_i$ is a function of the spatial coordinates at time $t+\Delta t$. That is, ${}^{t+2\Delta t}u_{i(^{t+\Delta t}x_1,\,^{t+\Delta t}x_2,\,^{t+\Delta t}x_3)}$. Besides

$$ {}^{t+\Delta t}_{t}\epsilon = \frac{1}{2}\left[{}^{t+\Delta t}_{t}x_{k,i}\, {}^{t+\Delta t}_{t}x_{k,j} - \delta_{ij}\right], $$

and

$$ \delta^{t+\Delta t}_{t}\epsilon = \frac{1}{2}\left[\delta^{t+\Delta t}_{t}x_{k,i}\, {}^{t+\Delta t}_{t}x_{k,j} + {}^{t+\Delta t}_{t}x_{k,i}\, \delta^{t+\Delta t}_{t}x_{k,j} - \delta(\delta_{ij})\right], \tag{3.12} $$

where $\delta(\delta_{ij}) = 0$ because it represents the variation of the delta Kronecker δ_{ij} which is a constant tensor. Now, it is necessary to find an expression for $\delta^{t+\Delta t}_{t}x_{i,j}$

$$ \delta^{t+\Delta t}_{t}x_{i,j} = \frac{\partial \delta^{t+\Delta t}x_i}{\partial {}^{t}x_j} = \frac{\partial \delta({}^{t}x_i + {}^{t+\Delta t}u_i)}{\partial {}^{t}x_j} = \delta(\delta_{ij}) + \frac{\partial \delta({}^{t+\Delta t}u_i)}{\partial {}^{t}x_j} = \frac{\partial \delta({}^{t+\Delta t}u_i)}{\partial {}^{t}x_j}; $$

but $\delta^{t+2\Delta t}u_i \cong \delta^{t+\Delta t}u_i$, then

$$ \delta^{t+\Delta t}_{t}x_{i,j} = \frac{\partial \delta({}^{t+\Delta t}u_i)}{\partial {}^{t}x_j} \cong \frac{\partial \delta({}^{t+2\Delta t}u_i)}{\partial {}^{t}x_j}. $$

Finally,

$$\delta_t^{t+\Delta t}x_{i,j} = \frac{\partial \delta({}^{t+2\Delta t}u_i)}{\partial {}^{t+\Delta t}x_p}\frac{\partial {}^{t+\Delta t}x_p}{\partial {}^{t}x_j} = \left({}^{t+2\Delta t}_{t+\Delta t}u_{i,p}\right)\left({}^{t}_{t+\Delta t}x_{p,j}\right). \tag{3.13}$$

Replacing this expression into Equation 3.12,

$$\begin{aligned}
\delta_t^{t+\Delta t}\epsilon_{ij} &= \frac{1}{2}\Big[\left(\delta^{t+2\Delta t}_{t+\Delta t}u_{k,p}\right){}^{t+\Delta t}_{t}x_{p,i}\,{}^{t+\Delta t}_{t}x_{k,j} + \underbrace{{}^{t+\Delta t}_{t}x_{k,i}\left(\delta^{t+2\Delta t}_{t+\Delta t}u_{k,n}\right){}^{t+\Delta t}_{t}x_{n,j}}_{\text{changing index } k \text{ by } p}\Big] \\
&= \frac{1}{2}\Big[{}^{t+\Delta t}_{t}x_{p,i}\left(\delta^{t+2\Delta t}_{t+\Delta t}u_{k,p}\right){}^{t+\Delta t}_{t}x_{k,j} + \underbrace{{}^{t+\Delta t}_{t}x_{p,i}\left(\delta^{t+2\Delta t}_{t+\Delta t}u_{p,n}\right){}^{t+\Delta t}_{t}x_{n,j}}_{\text{changing index } n \text{ by } k}\Big] \\
&= \frac{1}{2}\Big[{}^{t+\Delta t}_{t}x_{p,i}\left(\delta^{t+2\Delta t}_{t+\Delta t}u_{k,p}\right){}^{t+\Delta t}_{t}x_{k,j} + {}^{t+\Delta t}_{t}x_{p,i}\left(\delta^{t+2\Delta t}_{t+\Delta t}u_{p,k}\right){}^{t+\Delta t}_{t}x_{k,j}\Big] \\
&= {}^{t+\Delta t}_{t}x_{p,i}\Big[\frac{1}{2}\left(\delta^{t+2\Delta t}_{t+\Delta t}u_{k,p} + \delta^{t+2\Delta t}_{t+\Delta t}u_{p,k}\right)\Big]{}^{t+\Delta t}_{t}x_{k,j},
\end{aligned}$$

and according to Equation 3.11, it can be easily seen that

$$\delta_t^{t+\Delta t}\epsilon_{ij} = {}^{t+\Delta t}_{t}x_{p,i}\left[\delta_{t+\Delta t}e_{kp}\right]{}^{t+\Delta t}_{t}x_{k,j}. \tag{3.14}$$

Now, the left side of Equation 3.10 can be transformed into

$$\begin{aligned}
\int_{{}^{t+\Delta t}V} {}^{t+\Delta t}\tau_{ij}\,\delta_{t+\Delta t}e_{ij}\,d\,{}^{t+\Delta t}V = \int_{{}^{t+\Delta t}V} &\left(\frac{{}^{t+\Delta t}\rho}{{}^{t}\rho}\,{}^{t+\Delta t}_{t}x_{i,p}\,{}^{t+\Delta t}_{t}S_{pq}\,{}^{t+\Delta t}_{t}x_{j,q}\right) \\
&\left({}^{t}_{t+\Delta t}x_{n,i}\left[\delta^{t}_{t+\Delta t}\epsilon_{mn}\right]{}^{t}_{t+\Delta t}x_{m,j}\right)\,d\,{}^{t+\Delta t}V.
\end{aligned}$$

And because

$${}^{t+\Delta t}_{t}x_{i,p}\,{}^{t}_{t+\Delta t}x_{n,i} = \delta_{np}, \qquad \text{and} \qquad {}^{t+\Delta t}_{t}x_{j,q}\,{}^{t}_{t+\Delta t}x_{m,j} = \delta_{mq};$$

thus

$$\begin{aligned}
\int_{{}^{t+\Delta t}V} {}^{t+\Delta t}\tau_{ij}\,\delta_{t+\Delta t}e_{ij}\;d\,{}^{t+\Delta t}V &= \int_{{}^{t+\Delta t}V}\left(\frac{{}^{t+\Delta t}\rho}{{}^{t}\rho}\,\delta_{np}\delta_{mq}\,{}^{t+\Delta t}_{t}S_{pq}\,\delta_t^{t+\Delta t}\epsilon_{mn}\right)d\,{}^{t+\Delta t}V \\
&= \int_{{}^{t}V} {}^{t+\Delta t}_{t}S_{pq}\,\delta_t^{t+\Delta t}\epsilon_{pq}\,d\,{}^{t}V
\end{aligned}$$

where ${}^{t+\Delta t}\rho\,d\,{}^{t+\Delta t}V = {}^{t}\rho\,d\,{}^{t}V$. In this way,

$$\begin{aligned}
\int_{{}^{t}V} {}^{t+\Delta t}_{t}S_{pq}\,\delta_t^{t+\Delta t}\epsilon_{pq}\,d\,{}^{t}V = &\int_{{}^{t+\Delta t}V} {}^{t+\Delta t}\,f_i^B\,\delta^{t+\Delta t}u_i\,d\,{}^{t+\Delta t}V \\
&+ \int_{{}^{t+\Delta t}S_f} {}^{t+\Delta t}f_i^{S_f}\,\delta^{t+\Delta t}u_i^{S_f}\,d\,{}^{t+\Delta t}S.
\end{aligned} \tag{3.15}$$

This result is used for the development of the two general continuum mechanics incremental formulations of nonlinear problems: Total Lagrangian (TL) and Updated Lagrangian (UL). In the TL formulation all static and kinematic variables are referred to the initial configuration at time 0. Whereas in the UL formulation all the static and kinematic variables are referred to the last calculated configuration at time t (Bat96).

The result found in 3.15 is referred to configuration at time t, but instead, configuration at time 0 could be chosen. This means that any possible configuration between time 0 and t can be used to refer all the variables in 3.15. Therefore, it is also feasible to state that

$$\int_{t+\Delta t V} {}^{t+\Delta t}\tau_{ij}\, \delta_{t+\Delta t} e_{ij}\, d\, {}^{t+\Delta t}V = \int_{{}_0V} {}_0^{t+\Delta t}S_{pq}\, \delta_0^{t+\Delta t}\epsilon_{pq}\, d\, {}^0V, \tag{3.16}$$

and

$$\begin{aligned}\int_{{}_0V} {}_0^{t+\Delta t}S_{pq}\, \delta_0^{t+\Delta t}\epsilon_{pq}\, d\, {}^0V = &\int_{t+\Delta t V} {}^{t+\Delta t} f_i^B\, \delta^{t+\Delta t} u_i\, d\, {}^{t+\Delta t}V \\ &+ \int_{t+\Delta t S_f} {}^{t+\Delta t} f_i^{S_f}\, \delta^{t+\Delta t} u_i^{S_f}\, d\, {}^{t+\Delta t}S,\end{aligned} \tag{3.17}$$

which represents the general expression used for the TL formulation.

The right hand side of equations 3.15 and 3.17 is still written in terms of configuration at time $t + \Delta t$. To overcome this problem and for simplicity it will be assumed that the loading is deformation-independent. This implies that the load does not change its direction and magnitude as a function of the displacement. This specific type of loading is typically used to model concentrated loads which in reality are forces acting over a small surface area. The deformation-independent assumption allows to state that the load will be the same during the whole incremental process and the integration will be carried out over ${}^0V$. Hence

$$\begin{aligned}{}^{t+\Delta t}R &= \int_{t+\Delta t V} {}^{t+\Delta t} f_i^B\, \delta^{t+\Delta t} u_i\, d\, {}^{t+\Delta t}V + \int_{t+\Delta t S_f} {}^{t+\Delta t} f_i^{S_f}\, \delta^{t+\Delta t} u_i^{S_f}\, d\, {}^{t+\Delta t}S \\ &= \int_{{}_0V} {}^0 f_i^B\, \delta^0 u_i\, d\, {}^0V + \int_{{}_0S_f} {}^0 f_i^{S_f}\, \delta^0 u_i^{S_f}\, d\, {}^0S.\end{aligned} \tag{3.18}$$

Expressions 3.15 and 3.17 are simply the principle of virtual displacements written in terms of the Green-Lagrange strain tensor and the second Piola-Kirchhoff stresses. This expression represents a nonlinear system of equations

which in general cannot be solve directly. Therefore, *"an approximate solution can be obtained by referring all variables to a previously calculated known equilibrium configuration and linearising the resulting equation. This solution can be improved by an iteration process"*(Bat96). Hereafter, the solution at time t will be considered as the last calculated equilibrium configuration. Between time 0 and time t there is the whole path of time steps previously calculated by the iteration procedure. However, for the TL and UL formulations, only configurations at time 0 and t (not the whole path of time steps between them) are important. This fact occurs because all the static and kinematic variables are referred to times 0 and t.

3.3 Linearisation of the principle of virtual displacements. Total Lagrangian Formulation

In this report, the TL formulation has been chosen instead of the UL formulation. There is no apparent reason to take this decision; indeed, it does not matter what formulation is chosen *"if in the numerical solution the appropriate constitutive tensors are employed, identical results are obtained"*(Bat96).

First, it is appropriate to get the incremental decomposition for the second Piola-Kirchhoff stresses and the Green-Lagrange strain: According to Figure

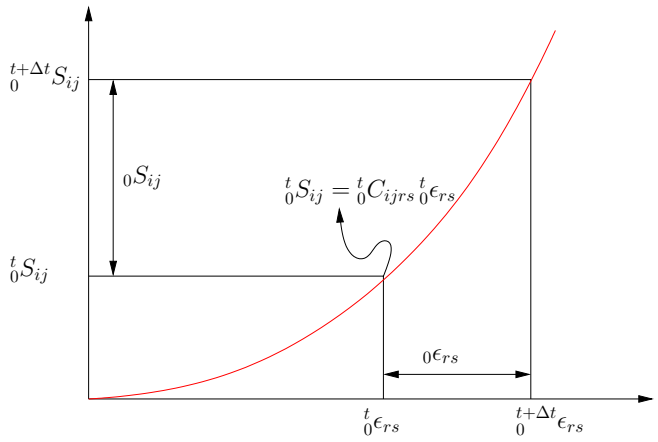

Figure 3.6: Incremetal decomposition of the stress and the strain tensors.

3.6, it can be appreciated that

$$\begin{aligned} {}^{t+\Delta t}_{0}S_{ij} &= {}^{t}_{0}S_{ij} + {}_{0}S_{ij} \\ {}^{t+\Delta t}_{0}\epsilon_{rs} &= {}^{t}_{0}\epsilon_{rs} + {}_{0}\epsilon_{rs}, \end{aligned} \tag{3.19}$$

${}^{t}_{0}C_{ijrs}$ represents a four order tensor which relates the second Piola-Kirchhoff stresses with the Green-Lagrange strains. In this particular case the ${}^{t}_{0}C_{ijrs}$ tensor takes place at time t but is measured in configuration at time 0. It is important to remember that ${}^{t}_{0}C_{ijrs}$ can be linear or non-linear. Indeed, the effectiveness of the iterative procedure and, whether a large or a small strain formulation is considered, depends on the use of appropriate stress-strain relationships. Note that the four order tensor ${}^{t}_{0}C_{ijrs}$ is different to the right Cauchy-Green deformation tensor ${}^{t}_{0}C_{ij}$, which is a second order tensor.

Equation 3.5 can be written as

$${}^{t+\Delta t}_{0}\epsilon_{ij} = \frac{1}{2}\left[\frac{\partial^{t+\Delta t}u_i}{\partial^0 x_j} + \frac{\partial^{t+\Delta t}u_j}{\partial^0 x_i} + \frac{\partial^{t+\Delta t}u_k}{\partial^0 x_i}\frac{\partial^{t+\Delta t}u_k}{\partial^0 x_j}\right],$$

where ${}^{t+\Delta t}u_i = {}^{t}u_i + u_i$, then

$$\begin{aligned} {}^{t+\Delta t}_{0}\epsilon_{ij} &= \frac{1}{2}\left[\frac{\partial^t u_i}{\partial^0 x_j} + \frac{\partial u_i}{\partial^0 x_j} + \frac{\partial^t u_j}{\partial^0 x_i} + \frac{\partial u_j}{\partial^0 x_i} + \left(\frac{\partial^t u_k}{\partial^0 x_i} + \frac{\partial u_k}{\partial^0 x_i}\right)\left(\frac{\partial^t u_k}{\partial^0 x_j} + \frac{\partial u_k}{\partial^0 x_j}\right)\right] \\ &= \frac{1}{2}\Big[\frac{\partial^t u_i}{\partial^0 x_j} + \frac{\partial u_i}{\partial^0 x_j} + \frac{\partial^t u_j}{\partial^0 x_i} + \frac{\partial u_j}{\partial^0 x_i} + \frac{\partial^t u_k}{\partial^0 x_i}\frac{\partial^t u_k}{\partial^0 x_j} + \\ &\qquad \frac{\partial^t u_k}{\partial^0 x_i}\frac{\partial u_k}{\partial^0 x_j} + \frac{\partial u_k}{\partial^0 x_i}\frac{\partial^t u_k}{\partial^0 x_j} + \frac{\partial u_k}{\partial^0 x_i}\frac{\partial u_k}{\partial^0 x_j}\Big] \\ &= \underbrace{\frac{1}{2}\left[\frac{\partial^t u_i}{\partial^0 x_j} + \frac{\partial^t u_j}{\partial^0 x_i} + \frac{\partial^t u_k}{\partial^0 x_i}\frac{\partial^t u_k}{\partial^0 x_j}\right]}_{{}^{t}_{0}\epsilon_{ij}} + \\ &\qquad \underbrace{\frac{1}{2}\left[\frac{\partial u_i}{\partial^0 x_j}\frac{\partial u_j}{\partial^0 x_i} + \frac{\partial^t u_k}{\partial^0 x_i}\frac{\partial u_k}{\partial^0 x_j} + \frac{\partial u_k}{\partial^0 x_i}\frac{\partial^t u_k}{\partial^0 x_j}\right]}_{{}_{0}e_{ij}} + \underbrace{\frac{1}{2}\frac{\partial u_k}{\partial^0 x_i}\frac{\partial u_k}{\partial^0 x_j}}_{{}_{0}\eta_{ij}}. \end{aligned}$$

Thus

$${}^{t+\Delta t}_{0}\epsilon_{ij} = {}^{t}_{0}\epsilon_{ij} + \underbrace{{}_{0}e_{ij} + {}_{0}\eta_{ij}}_{{}_{0}\epsilon_{ij}};$$

therefore, it can be said that

$$\delta^{t+\Delta t}_{0}\epsilon_{ij} = \delta({}^{t}_{0}\epsilon_{ij} + {}_{0}\epsilon_{ij}) = \delta^{t}_{0}\epsilon_{ij} + \delta_{0}\epsilon_{ij}, \tag{3.20}$$

but $\delta^t_0\epsilon_{ij} = 0$ because the variation is taken about the configuration at time $t + \Delta t$.

Replacing equations 3.19 and 3.20 into the principle of virtual displacements (Equation 3.17), the following expression is obtained

$$\int_{{}_0V} {}^{t+\Delta t}_{0}S_{ij}\, \delta^{t+\Delta t}_{0}\epsilon_{ij}\, d\,{}^0V = {}^{t+\Delta t}R$$

$$\int_{{}_0V} \left({}^{t}_{0}S_{ij} + {}_0S_{ij}\right) \underbrace{\left(\delta_0 e_{ij} + \delta_0\eta_{ij}\right)}_{\delta_0\epsilon_{ij}}\, d\,{}^0V = {}^{t+\Delta t}R$$

$$\int_{{}_0V} \left({}^{t}_{0}S_{ij}\, \delta_0 e_{ij} + {}^{t}_{0}S_{ij}\, \delta_0\eta_{ij} + {}_0S_{ij}\, \delta_0\epsilon_{ij}\right) d\,{}^0V = {}^{t+\Delta t}R$$

$$\underbrace{\int_{{}_0V} {}_0S_{ij}\, \delta_0\epsilon_{ij}\, d\,{}^0V}_{\text{term 1}} + \underbrace{\int_{{}_0V} {}^{t}_{0}S_{ij}\, \delta_0\eta_{ij}\, d\,{}^0V}_{\text{term 2}} = \underbrace{{}^{t+\Delta t}R}_{\text{term 3}} - \underbrace{\int_{{}_0V} {}^{t}_{0}S_{ij}\, \delta_0 e_{ij}}_{\text{term 4}}\,.$$

Terms 2, 3, and 4 are linear in the incremental displacements u_i, but term 1 is highly nonlinear. The linearity of terms 2, 3, and 4, with respect to u_i will be evident once the discrete finite element equations are assembled. Instead, term 1 has to be linearised, for that porpuse a Taylor series of expansion up to a first order of approximation is used. That is,

$${}^{t+\Delta t}_{0}S_{ij} = {}^{t}_{0}S_{ij} + \frac{\partial^t_0 S_{ij}}{\partial^t_0 \epsilon_{rs}}\, {}_0\epsilon_{rs}$$

$${}^{t+\Delta t}_{0}S_{ij} - {}^{t}_{0}S_{ij} = {}_0S_{ij} = {}^{t}_{0}C_{ijrs}\, {}_0\epsilon_{rs},$$

using this approximation, term 1 is transformed into

$$\begin{aligned}
\int_{{}_0V} {}_0S_{ij}\, \delta_0\epsilon_{ij}\, d\,{}^0V &= \int_{{}_0V} \left({}^{t}_{0}C_{ijrs}\, {}_0\epsilon_{rs}\right)\delta_0\epsilon_{ij}\, d\,{}^0V \\
&= \int_{{}_0V} {}^{t}_{0}C_{ijrs}\Big({}_0e_{rs} + {}_0\underbrace{\eta_{rs}}_{\text{neglect}}\Big)\delta\Big({}_0e_{ij} + {}_0\underbrace{\eta_{ij}}_{\text{neglect}}\Big)\, d\,{}^0V \\
&= \int_{{}_0V} {}^{t}_{0}C_{ijrs}\, {}_0e_{rs}\, \delta_0 e_{ij}\, d\,{}^0V.
\end{aligned}$$

The linearisation procedure explained here constitutes an enhanced deduction of the one published by reference (Bat96, pag. 525).

Finally, the linearised principle of virtual displacements in a TL formulation can be written as

$$\int_{{}_0V} {}^{t}_{0}C_{ijrs}\, {}_0e_{rs}\, \delta_0 e_{ij}\, d\,{}^0V + \int_{{}_0V} {}^{t}_{0}S_{ij}\, \delta_0\eta_{ij}\, d\,{}^0V = {}^{t+\Delta t}R - \int_{{}_0V} {}^{t}_{0}S_{ij}\, \delta_0 e_{ij}, \quad (3.21)$$

this expression is used directly in the Finite Element formulation for large displacements. The above equation can be written in matrix notation as

$$\delta\hat{\mathbf{u}}^T\Big(\int_{{}_0V} {}^t_0B_L^T\,{}^t_0C\,{}^t_0B_L\,d\,{}^0V + \int_{{}_0V} {}^t_0B_{NL}^T\,{}^t_0S\,{}^t_0B_{NL}\,d\,{}^0V\Big)\hat{\mathbf{u}} = \delta\hat{\mathbf{u}}^T\Big({}^{t+\Delta t}\mathbf{R} - \int_{{}_0V} {}^t_0B_L^T\,{}^t_0\mathbf{S}\,d\,{}^0V\Big),$$

and following the same procedure explained in section 2.1 yields to,

$$\Big({}^t_0K_L + {}^t_0K_{NL}\Big)\hat{\mathbf{u}} = {}^{t+\Delta t}\mathbf{R} - {}^t_0\mathbf{F}. \tag{3.22}$$

In the next chapters, matrices ${}^t_0K_L$, ${}^t_0K_{NL}$, and vectors ${}^{t+\Delta t}\mathbf{R}$, and ${}^t_0\mathbf{F}$ will be deduced for several types of elements.

Once the linear system of equations 3.22 is solved, it is precise to find how much difference there exists between the internal virtual work and the external virtual work, and continue with an iterative procedure until this difference tends to zero. The internal virtual work can be calculated with the state variables calculated by the system of finite equations, and the external virtual work is given by ${}^{t+\Delta t}R$.[7]

[7]this procedure is explained in more detail in (Bat96, pag. 526)

Chapter 4

Bar or Truss Elements

When begining with the study of the underlying theory used by the Finite Element Method, usually bars or truss elements are chosen as the first type of elements to be analysed. These elements are chosen because they are easy to define from the structural point of view; furthermore, the Finite Element equations can be mathematically deduced in a simple and understandable way. A truss element is defined as a structural part, which is capable of supporting loads only in the direction normal to its cross-sectional area. Therefore, the strains and the stresses can only be transmitted in that direction. It is also important to remark that the strains and the stresses are considered to be constant over the cross-sectional area of the element.

4.1 Bars under the small displacements hypothesis

Considering only small displacements and small deformations for a two-node bar element with only one degree of freedom per node, and with constant cross-sectional area, it can be easily deduced that its stiffness matrix is given by

$$^{(m)}K = \frac{E\,A}{L}\begin{bmatrix} 1 & -1 \\ -1 & 1 \end{bmatrix}, \tag{4.1}$$

where E is the linear-elastic modulus of the material, A is the value of the cross-sectional area, and L is the length of the bar. Hereafter this point, the superscript (m), which denotes the m-th element of the assemblage, will be ommited; this is done because henceforward only the FEM equations for single non-assembled elements will be stated.

To be able to arrive to the stiffness matrix 4.1, the Finite Element equations can be proposed in any convenient reference system. It is clear that if an inconvenient reference system is chosen, some mathematical problems in the deduction process might be obtained, but eventually, because of the Frame Indifference Principle[1] the same results must be achieved. The Frame Indifference Principle states that the frame of reference is only a mathematical artifice and it does not have any physical meaning. Therefore, it does not matter which frame of reference is chosen, the physical response of the structure analysed cannot be affected.

To aim towards the understanding of this principle, the FEM equations for a truss element will be stated in two different systems of reference; of course, the final results found must be similar. The problem to be solved can be defined as: A unidimensional truss element is located in the $x - y$ Cartesian plane, and it has been rotated a θ angle with respect to the x axis. The element has constant cross-sectional area A, a total length L, and its modulus of elasticity is E; see Figure 4.1a. Find the stiffness matrix of the element, stating the strain and the stress tensors both in a $x - y$ global Cartesian system, and in a $\widetilde{x} - \widetilde{y}$ local system.

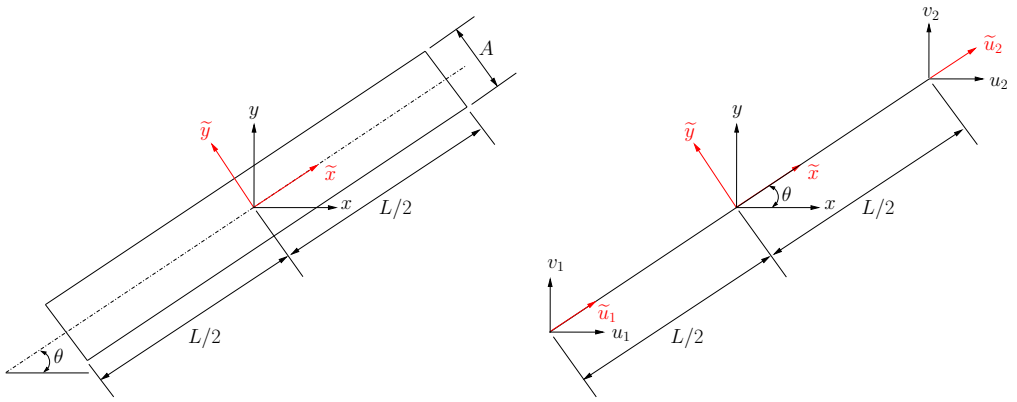

(a) Original 2–D geometry of the bar. (b) Truss element + degrees of freedom

Figure 4.1: Bar or truss element

First, a convenient local reference system $\widetilde{x} - \widetilde{y}$ which coincides with the principal axes of the element is chosen, see Figure 4.1. It is also important to remember that a truss element can only support tension or compression loads. For that reason, in the local system of reference, only degrees of freedom $\widetilde{u}_1$

[1]For an enhancement of this principle consult reference (Mal69)

and $\widetilde{u}_2$ along the longitudinal axis of the bar are considered, see Figure 4.1b. In this way, the strain and the stress tensors, $\widetilde{e_{ij}}$ and $\widetilde{\tau_{ij}}$ respectively, have values only for the direction normal to the cross-sectional area. This means that only the components $\widetilde{e_{11}}$ and $\widetilde{\tau_{11}}$ have values other than zero. The strain tensor $\widetilde{e_{ij}}$ can be written in matrix form as

$$\widetilde{e_{ij}} = \begin{bmatrix} \widetilde{e_{11}} & 0 \\ 0 & 0 \end{bmatrix} = \begin{bmatrix} \widetilde{e_{xx}} & 0 \\ 0 & 0 \end{bmatrix},$$

where $\widetilde{e_{xx}}$ is given by

$$\widetilde{e_{xx}} = \frac{\partial \widetilde{u}}{\partial \widetilde{x}}.$$

The global $x-y$ Cartesian system can be related to the local $\widetilde{x}-\widetilde{y}$ system via equations

$$\begin{aligned} x_{(\widetilde{x},\widetilde{y})} &= \widetilde{x}\cos\theta \; - \widetilde{y}\sin\theta \qquad & \widetilde{x}_{(x,y)} &= x\cos\theta \; + y\sin\theta \\ y_{(\widetilde{x},\widetilde{y})} &= \widetilde{x}\sin\theta \; + \widetilde{y}\cos\theta \qquad & \widetilde{y}_{(x,y)} &= -x\sin\theta \; + y\cos\theta\,. \end{aligned} \tag{4.2}$$

Even though the bar is a one dimensional element, in this particular case it is placed on a two dimensional space, and the z axis coincides with the $\widetilde{z}$ axis; therefore, this axis is not taken into account into the above equations. If the bar element would be located in the 3–D space with no coincidence between the z and $\widetilde{z}$ axes, then it would be necessary to modify the equations in 4.2.

Considering the complete bar as an assemblage of two nodes, one can assume a variational linear displacement between the two nodes of the element. Consequently, functions for the displacements can be constructed as

$$\begin{aligned} u_{(\widetilde{x})} &= h_{1(\widetilde{x})}u_1 + h_{2(\widetilde{x})}u_2 \\ v_{(\widetilde{x})} &= h_{1(\widetilde{x})}v_1 + h_{2(\widetilde{x})}v_2 \end{aligned} \qquad \widetilde{u}_{(\widetilde{x})} = h_{1(\widetilde{x})}\widetilde{u}_1 + h_{2(\widetilde{x})}\widetilde{u}_2 \tag{4.3}$$

where $h_{1(\widetilde{x})}$ and $h_{2(\widetilde{x})}$ are the unidimensional linear base functions for the truss element shown in Figure 4.1b, and they are given by

$$h_{1(\widetilde{x})} = \frac{1}{L}\left(\frac{L}{2} - \widetilde{x}\right) \qquad h_{2(\widetilde{x})} = \frac{1}{L}\left(\frac{L}{2} + \widetilde{x}\right).$$

In the global $x-y$ Cartesian system, the strain tensor e_{ij} has components $e_{11} = e_{xx}$, $e_{22} = e_{yy}$, and $e_{12} = e_{21} = e_{xy}$, which can be written in matrix form as

$$e_{ij} = \begin{bmatrix} e_{xx} & e_{xy} \\ e_{xy} & e_{yy} \end{bmatrix}.$$

This values are given by

$$e_{xx} = \frac{\partial u}{\partial x}, \qquad e_{yy} = \frac{\partial v}{\partial y}, \qquad \text{and} \qquad e_{xy} = \frac{1}{2}\left(\frac{\partial u}{\partial y} + \frac{\partial v}{\partial x}\right) = \frac{\gamma_{xy}}{2};$$

When computing the partial derivatives of $u_{(\widetilde{x})}$ and $v_{(\widetilde{x})}$ with respect to x and y, the chain rule should be used:

$$\begin{aligned} \frac{\partial}{\partial x} &= \frac{\partial}{\partial \widetilde{x}}\frac{\partial \widetilde{x}}{\partial x} + \frac{\partial}{\partial \widetilde{y}}\frac{\partial \widetilde{y}}{\partial x} \\ \frac{\partial}{\partial y} &= \frac{\partial}{\partial \widetilde{x}}\frac{\partial \widetilde{x}}{\partial y} + \frac{\partial}{\partial \widetilde{y}}\frac{\partial \widetilde{y}}{\partial y} \end{aligned} \longrightarrow \qquad \begin{bmatrix} \frac{\partial}{\partial x} \\ \\ \frac{\partial}{\partial y} \end{bmatrix} = \begin{bmatrix} \frac{\partial \widetilde{x}}{\partial x} & \frac{\partial \widetilde{y}}{\partial x} \\ \\ \frac{\partial \widetilde{x}}{\partial y} & \frac{\partial \widetilde{y}}{\partial y} \end{bmatrix} \begin{bmatrix} \frac{\partial}{\partial \widetilde{x}} \\ \\ \frac{\partial}{\partial \widetilde{y}} \end{bmatrix},$$

and in the same way

$$\begin{aligned} \frac{\partial}{\partial \widetilde{x}} &= \frac{\partial}{\partial x}\frac{\partial x}{\partial \widetilde{x}} + \frac{\partial}{\partial y}\frac{\partial y}{\partial \widetilde{x}} \\ \frac{\partial}{\partial \widetilde{y}} &= \frac{\partial}{\partial x}\frac{\partial x}{\partial \widetilde{y}} + \frac{\partial}{\partial y}\frac{\partial y}{\partial \widetilde{y}} \end{aligned} \longrightarrow \qquad \begin{bmatrix} \frac{\partial}{\partial \widetilde{x}} \\ \\ \frac{\partial}{\partial \widetilde{y}} \end{bmatrix} = \begin{bmatrix} \frac{\partial x}{\partial \widetilde{x}} & \frac{\partial y}{\partial \widetilde{x}} \\ \\ \frac{\partial x}{\partial \widetilde{y}} & \frac{\partial y}{\partial \widetilde{y}} \end{bmatrix} \begin{bmatrix} \frac{\partial}{\partial x} \\ \\ \frac{\partial}{\partial y} \end{bmatrix}.$$

Hence, using the equations in 4.2

$$\begin{bmatrix} \frac{\partial}{\partial x} \\ \\ \frac{\partial}{\partial y} \end{bmatrix} = \begin{bmatrix} \cos\theta & -\sin\theta \\ \\ \sin\theta & \cos\theta \end{bmatrix} \begin{bmatrix} \frac{\partial}{\partial \widetilde{x}} \\ \\ \frac{\partial}{\partial \widetilde{y}} \end{bmatrix},$$

and

$$\begin{bmatrix} \frac{\partial}{\partial \widetilde{x}} \\ \\ \frac{\partial}{\partial \widetilde{y}} \end{bmatrix} = \begin{bmatrix} \cos\theta & \sin\theta \\ \\ -\sin\theta & \cos\theta \end{bmatrix} \begin{bmatrix} \frac{\partial}{\partial x} \\ \\ \frac{\partial}{\partial y} \end{bmatrix}.$$

In this way, according to the relations in 4.3, it is possible to state that

$$\begin{aligned} \frac{\partial u}{\partial x} &= \frac{\partial h_{1(\widetilde{x})}}{\partial \widetilde{x}}\frac{\partial \widetilde{x}}{\partial x}u_1 + \frac{\partial h_{2(\widetilde{x})}}{\partial \widetilde{x}}\frac{\partial \widetilde{x}}{\partial x}u_2 \\ \frac{\partial u}{\partial y} &= \frac{\partial h_{1(\widetilde{x})}}{\partial \widetilde{x}}\frac{\partial \widetilde{x}}{\partial y}u_1 + \frac{\partial h_{2(\widetilde{x})}}{\partial \widetilde{x}}\frac{\partial \widetilde{x}}{\partial y}u_2 \\ \frac{\partial v}{\partial x} &= \frac{\partial h_{1(\widetilde{x})}}{\partial \widetilde{x}}\frac{\partial \widetilde{x}}{\partial x}v_1 + \frac{\partial h_{2(\widetilde{x})}}{\partial \widetilde{x}}\frac{\partial \widetilde{x}}{\partial x}v_2 \\ \frac{\partial v}{\partial y} &= \frac{\partial h_{1(\widetilde{x})}}{\partial \widetilde{x}}\frac{\partial \widetilde{x}}{\partial y}v_1 + \frac{\partial h_{2(\widetilde{x})}}{\partial \widetilde{x}}\frac{\partial \widetilde{x}}{\partial y}v_2. \end{aligned}$$

Now it is possible to compute the values of the strain tensors e_{ij} and $\widetilde{e_{ij}}$. That is,

$$
\begin{aligned}
e_{xx} &= \frac{\partial u}{\partial x} = -\frac{1}{L}\cos\theta\, u_1 + \frac{1}{L}\cos\theta\, u_2 \\
e_{xx} &= \frac{u_2 - u_1}{L}\cos\theta \\
\gamma_{xy} &= \frac{\partial u}{\partial y} + \frac{\partial v}{\partial x} = -\frac{1}{L}\sin\theta\, u_1 + \frac{1}{L}\sin\theta\, u_2 - \frac{1}{L}\cos\theta\, v_1 + \frac{1}{L}\cos\theta\, v_2 \\
\gamma_{xy} &= \frac{u_2 - u_1}{L}\sin\theta\, + \frac{v_2 - v_1}{L}\cos\theta \\
e_{yy} &= \frac{\partial v}{\partial y} = -\frac{1}{L}\sin\theta\, v_1 + \frac{1}{L}\sin\theta\, v_2 \\
e_{yy} &= \frac{v_2 - v_1}{L}\sin\theta \\
\widetilde{e_{xx}} &= \frac{\partial \widetilde{u}}{\partial \widetilde{x}} = -\frac{1}{L}\widetilde{u}_1 + \frac{1}{L}\widetilde{u}_2 = \frac{\widetilde{u}_2 - \widetilde{u}_1}{L},
\end{aligned}
$$

where e_{ij} written in matrix form is given by

$$
e_{ij} = \begin{bmatrix} e_{xx} & \frac{1}{2}\gamma_{xy} \\ \\ \frac{1}{2}\gamma_{xy} & e_{yy} \end{bmatrix}.
$$

In order to show that the state of strains at any point of bar is the same, no matter which system of reference has been chosen, it is necessary to transform e_{ij} into $\widetilde{e_{ij}}$. This transformation is carried out by the characteristic law for tensors

$$
\widetilde{e_{ij}} = P_{ik}\, P_{jl}\, e_{kl},
$$

where $P_{ik} = \cos(\widetilde{\phi}_i, \phi_k)$, and $\widetilde{\phi}_i$, ϕ_k are the director vectors of each frame of reference. For the particular case being analysed P_{ik} written in matrix form is given by

$$
P_{ik} = \begin{bmatrix} \cos\theta & \sin\theta \\ \\ -\sin\theta & \cos\theta \end{bmatrix}.
$$

In consequence,

$$\begin{aligned}
\widetilde{e_{11}} = \widetilde{e_{xx}} &= P_{1k}\, P_{1l}\, e_{kl} = P_{11} P_{1l}\, e_{1l} + P_{12}\, P_{1l}\, e_{2l} \\
&= P_{11} P_{11}\, e_{11} + P_{11} P_{12}\, e_{12} + P_{12} P_{11}\, e_{21} + P_{12} P_{12}\, e_{22} \\
&= \cos^2\theta\, e_{11} + 2\cos\theta\ \sin\theta\ e_{12} + \sin^2\theta\, e_{22} \\
&= \cos^2\theta\, e_{11} + \cos\theta\ \sin\theta\ \gamma_{12} + \sin^2\theta\, e_{22} \\
&= \frac{u_2 - u_1}{L}\cos^3\theta + \left[\frac{u_2 - u_1}{L}\sin\theta\ + \frac{v_2 - v_1}{L}\cos\theta\right]\cos\theta\ \sin\theta \\
&\quad + \frac{v_2 - v_1}{L}\sin^3\theta,
\end{aligned}$$

$$\begin{aligned}
\widetilde{e_{12}} = \frac{1}{2}\widetilde{\gamma_{xy}} &= P_{1k}\, P_{2l}\, e_{kl} = P_{11} P_{2l}\, e_{1l} + P_{12}\, P_{2l}\, e_{2l} \\
&= P_{11} P_{21}\, e_{11} + P_{11} P_{22}\, e_{12} + P_{12} P_{21}\, e_{21} + P_{12} P_{22}\, e_{22} \\
&= -\cos\theta\ \sin\theta\, e_{11} + \cos^2\theta\, e_{12} - \sin^2\theta\, e_{21} + \cos\theta\ \sin\theta\ e_{22} \\
&= -\cos\theta\ \sin\theta\, e_{11} + \cos^2\theta\, \frac{\gamma_{12}}{2} - \sin^2\theta\, \frac{\gamma_{12}}{2} + \cos\theta\ \sin\theta\ e_{22} \\
&= -\frac{u_2 - u_1}{L}\cos^2\theta\sin\theta\ - \left[\frac{u_2 - u_1}{L}\sin\theta\ + \frac{v_2 - v_1}{L}\cos\theta\right]\sin\theta\ \cos\theta \\
&\quad + \frac{v_2 - v_1}{L}\sin^2\theta\cos\theta\,,
\end{aligned}$$

$$\begin{aligned}
\widetilde{e_{22}} = \widetilde{e_{yy}} &= P_{2k}\, P_{2l}\, e_{kl} = P_{21} P_{2l}\, e_{1l} + P_{22}\, P_{2l}\, e_{2l} \\
&= P_{21} P_{21}\, e_{11} + P_{21} P_{22}\, e_{12} + P_{22} P_{21}\, e_{21} + P_{22} P_{22}\, e_{22} \\
&= \sin^2\theta\, e_{11} - 2\cos\theta\ \sin\theta\ e_{12} + \cos^2\ e_{22} \\
&= \sin^2\theta\, e_{11} - \cos\theta\ \sin\theta\ \gamma_{12} + \cos^2\ e_{22} \\
&= \frac{u_2 - u_1}{L}\cos\theta\ \sin^2\theta - \left[\frac{u_2 - u_1}{L}\sin\theta\ + \frac{v_2 - v_1}{L}\cos\theta\right]\cos\theta\ \sin\theta \\
&\quad + \frac{v_2 - v_1}{L}\cos^2\theta\sin\theta\,.
\end{aligned}$$

Subsequently, expressing u_1, u_2, v_1, and v_2 in terms of $\widetilde{u}_1$ and $\widetilde{u}_2$, it can be easily seen that

$$\begin{aligned}
u_1 &= \widetilde{u}_1 \cos\theta \qquad & u_2 &= \widetilde{u}_2 \cos\theta \\
v_1 &= \widetilde{u}_1 \sin\theta \qquad & v_2 &= \widetilde{u}_2 \sin\theta\,.
\end{aligned}$$

Hence,

$$\begin{aligned}
\widetilde{e_{xx}} =& \frac{\widetilde{u}_2 - \widetilde{u}_1}{L}\cos^4\theta + \left[\frac{\widetilde{u}_2 - \widetilde{u}_1}{L} + \frac{\widetilde{u}_2 - \widetilde{u}_1}{L}\right]\cos^2\theta\sin^2\theta + \frac{\widetilde{u}_2 - \widetilde{u}_1}{L}\sin^4\theta \\
\widetilde{e_{xx}} =& \frac{1}{L}\left[(\widetilde{u}_2 - \widetilde{u}_1)\cos^4\theta + 2(\widetilde{u}_2 - \widetilde{u}_1)\cos^2\theta\sin^2\theta + (\widetilde{u}_2 - \widetilde{u}_1)\sin^4\theta\right] \\
\widetilde{e_{xx}} =& \frac{(\widetilde{u}_2 - \widetilde{u}_1)}{L}\left[\cos^4\theta + \cos^2\theta\sin^2\theta + \sin^4\theta\right] = \frac{(\widetilde{u}_2 - \widetilde{u}_1)}{L}\left[\cos^2\theta + \sin^2\theta\right]^2 \\
\widetilde{e_{xx}} =& \frac{(\widetilde{u}_2 - \widetilde{u}_1)}{L},
\end{aligned}$$

$$\begin{aligned}
\widetilde{e_{yy}} =& \frac{\widetilde{u}_2 - \widetilde{u}_1}{L}\cos^2\theta\sin^2\theta - \left[2\frac{\widetilde{u}_2 - \widetilde{u}_1}{L}\right]\cos^2\theta\sin^2\theta + \frac{\widetilde{u}_2 - \widetilde{u}_1}{L}\cos^2\theta\sin^2\theta \\
\widetilde{e_{yy}} =& \frac{(\widetilde{u}_2 - \widetilde{u}_1)}{L}\left[\cos^2\theta\sin^2\theta - \cos^2\theta\sin^2\theta - \cos^2\theta\sin^2\theta + \cos^2\theta\sin^2\theta\right] \\
\widetilde{e_{yy}} =& 0,
\end{aligned}$$

$$\begin{aligned}
\frac{\widetilde{\gamma_{xy}}}{2} =& -\frac{\widetilde{u}_2 - \widetilde{u}_1}{L}\cos^3\theta\sin\theta + \frac{1}{2}\left[\frac{(\widetilde{u}_2 - \widetilde{u}_1)}{L}\cos\theta\,\sin\theta + \frac{(\widetilde{u}_2 - \widetilde{u}_1)}{L}\cos\theta\,\sin\theta\right] \\
& (\cos^2\theta - \sin^2\theta) + \frac{(\widetilde{u}_2 - \widetilde{u}_1)}{L} \\
\frac{\widetilde{\gamma_{xy}}}{2} =& \frac{\widetilde{u}_2 - \widetilde{u}_1}{L}\left[-\cos^3\theta\sin\theta + \cos^3\theta\sin\theta - \cos\theta\,\sin^3\theta + \cos\theta\,\sin^3\theta\right] \\
\frac{\widetilde{\gamma_{xy}}}{2} =& \widetilde{e_{xy}} = 0.
\end{aligned}$$

In this form, it was shown that tensor e_{ij} can be transformed into $\widetilde{e_{ij}}$, and the same results may be achieved employing any of the two particular systems of reference used so far.

To be able to calculate the stiffness matrix of the element via Equation 2.9, the finite element equations can be formulated either in the $x - y$ global Cartesian system or in the $\widetilde{x} - \widetilde{y}$ local system. In the local system of reference, the only component of the strain tensor $\widetilde{e_{ij}}$ different from zero is $\widetilde{e_{11}}$. This fact represents an advantage to compute the integral involved in Equation 2.9. Moreover, due to plane $\widetilde{y} - \widetilde{z}$ was chosen on purpose to be parallel to the cross-sectional area A of the bar, it can be considered as a constant or at least as a function of the $\widetilde{x}$ axis. Even more, in this local system the constitutive material properties described by tensor C_{ijmn}, can be fully described using only the Elastic Modulus E and this tensor does not have to be transformed into the global Cartesian system.

Stiffness matrix 4.1 was deduced for a two-node bar element with constant cross-sectional area A. Furthermore, a local reference system was used, and only one degree of freedom aligned with this local system was considered on each node. However, when several bar elements are connected and they are not aligned one another, it is necessary to rotate the local degrees of freedom into a global general system of reference. But even though the local degrees of freedom are rotated into a global system, it is still a good strategy to perform the integral for the stiffness matrix in the local coordinate system. To enhance this strategy, the finite element equations for the truss element shown in Figure 4.1 will be formulated in a Cartesian system $x-y$ with two degrees of freedom per node. This Cartesian system is going to be considered as the global system of reference. The degrees of freedom are going to be aligned with the x and y global Cartesian axes. Thereafter, the strain tensor e_{ij} is going to be rotated into the local reference system $\widetilde{x}-\widetilde{y}$ to obtain $\widetilde{e_{ij}}$, but the degrees of freedom will remain without rotation. In order to begin with this strategy, the equations for the strain tensor e_{ij} in the global Cartesian system are stated:

$$\begin{aligned} e_{xx} =& \frac{\partial h_1}{\partial \widetilde{x}}\frac{\partial \widetilde{x}}{\partial x}u_1 + \frac{\partial h_2}{\partial \widetilde{x}}\frac{\partial \widetilde{x}}{\partial x}u_2 \\ e_{xx} =& \left[\begin{array}{cccc} h_{1,\widetilde{x}}\cos\theta & 0 & h_{2,\widetilde{x}}\cos\theta & 0 \end{array}\right]\hat{\mathbf{u}}, \end{aligned}$$

where $h_{1,\widetilde{x}} = \frac{\partial h_1}{\partial \widetilde{x}}$, $h_{2,\widetilde{x}} = \frac{\partial h_2}{\partial \widetilde{x}}$, and $\hat{\mathbf{u}} = \left[\begin{array}{cccc} u_1 & v_1 & u_2 & v_2 \end{array}\right]^T$. Also

$$\begin{aligned} \frac{\gamma_{xy}}{2} =& \frac{1}{2}\left[\frac{\partial h_1}{\partial \widetilde{x}}\frac{\partial \widetilde{x}}{\partial y}u_1 + \frac{\partial h_2}{\partial \widetilde{x}}\frac{\partial \widetilde{x}}{\partial y}u_2 + \frac{\partial h_1}{\partial \widetilde{x}}\frac{\partial \widetilde{x}}{\partial x}v_1 + \frac{\partial h_2}{\partial \widetilde{x}}\frac{\partial \widetilde{x}}{\partial x}v_2\right] \\ \frac{\gamma_{xy}}{2} =& \left[\begin{array}{cccc} h_{1,\widetilde{x}}\sin\theta & h_{1,\widetilde{x}}\cos\theta & h_{2,\widetilde{x}}\sin\theta & h_{2,\widetilde{x}}\cos\theta \end{array}\right]\hat{\mathbf{u}}, \end{aligned}$$

and

$$\begin{aligned} e_{yy} =& \frac{\partial h_1}{\partial \widetilde{x}}\frac{\partial \widetilde{x}}{\partial y}v_1 + \frac{\partial h_2}{\partial \widetilde{x}}\frac{\partial \widetilde{x}}{\partial y}v_2 \\ e_{yy} =& \left[\begin{array}{cccc} 0 & h_{1,\widetilde{x}}\sin\theta & 0 & h_{2,\widetilde{x}}\sin\theta \end{array}\right]\hat{\mathbf{u}}. \end{aligned}$$

As it was stated before

$$\begin{aligned} \widetilde{e_{xx}} &= e_{xx}\cos^2\theta + 2\frac{\gamma_{xy}}{2}\cos\theta\sin\theta + e_{yy}\sin^2\theta \\ \widetilde{\gamma_{xy}} &= 0 \\ \widetilde{e_{yy}} &= 0; \end{aligned}$$

hence,

$$
\begin{aligned}
\widetilde{e_{xx}} =& \Big\{ \cos\theta \begin{bmatrix} h_{1,\tilde{x}} & 0 & h_{2,\tilde{x}} & 0 \end{bmatrix} \cos^2\theta \\
&+ 2\frac{1}{2} \begin{bmatrix} h_{1,\tilde{x}} \sin\theta & h_{1,\tilde{x}} \cos\theta & h_{2,\tilde{x}} \sin\theta & h_{2,\tilde{x}} \cos\theta \end{bmatrix} \cos\theta \sin\theta + \\
&+ \sin\theta \begin{bmatrix} 0 & h_{1,\tilde{x}} & 0 & h_{2,\tilde{x}} \end{bmatrix} \sin^2\theta \Big\} \hat{\mathbf{u}} \\
=& \Big\{ \begin{bmatrix} h_{1,\tilde{x}} \cos^3\theta & 0 & h_{2,\tilde{x}} \cos^3\theta & 0 \end{bmatrix} \\
&+ \begin{bmatrix} h_{1,\tilde{x}} \cos\theta \sin^2\theta & h_{1,\tilde{x}} \cos^2\theta \sin\theta & h_{2,\tilde{x}} \cos\theta \sin^2\theta & h_{2,\tilde{x}} \cos^2\theta \sin\theta \end{bmatrix} \\
&+ \begin{bmatrix} 0 & h_{1,\tilde{x}} \sin^3\theta & 0 & h_{2,\tilde{x}} \sin^3\theta \end{bmatrix} \Big\} \hat{\mathbf{u}} \\
\widetilde{e_{xx}} =& \begin{bmatrix} h_{1,\tilde{x}} \cos\theta & h_{1,\tilde{x}} \sin\theta & h_{2,\tilde{x}} \cos\theta & h_{2,\tilde{x}} \sin\theta \end{bmatrix} \hat{\mathbf{u}},
\end{aligned}
$$

and according to Equation 2.2, $\mathbf{e} = B\,\hat{\mathbf{u}}$, thus

$$
\begin{aligned}
\widetilde{e_{xx}} =& B\,\hat{\mathbf{u}} \\
\widetilde{e_{xx}} =& \begin{bmatrix} h_{1,\tilde{x}} \cos\theta & h_{1,\tilde{x}} \sin\theta & h_{2,\tilde{x}} \cos\theta & h_{2,\tilde{x}} \sin\theta \end{bmatrix} \hat{\mathbf{u}}.
\end{aligned}
$$

In this way, the strain tensor e_{ij} has been rotated into the local reference system to obtain $\widetilde{e_{ij}}$, but the global degrees of freedom are still in the global Cartesian system. According to Equation 2.9, the stiffness matrix of the element is given by

$$
\begin{aligned}
K &= \int_V B^T\, C\, B\, dV \\
&= \int_V \begin{bmatrix} -\frac{\cos\theta}{L} \\ -\frac{\sin\theta}{L} \\ \frac{\cos\theta}{L} \\ \frac{\sin\theta}{L} \end{bmatrix} E \begin{bmatrix} -\frac{\cos\theta}{L} & -\frac{\sin\theta}{L} & \frac{\cos\theta}{L} & \frac{\sin\theta}{L} \end{bmatrix} dV \\
&= EA \int_{-\frac{L}{2}}^{\frac{L}{2}} M\, dl,
\end{aligned}
$$

where

$$M = \frac{1}{L^2}\begin{bmatrix} \cos^2\theta & \cos\theta\,\sin\theta & -\cos^2\theta & -\cos\theta\,\sin\theta \\ \cos\theta\,\sin\theta & \sin^2\theta & -\cos\theta\,\sin\theta & -\sin^2\theta \\ -\cos^2\theta & -\cos\theta\,\sin\theta & \cos^2\theta & \cos\theta\,\sin\theta \\ -\cos\theta\,\sin\theta & -\sin^2\theta & \cos\theta\,\sin\theta & \sin^2\theta \end{bmatrix}.$$

Hence

$$K = \frac{EA}{L}\begin{bmatrix} \cos^2\theta & \cos\theta\,\sin\theta & -\cos^2\theta & -\cos\theta\,\sin\theta \\ \cos\theta\,\sin\theta & \sin^2\theta & -\cos\theta\,\sin\theta & -\sin^2\theta \\ -\cos^2\theta & -\cos\theta\,\sin\theta & \cos^2\theta & \cos\theta\,\sin\theta \\ -\cos\theta\,\sin\theta & -\sin^2\theta & \cos\theta\,\sin\theta & \sin^2\theta \end{bmatrix}. \quad (4.4)$$

The matrix above constitutes the general expression used for truss elements which are placed on a plane. Indeed, Expression 4.1 can be obtained assuming $\theta = 0$ in Equation 4.4, and considering only two degrees of freedom per node which are aligned with the main axis of the bar. The methodoly described herein to achieve the stiffness matrix 4.4 does not represent the traditional way described in FEM books; moreover, it introduces the basic mathematical foundations of shell analysis.

4.2 Bars under the large displacements hypothesis

In the previous section, only small displacements were considered. Therefore, in the evaluation of the stiffness matrix K all integrations were performed over the original volume of the bar. When considering the large displacement hypothesis, the use of the formulation described in chapter 3 becomes necessary and matrices ${}^t_0K_L$, ${}^t_0K_{NL}$, and vector ${}^t_0\mathbf{F}$ described therein must be calculated. A Total Lagrangian (TL) formulation will be used, but if instead, an Updated Lagrangian (UL) formulation is preferred, it could be deduced in a very similar way.

In this section the general case of a bar located in the plane will be addressed. The truss element is placed on a global ${}^0x_1 - {}^0x_2$ Cartesian system, and it has been rotated a θ angle with respect to the ${}^0x_1$ axis, see Figure 4.2.

As described in chapter 3, a time variable t describes the loading and the motion of the body. The aim is to evaluate the equilibrium positions of the complete body at the discrete time points $0, \Delta t, 2\Delta t, 3\Delta t, \ldots$, where Δt is an increment in time. Towards the solution of the problem, assume that the static

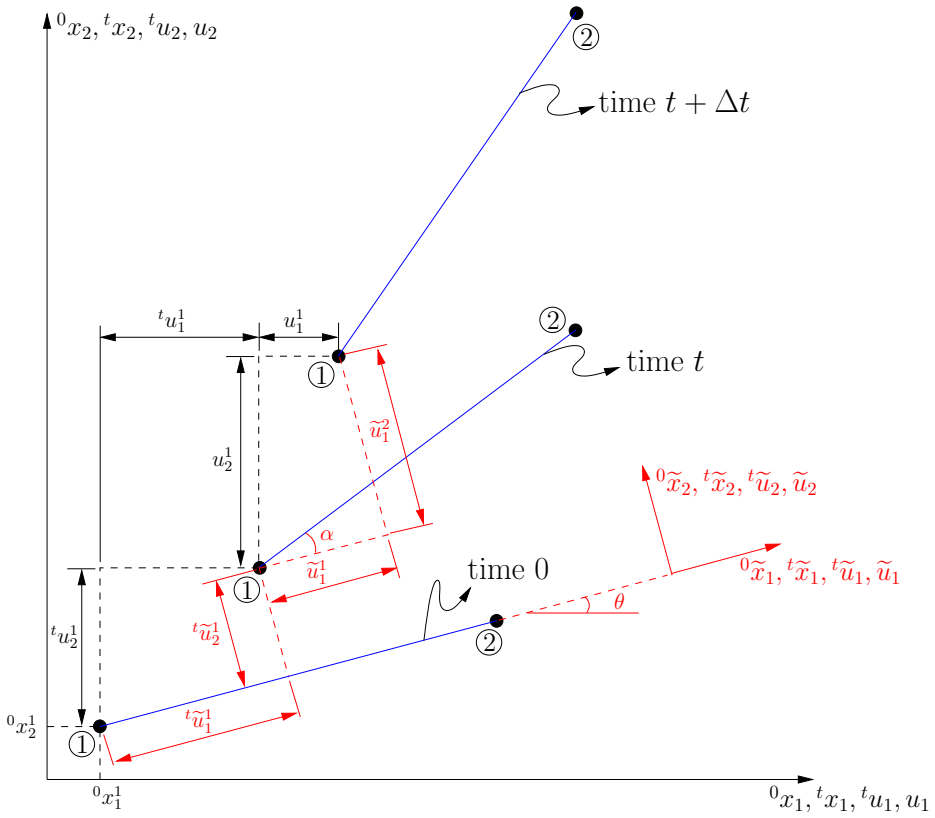

Figure 4.2: General 2–D Truss element in a large displacement analysis.

and kinematic variables for all time steps from time 0 to time t, inclusive, have been obtained already (Bat96).

Even though a large displacement scenario is being addressed, in a TL formulation the evaluation of the linear and nonlinear stiffness matrices, as well as vector ${}^t_0\mathbf{F}$ must be performed over the volume of the bar at time 0 (original volume of the element)[2]. Therefore, a good strategy would be to choose a local system of reference ${}^0\widetilde{x}_1 - {}^0\widetilde{x}_2$ aligned with the main axes of the element, see Figure 4.2. In this way, the strains and the stresses along the bar will only have non zero values in the position associated with the direction normal to the cross-sectional area. In consequence, only expressions for ${}_0\widetilde{e_{11}}$, $\delta_0\widetilde{\eta_{11}}$, and ${}^t_0\widetilde{\epsilon_{11}}$ must be found.

The element shown in Figure 4.2 is a two-node bar element with two dis-

[2]see chapter 3 for a better understanding of the TL formulation

placement degrees of freedom (dof) per node. The directions of the local dofs coincide with the directions of the axes of the local system of reference ${}^0\widetilde{x}_1 - {}^0\widetilde{x}_2$. These dofs are denoted by ${}^t\widetilde{u}_i^k$ and $\widetilde{u}_i^k$, where $i = 1, 2$ represents the directions of the local axes, and $k = 1, 2$ represents the node number associated to each dof. ${}^t\widetilde{u}_i^k$ represents the calculated values of the dofs for all the time steps from time 0 to time t; while $\widetilde{u}_i^k$ represents the unknown dofs from time t to time $t + \Delta t$.

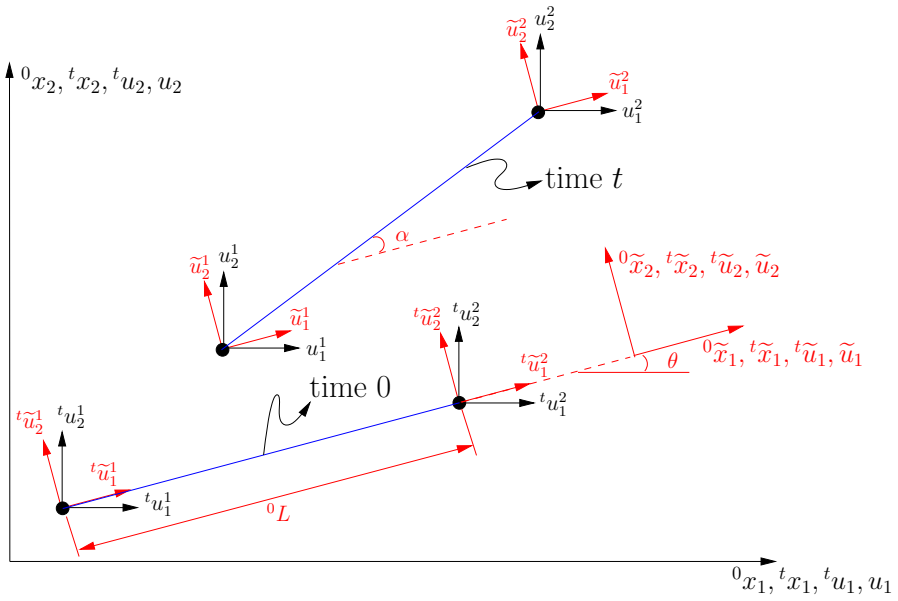

Figure 4.3: Degrees of freedom in the global Cartesian system ${}^0x_1 - {}^0x_2$, and in the local system ${}^0\widetilde{x}_1 - {}^0\widetilde{x}_2$

It is also possible to define global displacement dofs ${}^tu_i^k$ and u_i^k associated to the global Cartesian system ${}^0x_1 - {}^0x_2$. These dofs are aligned with the global Cartesian axes and can be easily written in terms of the local dofs or vice versa, as follows (see Figure 4.3):

$$\begin{aligned} {}^t\widetilde{u}_1^1 &= {}^tu_1^1 \cos\theta + {}^tu_2^1 \sin\theta & {}^t\widetilde{u}_1^2 &= {}^tu_1^2 \cos\theta + {}^tu_2^2 \sin\theta \\ {}^t\widetilde{u}_2^1 &= -{}^tu_1^1 \sin\theta + {}^tu_2^1 \cos\theta & {}^t\widetilde{u}_2^2 &= -{}^tu_1^2 \sin\theta + {}^tu_2^2 \cos\theta, \end{aligned} \tag{4.5}$$

or in matrix form

$$\underbrace{\begin{bmatrix} {}^t\widetilde{u}_1^1 \\ {}^t\widetilde{u}_2^1 \\ {}^t\widetilde{u}_1^2 \\ {}^t\widetilde{u}_2^2 \end{bmatrix}}_{{}^t\widetilde{\mathbf{u}}} = \underbrace{\begin{bmatrix} \cos\theta & \sin\theta & 0 & 0 \\ -\sin\theta & \cos\theta & 0 & 0 \\ 0 & 0 & \cos\theta & \sin\theta \\ 0 & 0 & -\sin\theta & \cos\theta \end{bmatrix}}_{M} \underbrace{\begin{bmatrix} {}^tu_1^1 \\ {}^tu_2^1 \\ {}^tu_1^2 \\ {}^tu_2^2 \end{bmatrix}}_{{}^t\mathbf{u}}, \tag{4.6}$$

where M is a rotation matrix which transforms local displacements dofs to the global Cartesian system. Matrix M can also be used to relate u_i^k with $\widetilde{u}_i^k$ applying the same procedure described above.

The local element longitudinal strains ${}_0\widetilde{e_{11}}$, $\delta_0\widetilde{\eta_{11}}$, and ${}_0^t\widetilde{\epsilon_{11}}$ written in terms of the local dofs are given by

$${}_0\widetilde{e_{11}} = \frac{\partial\,\widetilde{u}_1}{\partial\,{}^0\widetilde{x}_1} + \frac{\partial\,{}^t\widetilde{u}_k}{\partial\,{}^0\widetilde{x}_1}\frac{\partial\,\widetilde{u}_k}{\partial\,{}^0\widetilde{x}_1} \tag{4.7}$$

$$\delta_0\widetilde{\eta_{11}} = \delta\left[\frac{1}{2}\frac{\partial\,\widetilde{u}_k}{\partial\,{}^0\widetilde{x}_1}\frac{\partial\,\widetilde{u}_k}{\partial\,{}^0\widetilde{x}_1}\right] \tag{4.8}$$

$${}_0^t\widetilde{\epsilon_{11}} = \frac{\partial\,{}^t\widetilde{u}_1}{\partial\,{}^0\widetilde{x}_1} + \frac{1}{2}\frac{\partial\,{}^t\widetilde{u}_k}{\partial\,{}^0\widetilde{x}_1}\frac{\partial\,{}^t\widetilde{u}_k}{\partial\,{}^0\widetilde{x}_1}. \tag{4.9}$$

However, *"in finite element formulations, the natural coordinate system has been found to be quite effective in formulating the element properties. The natural coordinate system is a local system in which a point within an element will be expressed by a dimensionless set of numbers whose magnitude never exceed unity. Moreover, this systems will be so defined that the nodal points will have unit magnitude or zero, or a convenient set of fractions. This type of expressing the coordinates also facilitates the integration to compute element stiffness."*(Kri95) This strategy is usually known as the iso parametric finite element formulation.

Therefore, to use this strategy, one has to relate the original non-natural coordinates of the truss element (which could be those measured in the local or in the global Cartesian system) to the natural iso parametric coordinates, see Figure 4.4. The local coordinates of the bar can be related to de natural system trough,

$${}^0\widetilde{x}_1 = h_{1(r)}\,{}^0\widetilde{x}_1^1 + h_{2(r)}\,{}^0\widetilde{x}_1^2, \qquad {}^t\widetilde{x}_1 = h_{1(r)}\,{}^t\widetilde{x}_1^1 + h_{2(r)}\,{}^t\widetilde{x}_1^2; \tag{4.10}$$

where $h_{1(r)}$ and $h_{2(r)}$ are the so-called interpolation functions, which for this particular case are given by

$$h_{1(r)} = \frac{1}{2}(1-r) \qquad h_{2(r)} = \frac{1}{2}(1+r). \tag{4.11}$$

Here, $h_{1(r)}$ and $h_{2(r)}$ are functions only of the natural variable $r \rightarrow -1 \leq r \leq 1$, which is aligned with the longitudinal axis of the element, see Figure 4.4.

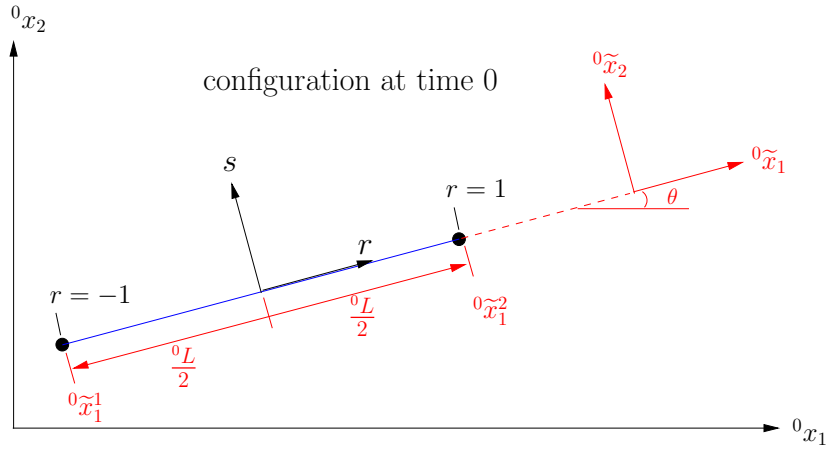

Figure 4.4: Element in the global and in the natural coordinate system.

"The principal idea of the iso parametric finite element formulation is to achieve the relationship between the element displacements at any point and the element nodal point displacements directly through the use of interpolation functions."(Bat96). Similarly as with equations 4.10, expressions for the displacements ${}^t\widetilde{u}_i$ and $\widetilde{u}_i$ using the interpolation functions can be found. That is,

$$ {}^t\widetilde{u}_i = h_{1(r)}\,{}^t\widetilde{u}_i^1 + h_{2(r)}\,{}^t\widetilde{u}_i^2, \qquad \widetilde{u}_i = h_{1(r)}\,\widetilde{u}_i^1 + h_{2(r)}\,\widetilde{u}_i^2. \tag{4.12} $$

or in matrix form

$$ {}^t\widetilde{u}_i = H\,{}^t\widetilde{\hat{\mathbf{u}}}, \qquad \widetilde{u}_i = H\,\widetilde{\hat{\mathbf{u}}}; $$

where

$$ H = \begin{bmatrix} h_{1(r)} & 0 & h_{2(r)} & 0 \\ 0 & h_{1(r)} & 0 & h_{2(r)} \end{bmatrix}, \qquad {}^t\widetilde{\hat{\mathbf{u}}} = \begin{bmatrix} {}^t\widetilde{u}_1^1 \\ {}^t\widetilde{u}_2^1 \\ {}^t\widetilde{u}_1^2 \\ {}^t\widetilde{u}_2^2 \end{bmatrix} \quad \text{and} \quad \widetilde{\hat{\mathbf{u}}} = \begin{bmatrix} \widetilde{u}_1^1 \\ \widetilde{u}_2^1 \\ \widetilde{u}_1^2 \\ \widetilde{u}_2^2 \end{bmatrix}. $$

Remember that the values of ${}^t\widetilde{\hat{\mathbf{u}}}$ are all known because they represent the solutions for the static and kinematic variables for all time steps from time 0 to time t, inclusive. Instead, $\widetilde{\hat{\mathbf{u}}}$ represents the unknown values of the variables at time $t + \Delta t$.

Now it is possible to write Expressions 4.7, 4.8, and 4.9 in terms of the natural coordinates. Using the chain rule one obtains,

$$ {}_0\widetilde{e_{11}} = \frac{\partial\,\widetilde{u}_1}{\partial\,r}\frac{\partial\,r}{\partial\,{}^0\widetilde{x}_1} + \frac{\partial\,{}^t\widetilde{u}_k}{\partial\,r}\frac{\partial\,r}{\partial\,{}^0\widetilde{x}_1}\,\frac{\partial\,\widetilde{u}_k}{\partial\,r}\frac{\partial\,r}{\partial\,{}^0\widetilde{x}_1} \tag{4.13} $$

$$ \delta\,{}_0\widetilde{\eta_{11}} = \delta\left[\frac{1}{2}\frac{\partial\,\widetilde{u}_k}{\partial\,r}\frac{\partial\,r}{\partial\,{}^0\widetilde{x}_1}\,\frac{\partial\,\widetilde{u}_k}{\partial\,r}\frac{\partial\,r}{\partial\,{}^0\widetilde{x}_1}\right] \tag{4.14} $$

$$ {}^t_0\widetilde{\epsilon_{11}} = \frac{\partial\,{}^t\widetilde{u}_1}{\partial\,r}\frac{\partial\,r}{\partial\,{}^0\widetilde{x}_1} + \frac{1}{2}\frac{\partial\,{}^t\widetilde{u}_k}{\partial\,r}\frac{\partial\,r}{\partial\,{}^0\widetilde{x}_1}\,\frac{\partial\,{}^t\widetilde{u}_k}{\partial\,r}\frac{\partial\,r}{\partial\,{}^0\widetilde{x}_1}. \tag{4.15} $$

All the terms in the above equations can be easily found by deriving the expressions in 4.10 and in 4.12. The term $\frac{\partial^0\widetilde{x}_1}{\partial r}$ is known as the Jacobian $({}^0\widetilde{J})$, and in this case, it relates the length of the element in the local reference system to the length of element in the natural coordinate system. From 4.10, ${}^0\widetilde{J}$ can be calculated as

$$ {}^0\widetilde{J} = \frac{\partial^0\widetilde{x}_1}{\partial r} = \frac{\partial h_{1(r)}}{\partial r}\,{}^0\widetilde{x}_1^1 + \frac{\partial h_{2(r)}}{\partial r}\,{}^0\widetilde{x}_1^2 = h_{1,r}\,{}^0\widetilde{x}_1^1 + h_{2,r}\,{}^0\widetilde{x}_1^2 $$

$$ {}^0\widetilde{J} = -\frac{1}{2}\,{}^0\widetilde{x}_1^1 + \frac{1}{2}\,{}^0\widetilde{x}_1^2 = \frac{1}{2}\big({}^0\widetilde{x}_1^2 - {}^0\widetilde{x}_1^1\big), $$

and according to Figure 4.4

$$ {}^0\widetilde{J} = \frac{\partial^0\widetilde{x}_1}{\partial r} = \frac{1}{2}\big[-{}^0\widetilde{x}_1^2 - (-{}^0\widetilde{x}_1^2 - {}^0L)\big] = \frac{{}^0L}{2}; $$

However, in expressions 4.13 to 4.15 it is necessary to calculate the inverse of the Jacobian $({}^0\widetilde{J}^{-1} = \frac{\partial\,r}{\partial\,{}^0\widetilde{x}_1})$ instead of ${}^0\widetilde{J}$. For the particular case being analysed

$$ {}^0\widetilde{J}^{-1} = \frac{\partial\,r}{\partial\,{}^0\widetilde{x}_1} = \frac{2}{{}^0L}. \tag{4.16} $$

Strictly talking, the Jacobian operator is a 3×3 matrix *"relating the natural coordinate derivatives to the local coordinate derivatives"*(Bat96)[3]; that means

$$ \begin{bmatrix} \partial/\partial r \\ \partial/\partial s \\ \partial/\partial t \end{bmatrix} = \underbrace{\begin{bmatrix} \frac{\partial^0\widetilde{x}_1}{\partial r} & \frac{\partial^0\widetilde{x}_2}{\partial r} & \frac{\partial^0\widetilde{x_3}}{\partial r} \\ \frac{\partial^0\widetilde{x}_1}{\partial s} & \frac{\partial^0\widetilde{x}_2}{\partial s} & \frac{\partial^0\widetilde{x_3}}{\partial s} \\ \frac{\partial^0\widetilde{x}_1}{\partial t} & \frac{\partial^0\widetilde{x}_2}{\partial t} & \frac{\partial^0\widetilde{x_3}}{\partial t} \end{bmatrix}}_{{}^0\widetilde{J}} \begin{bmatrix} \partial/\partial^0\widetilde{x}_1 \\ \partial/\partial^0\widetilde{x}_2 \\ \partial/\partial^0\widetilde{x}_3 \end{bmatrix}, $$

[3]see reference (Bat96, pag 346-347) for a better explanation.

where r, s, and t represent the axes of the natural coordinate system. For the truss element being studied the Jacobian is given by

$$ {}^{0}\widetilde{J} = \begin{bmatrix} \frac{{}^{0}L}{2} & 0 & 0 \\ 0 & \frac{{}^{0}h}{2} & 0 \\ 0 & 0 & \frac{{}^{0}d}{2} \end{bmatrix} $$

where ${}^{0}h$ and ${}^{0}d$ are the dimensions of the truss along the axes ${}^{0}\widetilde{x}_2$ and ${}^{0}\widetilde{x}_3$ respectively. Appendix B upholds this result. In consequence,

$$ {}^{0}\widetilde{J}^{-1} = \begin{bmatrix} \frac{\partial r}{\partial \widetilde{x}_1} & \frac{\partial s}{\partial \widetilde{x}_1} & \frac{\partial t}{\partial \widetilde{x}_1} \\ \frac{\partial r}{\partial \widetilde{x}_2} & \frac{\partial s}{\partial \widetilde{x}_2} & \frac{\partial t}{\partial \widetilde{x}_2} \\ \frac{\partial r}{\partial \widetilde{x}_3} & \frac{\partial s}{\partial \widetilde{x}_3} & \frac{\partial t}{\partial \widetilde{x}_3} \end{bmatrix} = \begin{bmatrix} \frac{2}{{}^{0}L} & 0 & 0 \\ 0 & \frac{2}{{}^{0}h} & 0 \\ 0 & 0 & \frac{2}{{}^{0}d} \end{bmatrix}, $$

for that reason $\partial r / \partial \widetilde{x}_1 = \frac{2}{{}^{0}L}$.

4.2.1 A general 2–D expression for ${}_{0}\widetilde{e_{11}}$

By this time, getting appropriate expressions for ${}_{0}\widetilde{e_{11}}$, ${}_{0}\widetilde{\eta_{11}}$, and ${}^{t}_{0}\widetilde{\epsilon_{11}}$ written in terms of the state variables of the problem might be easily accomplished. Beginning with ${}_{0}\widetilde{e_{11}}$, that would be

$$ {}_{0}\widetilde{e_{11}} = \underbrace{\frac{\partial r}{\partial\, {}^{0}\widetilde{x}_1}}_{{}^{0}\widetilde{J}^{-1}} \frac{\partial\, \widetilde{u}_1}{\partial r} + \Big(\underbrace{\frac{\partial r}{\partial\, {}^{0}\widetilde{x}_1}}_{{}^{0}\widetilde{J}^{-1}} \Big)^2 \frac{\partial\, {}^{t}\widetilde{u}_k}{\partial r} \frac{\partial\, \widetilde{u}_k}{\partial r} $$

$$ {}_{0}\widetilde{e_{11}} = \frac{2}{{}^{0}L} \underbrace{\begin{bmatrix} h_{1,r} & 0 & h_{2,r} & 0 \end{bmatrix}}_{\frac{\partial\, \widetilde{u}_1}{\partial r}} \widetilde{\hat{\mathbf{u}}} + \frac{4}{{}^{0}L^2} \underbrace{\left[\begin{bmatrix} h_{1,r} & 0 & h_{2,r} & 0 \\ 0 & h_{1,r} & 0 & h_{2,r} \end{bmatrix} {}^{t}\widetilde{\hat{\mathbf{u}}} \right]^T}_{\frac{\partial\, {}^{t}\widetilde{u}_k}{\partial r}} $$

$$ \underbrace{\begin{bmatrix} h_{1,r} & 0 & h_{2,r} & 0 \\ 0 & h_{1,r} & 0 & h_{2,r} \end{bmatrix} \widetilde{\hat{\mathbf{u}}}}_{\frac{\partial\, \widetilde{u}_k}{\partial r}}, $$

and if $\widetilde{\hat{\mathbf{u}}}$ and ${}^{t}\widetilde{\hat{\mathbf{u}}}$ are transformed into the global Cartesian system using the rotation matrix M used in 4.6; hence,

$$
\begin{aligned}
{}_0\widetilde{e_{11}} =& \frac{2}{{}_0L}\begin{bmatrix} h_{1,r} & 0 & h_{2,r} & 0 \end{bmatrix} M\,\hat{\mathbf{u}} + \frac{4}{{}_0L^2}\,{}^{t}\hat{\mathbf{u}}^T M^T \underbrace{\begin{bmatrix} h_{1,r} & 0 & h_{2,r} & 0 \\ 0 & h_{1,r} & 0 & h_{2,r} \end{bmatrix}^T}_{H,r} \\
& \underbrace{\begin{bmatrix} h_{1,r} & 0 & h_{2,r} & 0 \\ 0 & h_{1,r} & 0 & h_{2,r} \end{bmatrix}}_{H,r} M\,\hat{\mathbf{u}} \\
=& \frac{2}{{}_0L}\begin{bmatrix} h_{1,r} & 0 & h_{2,r} & 0 \end{bmatrix} M\,\hat{\mathbf{u}} + \\
& \frac{4}{{}_0L^2}\,{}^{t}\hat{\mathbf{u}}^T \begin{bmatrix} (h_{1,r})^2 & 0 & h_{1,r}h_{2,r} & 0 \\ 0 & (h_{1,r})^2 & 0 & h_{1,r}h_{2,r} \\ h_{1,r}h_{2,r} & 0 & (h_{2,r})^2 & 0 \\ 0 & h_{1,r}h_{2,r} & 0 & (h_{2,r})^2 \end{bmatrix} M^T M\,\hat{\mathbf{u}},
\end{aligned}
$$

but M is an orthogonal matrix, then $M^T M = I$, where I is the identity matrix; therefore,

$$
\begin{aligned}
{}_0\widetilde{e_{11}} =& \frac{2}{{}_0L}\begin{bmatrix} h_{1,r}\cos\theta & h_{1,r}\sin\theta & h_{2,r}\cos\theta & h_{2,r}\sin\theta \end{bmatrix}\hat{\mathbf{u}} + \\
& \frac{4}{{}_0L^2}\begin{bmatrix} \frac{1}{4}({}^{t}u_1^1 - {}^{t}u_1^2) & \frac{1}{4}({}^{t}u_2^1 - {}^{t}u_2^2) & \frac{1}{4}(-{}^{t}u_1^1 + {}^{t}u_1^2) & \frac{1}{4}(-{}^{t}u_2^1 + {}^{t}u_2^2) \end{bmatrix}\hat{\mathbf{u}} \\
=& \frac{1}{{}_0L}\left\{\begin{bmatrix} -\cos\theta & -\sin\theta & \cos\theta & \sin\theta \end{bmatrix} + \right. \\
& \left.\begin{bmatrix} \frac{{}^{t}u_1^1 - {}^{t}u_1^2}{{}_0L} & \frac{{}^{t}u_2^1 - {}^{t}u_2^2}{{}_0L} & \frac{{}^{t}u_1^2 - {}^{t}u_1^1}{{}_0L} & \frac{{}^{t}u_2^2 - {}^{t}u_2^1}{{}_0L} \end{bmatrix}\right\}\hat{\mathbf{u}} \\
=& \underbrace{\frac{1}{{}_0L}\begin{bmatrix} \frac{{}^{t}u_1^1 - {}^{t}u_1^2}{{}_0L} - \cos\theta & \frac{{}^{t}u_2^1 - {}^{t}u_2^2}{{}_0L} - \sin\theta & \frac{{}^{t}u_1^2 - {}^{t}u_1^1}{{}_0L} + \cos\theta & \frac{{}^{t}u_2^2 - {}^{t}u_2^1}{{}_0L} + \sin\theta \end{bmatrix}}_{{}^{t}_{0}B_L}\hat{\mathbf{u}};
\end{aligned}
\tag{4.17}
$$

${}^{t}_{0}B_L$ is known as the linear strain displacement matrix. Consequently

$$
{}_0\widetilde{e_{11}} = {}^{t}_{0}B_L\,\hat{\mathbf{u}}.
$$

Matrix ${}^{t}_{0}B_L$ is used to calculate matrix ${}^{t}_{0}K_L$ appearing in Equation 3.22. ${}^{t}_{0}K_L$ is known as the linear stiffness matrix of the element.

4.2.2 A general 2–D expression for $\delta_0\widetilde{\eta_{11}}$

An expression for $\delta_0\widetilde{\eta_{11}}$ can also be obtained by following the same strategy used to get ${}_0\widetilde{e_{11}}$, that is

$$\begin{aligned}\delta_0\widetilde{\eta_{11}} =&\delta\Big[\frac{1}{2}\frac{\partial\,\widetilde{u}_k}{\partial\,r}\underbrace{\frac{\partial\,r}{\partial\,{}^0\widetilde{x}_1}}_{{}_0\widetilde{f}^{-1}}\frac{\partial\,\widetilde{u}_k}{\partial\,r}\underbrace{\frac{\partial\,r}{\partial\,{}^0\widetilde{x}_1}}_{{}_0\widetilde{f}^{-1}}\Big]\\ =&\frac{1}{2}\frac{\partial\,\widetilde{u}_k}{\partial\,r}\frac{\partial\,r}{\partial\,{}^0\widetilde{x}_1}\delta\left[\frac{\partial\,\widetilde{u}_k}{\partial\,r}\frac{\partial\,r}{\partial\,{}^0\widetilde{x}_1}\right]+\frac{\partial\,\widetilde{u}_k}{\partial\,r}\frac{\partial\,r}{\partial\,{}^0\widetilde{x}_1}\delta\left[\frac{1}{2}\frac{\partial\,\widetilde{u}_k}{\partial\,r}\frac{\partial\,r}{\partial\,{}^0\widetilde{x}_1}\right],\end{aligned}$$

and $\delta\frac{\partial\,r}{\partial\,{}^0\widetilde{x}_1}=0$ because the variation is taken with respect to displacements $\widetilde{u}_k$; hence,

$$\begin{aligned}\delta_0\widetilde{\eta_{11}} =&\delta\left[\frac{\partial\,\widetilde{u}_k}{\partial\,r}\right]\frac{\partial\,r}{\partial\,{}^0\widetilde{x}_1}\frac{\partial\,\widetilde{u}_k}{\partial\,r}\frac{\partial\,r}{\partial\,{}^0\widetilde{x}_1}\\ =&\underbrace{\left[\left[\begin{array}{cccc}h_{1,r}&0&h_{2,r}&0\\0&h_{1,r}&0&h_{2,r}\end{array}\right]\delta\widetilde{\hat{\mathbf{u}}}\right]^T}_{\frac{\partial\,{}^t\widetilde{u}_k}{\partial\,r}}\frac{2}{{}^0L}\underbrace{\left[\begin{array}{cccc}h_{1,r}&0&h_{2,r}&0\\0&h_{1,r}&0&h_{2,r}\end{array}\right]\widetilde{\hat{\mathbf{u}}}}_{\delta\frac{\partial\,\widetilde{u}_k}{\partial\,r}}\frac{2}{{}^0L}.\end{aligned}$$

Moreover, if $\widetilde{\hat{\mathbf{u}}}$ is transformed into the global Cartesian system using the rotation matrix M used in 4.6, then

$$\delta_0\widetilde{\eta_{11}}=\delta\hat{\mathbf{u}}^TM^T\left[\begin{array}{cccc}h_{1,r}&0&h_{2,r}&0\\0&h_{1,r}&0&h_{2,r}\end{array}\right]^T\frac{2}{{}^0L}\left[\begin{array}{cccc}h_{1,r}&0&h_{2,r}&0\\0&h_{1,r}&0&h_{2,r}\end{array}\right]M\,\hat{\mathbf{u}}\,\frac{2}{{}^0L}$$

Remember that $\delta(M\,\hat{\mathbf{u}})=M\,\delta\hat{\mathbf{u}}$ because $\delta M=0$. Now, arranging terms and accounting for $M^TM=I$,

$$\delta_0\widetilde{\eta_{11}}=\delta\hat{\mathbf{u}}^T\underbrace{\left[\begin{array}{cccc}h_{1,r}&0&h_{2,r}&0\\0&h_{1,r}&0&h_{2,r}\end{array}\right]^T\frac{2}{{}^0L}}_{[{}^t_0B_{NL}]^T}\underbrace{\left[\begin{array}{cccc}h_{1,r}&0&h_{2,r}&0\\0&h_{1,r}&0&h_{2,r}\end{array}\right]\frac{2}{{}^0L}}_{{}^t_0B_{NL}}\hat{\mathbf{u}},\tag{4.18}$$

where ${}^t_0B_{NL}$ is known as the non-linear strain displacement matrix. Consequently

$$\delta_0\widetilde{\eta_{11}}=\delta\hat{\mathbf{u}}^T\frac{4}{{}^0L^2}\left[\begin{array}{cccc}(h_{1,r})^2&0&h_{1,r}h_{2,r}&0\\0&(h_{1,r})^2&0&h_{1,r}h_{2,r}\\h_{1,r}h_{2,r}&0&(h_{2,r})^2&0\\0&h_{1,r}h_{2,r}&0&(h_{2,r})^2\end{array}\right]\hat{\mathbf{u}}.$$

Finally, giving numerical values to the matrix above, the final expression for $\delta_0\widetilde{\eta_{11}}$ is obtained:

$$\delta_0\widetilde{\eta_{11}} = \delta\hat{\mathbf{u}}^T \frac{1}{{}^0L^2} \begin{bmatrix} 1 & 0 & -1 & 0 \\ 0 & 1 & 0 & -1 \\ -1 & 0 & 1 & 0 \\ 0 & -1 & 0 & 1 \end{bmatrix} \hat{\mathbf{u}}. \tag{4.19}$$

This expression can be directly used to calculate the non-linear stiffness matrix ${}^t_0K_{NL}$.

4.2.3 A general 2–D expression for ${}^t_0\widetilde{\epsilon_{11}}$

Within this TL large displacement formulation for truss elements, it is inevitable to deal with the strain ${}^t_0\widetilde{\epsilon_{11}}$[4]. Therefore, an expression for it must also be found. Following the same strategy used for ${}_0\widetilde{e_{11}}$ and $\delta_0\widetilde{\eta_{11}}$,

$$\begin{aligned} {}^t_0\widetilde{\epsilon_{11}} =& \underbrace{\frac{\partial r}{\partial\, {}^0\widetilde{x}_1}}_{{}^0\widetilde{j}^{-1}} \frac{\partial\, {}^t\widetilde{u}_1}{\partial r} + \frac{1}{2}\Big(\underbrace{\frac{\partial r}{\partial\, {}^0\widetilde{x}_1}}_{{}^0\widetilde{j}^{-1}}\Big)^2 \frac{\partial\, {}^t\widetilde{u}_k}{\partial r} \frac{\partial\, {}^t\widetilde{u}_k}{\partial r} \\ =& \frac{2}{{}^0L} \underbrace{\begin{bmatrix} h_{1,r} & 0 & h_{2,r} & 0 \end{bmatrix} {}^t\widetilde{\hat{\mathbf{u}}}}_{\frac{\partial\, \widetilde{u}_1}{\partial r}} + \frac{1}{2}\frac{4}{{}^0L^2} \underbrace{\left[\begin{bmatrix} h_{1,r} & 0 & h_{2,r} & 0 \\ 0 & h_{1,r} & 0 & h_{2,r} \end{bmatrix} {}^t\widetilde{\hat{\mathbf{u}}} \right]^T}_{\frac{\partial\, {}^t\widetilde{u}_k}{\partial r}} \\ & \underbrace{\begin{bmatrix} h_{1,r} & 0 & h_{2,r} & 0 \\ 0 & h_{1,r} & 0 & h_{2,r} \end{bmatrix} {}^t\widetilde{\hat{\mathbf{u}}}}_{\frac{\partial\, \widetilde{u}_k}{\partial r}}. \end{aligned}$$

Now if ${}^t\widetilde{\hat{\mathbf{u}}}$ is transformed into the global Cartesian system using the rotation matrix M used in 4.6, it follows that

$$\begin{aligned} {}^t_0\widetilde{\epsilon_{11}} =& \frac{2}{{}^0L} \begin{bmatrix} h_{1,r} & 0 & h_{2,r} & 0 \end{bmatrix} M\, {}^t\hat{\mathbf{u}} + \frac{1}{2}\frac{4}{{}^0L^2}\, {}^t\hat{\mathbf{u}}^T M^T \begin{bmatrix} h_{1,r} & 0 & h_{2,r} & 0 \\ 0 & h_{1,r} & 0 & h_{2,r} \end{bmatrix}^T \\ & \begin{bmatrix} h_{1,r} & 0 & h_{2,r} & 0 \\ 0 & h_{1,r} & 0 & h_{2,r} \end{bmatrix} M\, {}^t\hat{\mathbf{u}} \\ =& \frac{1}{{}^0L} \begin{bmatrix} -1 & 0 & 1 & 0 \end{bmatrix} M\, \hat{\mathbf{u}} + \frac{1}{2}\frac{1}{{}^0L^2}\, {}^t\hat{\mathbf{u}}^T \begin{bmatrix} 1 & 0 & -1 & 0 \\ 0 & 1 & 0 & -1 \\ -1 & 0 & 1 & 0 \\ 0 & -1 & 0 & 1 \end{bmatrix} {}^t\hat{\mathbf{u}}, \end{aligned}$$

[4] check on chapter 3 for a better understanding of this strain measure

and making some matrix multiplications,

$$
\begin{aligned}
{}^{t}_{0}\widetilde{\epsilon_{11}} =& \frac{1}{{}_{0}L}\left[\begin{array}{cccc} -\cos\theta & -\sin\theta & \cos\theta & \sin\theta \end{array}\right] {}^{t}\hat{\mathbf{u}} + \\
& \frac{1}{2}\frac{1}{{}_{0}L^{2}}\left[\begin{array}{cccc} ({}^{t}u_1^1 - {}^{t}u_1^2) & ({}^{t}u_2^1 - {}^{t}u_2^2) & (-{}^{t}u_1^1 + {}^{t}u_1^2) & (-{}^{t}u_2^1 + {}^{t}u_2^2) \end{array}\right] {}^{t}\hat{\mathbf{u}} \\
{}^{t}_{0}\widetilde{\epsilon_{11}} =& \frac{1}{{}_{0}L}\Big\{\Big[-{}^{t}u_1^1\cos\theta - {}^{t}u_2^1\sin\theta + {}^{t}u_1^2\cos\theta + {}^{t}u_2^2\sin\theta\Big] + \\
& \Big[\frac{({}^{t}u_1^1 - {}^{t}u_1^2){}^{t}u_1^1}{2\,{}^{0}L} + \frac{({}^{t}u_2^1 - {}^{t}u_2^2){}^{t}u_2^1}{2\,{}^{0}L} + \frac{({}^{t}u_1^2 - {}^{t}u_1^1){}^{t}u_1^2}{2\,{}^{0}L} + \frac{({}^{t}u_2^2 - {}^{t}u_2^1){}^{t}u_2^2}{2\,{}^{0}L}\Big]\Big\}
\end{aligned}
\tag{4.20}
$$

The expression above represents the Green-Lagrange strain occurring at time t but measured in configuration 0. Now, it is possible to compute the Second Piola-Kirchhoff stress tensor ${}^{t}_{0}\widetilde{S_{11}}$. This can be done using the constitutive material realtion, e.g. Assume that the ${}^{t}_{0}\widetilde{S_{11}}$ is given in terms of ${}^{t}_{0}\widetilde{\epsilon_{11}}$ via a generalised Hook's law; it means that,

$$
{}^{t}_{0}\widetilde{S_{11}} = {}^{t}_{0}\widetilde{C_{1111}}\,{}^{t}_{0}\widetilde{\epsilon_{11}}. \tag{4.21}
$$

Considering that the load to be applied to the truss element is deformation-independent[5], all the terms involved in the linearised Principle of Virtual Displacements (Equation 3.21) can be quantified. This is possible using the strain-displacement relations 4.17, 4.19, and 4.20, together with the stress relation 4.21. It means that the iterative Newton Raphson procedure explained in chapter 3 can begin. If the procedure is converging, the solution of the non-linear equations might be achieved when the difference between the internal virtual work and the external virtual work tends to be zero.

In order to gain more insight on the appropriate construction of matrices ${}^{t}_{0}K_L$, ${}^{t}_{0}K_{NL}$, and vector ${}^{t}_{0}\mathbf{F}$; the example proposed by reference (Bat96, pag. 544-547) is solved in Appendix C. Although this exercise is fully solved in reference (Bat96), the solution appearing in Appendix C offers more details and corroborates the validity of Expressions 4.17 to 4.21.

[5] check into Equation 3.18 for a better understanding of this assumption

Chapter 5

Beam Elements

Although beams elements are bar-like elements whose geometry can be easily described, the underlying physics used for them is not trivial. For that reason, the theory of Finite Elements requires a deeper insight compared to elements such as 2–D plane stress or 1–D bars. A beam can be defined as *"a bar-like structural member whose primary function is to support transverse loading and carry it to the supports. By bar-like it is meant that one of the dimensions is considerably larger than the other two. This dimension is called the longitudinal dimension o the beam"*(Fel08).

5.1 Euler-Bernoulli and Timoshenko beams

"Because beams are actually 3–D solids, all models necessarily involve some form of approximations to the underlying physics"(Fel08). The most well known and highly used theories of beams are: Euler-Bernoulli and Thimoshenko. Both of them agree that mainly, a beam can support transverse loading due to the action of bending or flexure. However, the biggest difference between them lies in the exclusion or not of the shear deformations. Even though this aspect is not taken into account by the Euler-Bernoulli theory, good results are obtained as long as the element is thin enough to almost neglect the shear effects. By the other hand, due to the inclusion of this variable into the Timoshenko theory, slightly thicker structures can be analysed more accurately.

The bending action taking place in a beam *"produces compressive longitudinal stresses in one side of the beam and tensile stresses in the other. The two regions are separated by a neutral surface of zero stress"*(Fel08). Commonly, a beam element is represented by a 1–D straight or curved line. This line coincides with the neutral stress-free mid-surface of the element; Indeed, the real

3–D displacements of the beam are written in terms of the mid-surface displacements and rotations. In the Timoshenko theory, the transverse displacement of the neutral surface and its angular rotation are treated as independent variables. Therefore, when using FEM, these variables can be interpolated independently via an iso parametric formulation, but of course an additional kinematic expression relating them has to be stated.

In this study, only Timoshenko beams will be addressed. This theory has been preferred becuase (i) an iso parametric formulation can be easily implemented, and because (ii) the transverse displacements and the rotations of the mid-surface are interpolated independently, *"the inter-element continuity conditions of these variables can be satisfied directly, as in the analysis of continua"*(Bat96).

5.2 Timoshenko beams fundamentals

As it was said before, this theory takes into account shear deformations. Therefore, a plane section originally normal to the neutral surface of the beam, will not remain normal after deformation, see Figure 5.1.

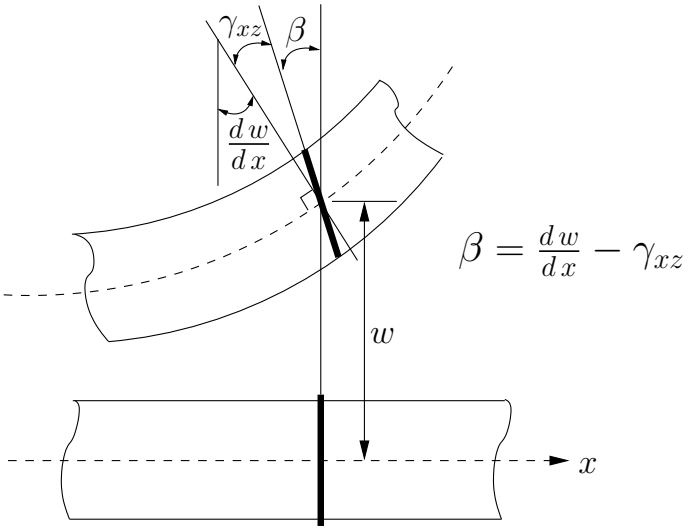

Figure 5.1: Deformation of cross section. Figure taken from (Bat96)

"The total rotation of the plane originally normal to the neutral axis of the beam is given by the rotation of the tangent to the neutral axis $\frac{dw}{dx}$ *and*

the shear deformation γ_{xz}, where γ_{xz} is a constant shearing strain across the section"(Bat96). That is,

$$\beta = \frac{d\,w}{d\,x} - \gamma_{xz}. \tag{5.1}$$

The fact that γ_{xz} is considered as a constant value is merely an approximation. In reality, a strain γ_a varies throughout the cross-section of the beam as well as the corresponding stress τ_a associated to it, see Figure 5.2. These two quantities can be related by

$$\tau_a = G\,\gamma_a,$$

where G is the shear modulus. It is also important to remember that the actual shear stress acting over the cross-section area is given by

$$\tau_a = \frac{\mathbf{V_a}}{d\,A},$$

where $\mathbf{V_a}$ is the actual shear force acting over a differential area $d\,A$.

"Since the actual shearing stress and strain vary over the section, the shearing strain γ_{xz} in 5.1 is an equivalent constant strain on a corresponding shear area A_s"(Bat96), see Figure 5.2.

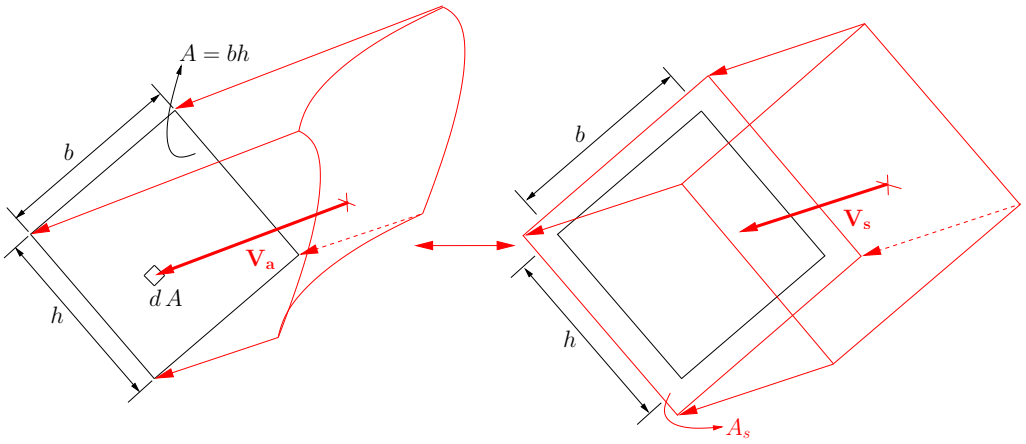

Figure 5.2: Real shear stress on the left vs. assumed constant shear stress on the right.

Consequently, a constant stress τ_{xz} can be associated to γ_{xz} via $\tau_{xz} = G\,\gamma_{xz}$, where τ_{xz} can be calculated as $\tau_{xz} = \frac{\mathbf{V_s}}{A_s}$. $\mathbf{V_s}$ is therefore defined as an equivalent constant shear force acting over A_s. If a closer look is taken to Figure 5.2, it can be noted that the drawn direction for the force vectors $\mathbf{V_a}$

and $\mathbf{V_s}$ do not coincide with the reality. They only have been drawn like that in order to sketch their variation all over the cross-section area.

The actual shear strain energy $\mathbf{U}_{\text{shear}}$ of a beam can be calculated as

$$\mathbf{U}_{\text{shear}} = \frac{1}{2}\int_V \tau_a \gamma_a \, dV;$$

however, if the constant shear strain γ_{xz} and stress τ_{xz} are used instead of γ_a and τ_a; thus, a non-real shear strain energy would be predicted. To overcome this problem, a correction factor k has to be introduced into the calculation of $\mathbf{U}_{\text{shear}}$, that is

$$\mathbf{U}_{\text{shear}} = k\,\frac{1}{2}\int_V \tau_{xz}\,\gamma_{xz}\,dV.$$

Several articles have been written with the aim of calculating this correction factor[1]. For rectangular cross-section area, K.J Bathe proposes a k-value of $\frac{5}{6}$.

5.3 Displacement-based formulation for a two-node Timoshenko beam

In this section the Finite Element Formulation for a two-node Timoshenko beam will be discussed. However, higher order elements can be implemented in the same way.

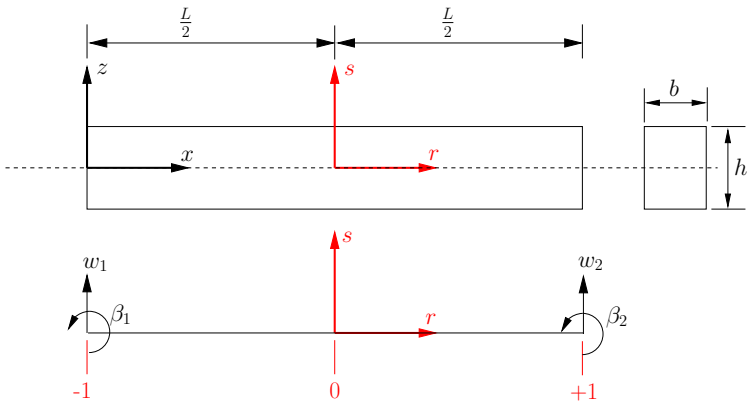

Figure 5.3: Two-node straight Timoshenko beam. Figure taken from (Bat96, pag. 402)

[1] see references (Bat96, pag. 399-400) and (GK07)

The beam to be analysed has a constant rectangular cross-sectional area and its total length is L, see Figure 5.3. Each node has two degrees of freedom: w_i and θ_i.

The expression bellow applies the Minimum Total Potential Energy Principle (Equation 1.1) to the particular beam problem being considered,

$$\Pi = \mathbf{U}_{\text{bending}} + \mathbf{U}_{\text{shear}} - \mathbf{W}_{\text{bending}} - \mathbf{W}_{\text{shear}}$$

$$\Pi = \underbrace{\frac{EI}{2}\int_0^L \Big(\frac{d\,\beta}{d\,x}\Big)^2 d\,x}_{\mathbf{U}_{\text{bending}}} + \underbrace{\frac{GA\,k}{2}\int_0^L \Big(\frac{d\,w}{d\,x} - \beta\Big)^2 d\,x}_{\mathbf{U}_{\text{shear}}} - \underbrace{\int_0^L p\,w\,d\,x}_{\mathbf{W}_{\text{bending}}} - \underbrace{\int_0^L w\,\beta\,d\,x}_{\mathbf{W}_{\text{shear}}},$$

where p and m represent the tranverse and moment loading per unit length respectively.

Next, if the first variation of Π with respect to w and β is taken and the result is equalised to zero; thus, the principle of virtual displacements will be obtained. Namely,

$$EI\int_0^L \Big(\frac{d\,\beta}{d\,x}\Big)\delta\Big(\frac{d\,\beta}{d\,x}\Big)d\,x + GA\,k\int_0^L \Big(\frac{d\,w}{d\,x} - \beta\Big)\Big(\delta\frac{d\,w}{d\,x} - \delta\beta\Big)d\,x = \int_0^L p\,\delta w\,d\,x + \int_0^L m\,\delta\beta\,d\,x. \tag{5.2}$$

Employing the iso parametric formulation discussed in chapter 4, the transverse displacements w and the rotations β can be interpolated as,

$$w = h_{1(r)}w_1 + h_{2(r)}w_2, \qquad \beta = h_{1(r)}\beta_1 + h_{2(r)}\beta_2,$$

where $h_{1(r)}$ and $h_{2(r)}$ are the so-called interpolation functions stated in 4.11.

If a vector $\hat{\mathbf{u}}^T = \begin{bmatrix} w_1 & \beta_1 & w_2 & \beta_2 \end{bmatrix}$ containing all the degrees of freedom of the beam is defined; hence, the expressions above can be written in matrix form. That is

$$w = \underbrace{\begin{bmatrix} h_{1(r)} & 0 & h_{2(r)} & 0 \end{bmatrix}}_{H_w}\hat{\mathbf{u}}, \qquad \beta = \underbrace{\begin{bmatrix} 0 & h_{1(r)} & 0 & h_{2(r)} \end{bmatrix}}_{H_\beta}\hat{\mathbf{u}}; \tag{5.3}$$

and consequently,

$$\frac{d\,w}{d\,x} = \underbrace{\frac{\partial r}{\partial x}\begin{bmatrix} h_{1,r} & 0 & h_{2,r} & 0 \end{bmatrix}}_{B_w}\hat{\mathbf{u}}, \qquad \frac{d\,\beta}{d\,x} = \underbrace{\frac{\partial r}{\partial x}\begin{bmatrix} 0 & h_{1,r} & 0 & h_{2,r} \end{bmatrix}}_{B_\beta}\hat{\mathbf{u}}, \tag{5.4}$$

where $\frac{\partial r}{\partial x} = J^{-1}$ is the inverse of the Jacobian. Replacing these expressions into Equation 5.2 yields to,

$$\delta\hat{\mathbf{u}}^T\Big\{EI\int_{-1}^{+1} B_\beta^T B_\beta \,\mathrm{det}J\,d\,r + GA\,k\int_{-1}^{+1}\Big(B_w - H_\beta\Big)^T\Big(B_w - H_\beta\Big)\,\mathrm{det}J\,d\,r\Big\}\hat{\mathbf{u}} = \delta\hat{\mathbf{u}}^T\Big\{\int_{-1}^{+1} H_w^T\,p\,\mathrm{det}J\,d\,r + \int_{-1}^{+1} H_\beta^T\,m\,\mathrm{det}J\,d\,r\Big\}. \tag{5.5}$$

In order to perform the integrals in the convected-natural coordinate system, it is necessary to replace $d\,x = \mathrm{det}J\,d\,r$, and the upper and lower integration limits have to be change for -1 and +1 respectively.[2]

Following the procedure shown in chapter 2, Expression 5.5 transforms into

$$K\,\hat{\mathbf{u}} = \mathbf{R},$$

where

$$K = EI\int_{-1}^{+1} B_\beta^T B_\beta \,\mathrm{det}J\,d\,r + GA\,k\int_{-1}^{+1}\Big(B_w - H_\beta\Big)^T\Big(B_w - H_\beta\Big)\,\mathrm{det}J\,d\,r, \tag{5.6}$$

and

$$\mathbf{R} = \int_{-1}^{+1} H_w^T\,p\,\mathrm{det}J\,d\,r + \int_{-1}^{+1} H_\beta^T\,m\,\mathrm{det}J\,d\,r.$$

The Jacobian value for a two-node beam element turns out to be the same Jacobian of a two-node bar-like element. Therefore, according to chapter 4, $\frac{\partial r}{\partial x} = \frac{2}{L}$, and also $\mathrm{det}J = \frac{L}{2}$ because only 1–D integrals are pursued. Considering a k-factor value of 1, Equation 5.6 turns into,

$$K = \begin{bmatrix} \frac{Gh}{L} & \frac{Gh}{2} & -\frac{Gh}{L} & \frac{Gh}{2} \\ \frac{Gh}{2} & \frac{GhL}{3} + \frac{EI}{L} & -\frac{Gh}{2} & \frac{GhL}{6} - \frac{EI}{L} \\ -\frac{Gh}{L} & -\frac{Gh}{2} & \frac{Gh}{L} & \frac{Gh}{2} \\ \frac{Gh}{2} & \frac{GhL}{6} - \frac{EI}{L} & -\frac{Gh}{2} & \frac{GhL}{3} + \frac{EI}{L} \end{bmatrix}. \tag{5.7}$$

Stiffness matrix K was deduced based on a pure displacement-based formulation. *"The use of this element cannot be recommended because the shearing*

[2]Reference (Bat96, pag. 347) explains the reason why this change has to be done.

deformations are not represented to sufficient accuracy. This deficiency is particularly pronounced when the element is thin"(Bat96). The lack of performance exhibited by this element can be easily seen if the terms associated with the strain energy of the element are analysed:

$$\begin{aligned}
\mathbf{U}_{\text{element}} &= \mathbf{U}_{\text{bending}} + \mathbf{U}_{\text{shear}} \\
\mathbf{U}_{\text{element}} &= \frac{EI}{2}\int_0^L \left(\frac{d\,\beta}{d\,x}\right)^2 d\,x + \frac{GA\,k}{2}\int_0^L \left(\frac{d\,w}{d\,x} - \beta\right)^2 d\,x \\
\widetilde{\mathbf{U}}_{\text{element}} = \frac{2}{EI}\mathbf{U}_{\text{element}} &= \int_0^L \left(\frac{d\,\beta}{d\,x}\right)^2 d\,x + \frac{GA\,k}{EI}\int_0^L \left(\frac{d\,w}{d\,x} - \beta\right)^2 d\,x,
\end{aligned}$$

the pseudo strain energy $\widetilde{\mathbf{U}}$ *"shows the relative importance of the bending and shearing contributions to the stiffness matrix of an element"*(Bat96). If a closer look is taken to the factor $\frac{GA\,k}{EI}$ in the shearing term, it can be noted that the thinner the element is, the higher the factor $\frac{GA\,k}{EI}$ becomes; indeed, its value increases exponentially when the thickness of the element decreases. This unexpected behaviour makes the beam to be much stiffer than it should be. In consequence, *"this error results into much smaller displacements and rotations than the exact values when the beam structure analysed is thin. The very stiff behaviour exhibited by the thin elements has been referred to as element shear locking"*(Bat96).

In fact, reference (Bat96, pag. 405-406) analyses the case of a displacement-based two-node cantilever beam subjected to only a moment applied at the tip of the beam, and intentionally a zero shear strain all over the domain of the beam has been enforced. The equations obtained show that this situation can only be achieved when all the degrees of freedom are zero, in other words: $w_1 = \theta_1 = w_2 = \theta_2 = 0$. This of course constitutes a non-logic result that has to be avoided somehow. Therefore, it would be valuable if for a thin element, the Timoshenko formulation could predict accurately small shearing deformations. In this way, this theory could be used either for thick or thin elements.

Several alternative procedures have been proposed to overcome the shear locking problem exhibited by the displacement-based formulation. Mixed formulations have emerged as an easy and understandable way to correct this deficiency.

5.4 Mixed Formulations

So far, the functional used to quantify the total potential energy of a structural element has been written as

$$\underbrace{\Pi_{(u_i,\partial u_i/\partial x_j)}}_{\text{total potential energy}} = \frac{1}{2}\int_V e_{ij}\, C_{ijmn}\, e_{mn}\, dV - \int_V f_i^B u_i\, dV - \int_{S_f} f_i^{S_f} u_i^{S_f}\, dS. \quad (5.8)$$

Indeed, when deducing the displacement-based finite element formulation, it is tacitly implicit that the strain tensor can be always expressed in terms of the nodal degrees of freedom of the element being analysed via the equation

$$e_{ij} = \frac{1}{2}(u_{i,j} + u_{j,i}).$$

Therefore, the strains do not appear like an extra degree of freedom to be calculated and Expression 5.8 can be written only in terms of the nodal displacements and, depending on the type of element being used, also in terms of the nodal rotations.

"Various extended variational principles can be used as the basis of a finite element formulation, and the use of many different finite element interpolations can be pursued"(Bat96). Assume that a strain field e_{ij} is wanted to be imposed, in other words, the strain field is going to be treated as an independent state variable. Thus, using Lagrange Multipliers this condition can be accomplished by modifying Equation 5.8 as

$$\Pi^* = \Pi - \int_V \lambda_{ij}(e_{ij} - e_{ij}^{\mathrm{DI}})\, d\, V, \quad (5.9)$$

where λ_{ij} is a new state variable which is referred to as a Lagrange multiplier, e_{ij}^{DI} is the strain field calculated from the displacements and the superscript DI makes reference to it, and e_{ij} also represents a new independent state variable. In consequence, in a subsequent finite element formulation based on this modified functional, different interpolations must be used for λ_{ij}, e_{ij}, and for the displacements u_i.

The new defined functional only adds one extra term to the Minimum Total Potential Energy Principle. In order to uphold this principle, the new added term must tend to be zero, otherwise an extra amount of energy would be being introduced into the principle. The tendency of this term to be zero is explicitly revealed by the way it has been written. Certainly, e_{ij} and e_{ij}^{DI} represent the same quantity; however, they are evaluated by different ways.

Hence, it is completely reasonable to say that the difference between these two quantities must tend to be zero.

Due to the variational principle expressed in Equation 5.9 represents a summation of energy quantities, the introduced extra term must also have energy units. Thus, the state variable λ_{ij} can be identified as the stress τ_{ij}. Thus Π^* can be rewritten as

$$\begin{aligned}\Pi^* &= \Pi - \int_V \tau_{ij}(e_{ij} - e_{ij}^{\mathrm{DI}})\, d\,V \\ &= \Pi - \int_V C_{ijmn}\, e_{mn}(e_{ij} - e_{ij}^{\mathrm{DI}})\, d\,V \\ &= \frac{1}{2}\int_V e_{ij}\, C_{ijmn}\, e_{mn}\, dV - \int_V f_i^B u_i\, dV - \int_{S_f} f_i^{S_f} u_i^{S_f}\, dS \\ &\qquad - \int_V C_{ijmn}\, e_{mn}(e_{ij} - e_{ij}^{\mathrm{DI}})\, d\,V,\end{aligned}$$

this expression is known as the Hellinger-Reissner functional and it would be used as the basis for the formulation of a mixed shear locking free two-node beam element. For that purpose, the Hellinger-Reissner functional has to be specialised to the specific conditions of the problem to be modelled. Those conditions are: (a) Consider a linear variations of the displacements w and rotations β, (b) assume a constant shear strain γ_{xz} throughout the domain of the element, and (c) the strain e_{11} will be calculated from the transverse displacements w and from the rotations β.

According to the above conditions, only the shear strain $\gamma_{xz} = \gamma_{12}$ is going to be treated as an independent state variable while the strain e_{11} is going to be calculated from the displacements and rotations. The specialised functional is therefore,

$$\begin{aligned}\Pi^* &= \frac{1}{2}\int_V e_{ij}\, C_{ijmn}\, e_{mn}\, dV - \underbrace{\int_V f_i^B u_i\, dV - \int_{S_f} f_i^{S_f} u_i^{S_f}\, dS}_{\text{Boundary Terms}} \\ &\qquad - \int_V \underbrace{\tau_{12}}_{\lambda_{12}}(\gamma_{12} - \gamma_{12}^{\mathrm{DI}})\, d\,V, \\ &= \frac{1}{2}\int_V e_{11}\, E\, e_{11}\, dV + \frac{1}{2}\int_V \gamma_{12}\, G\, \gamma_{12}\, dV - \text{Boundary Terms} \\ &\qquad - \int_V \gamma_{12}\, G\, \gamma_{12}\, dV + \int_V \gamma_{12}\, G\, \gamma_{12}^{\mathrm{DI}}\, dV,\end{aligned}$$

where the relations $e_{11}\, C_{11mn}\, e_{mn} = e_{11}\, E\, e_{11}$ and $e_{12}\, C_{12mn}\, e_{mn} = \gamma_{12}\, G\, \gamma_{12}$ have been used according to the Hook's Law for elastic materials. As it was remarked in the listed problem conditions, e_{11} will not be treated as an independent state variable. Hence, $e_{11} = e_{xx}^{\mathrm{DI}}$; moreover, $\gamma_{12} = \gamma_{xz}$, then

$$\begin{aligned}\Pi^* &= \frac{1}{2}\int_V e_{xx}^{\mathrm{DI}}\, E\, e_{xx}^{\mathrm{DI}}\, dV + \frac{1}{2}\int_V \gamma_{xz}\, G\, \gamma_{xz}\, dV - \text{Boundary Terms} \\ &\qquad - \int_V \gamma_{xz}\, G\, \gamma_{xz}\, dV + \int_V \gamma_{xz}\, G\, \gamma_{xz}^{\mathrm{DI}}\, dV \\ &= \frac{1}{2}\int_V e_{xx}^{\mathrm{DI}}\, E\, e_{xx}^{\mathrm{DI}}\, dV - \frac{1}{2}\int_V \gamma_{xz}\, G\, \gamma_{xz}\, dV + \int_V \gamma_{xz}\, G\, \gamma_{xz}^{\mathrm{DI}}\, dV - \text{Boundary T.}\end{aligned}$$

Once the functional has been specialised to the particular problem to be modelled, the stationary conditions $\delta\Pi^* = 0$ is invoked. The variation is taken with respect to the state variables of the problem, in this case the displacements and the shear strain. Reference (Bat96, pag. 274-276) solves this particular problem and states the finite element equations arriving to the stiffness matrix of the element,

$$K = \begin{bmatrix} \frac{GA}{L} & \frac{GA}{2} & -\frac{GA}{L} & \frac{GA}{2} \\ \frac{GA}{2} & \frac{GAL}{4} + \frac{EI}{L} & -\frac{GA}{2} & \frac{GAL}{4} - \frac{EI}{L} \\ -\frac{GA}{L} & -\frac{GA}{2} & \frac{GA}{L} & -\frac{GA}{2} \\ \frac{GA}{2} & \frac{GAL}{4} - \frac{EI}{L} & -\frac{GA}{2} & \frac{GAL}{4} + \frac{EI}{L} \end{bmatrix}.$$

Static condensation on the degrees of freedom corresponding to the shear strain γ_{xz} has been used in order to obtain a final stiffness matrix dependent only on the displacements dofs.

"It is interesting to note that a pure displacement formulation would give a very similar stiffness matrix. However, the element predictive capability of the pure displacement-based formulation is drastically different, displaying a behaviour that is too stiff when the element is thin"(Bat96). Physically what happens is that the Hellinger-Reissner functional has attached the shear strain γ_{xz} (which has been interpolated independently) to the shear strain $\gamma_{xz}^{\mathrm{DI}}$ calculated from the displacements. Indeed, this physic attachment can also be imposed with a different strategy: It is already known that for a Timoshenko beam the following kinematic relations can be applied:

$$u = -z\beta \qquad e_{xx}^{\mathrm{DI}} = \frac{\partial u}{\partial x} = -z\frac{\partial \beta}{\partial x} \qquad \gamma_{xz}^{\mathrm{DI}} = \frac{\partial w}{\partial x} - \beta,$$

where the superscript DI highlights that these quantities have been evaluated from the displacements. The transversal displacements w and rotations β are interpolated as stated in Equation 5.3; In the same way, derivatives $\frac{\partial w}{\partial x}$ and $\frac{\partial \beta}{\partial x}$ are interpolated as it is expressed in Equation 5.4.

According to this interpolations, the shear strain $\gamma_{xz}^{\mathrm{DI}}$ can be expressed as

$$\gamma_{xz}^{\mathrm{DI}} = \frac{1}{L}(w_2 - w_1) - \frac{(1-r)}{2}\beta_1 - \frac{(1+r)}{2}\beta_2.$$

Now imagine that the shear strain is also wanted to be interpolated independently; however, it is conditioned to be a constant value along the domain of the element, that is

$$\gamma_{xz} = B_s\, \gamma_{xz}^1 = [1]\, \gamma_{xz}^1.$$

Where B_s is the strain interpolation matrix, and γ_{xz}^1 is the only one degree of freedom utilised to interpolate the the shear strain. γ_{xz}^1 has been located at $r = 0$ on purpose to make it coincide with a Gauss point. This fact is important in order to pass the Inf-Sup test.[3] *"This test is the basic mathematical criterion that determines whether a mixed finite element discretisation is stable and convergent (and hence will yield a reliable solution)"*(Bat96). Indeed, when interpolating the shear strain, it is also recommended to use an interpolation function with a lower polynomial degree than the one use for the displacements. This means that the decision of considering a constant shear strain for the two-node element was not taken randomly.

Next, suppose that it is wished to impose the condition that the interpolated strain field γ_{xz} be equal to the strain $\gamma_{xz}^{\mathrm{DI}}$ calculated from the displacements. However, $\gamma_{xz}^{\mathrm{DI}}$ is a linear function and γ_{xz} has been interpolated as a constant value. This problem is overcomed by obligating γ_{xz} to be equal to $\gamma_{xz}^{\mathrm{DI}}\Big|_{r=0}$ evaluated in $r = 0$. In this form,

$$\gamma_{xz} = \gamma_{xz}^{\mathrm{DI}}\Big|_{r=0} = \frac{(w_2 - w_1)}{L} - \frac{(\beta_1 + \beta_2)}{2}$$
$$\gamma_{xz} = \underbrace{\begin{bmatrix} -\frac{1}{L} & -\frac{1}{2} & \frac{1}{L} & -\frac{1}{2} \end{bmatrix}}_{\beta_\gamma} \hat{\mathbf{u}}.$$

Hence, in an implicit way, the same mixed formulation already discussed at the beginning of this section is being used. Thus, the principle of virtual

[3] A detailed explanation of this test is carried out by reference (Bat96, pag. 300-337)

displacements can be written as,

$$\delta\hat{\mathbf{u}}^T \underbrace{\left\{ EI \int_{-1}^{+1} B_\beta^T B_\beta \, \mathrm{det}J \, d\, r + GA\, k \int_{-1}^{+1} \beta_\gamma^T \, \beta_\gamma \, \mathrm{det}J \, d\, r \right\}}_{K} \hat{\mathbf{u}} = \delta\hat{\mathbf{u}}^T \, \mathbf{R}.$$

Then, K can be calculated as

$$K = EI \int_{-1}^{+1} \frac{4}{L^2} \begin{bmatrix} 0 \\ -\frac{1}{2} \\ 0 \\ \frac{1}{2} \end{bmatrix} \begin{bmatrix} 0 & -\frac{1}{2} & 0 & -\frac{1}{2} \end{bmatrix} \mathrm{det}J \, d\, r$$
$$+ GA\, k \int_{-1}^{+1} \begin{bmatrix} -\frac{1}{L} \\ -\frac{1}{2} \\ \frac{1}{L} \\ -\frac{1}{2} \end{bmatrix} \begin{bmatrix} -\frac{1}{L} & -\frac{1}{2} & \frac{1}{L} & -\frac{1}{2} \end{bmatrix} \mathrm{det}J \, d\, r,$$

and solving the matrix operations indicated yields to

$$K = \frac{EI}{L} \int_{-1}^{+1} \frac{4}{L^2} \begin{bmatrix} 0 & 0 & 0 & 0 \\ 0 & \frac{1}{4} & 0 & -\frac{1}{4} \\ 0 & 0 & 0 & 0 \\ 0 & -\frac{1}{4} & 0 & \frac{1}{4} \end{bmatrix} \frac{L}{2} \, d\, r$$
$$+ GA\, k \int_{-1}^{+1} \begin{bmatrix} \frac{1}{L^2} & \frac{1}{2L} & -\frac{1}{L^2} & \frac{1}{2L} \\ \frac{1}{2L} & \frac{1}{4} & -\frac{1}{2L} & \frac{1}{4} \\ -\frac{1}{L^2} & -\frac{1}{2L} & \frac{1}{L^2} & -\frac{1}{2L} \\ \frac{1}{2L} & \frac{1}{4} & -\frac{1}{2L} & \frac{1}{4} \end{bmatrix} \frac{L}{2} \, d\, r.$$

Finally, assuming a k-factor = 1, the stiffness matrix K is given by

$$K = \begin{bmatrix} \frac{GA}{L} & \frac{GA}{2} & -\frac{GA}{L} & \frac{GA}{2} \\ \frac{GA}{2} & \frac{GAL}{4} + \frac{EI}{L} & -\frac{GA}{2} & \frac{GAL}{4} - \frac{EI}{L} \\ -\frac{GA}{L} & -\frac{GA}{2} & \frac{GA}{L} & -\frac{GA}{2} \\ \frac{GA}{2} & \frac{GAL}{4} - \frac{EI}{L} & -\frac{GA}{2} & \frac{GAL}{4} + \frac{EI}{L} \end{bmatrix}.$$

As expected, this matrix is exactly the same matrix that was obtained before. This means that either the first or the second strategy can be used to generate the stiffness matrix of the element. *"In addition, the stiffness matrix of these elements can be evaluated efficiently by simply integrating the displacement-based model with one-point Gauss integration for the two-node element. Namely, using this strategy the transverse shear strain is assumed to be constant, and the contribution from the bending deformation is still evaluated exactly. This computational approach may be called reduced integration of the displacement-based element but in fact is actually a full integration of the mixed interpolated element"*(Bat96).

Chapter 6

Plane Stress Elements

In continuum structural mechanics, a state of plane-stress occurs when a stress distribution in which $\tau_{33} = \tau_{13} = \tau_{23} = 0$ takes place throughout the domain of a deformable object. *"The simplest physical problem, for which these stress conditions are a good approximation is the flat plate loaded symmetrically with respect to the midplane of the plate"*(CS97); additionally, all the plate support conditions must also be symmetric about the midplane. A differential portion of a plane-stress plate with dimensions $d\,x \times d\,y \times h$ is shown in Figure 6.1, where h represents the thickness of the plate. As it can be seen, the normal and the shear stress components in the x_3 direction are zero; that is the reason why, models including plane-stress distributions are usually treated as 2–D problems. In fact, the original 3–D domain of the plate V is represented by

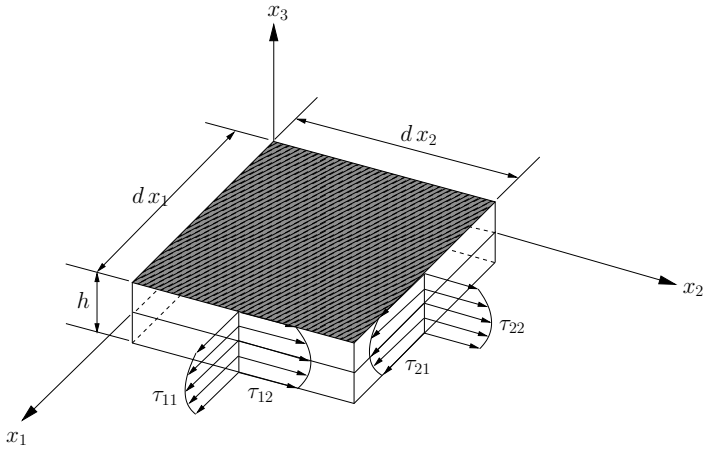

Figure 6.1: Non-zero stresses present in a plane-stress state.

its midplane Ω.

Similarly, the surface located between the upper and the lower faces of the plate is collapsed into a curve Γ which is the boundary of Ω, see Figure 6.2. In consequence, only in-plane boundary conditions are allowed by the plane-stress model; therefore, the symmetric tractions forces distributed over the traction surface S_f have to be collapsed into a curve Γ_f. Regularly, this is achieved in the following way: Traction forces $f_i^{S_f}$ are of course a function of S_f, but $S_f = \Gamma_f\, h$, see Figure 6.2. However, due to the traction forces are assumed to

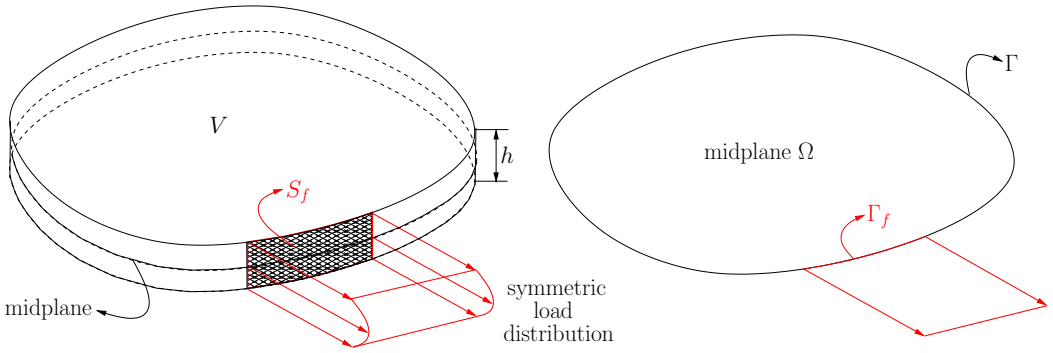

Figure 6.2: Original plate-like element and its 2–D plane-stress representation

be symmetric with respect to the midplane Ω, it is possible to express $f_i^{S_f}$ in terms of $f_i^{\Gamma_f}$ as

$$f_i^{S_f} = \int_{-\frac{h}{2}}^{\frac{h}{2}} f_i^{\Gamma_f}\, d\, h;$$

indeed, it is also very frequent to assume that the symmetric load distribution does not vary with the thickness h of the element. In this case,

$$f_i^{S_f} = h\, f_i^{\Gamma_f};$$

in this way, $f_i^{S_f}$ is expressed as a function of Γ_f. Taking into account this result, the Minimum Total Potential Energy Principle (Equation 1.1) applied to the plane-stress problem is given by,

$$\Pi = \frac{1}{2} h \int_\Omega \tau_{ij}\, e_{ij}\, d\,\Omega - h \int_\Omega f_i^B u_i\, d\Omega - h \int_{\Gamma_f} f_i^{\Gamma_f} u_i^{\Gamma_f}\, d\Gamma, \tag{6.1}$$

with $i = 1, 2$ and $j = 1, 2$. In the above functional, it has been assumed that the stress tensor τ_{ij} do not vary with h and, therefore, it is only a function

of the domain Ω. The fact that a constant stress value with respect to the thickness of the plate is being used is merely an assumption that has to be evaluated somehow to check how much the final resuts can be affected. Instead, an average constant stress tensor could be used, that is

$$\overline{\tau_{ij}} = \frac{1}{h}\int_{-\frac{h}{2}}^{\frac{h}{2}} \tau_{ij}\, d\, h;$$

in spite of this, for simplicity it would be assumed that the in-plane displacements, strains, and stresses are constant through the thickness of the element and, accordingly, Functional 6.1 can be directly used. By invoking the stationary of Functional 6.1 and using the same procedure explained in chapter 2, the finite element equations for a small deformation displacement-based plane-stress element can be easily deduced. This deduction is published and widely analysed by references (Bat96, pag.170-175) and (ZT00); consequently, it will not be discussed in this text. Instead, a displacement-based large deformation formulation will be addressed.

6.1 Plane-Stress elements under the large displacement hypothesis

Large deformation elements, in general, constitute a better approximation to the real behaviour of deformable structures and, of course cover a bigger range of engineering problems. However, the models developed for them require a bigger physical, mathematical, and computational effort. In this section the displacement-based Total Lagrangian formulation for a plane-stress element will be discussed. Basically, the finite element equations required to calculate the stiffness matrices ${}^t_0K_L$, ${}^t_0K_{NL}$, and vector ${}^t_0\mathbf{F}$ will be stated. The formulation presented in this section represents merely an extension to what has been already published by reference (Bat96, pag. 549-553). This material has been rewritten here in order to enhance and clarify the concepts discussed therein.

"Consider a typical two-dimensional element in its configuration at time 0 *and at time t, as illustrated in Figure 6.3."*(Bat96). The Cartesian coordinates

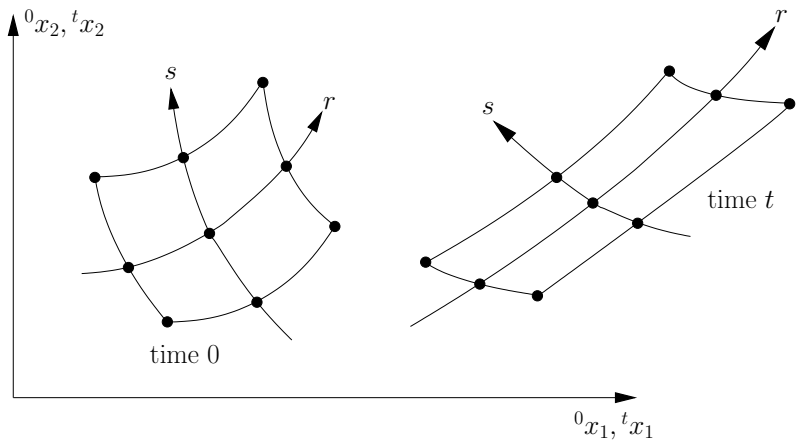

Figure 6.3: Two-dimensional element shown in the ${}^tx_1, {}^tx_2$ plane. Figure taken from (Bat96, pag. 550).

${}^0x_i$ and ${}^tx_i$ plus the element displacements ${}^tu_i$ and u_i can be interpolated as

$$ {}^0x_i = \sum_{k=1}^{n} h_{k(r,s)}\, {}^0x_i^k \qquad {}^tx_i = \sum_{k=1}^{n} h_{k(r,s)}\, {}^tx_i^k \tag{6.2} $$

$$ {}^tu_i = \sum_{k=1}^{n} h_{k(r,s)}\, {}^tu_i^k \qquad u_i = \sum_{k=1}^{n} h_{k(r,s)}\, u_i^k, \tag{6.3} $$

where $h_{k(r,s)}$ are the so-called interpolation functions written in terms of the natural coordinates $r - s$. The geometry of the element is described by n Cartesian points which normally coincide with the displacements nodes of the element. Figure 6.3 shows a 9-node element; nevertheless, the amount of nodes used can vary depending on the particular purpose pursued with the utilisation of the element.

The Total Lagrangian linearised principle of virtual displacements for the plane-stress model written in matrix form is given by

$$ \Big(\underbrace{h \int_{{}^0\Omega} {}^t_0B_L^T \, {}^t_0C \, {}^t_0B_L \, d\,{}^0\Omega}_{{}^t_0K_L} + \underbrace{h \int_{{}^0\Omega} {}^t_0B_{NL}^T \, {}^t_0S \, {}^t_0B_{NL} \, d\,{}^0\Omega}_{{}^t_0K_{NL}} \Big) \hat{\mathbf{u}} = $$

$$ {}^{t+\Delta t}R - \underbrace{h \int_{{}^0\Omega} {}^t_0B_L^T \, {}^t_0\mathbf{S} \, d\,{}^0\Omega}_{{}^t_0\mathbf{F}} . \tag{6.4} $$

The large displacement formulation being discussed in this text has been deduced to predict accurately large displacements and large strains. *"Clearly, the finite element equilibrium equations contain the displacement and strain-displacement matrices plus the constitutive matrix of the material. Therefore, in order for a formulation to be applicable to a certain response prediction, it is imperative that both the kinematic and the constitutive descriptions be appropriate"*(Bat96). However, small strain material laws are also admitted; in this way, large displacements but small strain predictions can be achieved.

Assuming that the plane-stress Hook's Law for small displacements is going to be used to describe the material behaviour, then

$$ {}^{t}_{0}C = \frac{E}{1-\nu^2} \begin{bmatrix} 1 & \nu & 0 \\ \nu & 1 & 0 \\ 0 & 0 & \frac{1-\nu}{2} \end{bmatrix}. $$

Note that although ${}^{t}_{0}C_{ijrs}$ is a four order tensor, it has been represented as a square matrix just in order to fulfil the generalised Hook's Law

$$ \begin{bmatrix} {}^{t}_{0}S_{11} \\ {}^{t}_{0}S_{22} \\ {}^{t}_{0}S_{12} \end{bmatrix} = \begin{bmatrix} 1 & \nu & 0 \\ \nu & 1 & 0 \\ 0 & 0 & \frac{1-\nu}{2} \end{bmatrix} \begin{bmatrix} {}^{t}_{0}\epsilon_{11} \\ {}^{t}_{0}\epsilon_{22} \\ {}^{t}_{0}\epsilon_{12} \end{bmatrix}. \tag{6.5} $$

By the other hand, when intending to compute matrix ${}^{t}_{0}B_L$, it is essential to remember that in a Total Lagrangian formulation,

$$ {}_0e_{ij} = \frac{1}{2}\Big[\frac{\partial u_i}{\partial {}^0x_j}\frac{\partial u_j}{\partial {}^0x_i}\Big] + \underbrace{\frac{1}{2}\Big[\frac{\partial {}^t u_k}{\partial {}^0x_i}\frac{\partial u_k}{\partial {}^0x_j} + \frac{\partial u_k}{\partial {}^0x_i}\frac{\partial {}^t u_k}{\partial {}^0x_j}\Big]}_{\text{initial displacement effect}} $$

$$ {}_0e_{ij} = \underbrace{\frac{1}{2}\Big({}_0u_{i,j} + {}_0u_{j,i}\Big)}_{{}_0e^{*}_{ij}} + \underbrace{\frac{1}{2}\Big({}^{t}_{0}u_{p,i}\ {}_0u_{p,j} + {}_0u_{p,i}\ {}^{t}_{0}u_{p,j}\Big)}_{{}_0e^{**}_{ij}}; $$

thus, ${}_0e_{ij} = {}_0e^{*}_{ij} + {}_0e^{**}_{ij}$.

6.1.1 A general expression for ${}^{t}_{0}B_L$

For simplicity, the linear strain ${}_0e_{ij}$ has been expressed as the addition of ${}_0e^{*}_{ij}$ and the initial displacement effect ${}_0e^{**}_{ij}$. The first term ${}_0e^{*}_{ij}$ can be developed

in the following way

$$
\begin{aligned}
{}_0e^*_{11} &= \frac{1}{2}\left[\frac{\partial u_1}{\partial {}^0x_1}\frac{\partial u_1}{\partial {}^0x_1}\right] = \frac{\partial u_1}{\partial {}^0x_1} \\
{}_0e^*_{22} &= \frac{1}{2}\left[\frac{\partial u_2}{\partial {}^0x_2}\frac{\partial u_2}{\partial {}^0x_2}\right] = \frac{\partial u_2}{\partial {}^0x_2} \\
{}_0e^*_{12} &= \frac{1}{2}\left[\frac{\partial u_1}{\partial {}^0x_2}\frac{\partial u_2}{\partial {}^0x_1}\right] = \frac{1}{2}\gamma^*_{12} = {}_0e^*_{21}.
\end{aligned}
$$

Next, based on the interpolations stated in 6.3, ${}_0e^*_{11}$ can computed as

$${}_0e^*_{11} = \frac{\partial h_{1(r,s)}}{\partial {}^0x_1}u^1_1 + \frac{\partial h_{2(r,s)}}{\partial {}^0x_1}u^2_1 + \frac{\partial h_{3(r,s)}}{\partial {}^0x_1}u^3_1 + \cdots + \frac{\partial h_{n(r,s)}}{\partial {}^0x_1}u^n_1.$$

If a vector $\hat{\mathbf{u}}^T = \begin{bmatrix} u^1_1 & u^1_2 & u^2_1 & u^2_2 & u^3_1 & u^3_2 & \dots & u^2_n & u^2_n \end{bmatrix}$ containing all the displacements degrees of freedom is defined, the above expression can be rewritten in matrix form, namely

$${}_0e^*_{11} = \begin{bmatrix} {}_0h_{1,1} & 0 & {}_0h_{2,1} & 0 & {}_0h_{3,1} & 0 & \dots & {}_0h_{n,1} & 0 \end{bmatrix}\hat{\mathbf{u}},$$

where ${}_0h_{k,j} = \frac{\partial h_{k(r,s)}}{\partial {}^0x_j}$. The same strategy can be used with ${}_0e^*_{22}$ and ${}_0e^*_{12}$, hence

$$
\begin{bmatrix} {}_0e^*_{11} \\ {}_0e^*_{22} \\ {}_0\gamma^*_{12} \end{bmatrix} = \underbrace{\begin{bmatrix} {}_0h_{1,1} & 0 & {}_0h_{2,1} & 0 & {}_0h_{3,1} & 0 & \dots & {}_0h_{n,1} & 0 \\ 0 & {}_0h_{1,2} & 0 & {}_0h_{2,2} & 0 & {}_0h_{3,2} & \dots & 0 & {}_0h_{n,2} \\ {}_0h_{1,2} & {}_0h_{1,1} & {}_0h_{2,2} & {}_0h_{2,1} & {}_0h_{3,2} & {}_0h_{3,1} & \dots & {}_0h_{n,2} & {}_0h_{n,1} \end{bmatrix}}_{{}^t_0B^*_L}\hat{\mathbf{u}}.
$$

However, it is important to note that each value ${}_0h_{k,j}$ inside matrix ${}^t_0B^*_L$ is a function of r and s, thus

$${}_0h_{k,j} = \frac{\partial h_{k(r,s)}}{\partial {}^0x_j} = \frac{\partial h_{k(r,s)}}{\partial r}\frac{\partial r}{\partial {}^0x_j} + \frac{\partial h_{k(r,s)}}{\partial s}\frac{\partial s}{\partial {}^0x_j}. \tag{6.6}$$

For that reason, Expression 6.6 must be used to calculate each position of matrix ${}^t_0B^*_L$.

The term ${}_0e^{**}_{ij}$ can be expressed in terms of the vector of displacements degrees of freedom $\hat{\mathbf{u}}$ somehow similarly as ${}_0e^*_{ij}$. Each one of the components

of tensor ${}_0e_{ij}^{**}$ are

$$
\begin{aligned}
{}_0e_{11}^{**} &= \frac{1}{2}\left[\frac{\partial^t u_k}{\partial^0 x_1}\frac{\partial u_k}{\partial^0 x_1} + \frac{\partial u_k}{\partial^0 x_1}\frac{\partial^t u_k}{\partial^0 x_1}\right] = \frac{\partial^t u_k}{\partial^0 x_1}\frac{\partial u_k}{\partial^0 x_1} \\
{}_0e_{22}^{**} &= \frac{1}{2}\left[\frac{\partial^t u_k}{\partial^0 x_2}\frac{\partial u_k}{\partial^0 x_2} + \frac{\partial u_k}{\partial^0 x_2}\frac{\partial^t u_k}{\partial^0 x_2}\right] = \frac{\partial^t u_k}{\partial^0 x_2}\frac{\partial u_k}{\partial^0 x_2} \\
{}_0e_{12}^{**} &= \frac{1}{2}\left[\frac{\partial^t u_k}{\partial^0 x_1}\frac{\partial u_k}{\partial^0 x_2} + \frac{\partial u_k}{\partial^0 x_1}\frac{\partial^t u_k}{\partial^0 x_2}\right] = \frac{1}{2}\gamma_{12}^{**} = {}_0e_{21}^{**},
\end{aligned}
$$

and each component can be developed as

$$
\begin{aligned}
{}_0e_{11}^{**} &= \frac{\partial^t u_1}{\partial^0 x_1}\frac{\partial u_1}{\partial^0 x_1} + \frac{\partial^t u_2}{\partial^0 x_1}\frac{\partial u_2}{\partial^0 x_1} \\
{}_0e_{22}^{**} &= \frac{\partial^t u_1}{\partial^0 x_2}\frac{\partial u_1}{\partial^0 x_2} + \frac{\partial^t u_2}{\partial^0 x_2}\frac{\partial u_2}{\partial^0 x_2} \\
{}_0\gamma_{12}^{**} &= \frac{\partial^t u_1}{\partial^0 x_1}\frac{\partial u_1}{\partial^0 x_2} + \frac{\partial^t u_2}{\partial^0 x_1}\frac{\partial u_2}{\partial^0 x_2} + \frac{\partial u_1}{\partial^0 x_1}\frac{\partial^t u_1}{\partial^0 x_2} + \frac{\partial u_2}{\partial^0 x_1}\frac{\partial^t u_2}{\partial^0 x_2}.
\end{aligned}
$$

Next, based on expressions 6.3, derivatives of the form $\frac{\partial^t u_i}{\partial^0 x_j}$ can be easily computed, that is

$$
\begin{aligned}
\frac{\partial^t u_1}{\partial^0 x_1} &= \sum_{k=1}^{n} {}_0h_{k,1}\,{}^t u_1^k = l_{11} \qquad & \frac{\partial^t u_1}{\partial^0 x_2} &= \sum_{k=1}^{n} {}_0h_{k,2}\,{}^t u_1^k = l_{12} \\
\frac{\partial^t u_2}{\partial^0 x_1} &= \sum_{k=1}^{n} {}_0h_{k,1}\,{}^t u_2^k = l_{21} \qquad & \frac{\partial^t u_2}{\partial^0 x_2} &= \sum_{k=1}^{n} {}_0h_{k,2}\,{}^t u_2^k = l_{22}.
\end{aligned}
$$

Hence,

$$
\begin{aligned}
{}_0e_{11}^{**} &= l_{11}\frac{\partial u_1}{\partial^0 x_1} + l_{21}\frac{\partial u_2}{\partial^0 x_1} \\
&= l_{11}\left[\begin{array}{cccccccc} {}_0h_{1,1} & 0 & {}_0h_{2,1} & 0 & \dots & {}_0h_{n,1} & 0 \end{array}\right]\hat{\mathbf{u}} \\
&\qquad + l_{21}\left[\begin{array}{cccccccc} 0 & {}_0h_{1,1} & 0 & {}_0h_{2,1} & \dots & 0 & {}_0h_{n,1} \end{array}\right]\hat{\mathbf{u}} \\
&= \left[\begin{array}{cccccccc} l_{11}\,{}_0h_{1,1} & l_{21}\,{}_0h_{1,1} & l_{11}\,{}_0h_{2,1} & l_{21}\,{}_0h_{2,1} & \dots & l_{11}\,{}_0h_{n,1} & l_{21}\,{}_0h_{n,1} \end{array}\right]\hat{\mathbf{u}}.
\end{aligned}
$$

In a similar way ${}_0e_{22}^{**}$ and ${}_0\gamma_{12}^{**}$ can be calculated. Finally,

$$
{}_0\mathbf{e}^{**} = {}_0^t B_L^{**}\ \hat{\mathbf{u}},
$$

where $[{}_0\mathbf{e}^{**}]^T = \left[\begin{array}{ccc} {}_0e_{11}^{**} & {}_0e_{22}^{**} & {}_0\gamma_{12}^{**} \end{array}\right]$, and

$$
{}^t_0B^{**}_L =
\begin{bmatrix}
l_{11}\,{}_0h_{1,1} & l_{21}\,{}_0h_{1,1} & l_{11}\,{}_0h_{2,1} & l_{21}\,{}_0h_{2,1} & \dots & l_{11}\,{}_0h_{n,1} & l_{21}\,{}_0h_{n,1} \\
l_{12}\,{}_0h_{1,2} & l_{22}\,{}_0h_{1,2} & l_{12}\,{}_0h_{2,2} & l_{22}\,{}_0h_{2,2} & \dots & l_{12}\,{}_0h_{n,2} & l_{22}\,{}_0h_{n,2} \\
l_{11}\,{}_0h_{1,2}+ & l_{21}\,{}_0h_{1,2}+ & l_{11}\,{}_0h_{2,2}+ & l_{21}\,{}_0h_{2,2}+ & & l_{11}\,{}_0h_{n,2}+ & l_{21}\,{}_0h_{n,2}+ \\
l_{12}\,{}_0h_{1,1} & l_{22}\,{}_0h_{1,1} & l_{12}\,{}_0h_{2,1} & l_{22}\,{}_0h_{2,1} & \dots & l_{12}\,{}_0h_{n,1} & l_{22}\,{}_0h_{n,1}
\end{bmatrix}.
$$

In this way,

$$
{}_0\mathbf{e} = {}^t_0B_L\,\hat{\mathbf{u}}
$$

where ${}^t_0B_L = {}^t_0B^*_L + {}^t_0B^{**}_L$. Note that matrix ${}^t_0B_L$ is also used to calculate vector ${}^t_0\mathbf{F}$, see Equation 6.4; but additionally, a vector ${}^t_0\mathbf{S}$ listing all the components of the Second Piola-Kirchhoff stress tensor must be computed. Each component of vector ${}^t_0\mathbf{S}$ can be calculated directly from the generalised Hook's Law (Equation 6.5) for linear-elastic materials.

6.1.2 A general expression for ${}^t_0B_{NL}$

In chapter 3 it was shown that the non-linear stiffness matrix ${}^t_0K_{NL}$ comes from the evaluation of $\int_{{}_0V} {}^t_0S_{ij}\,\delta_0\eta_{ij}\,d\,{}^0V$, which is an inner term of the linearised principle of virtual displacements (Equation 3.21). Under plane-stress conditions this term can be specialised into

$$
\int_{{}_0V} {}^t_0S_{ij}\,\delta_0\eta_{ij}\,d\,{}^0V = h\int_{{}_0\Omega} {}^t_0S_{ij}\,\delta_0\eta_{ij}\,d\,{}^0\Omega, \tag{6.7}
$$

or in matrix notation

$$
h\int_{{}_0\Omega} {}^t_0S_{ij}\,\delta_0\eta_{ij}\,d\,{}^0\Omega = \delta\hat{\mathbf{u}}^T\Big(h\int_{{}_0\Omega} {}^t_0B^T_{NL}\,{}^t_0S\,{}^t_0B_{NL}\,d\,{}^0\Omega\Big)\hat{\mathbf{u}}. \tag{6.8}
$$

Because $\delta_0\eta_{ij} = \delta\Big(\frac{1}{2}\frac{\partial u_p}{\partial {}^0x_i}\frac{\partial u_p}{\partial {}^0x_j}\Big)$, Equation 6.7 can be developed as

$$
\begin{aligned}
h\int_{{}_0\Omega} {}^t_0S_{ij}\,\delta_0\eta_{ij}\,d\,{}^0\Omega &= h\int_{{}_0\Omega} {}^t_0S_{ij}\Big[\frac{1}{2}\frac{\partial u_p}{\partial {}^0x_i}\,\delta\Big(\frac{\partial u_p}{\partial {}^0x_j}\Big) + \frac{1}{2}\,\delta\Big(\frac{\partial u_p}{\partial {}^0x_i}\Big)\frac{\partial u_p}{\partial {}^0x_j}\Big]d\,{}^0\Omega \\
&= h\int_{{}_0\Omega} {}^t_0S_{ij}\Big[\frac{1}{2}\frac{\partial u_1}{\partial {}^0x_i}\,\delta\Big(\frac{\partial u_1}{\partial {}^0x_j}\Big) + \frac{1}{2}\frac{\partial u_2}{\partial {}^0x_i}\,\delta\Big(\frac{\partial u_2}{\partial {}^0x_j}\Big) \\
&\qquad + \frac{1}{2}\,\delta\Big(\frac{\partial u_1}{\partial {}^0x_i}\Big)\frac{\partial u_1}{\partial {}^0x_j} + \frac{1}{2}\,\delta\Big(\frac{\partial u_2}{\partial {}^0x_i}\Big)\frac{\partial u_2}{\partial {}^0x_j}\Big]d\,{}^0\Omega.
\end{aligned}
$$

Moreover, evaluating indices i, j, adding common terms, and taking into account that ${}^t_0S_{ij} = {}^t_0S_{ji}$, yields to

$$\begin{aligned} h\int_{{}_0\Omega} {}^t_0S_{ij}\,\delta_0\eta_{ij}\,d\,{}^0\Omega = h\int_{{}_0\Omega}\Big[\quad & {}^t_0S_{11}\frac{\partial u_1}{\partial {}^0x_1}\,\delta\Big(\frac{\partial u_1}{\partial {}^0x_1}\Big) + {}^t_0S_{12}\frac{\partial u_1}{\partial {}^0x_1}\,\delta\Big(\frac{\partial u_1}{\partial {}^0x_2}\Big) + \\ & {}^t_0S_{12}\frac{\partial u_1}{\partial {}^0x_2}\,\delta\Big(\frac{\partial u_1}{\partial {}^0x_1}\Big) + {}^t_0S_{22}\frac{\partial u_1}{\partial {}^0x_2}\,\delta\Big(\frac{\partial u_1}{\partial {}^0x_2}\Big) + \\ & {}^t_0S_{11}\frac{\partial u_2}{\partial {}^0x_1}\,\delta\Big(\frac{\partial u_2}{\partial {}^0x_1}\Big) + {}^t_0S_{12}\frac{\partial u_2}{\partial {}^0x_1}\,\delta\Big(\frac{\partial u_2}{\partial {}^0x_2}\Big) + \\ & {}^t_0S_{12}\frac{\partial u_2}{\partial {}^0x_2}\,\delta\Big(\frac{\partial u_2}{\partial {}^0x_1}\Big) + {}^t_0S_{22}\frac{\partial u_2}{\partial {}^0x_2}\,\delta\Big(\frac{\partial u_2}{\partial {}^0x_2}\Big)\Big]\,d\,{}^0\Omega. \end{aligned} \tag{6.9}$$

According to Equation 6.8, the expression above must be written somehow in matrix form, that is

$$h\int_{{}_0\Omega} {}^t_0S_{ij}\,\delta_0\eta_{ij}\,d\,{}^0\Omega = \delta\hat{\mathbf{u}}^T\Big(h\int_{{}_0\Omega} {}^t_0B^T_{NL}\;{}^t_0S\;{}^t_0B_{NL}\;d\,{}^0\Omega\Big)\hat{\mathbf{u}}.$$

Reference (Bat96) has come up with an effective and simple way to do it: Define a vector ${}_0\mathbf{A}$ containing all the values of the second order tensor $\frac{\partial u_p}{\partial {}^0x_j}$; namely,

$${}_0\mathbf{A} = \begin{bmatrix} \frac{\partial u_1}{\partial {}^0x_1} \\ \\ \frac{\partial u_1}{\partial {}^0x_2} \\ \\ \frac{\partial u_2}{\partial {}^0x_1} \\ \\ \frac{\partial u_2}{\partial {}^0x_2} \end{bmatrix} \qquad \delta_0\mathbf{A} = \begin{bmatrix} \delta\frac{\partial u_1}{\partial {}^0x_1} \\ \\ \delta\frac{\partial u_1}{\partial {}^0x_2} \\ \\ \delta\frac{\partial u_2}{\partial {}^0x_1} \\ \\ \delta\frac{\partial u_2}{\partial {}^0x_2} \end{bmatrix}.$$

Furthermore, a matrix ${}^t_0S$ with the form

$${}^t_0S = \begin{bmatrix} {}^t_0S_{11} & {}^t_0S_{12} & 0 & 0 \\ {}^t_0S_{12} & {}^t_0S_{22} & 0 & 0 \\ 0 & 0 & {}^t_0S_{11} & {}^t_0S_{12} \\ 0 & 0 & {}^t_0S_{12} & {}^t_0S_{22} \end{bmatrix}$$

is defined. The product $\delta_0\mathbf{A}^T\,{}^t_0S\,{}_0\mathbf{A}$ is therefore,

$$\delta_0\mathbf{A}^T\,{}^t_0S\,{}_0\mathbf{A} = \delta_0\mathbf{A}^T \begin{bmatrix} {}^t_0S_{11} & {}^t_0S_{12} & 0 & 0 \\ {}^t_0S_{12} & {}^t_0S_{22} & 0 & 0 \\ 0 & 0 & {}^t_0S_{11} & {}^t_0S_{12} \\ 0 & 0 & {}^t_0S_{12} & {}^t_0S_{22} \end{bmatrix} {}_0\mathbf{A}$$

$$= \begin{bmatrix} {}^t_0S_{11}\delta\frac{\partial u_1}{\partial^0 x_1}+ & {}^t_0S_{12}\delta\frac{\partial u_1}{\partial^0 x_1}+ & {}^t_0S_{11}\delta\frac{\partial u_2}{\partial^0 x_1}+ & {}^t_0S_{12}\delta\frac{\partial u_2}{\partial^0 x_1}+ \\ {}^t_0S_{12}\delta\frac{\partial u_1}{\partial^0 x_2} & {}^t_0S_{22}\delta\frac{\partial u_1}{\partial^0 x_2} & {}^t_0S_{12}\delta\frac{\partial u_2}{\partial^0 x_2} & {}^t_0S_{22}\delta\frac{\partial u_2}{\partial^0 x_2} \end{bmatrix} \begin{bmatrix} \frac{\partial u_1}{\partial^0 x_1} \\ \frac{\partial u_1}{\partial^0 x_2} \\ \frac{\partial u_2}{\partial^0 x_1} \\ \frac{\partial u_2}{\partial^0 x_2} \end{bmatrix};$$

thus,

$$\begin{aligned} \delta_0\mathbf{A}^T\,{}^t_0S\,{}_0\mathbf{A} = {}& {}^t_0S_{11}\frac{\partial u_1}{\partial^0 x_1}\,\delta\Big(\frac{\partial u_1}{\partial^0 x_1}\Big) + {}^t_0S_{12}\frac{\partial u_1}{\partial^0 x_1}\,\delta\Big(\frac{\partial u_1}{\partial^0 x_2}\Big) + {}^t_0S_{12}\frac{\partial u_1}{\partial^0 x_2}\,\delta\Big(\frac{\partial u_1}{\partial^0 x_1}\Big) + \\ & {}^t_0S_{22}\frac{\partial u_1}{\partial^0 x_2}\,\delta\Big(\frac{\partial u_1}{\partial^0 x_2}\Big) + {}^t_0S_{11}\frac{\partial u_2}{\partial^0 x_1}\,\delta\Big(\frac{\partial u_2}{\partial^0 x_1}\Big) + {}^t_0S_{12}\frac{\partial u_2}{\partial^0 x_1}\,\delta\Big(\frac{\partial u_2}{\partial^0 x_2}\Big) + \\ & {}^t_0S_{12}\frac{\partial u_2}{\partial^0 x_2}\,\delta\Big(\frac{\partial u_2}{\partial^0 x_1}\Big) + {}^t_0S_{22}\frac{\partial u_2}{\partial^0 x_2}\,\delta\Big(\frac{\partial u_2}{\partial^0 x_2}\Big). \end{aligned}$$

The result above can be directly related to Equation 6.9 in the following way,

$$\begin{aligned} h\int_{{}_0\Omega} \delta_0\mathbf{A}^T\,{}^t_0S\,{}_0\mathbf{A}\; d\,{}^0\Omega &= h\int_{{}_0\Omega} {}^t_0S_{ij}\,\delta_0\eta_{ij}\,d\,{}^0\Omega \\ &= \delta\hat{\mathbf{u}}^T\Big(h\int_{{}_0\Omega} {}^t_0B^T_{NL}\;{}^t_0S\;{}^t_0B_{NL}\;d\,{}^0\Omega\Big)\hat{\mathbf{u}}. \end{aligned}$$

This means that

$${}_0\mathbf{A} = {}^t_0B_{NL}\;\hat{\mathbf{u}}, \qquad \text{and} \qquad \delta_0\mathbf{A}^T = \delta\hat{\mathbf{u}}^T\;{}^t_0B^T_{NL}.$$

Therefore

$${}_0\mathbf{A} = \begin{bmatrix} \frac{\partial u_1}{\partial^0 x_1} \\ \frac{\partial u_1}{\partial^0 x_2} \\ \frac{\partial u_2}{\partial^0 x_1} \\ \frac{\partial u_2}{\partial^0 x_2} \end{bmatrix} = \underbrace{\begin{bmatrix} {}_0h_{1,1} & 0 & {}_0h_{2,1} & 0 & \dots & {}_0h_{n,1} & 0 \\ {}_0h_{1,2} & 0 & {}_0h_{2,2} & 0 & \dots & {}_0h_{n,2} & 0 \\ 0 & {}_0h_{1,1} & 0 & {}_0h_{2,1} & \dots & 0 & {}_0h_{n,1} \\ 0 & {}_0h_{1,2} & 0 & {}_0h_{2,2} & \dots & 0 & {}_0h_{n,2} \end{bmatrix}}_{{}^t_0B_{NL}} \hat{\mathbf{u}}.$$

If instead, an Updated Lagrangian formulation is pursued, a similar methodology to deduce ${}^{t}_{t}B_L$ and ${}^{t}_{t}B_{NL}$ can be employed. Reference (Bat96, pag. 553) shows the values of these matrices.

The complete linearised principle of virtual displacements requires also a load vector ${}^{t+\Delta t}\mathbf{R}$. As it was said in chapter 3 for the calculation of this vector, it is assumed that the loading is deformation-independent. For that reason, a small displacement formulation can be used. Reference (Bat96, pag. 173-175) calculates the load vector when a linearly varying surface pressure distribution is applied over the edge of a plane-stress element.

Chapter 7

Shell Elements

A shell can be defined as *"a thin body bounded by two nearby surfaces separated by a small distance h. If the bounding surfaces are not closed, then the shell has edges and the distance between such edges is normally large compared with the thickness"*(WT03). When an external force is being applied to a shell structure, mainly two types of internal forces are produced: Membrane forces, and bending forces. Membrane forces act tangent to the midplane of the element; therefore, axial forces and membrane shears are part of this type of internal force. In the other hand, flexural effects, twisting, and transverse shear are considered as part of the bending forces.

Shells are usually curved structures, and due to that curvature remarkable external forces can be supported without fracture or damage. This feature is attributed to the fact that when external loads are applied to egg-like structures (shell structures with high positive non-zero Gaussian curvatures), no inextensional deformation is feasible or at least it is too small to be considered; thus, external loads are supported mainly by the membrane internal forces. With inextensional deformation it is meant that the length and the curvature of any line drawn over the surface of the shell remains unchanged after deformation.

Due to the remarkable stiffness behaviour exhibited by shells and the low amount of material used for it; nowadays, these kind of structures are getting lots of followers in the engineering world. In consequence, this kind of structures are more common everyday, and scientists are keen with the idea of developing efficient and accurate models to predict their behaviour. When attempting to study shell models, *"Although a rectangular system may be inscribed conveniently in certain bodies, deformation carries the straight lines and planes to curved lines and surfaces; rectangular coordinates are deformed*

into arbitrary Curvilinear coordinates"(WT03). For that reason, somehow it is necessary to deal with Curvilinear coordinates.

7.1 A brief introduction to Curvilinear coordinates

The following Curvilinear coordinates explanation to be discussed herein has been based on reference (WT03). An enhanced and clearer explanation of this topic is available therein.

In Figure 7.1 arbitrary Curvilinear coordinates θ^i are going to be expressed in terms of the Cartesian coordinates x_i. Coordinates x_i were chosen simply for easy understanding; however, instead of x_i some other system of coordinates could be chosen.

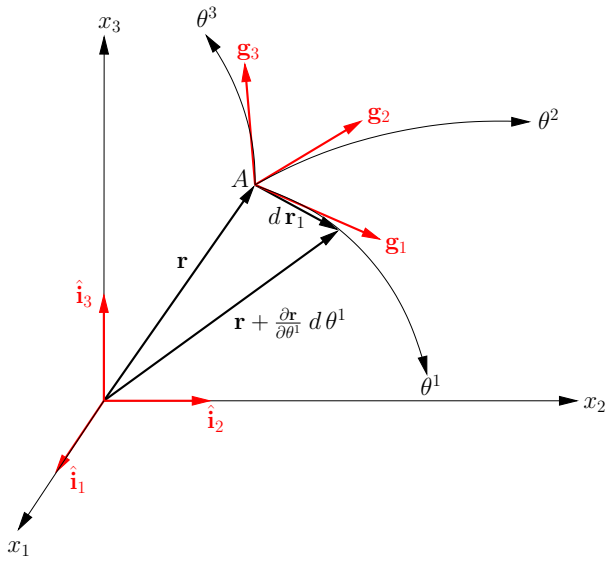

Figure 7.1: Curvilinear coordinate lines and surfaces. Figure taken from (WT03).

The vector $\mathbf{r}$ in Figure 7.1 indicates the position of point A. This position can be described either in Cartesian or Curvilinear coordinates, namely

$$\mathbf{r}_{(x_1,x_2,x_3)} = x_i\,\hat{\mathbf{i}}_i, \qquad \mathbf{r}_{(\theta^1,\theta^2,\theta^3)} = \theta^i\,\mathbf{g}_i.$$

Also, assume that there exist a set of equations relating coordinates x_i in terms of θ^i and vice versa; that is,

$$x_i = x_{i(\theta^1,\theta^2,\theta^3)}, \qquad \theta^i = \theta_{i(x_1,x_2,x_3)}.$$

"A differential change $d\,\theta^i$ is accompanied by a change $d\,\mathbf{r}_i$ tangent to the θ^i line; a change in θ^1 only causes the increment $d\,\mathbf{r}_1$ illustrated in Figure 7.1. It follows that the vector

$$\mathbf{g}_i \cong \frac{\partial \mathbf{r}}{\partial \theta^i} = \frac{\partial x_j}{\partial \theta^i}\hat{\imath}_j$$

is tangent to the θ^i curve"(WT03). The triad of vectors $\mathbf{g}_i$ will be referred to as the covariant base in this text. A triad of vectors $\mathbf{g}^i$ which are normal to the covariant base vectors can also be defined such that,

$$\mathbf{g}^i \cdot \mathbf{g}_j = \delta^i_j, \tag{7.1}$$

where δ^i_j is the Kronecker delta. This symbol can be written with the indices in any position and it will always mean the same; that is,

$$\delta_{ij} = \delta_{ji} = \delta^i_j = \delta^{ij} = \delta^{ji}.$$

Vectors $\mathbf{g}^i$ are referred to as contravariant base vectors in this text. Note that the notation $\mathbf{g}_i$ or $\mathbf{g}^i$ represents a triad of 3–D vectors. In other words,

$$\mathbf{g}_i = \begin{bmatrix} \mathbf{g}_1 \\ \mathbf{g}_2 \\ \mathbf{g}_3 \end{bmatrix}, \qquad \mathbf{g}^i = \begin{bmatrix} \mathbf{g}^1 \\ \mathbf{g}^2 \\ \mathbf{g}^3 \end{bmatrix}.$$

The differential vector $d\,\mathbf{r}$ can be approximated via a first order Taylor approximation as (see Figure 7.1),

$$d\,\mathbf{r} = \frac{\partial \mathbf{r}}{\partial \theta^i} d\,\theta^i = \mathbf{g}_i\, d\,\theta^i, \tag{7.2}$$

and its length $(d\,l)^2$ is given by

$$(d\,l)^2 = d\,\mathbf{r}\; d\,\mathbf{r} = (\mathbf{g}_i \cdot \mathbf{g}_j)\, d\,\theta^i\, d\,\theta^j. \tag{7.3}$$

"Any vector can be expressed as a linear combination of the base vectors $\mathbf{g}_i$ or $\mathbf{g}^i$"(WT03). Figure 7.2 shows a 2–D vector $\mathbf{R}$ expressed as a combination of the Cartesian base vectors $\hat{\imath}_i$, as well as a combination of $\mathbf{g}_i$ and $\mathbf{g}^i$. That is,

$$\mathbf{R} = R_i\,\hat{\imath}_i = R^i\,\mathbf{g}_i = R_i\,\mathbf{g}^i,$$

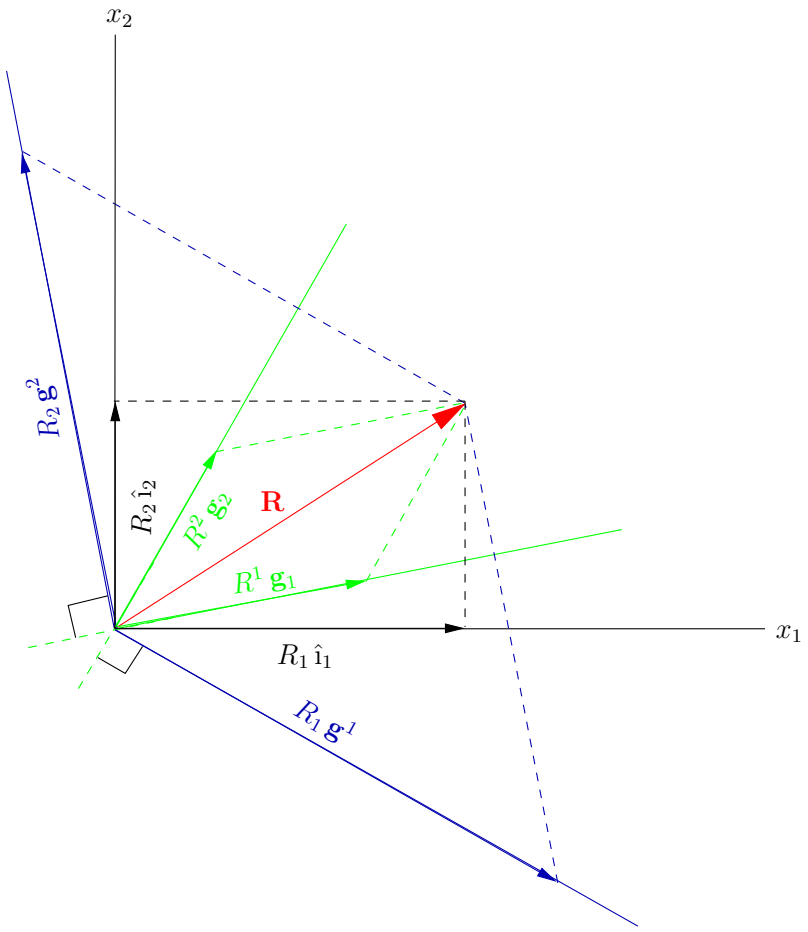

Figure 7.2: Representation of a 2–D vector using Cartesian, covariant, and contravariant bases.

where the length of vectors $\mathbf{g}_i$ and $\mathbf{g}^i$ is not necessarily equal to one. R_i and R^i are known as covariant and contravariant components respectively. In general, the covariant basis is chosen conveniently depending on the problem to be analysed, and after the contravariant basis is calculated via Equation 7.1. In a similar way as stated for vectors, tensors can be expressed in a covariant or a contravariant basis. e.g. The Cauchy stress tensor can be expressed as

$$\tau = \widetilde{\tau}^{ij}\,\mathbf{g}_i\,\mathbf{g}_j, \qquad \tau = \widetilde{\tau}_{ij}\,\mathbf{g}^i\,\mathbf{g}^j.$$

Expression 7.3 represents the basic relation used to define the Green-Lagrange strain tensor in Curvilinear coordinates. e.g. In a large deformation formula-

tion, the Green-Lagrange tensor taking place at time $t + \Delta t$ but measured at time t can be written as

$$ {}^{t+\Delta t}_{t}\widetilde{\epsilon} = {}^{t+\Delta t}_{t}\widetilde{\epsilon}_{ij}\, \mathbf{g}^i\, \mathbf{g}^j, $$

where the covariant component ${}^{t+\Delta t}_{t}\widetilde{\epsilon}_{ij}$ can be computed as

$$ {}^{t+\Delta t}_{t}\widetilde{\epsilon}_{ij} = \frac{1}{2}\Big({}^{t+\Delta t}\mathbf{g}_i \cdot {}^{t+\Delta t}\mathbf{g}_j - {}^{t}\mathbf{g}_i \cdot {}^{t}\mathbf{g}_j \Big). \tag{7.4} $$

As shown in Equation 7.2, the base vectors ${}^{t+\Delta t}\mathbf{g}_i$ and ${}^{t}\mathbf{g}_i$ are given by

$$ {}^{t}\mathbf{g}_i = \frac{\partial\, {}^{t}\mathbf{r}}{\partial\, {}^{t}\theta^i} \qquad \text{and} \qquad {}^{t+\Delta t}\mathbf{g}_i = \frac{\partial({}^{t}\mathbf{r} + \mathbf{u})}{\partial\, {}^{t}\theta^i} $$

respectively. However, the details for the large deformation problem will be addressed later in this chapter.

7.1.1 Minimum Total Potential Energy (MTPE) Principle in Curvilinear Coordinates

In chapter 1 it was said that the Total Potential Energy Π of a system subjected to deformation, equals to the difference between the strain energy $\mathbf{U}$ stored in the deformed object, and the potential energy of the loads $\mathbf{W}$. Namely,

$$ \Pi = \mathbf{U} - \mathbf{W}. $$

Recalling the fact that an expression written in tensorial form holds in any coordinate system, the MTPE Principle can also be expressed in a Curvilinear basis. Thus, the strain energy stored in an object can be quantify as,

$$ \begin{aligned} \mathbf{U} &= \int_V \frac{1}{2}(\widetilde{\tau} \cdot \widetilde{e})\, dV = \frac{1}{2}\int_V (\widetilde{\tau}^{\,mn}\, \mathbf{g}_m\, \mathbf{g}_n) \cdot (\widetilde{e}_{ij}\, \mathbf{g}^i\, \mathbf{g}^j)\, dV \\ &= \frac{1}{2}\int_V \widetilde{\tau}^{\,mn}\, \widetilde{e}_{ij}\, \delta^i_m\, \delta^j_n\, dV = \frac{1}{2}\int_V \widetilde{\tau}^{\,ij}\, \widetilde{e}_{ij}\, dV. \end{aligned} $$

However, a consistent Curvilinear expression for the differential volume dV must be amended. A differential volume dV with dimensions $d\theta^1 \times d\theta^2 \times d\theta^3$ is shown in figure 7.3. This volume can be approached as

$$ \begin{aligned} dV =& d\,\mathbf{r}_1 \cdot (d\,\mathbf{r}_2 \times d\,\mathbf{r}_3) = \frac{\partial \mathbf{r}}{\partial \theta^1}\, d\,\theta^1 \cdot \Big(\frac{\partial \mathbf{r}}{\partial \theta^2}\, d\,\theta^2 \times \frac{\partial \mathbf{r}}{\partial \theta^3}\, d\,\theta^3 \Big) \\ =& \frac{\partial \mathbf{r}}{\partial \theta^1} \cdot \Big(\frac{\partial \mathbf{r}}{\partial \theta^2} \times \frac{\partial \mathbf{r}}{\partial \theta^3} \Big) d\,\theta^1\, d\,\theta^2\, d\,\theta^3 = \mathbf{g}_1 \cdot (\mathbf{g}_2 \times \mathbf{g}_3)\, d\,\theta^1\, d\,\theta^2\, d\,\theta^3, \end{aligned} $$

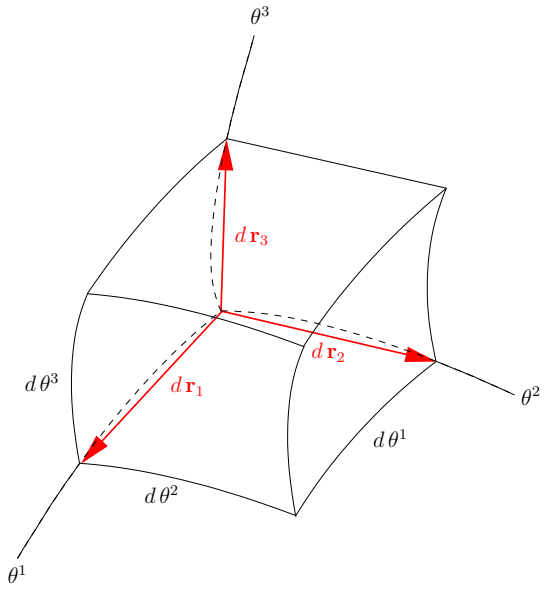

Figure 7.3: Elemental parallelepiped. Figure taken from reference (WT03).

but the product $\mathbf{g}_1 \cdot (\mathbf{g}_2 \times \mathbf{g}_3)$ can be rewritten in the following way:

$$\mathbf{g}_1 \cdot (\mathbf{g}_2 \times \mathbf{g}_3) = \det \begin{vmatrix} \mathbf{g}_1 \\ \mathbf{g}_2 \\ \mathbf{g}_3 \end{vmatrix} = \det \begin{vmatrix} \frac{\partial \mathbf{r}}{\partial \theta^1} \\ \frac{\partial \mathbf{r}}{\partial \theta^2} \\ \frac{\partial \mathbf{r}}{\partial \theta^3} \end{vmatrix} = \det \underbrace{\begin{vmatrix} \frac{\partial r_1}{\partial \theta^1} & \frac{\partial r_2}{\partial \theta^1} & \frac{\partial r_3}{\partial \theta^1} \\ \frac{\partial r_1}{\partial \theta^2} & \frac{\partial r_2}{\partial \theta^2} & \frac{\partial r_3}{\partial \theta^2} \\ \frac{\partial r_1}{\partial \theta^3} & \frac{\partial r_2}{\partial \theta^3} & \frac{\partial r_3}{\partial \theta^3} \end{vmatrix}}_{\text{Jacobian}}.$$

In consequence, $\mathbf{g}_1 \cdot (\mathbf{g}_2 \times \mathbf{g}_3) = \det J$ and therefore,

$$d\,V = \det J\, d\,\theta^1\, d\,\theta^2\, d\,\theta^3.$$

In this way, the Minimun Total Potential Energy principle in Curvilinear coordinates can be written as

$$\Pi = \frac{1}{2} \int_V \widetilde{\tau}^{\,ij}\, \widetilde{e}_{ij}\ \det J\, d\,\theta^1\, d\,\theta^2\, d\,\theta^3 - \mathbf{W}.$$

The term $\mathbf{W}$ can either be expressed in Curvilinear coordinates or in any other system. It depends basically on the problem to be addressed, and the convenience of expressing it either in a Curvilinear or in a Cartesian system of reference.

7.2 Mixed Plate/Shell elements for small displacements

Before facing the problem of shell elements, a different but very close type of element named as plate will be introduced. The biggest difference between plate and shell elements is that in plates elements no in-plane deformations are taken into account. Therefore, only transversal deformations + rotations are considered, see Figure 7.4.

Normally, in plate/shell analysis two main assumptions are made: *"i) the stress through the thickness of the plate/shell is zero, and ii) material particles that are originally on a straight line perpendicular to the mid-surface of the plate/shell remain on a straight line during deformations"*(Bat96). However, when dealing with plates/shells problems, it is common to cope with loads which are perpendicular to the mid-surface of the object. Therefore, it is reasonable to think that the first assumption is far away to be possible, because when a load is applied perpendicular to a surface area, the stress component in that direction do not vanish. Nevertheless, this assumption begins to make more sense once it is known that in spite of the stress component perpendicular to the mid-surface is different than zero, its value is very small compared to the the other stress components generated by the load; for that reason, it is not considered.

7.2.1 Plate Elements

Basically, plates elements can be considered as an extention of beam elements, see Figure 7.4. In consequence, the same assumptions made for beams can be used for plates elements. Reissner-Mindlin plate theory extends Timoshenko beams assumptions to plates elements. Based on this plate theory, the finite element equations for a displacement-based finite element can be easily stated. This displacement-based element is explained by reference (Bat96, pag. 420-424) and will not be discussed in this text. Instead, a mixed plate element will be addressed with the intention of avoiding the shear locking phenomenon explained in section 5.4. The finite element equations will be written in Curvilinear coordinates in order to introduce shell elements.

Going back to Figure 7.1, imagine that the convected natural coordinates r, s, t represent the Curvilinear coordinates $\theta^1, \theta^2, \theta^3$; hence, vector $\mathbf{r}$ can be described either in Cartesian or Curvilinear coordinates as

$$\mathbf{r}_{(x_1,x_2,x_3)} = x_i\,\hat{\mathbf{i}}_i \qquad \mathbf{r}_{(r^1,r^2,r^3)} = r^i\,\mathbf{g}_i,$$

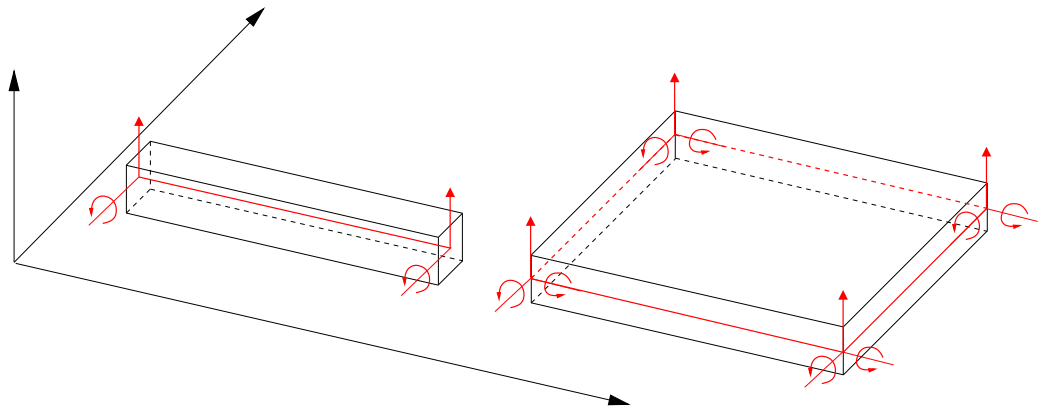

Figure 7.4: Plate element as an extention of a beam element.

where $x_1 = x$, $x_2 = y$, $x_3 = z$, and $r^1 = r$, $r^2 = s$, $r^3 = t$. The natural coordinates will vary from -1 to 1; consequently, the covariant vectors will be given by

$$\mathbf{g}_i = \frac{\partial x_m}{\partial r^i}\,\hat{\imath}_m.$$

In this way, a Curvilinear natural system of reference is being used. The axes r, s, and t are therefore curves, and the coordinates of the object (r, s, t) vary from -1 to 1. In general, when describing an object with a Curvilinear reference system, the coordinates of any point do not coincide with its real length, whereas in a Cartesian system the coordinates (x, y, z) of any point do coincide with its real length.

The small displacement strain tensor $\widetilde{e}_{ij}$ in Curvilinear coordinates can be obtained directly from the Green-Lagrange strain tensor by neglecting the non-linear part of it; that is,

$$\overset{t}{_0}\widetilde{\epsilon}_{ij} = \frac{1}{2}\Big({}^t\mathbf{g}_i \cdot {}^t\mathbf{g}_j - {}^0\mathbf{g}_i \cdot {}^0\mathbf{g}_j\Big),$$

where the time t corresponds to the deformed configuration and time 0 to the undeformed. Thus,

$$\overset{t}{_0}\widetilde{\epsilon}_{ij} = \frac{1}{2}\Big(\frac{\partial {}^t\mathbf{r}}{\partial r^i} \cdot \frac{\partial {}^t\mathbf{r}}{\partial r^j} - \frac{\partial \mathbf{r}}{\partial r^i} \cdot \frac{\partial \mathbf{r}}{\partial r^j}\Big),$$

but ${}^t\mathbf{r} = \mathbf{r} + \mathbf{u}$; hence,

$$
\begin{aligned}
{}^t_0\widetilde{\epsilon}_{ij} &= \frac{1}{2}\Big[\Big(\frac{\partial \mathbf{r}}{\partial r^i} + \frac{\partial \mathbf{u}}{\partial r^i}\Big)\cdot\Big(\frac{\partial \mathbf{r}}{\partial r^j} + \frac{\partial \mathbf{u}}{\partial r^j}\Big) - \Big(\frac{\partial \mathbf{r}}{\partial r^i}\cdot\frac{\partial \mathbf{r}}{\partial r^j}\Big)\Big] \\
&= \frac{1}{2}\Big[\Big(\frac{\partial \mathbf{r}}{\partial r^i}\cdot\frac{\partial \mathbf{r}}{\partial r^j}\Big) + \Big(\frac{\partial \mathbf{r}}{\partial r^i}\cdot\frac{\partial \mathbf{u}}{\partial r^j}\Big) + \Big(\frac{\partial \mathbf{u}}{\partial r^i}\cdot\frac{\partial \mathbf{r}}{\partial r^j}\Big) + \Big(\frac{\partial \mathbf{u}}{\partial r^i}\cdot\frac{\partial \mathbf{u}}{\partial r^j}\Big) - \Big(\frac{\partial \mathbf{r}}{\partial r^i}\cdot\frac{\partial \mathbf{r}}{\partial r^j}\Big)\Big].
\end{aligned}
$$

Adding similar terms and not considering the non-linear term $\left(\frac{\partial \mathbf{u}}{\partial r^i}\cdot\frac{\partial \mathbf{u}}{\partial r^j}\right)$, yields to the small strain tensor

$$
\begin{aligned}
\widetilde{e}_{ij} &= \frac{1}{2}\Big[\Big(\frac{\partial \mathbf{r}}{\partial r^i}\cdot\frac{\partial \mathbf{u}}{\partial r^j}\Big) + \Big(\frac{\partial \mathbf{u}}{\partial r^i}\cdot\frac{\partial \mathbf{r}}{\partial r^j}\Big)\Big] \\
\widetilde{e}_{ij} &= \frac{1}{2}\Big[\Big(\frac{\partial x_m}{\partial r^i}\frac{\partial u_m}{\partial r^j}\Big) + \Big(\frac{\partial u_m}{\partial r^i}\frac{\partial x_m}{\partial r^j}\Big)\Big].
\end{aligned} \tag{7.5}
$$

Remember that in Curvilinear coordinates it is necessary to have a set of equations relating x_i with r^i and vice versa. Towards that goal, and taking into account that a finite element formulation is pursued, the geometry of the element can be interpolated via the base functions $h_{k(r,s)}$. For simplicity, a non-square 4-node flat plate whose midplane lies over the $x-y$ plane will be considered, see Figure 7.5. Equations relating x_i with r^i are therefore:

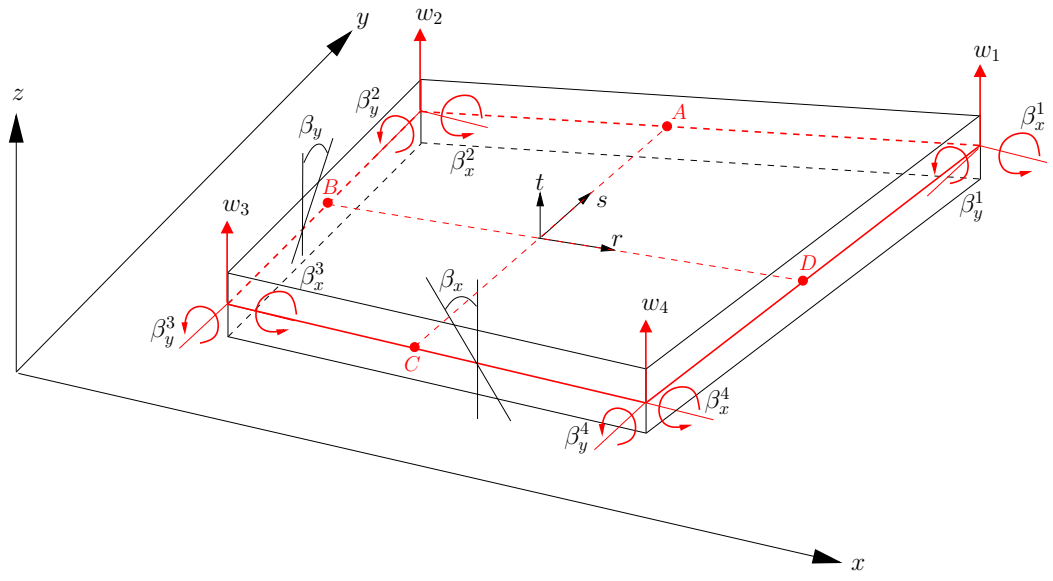

Figure 7.5: 4-node Plate element and its degrees of freedom.

$$x_{(r,s)} = \sum_{k=1}^{4} h_{k(r,s)} x_k, \qquad y_{(r,s)} = \sum_{k=1}^{4} h_{k(r,s)} y_k, \qquad z_{(t)} = \frac{t}{2} h, \tag{7.6}$$

where h represents the thickness of the plate. Due to the Reissner-Mindlin theory, the displacements of the plate can be expressed as

$$u = -z\beta_{x(r,s)}, \qquad v = -z\beta_{y(r,s)}, \qquad w = w_{(r,s)},$$

where β_x and β_y are the rotations about the x and y axes. These rotations have been expressed as a function of the convected natural coordinates r, s because in the finite element formulation they will be interpolated via the shape functions $h_{k(r,s)}$. Because z is a function of t, note that displacements u and v are functions of (r, s, t). In consequence, u and v can be rewritten as,

$$u_{(r,s,t)} = -\frac{t}{2} h\, \beta_{x(r,s)}, \qquad v_{(r,s,t)} = -\frac{t}{2} h\, \beta_{y(r,s)}, \tag{7.7}$$

and rotations β_x, β_y plus the displacement w can be interpolated as

$$\beta_{x(r,s)} = -\sum_{k=1}^{4} h_{k(r,s)}\, \beta_y^k, \qquad \beta_{y(r,s)} = \sum_{k=1}^{4} h_{k(r,s)}\, \beta_x^k, \qquad w_{(r,s)} = \sum_{k=1}^{4} h_{k(r,s)}\, w_k. \tag{7.8}$$

In a small displacement Curvilinear scenario, the principle of virtual displacements for a plate element written in matrix form would be,

$$\int_r \int_s \int_t \begin{bmatrix} \delta\widetilde{e}_{rr} & \delta\widetilde{e}_{ss} & \delta\widetilde{\gamma}_{rs} \end{bmatrix} \widetilde{C}_{\text{bend}} \begin{bmatrix} \widetilde{e}_{rr} \\ \widetilde{e}_{ss} \\ \widetilde{\gamma}_{rs} \end{bmatrix} \det J\, dr\, ds\, dt + \int_r \int_s \int_t \begin{bmatrix} \delta\widetilde{\gamma}_{rt} & \delta\widetilde{\gamma}_{st} \end{bmatrix} \widetilde{C}_{\text{shear}} \begin{bmatrix} \widetilde{\gamma}_{rt} \\ \widetilde{\gamma}_{st} \end{bmatrix} \det J\, dr\, ds\, dt = \delta\hat{\mathbf{u}}^T\, \mathbf{R}. \tag{7.9}$$

Matrices $\widetilde{C}_{\text{bend}}$ and $\widetilde{C}_{\text{shear}}$ represent the bending and shear constitutive material properties written in Curvilinear coordinates. Using the Hook's Law for linear elastic materials, these matrices in a Cartesian system are given by,

$$C_{\text{bend}} = \frac{E}{1-\nu^2} \begin{bmatrix} 1 & \nu & 0 \\ \nu & 1 & 0 \\ 0 & 0 & \frac{1-\nu}{2} \end{bmatrix} \qquad C_{\text{shear}} = \frac{Ek}{2(1+\nu)} \begin{bmatrix} 1 & 0 \\ 0 & 1 \end{bmatrix};$$

however, these matrices have to be written in Curvilinear coordinates. For that purpose, the four order tensor C_{ijkl} has to be transformed into Curvilinear coordinates according to

$$\widetilde{C}^{pqrs} = (\mathbf{g}^p \cdot \hat{\mathbf{i}}_i)(\mathbf{g}^q \cdot \hat{\mathbf{i}}_j)(\mathbf{g}^r \cdot \hat{\mathbf{i}}_k)(\mathbf{g}^s \cdot \hat{\mathbf{i}}_l) C_{ijkl}.$$

Once the tensor $\widetilde{C}^{pqrs}$ is obtained, the bending and a shear components of $\widetilde{C}^{pqrs}$ have to be written in two different matrices $\widetilde{C}_{\text{bend}}$ and $\widetilde{C}_{\text{shear}}$.

Following the same strategy used in the mixed formulation for Timoshenko beams explained in section 5.4, expressions for $\widetilde{e}_{rr}$, $\widetilde{e}_{ss}$, and $\widetilde{\gamma}_{rs}$ calculated from the displacement must be found, this can be achieved as it is shown in reference [pag. 420-424](Bat96). On the other hand, the shear strains $\widetilde{\gamma}_{rt}$ and $\widetilde{\gamma}_{st}$ have to be interpolated independently as,

$$\widetilde{\gamma}_{rt} = \frac{1}{2}(1+s)\widetilde{\gamma}^A_{rt} + \frac{1}{2}(1-s)\widetilde{\gamma}^C_{rt} \tag{7.10}$$

$$\widetilde{\gamma}_{st} = \frac{1}{2}(1+s)\widetilde{\gamma}^D_{st} + \frac{1}{2}(1-s)\widetilde{\gamma}^B_{st} \tag{7.11}$$

"where $\widetilde{\gamma}^A_{rt}$, $\widetilde{\gamma}^C_{rt}$, $\widetilde{\gamma}^D_{st}$, and $\widetilde{\gamma}^B_{st}$ are the (physical) shear strains at points A, B, C, and D (see Figure 7.5) evaluated by the displacement and section rotations in 7.8"(Bat96).

The bending strains $\widetilde{e}_{rr}$, $\widetilde{e}_{ss}$, and $\widetilde{\gamma}_{rs}$ can be computed directly form Equation 7.5; that is,

$$\widetilde{e}_{11} = \widetilde{e}_{rr} = \frac{\partial x_m}{\partial r^1}\frac{\partial u_m}{\partial r^1} = \frac{\partial x_1}{\partial r^1}\frac{\partial u_1}{\partial r^1} + \frac{\partial x_2}{\partial r^1}\frac{\partial u_2}{\partial r^1} + \frac{\partial x_3}{\partial r^1}\frac{\partial u_3}{\partial r^1}$$

$$\widetilde{e}_{22} = \widetilde{e}_{ss} = \frac{\partial x_m}{\partial r^2}\frac{\partial u_m}{\partial r^2} = \frac{\partial x_1}{\partial r^2}\frac{\partial u_1}{\partial r^2} + \frac{\partial x_2}{\partial r^2}\frac{\partial u_2}{\partial r^2} + \frac{\partial x_3}{\partial r^2}\frac{\partial u_3}{\partial r^2}$$

$$\widetilde{\gamma}_{12} = \widetilde{\gamma}_{rs} = \frac{\partial x_m}{\partial r^1}\frac{\partial u_m}{\partial r^2} + \frac{\partial u_m}{\partial r^1}\frac{\partial x_m}{\partial r^2} = \frac{\partial x_1}{\partial r^1}\frac{\partial u_1}{\partial r^2} + \frac{\partial x_2}{\partial r^1}\frac{\partial u_2}{\partial r^2} + \frac{\partial x_3}{\partial r^1}\frac{\partial u_3}{\partial r^2} + \frac{\partial u_1}{\partial r^1}\frac{\partial x_1}{\partial r^2} + \frac{\partial u_2}{\partial r^1}\frac{\partial x_2}{\partial r^2} + \frac{\partial u_3}{\partial r^1}\frac{\partial x_3}{\partial r^2}.$$

The terms $\frac{\partial x_3}{\partial r^1} = \frac{\partial z}{\partial r}$ and $\frac{\partial x_3}{\partial r^2} = \frac{\partial z}{\partial s}$ are equal to zero because z is only a function of t. Therefore, the above expressions reduce to,

$$\widetilde{e}_{rr} = \frac{\partial x}{\partial r}\frac{\partial u}{\partial r} + \frac{\partial y}{\partial r}\frac{\partial v}{\partial r}$$

$$\widetilde{e}_{ss} = \frac{\partial x}{\partial s}\frac{\partial u}{\partial s} + \frac{\partial y}{\partial s}\frac{\partial v}{\partial s}$$

$$\widetilde{\gamma}_{rs} = \frac{\partial x}{\partial r}\frac{\partial u}{\partial s} + \frac{\partial y}{\partial r}\frac{\partial v}{\partial s} + \frac{\partial u}{\partial r}\frac{\partial x}{\partial s} + \frac{\partial v}{\partial r}\frac{\partial y}{\partial s}.$$

If a vector containing all the degrees of freedom of the plate element is defined as,

$$\hat{\mathbf{u}} = \left[\begin{array}{cccccccccccc} w_1 & \beta^1_x & \beta^1_y & w_2 & \beta^2_x & \beta^2_y & w_3 & \beta^3_x & \beta^3_y & w_4 & \beta^4_x & \beta^4_y \end{array}\right],$$

and using Equations 7.6, 7.7, and 7.8; the bending strains $\widetilde{e}_{rr}$, $\widetilde{e}_{ss}$, and $\widetilde{\gamma}_{rs}$ can be easily written as the multiplication of a strain-displacement matrix B and the vector $\hat{\mathbf{u}}$ as stated by Equation 2.2.

In the other hand, shear strains $\widetilde{\gamma}_{rt}$ and $\widetilde{\gamma}_{st}$ are interpolated independently according to Equations 7.10 and 7.11. However, the shear strains evaluated at points A, B, C, and D must be computed from the displacement kinematic relations. Following this strategy, and using Equation 7.5, the shear strains are given by

$$\widetilde{\gamma}_{13} = \widetilde{\gamma}_{rt} = \frac{\partial x_m}{\partial r^1}\frac{\partial u_m}{\partial r^3} + \frac{\partial u_m}{\partial r^1}\frac{\partial x_m}{\partial r^3} = \frac{\partial x_1}{\partial r^1}\frac{\partial u_1}{\partial r^3} + \frac{\partial x_2}{\partial r^1}\frac{\partial u_2}{\partial r^3} + \frac{\partial x_3}{\partial r^1}\frac{\partial u_3}{\partial r^3} + \frac{\partial u_1}{\partial r^1}\frac{\partial x_1}{\partial r^3} + \frac{\partial u_2}{\partial r^1}\frac{\partial x_2}{\partial r^3} + \frac{\partial u_3}{\partial r^1}\frac{\partial x_3}{\partial r^3}$$

$$\widetilde{\gamma}_{23} = \widetilde{\gamma}_{st} = \frac{\partial x_m}{\partial r^2}\frac{\partial u_m}{\partial r^3} + \frac{\partial u_m}{\partial r^2}\frac{\partial x_m}{\partial r^3} = \frac{\partial x_1}{\partial r^2}\frac{\partial u_1}{\partial r^3} + \frac{\partial x_2}{\partial r^2}\frac{\partial u_2}{\partial r^3} + \frac{\partial x_3}{\partial r^2}\frac{\partial u_3}{\partial r^3} + \frac{\partial u_1}{\partial r^2}\frac{\partial x_1}{\partial r^3} + \frac{\partial u_2}{\partial r^2}\frac{\partial x_2}{\partial r^3} + \frac{\partial u_3}{\partial r^2}\frac{\partial x_3}{\partial r^3}.$$

Due to the particular geometry chosen for the plate, $\frac{\partial x_3}{\partial r^1} = \frac{\partial z}{\partial r} = 0$, $\frac{\partial x_3}{\partial r^2} = \frac{\partial z}{\partial s} = 0$, $\frac{\partial x_1}{\partial r^3} = \frac{\partial x}{\partial t} = 0$, and $\frac{\partial x_2}{\partial r^3} = \frac{\partial y}{\partial t} = 0$; hence the above expressions reduce to,

$$\widetilde{\gamma}_{rt} = \frac{\partial x}{\partial r}\frac{\partial u}{\partial t} + \frac{\partial y}{\partial r}\frac{\partial v}{\partial t} + \frac{\partial w}{\partial r}\frac{\partial z}{\partial t}$$

$$\widetilde{\gamma}_{st} = \frac{\partial x}{\partial s}\frac{\partial u}{\partial t} + \frac{\partial y}{\partial s}\frac{\partial v}{\partial t} + \frac{\partial w}{\partial s}\frac{\partial z}{\partial t}.$$

The shear strains $\widetilde{\gamma}^A_{rt}$, $\widetilde{\gamma}^C_{rt}$, $\widetilde{\gamma}^D_{st}$, and $\widetilde{\gamma}^B_{st}$ can be obtained by simply evaluating the above expression at the corresponding points, such that

$$A(r=0,\, s=1,\, t=0) \qquad B(r=-1,\, s=0,\, t=0)$$
$$C(r=0,\, s=-1,\, t=0) \qquad D(r=1,\, s=0,\, t=0).$$

For example $\widetilde{\gamma}^A_{rt}$ can be computed as,

$$\widetilde{\gamma}^A_{rt} = \frac{\partial x}{\partial r}\Big|^A \frac{\partial u}{\partial t}\Big|^A + \frac{\partial y}{\partial r}\Big|^A \frac{\partial v}{\partial t}\Big|^A + \frac{\partial w}{\partial r}\Big|^A \frac{\partial z}{\partial t}\Big|^A,$$

where according to Equations 7.6, 7.7, and 7.8,

$$\frac{\partial x}{\partial r}\Big|^A = \frac{1}{2}(x_1 - x_2), \qquad \frac{\partial y}{\partial r}\Big|^A = \frac{1}{2}(y_1 - y_2), \qquad \frac{\partial z}{\partial t}\Big|^A = \frac{h}{2},$$
$$\frac{\partial u}{\partial t}\Big|^A = \frac{1}{2}(\beta^1_y + \beta^2_y)\frac{h}{2}, \qquad \frac{\partial v}{\partial t}\Big|^A = -\frac{1}{2}(\beta^1_x + \beta^2_x)\frac{h}{2}, \qquad \frac{\partial w}{\partial r}\Big|^A = \frac{1}{2}(w_1 - w_2).$$

Therefore, $\widetilde{\gamma}_{rt}^{A}$ is given by

$$\widetilde{\gamma}_{rt}^{A} = \frac{h}{8}(x_1 - x_2)(\beta_y^1 + \beta_y^2) - \frac{h}{8}(y_1 - y_2)(\beta_x^1 + \beta_x^2) + \frac{h}{4}(w_1 - w_2).$$

The remaining shear strains at points B, C, and D can be calculated in the same way. Once all the terms appearing in Equation 7.9 are calculated, the stiffness matrix of the element can be simply assembled in the same way as it has been shown in the previous chapters.

7.2.2 Shell Elements

The small diplacement formulation presented by reference (Bat96) for this kind of elements represents the basis for a large displacement shell formulation. For that reason, not many details will be discussed in this section as they will be included as part of the large displacement shell formulation, see section 7.3.

In a finite element formulation, displacement-based shell elements also suffer from the shear locking phenomenon. Indeed, when dealing with curved elements, the element can also lock because some spurious membrane strains may appear. Therefore, a mixed formulation is suggested to overtake this situation. The strategy to follow is the same followed so far: *"the objective is to interpolate the membrane and shear strains components independently and tie these interpolations to the usual displacements interpolations"*(Bat96). In a Curvilinear natural reference system, the membrane strain components are $\widetilde{e}_{rr}$, $\widetilde{e}_{ss}$, $\widetilde{e}_{rs}$, whereas the shear strains are $\widetilde{e}_{rt}$ and $\widetilde{e}_{st}$. The details of this small displacement curvilinear element are discussed by reference (Bat96, pag. 443-446).

7.3 Mixed Shell Elements under the large displacement hypothesis

From the very beginning of this study, the biggest and most important objective has been the formulation, implementation, and validation of a shell element based on a large displacement hypothesis. For that purpose, several formulations are available in the literature, see references (APK02), (Fel08), (ZT00), (WT03), and (Cri01). However, throughout this study, reference (Bat96) has been followed in order to get to the shell formulation proposed by K.J. Bathe. Towards that aim, it has been considered as convenient first

to fully understand the finite element formulation proposed by K.J. Bathe for bars, beams, and plane stress elements before arriving to shell elements.

As it was said in the previous sections, a mixed formulation usually represents a better and a more efficient way to predict the behaviour of shell elements. Therefore, a 4-node mixed shell element has been chosen to be implemented, see Figure 7.6. The element has been proposed by K.J. Bathe and E.N. Devorkin in reference (DB84), and exhibits the following characteristics: *"(i) The element is able to represent the six rigid body modes, (ii) it also can approximate the Kirchhoff-Love hypothesis of negligible shear deformation effects and can be used for thin shells, and (iii) the element does not contain spurious energy modes"*(DB84). When talking about the six rigid

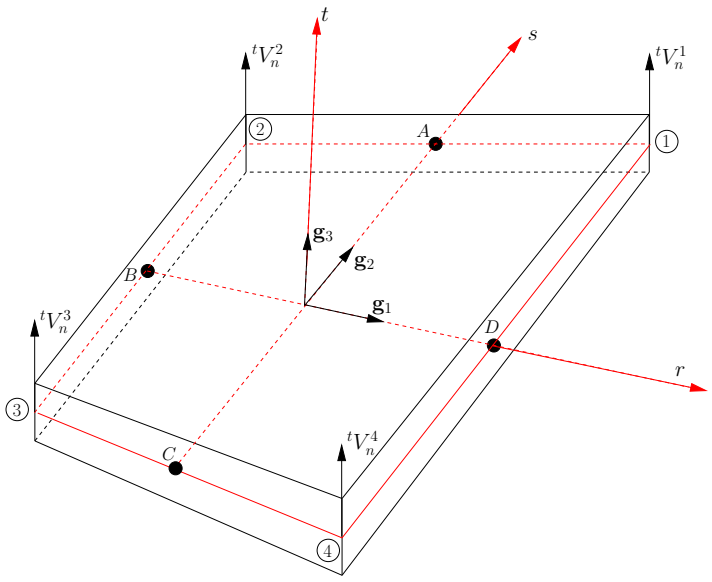

Figure 7.6: 4-node shell element. Figure taken from reference (Bat96)

body modes, it is meant that zero strains are obtained when any node of the element is subjected to rigid body motions.

In section 5.4 it was shown that when dealing with a mixed formulation the Lagrange Multiplier method can be used to modify the functional to be minimised. The modified functional Π^* written in Curvilinear coordinates under a Total Lagrangian (TL) large displacement formulation can be written

as,

$$\Pi^* = \frac{1}{2}\int_{{}^0V} {}_0^{t+\Delta t}\widetilde{S}^{ij}\ {}_0^{t+\Delta t}\widetilde{\epsilon}_{ij}\, d\,{}^0V + \int_{{}^0V} \underbrace{{}_0^{t+\Delta t}\widetilde{S}^{13}}_{\lambda_{13}}({}_0^{t+\Delta t}\widetilde{\epsilon}_{13} - {}_0^{t+\Delta t}\widetilde{\epsilon}^{\,\mathrm{DI}}_{13})\, d\,{}^0V + \int_{{}^0V} \underbrace{{}_0^{t+\Delta t}\widetilde{S}^{23}}_{\lambda_{23}}({}_0^{t+\Delta t}\widetilde{\epsilon}_{23} - {}_0^{t+\Delta t}\widetilde{\epsilon}^{\,\mathrm{DI}}_{23})\, d\,{}^0V - \mathbf{W}.$$

However, in section 5.4 it was also explained that instead of following the formal rigorous mathematical procedure to obtain a mixed stiffness matrix, a shortcut (which in reality represents the same exact procedure) will lead to the same results. The shortcut suggests to interpolate the shear strains ${}_0^{t+\Delta t}\widetilde{\epsilon}_{13}$ and ${}_0^{t+\Delta t}\widetilde{\epsilon}_{23}$ in an independent way, and tie the interpolations to the expressions obtained for ${}_0^{t+\Delta t}\widetilde{\epsilon}^{\,\mathrm{DI}}_{13}$ and ${}_0^{t+\Delta t}\widetilde{\epsilon}^{\,\mathrm{DI}}_{23}$ using the kinematic displacement-based equations. *"The result is that the stiffness matrix is then obtained corresponding to only the same nodal point variables (displacements and section rotations) as are used for the displacement-based elements"*(Bat96). The independent interpolations to be used for the shear strains are,

$${}_0^{t+\Delta t}\widetilde{\epsilon}_{13} = \frac{1}{2}(1+s)\,{}_0^{t+\Delta t}\widetilde{\epsilon}^{A}_{13} + \frac{1}{2}(1-s)\,{}_0^{t+\Delta t}\widetilde{\epsilon}^{C}_{13} \tag{7.12}$$

$${}_0^{t+\Delta t}\widetilde{\epsilon}_{23} = \frac{1}{2}(1+r)\,{}_0^{t+\Delta t}\widetilde{\epsilon}^{D}_{23} + \frac{1}{2}(1-r)\,{}_0^{t+\Delta t}\widetilde{\epsilon}^{B}_{23}, \tag{7.13}$$

where ${}_0^{t+\Delta t}\widetilde{\epsilon}^{A}_{13}$, ${}_0^{t+\Delta t}\widetilde{\epsilon}^{B}_{23}$, ${}_0^{t+\Delta t}\widetilde{\epsilon}^{C}_{13}$, and ${}_0^{t+\Delta t}\widetilde{\epsilon}^{D}_{23}$ are the shear strains obtained from the kinematic displacement-based equations and evaluated at points A, B, C, and D.

The geometry of the shell element can be interpolated as,

$${}^t x_i = \sum_{k=1}^{4} h_{k(r,s)}\, {}^t x_i^k + \sum_{k=1}^{4} \frac{t}{2} a_k h_{k(r,s)}\, {}^t V_{ni}^k, \tag{7.14}$$

where t represents any deformation configuration taking place during the deformation process. a_k is the thickness of the element measured along vector ${}^t\mathbf{V}_n^k$; in consequence, vector ${}^t\mathbf{V}_n^k$ is a director vector not necessarily normal to the mid-surface of the element, see Figure 7.7.

Remember that in a large displacement formulation the displacements ${}^t u_i$ and u_i are given by,

$${}^t u_i = {}^t x_i - {}^0 x_i \qquad u_i = {}^{t+\Delta t} x_i - {}^t x_i.$$

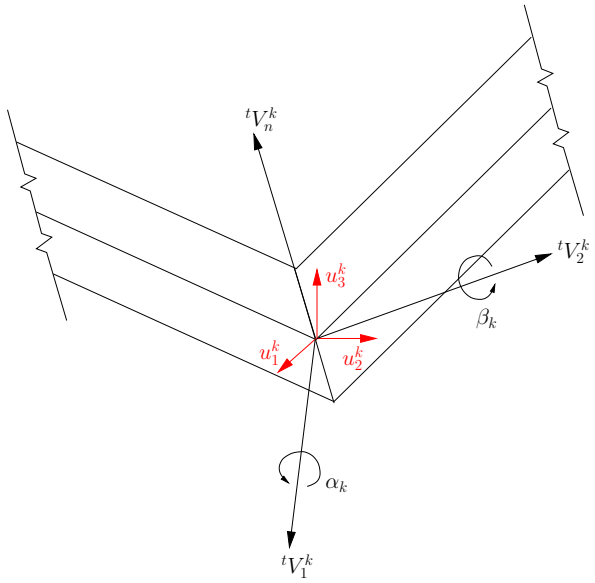

Figure 7.7: Local system of orthogonal vectors. Figure taken from reference (Bat96)

Thus, according to Equation 7.14 the displacements ${}^tu_i$ and u_i can be rewritten as,

$$ {}^tu_i = \sum_{k=1}^{4} h_{k(r,s)}\, {}^tu_i^k + \sum_{k=1}^{4} \frac{t}{2} a_k h_{k(r,s)} \left({}^tV_{ni}^k - {}^0V_{ni}^k \right) \tag{7.15} $$

$$ u_i = \sum_{k=1}^{4} h_{k(r,s)}\, u_i^k + \sum_{k=1}^{4} \frac{t}{2} a_k h_{k(r,s)} \underbrace{\left({}^{t+\Delta t}V_{ni}^k - {}^tV_{ni}^k \right)}_{V_{ni}^k}. \tag{7.16} $$

"The vector components of V_{ni}^k are expressed in terms of rotations about two vectors that are orthogonal to ${}^t\mathbf{V}_n^k$. These two vectors ${}^t\mathbf{V}_1^k$ and ${}^t\mathbf{V}_2^k$ are defined at time 0 using

$$ {}^0\mathbf{V}_1^k = \frac{\hat{\jmath} \times {}^0\mathbf{V}_n^k}{||\hat{\jmath} \times {}^0\mathbf{V}_n^k||_2} \qquad \text{and} \qquad {}^0\mathbf{V}_2^k = {}^0\mathbf{V}_n^k \times {}^0\mathbf{V}_1^k, $$

where ${}^0\mathbf{V}_1^k = \hat{\mathbf{k}}$ if ${}^0\mathbf{V}_n^k$ is parallel to $\hat{\jmath}$"(Bat96). Now it is necessary to find a way to express the rotations that vector ${}^0\mathbf{V}_n^k$ suffers due to the deformation process in terms of the ${}^t\mathbf{V}_1^k$ and ${}^t\mathbf{V}_2^k$. For that purpose, the formulation proposed by reference (Arg82) will be followed. Consequently, almost the literal

procedure explained by reference (Arg82) will be written in this text in order to clarify this concept and gain a better understanding.

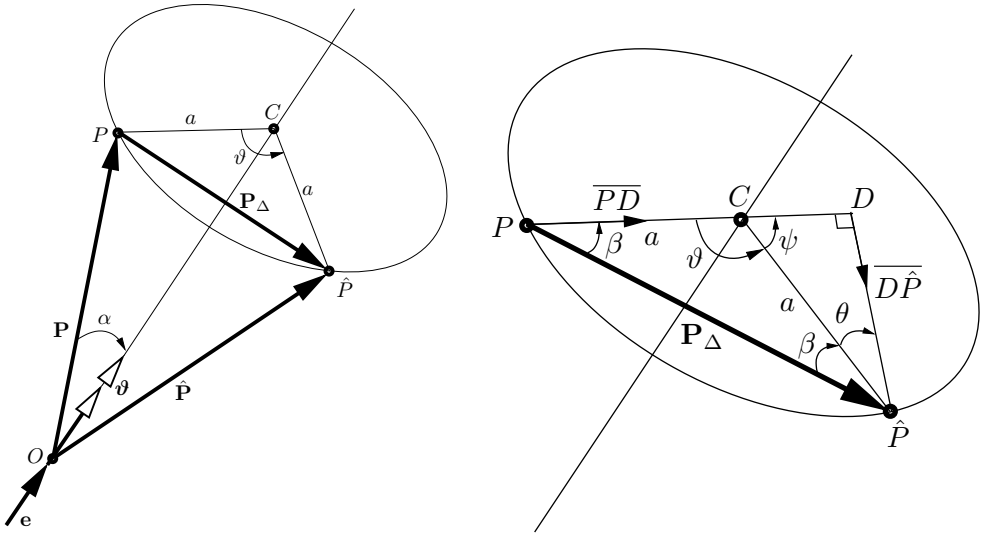

(a) rotational pseudo-vector $\boldsymbol{\vartheta}$ (b) Auxiliary construction to obtain $\mathbf{P}_\Delta$

Figure 7.8: Construction of a transformation matrix for an arbitrary rotational pseudo-vector $\boldsymbol{\vartheta}$. Figure taken from reference (Arg82).

Imagine that a finite rotation with magnitude ϑ is taking place around an axis whose director vector is $\mathbf{e}$, see Figure 7.8a. Subsequently, a pseudo-rotational vector $\boldsymbol{\vartheta} = \vartheta\mathbf{e}$ is defined. Its components in any orthogonal system are given by: e.g. in a Cartesian system,

$$\boldsymbol{\vartheta} = \vartheta_x \hat{\imath} + \vartheta_y \hat{\jmath} + \vartheta_z \hat{\mathrm{k}};$$

however, any other orthogonal system could have been chosen. Only for small deformations, the components ϑ_x, ϑ_y, and ϑ_z can be interpreted as rotations about the x, y, and z axes respectively.

Now *"consider a vector* $\mathbf{P}$ *which as a result of the application of* $\boldsymbol{\vartheta}$ *is transported to a new position* $\hat{\mathbf{P}}$*"*(Arg82); therefore, in accordance with Figure 7.8a it is possible to state that,

$$\hat{\mathbf{P}} = \mathbf{P} + \mathbf{P}_\Delta. \tag{7.17}$$

Figure 7.8b shows an auxiliary construction to quantify $\mathbf{P}_\Delta$. A line $\overline{D\hat{P}}$ has been drawn normal to line $\overline{PC}$. In consequence, vector $\overline{D\hat{P}}$ is also normal to

the plane OPC and points in the direction $(\mathbf{e} \times \mathbf{P})$. Moreover, it can be easily seen that,

$$\mathbf{P}_\Delta = \overline{PD} + \overline{D\hat{P}}.$$

Vectors $\overline{PD}$ and $\overline{D\hat{P}}$ can be quantified in the following way: According to Figure 7.8b, the following relations can be stated:

$$90 + \beta + \beta + \theta = 180 \qquad 90 + \psi + \theta = 180 \qquad \vartheta + \psi = 180.$$

Equating these expressions yields to,

$$\theta = \vartheta - 90, \tag{7.18}$$

and because the triangle $\hat{P}DC$ is rectangular, the magnitude of $\overline{D\hat{P}}$ is given by

$$||\overline{D\hat{P}}|| = a\,\cos\theta = a\,\cos\left(\vartheta - 90\right) = a\,\sin\vartheta.$$

On the other hand, the magnitude of $(\mathbf{e} \times \mathbf{P})$ is equal to

$$||(\mathbf{e} \times \mathbf{P})|| = 1 \cdot ||\mathbf{P}||\sin\alpha = ||\mathbf{P}||\frac{a}{||\mathbf{P}||} = a;$$

therefore,

$$\overline{D\hat{P}} = \frac{(\mathbf{e} \times \mathbf{P})}{a}\,a\,\sin\vartheta = \frac{\sin\vartheta}{\vartheta}(\boldsymbol{\vartheta} \times \mathbf{P}) \qquad \text{due to} \qquad \mathbf{e} = \frac{\boldsymbol{\vartheta}}{\vartheta}.$$

In the same way, vector $\overline{PD}$ needs to be quantified. $\overline{PD}$ is perpendicular to $(\mathbf{e} \times \mathbf{P})$ as well as perpendicular to $\mathbf{e}$, see Figure 7.8a. The direction of $\overline{PD}$ is therefore given by the product $\mathbf{e} \times (\mathbf{e} \times \mathbf{P})$. Furthermore, due to the fact that $||(\mathbf{e} \times \mathbf{P})|| = a$ and $||\mathbf{e}|| = 1$, the magnitude of the director vector $||\mathbf{e} \times (\mathbf{e} \times \mathbf{P})|| = a$. Looking at Figure 7.8b, it can be noted that the magnitude of $\overline{PD}$ is given by,

$$||\overline{PD}|| = a + a\sin\theta$$

and using Equation 7.18 yields to

$$||\overline{PD}|| = a - a\sin(\vartheta - 90) = a - a\cos\vartheta = a(1 - \cos\vartheta) = 2\sin^2(\vartheta/2)a.$$

Finally, vector $\overline{PD}$ can be expressed as,

$$\begin{aligned}\overline{PD} &= 2\sin^2(\vartheta/2)a\,\frac{(\mathbf{e} \times (\mathbf{e} \times \mathbf{P}))}{a} = 2\sin^2(\vartheta/2)(\boldsymbol{\vartheta} \times (\boldsymbol{\vartheta} \times \mathbf{P}))\frac{1}{\vartheta}\frac{1}{\vartheta} \\ &= 2\sin^2(\vartheta/2)(\boldsymbol{\vartheta} \times (\boldsymbol{\vartheta} \times \mathbf{P}))\frac{\frac{1}{2}\frac{1}{2}}{\frac{\vartheta}{2}\frac{\vartheta}{2}} = \frac{1}{2}\frac{\sin^2(\vartheta/2)}{(\vartheta/2)^2}(\boldsymbol{\vartheta} \times (\boldsymbol{\vartheta} \times \mathbf{P})).\end{aligned}$$

Coming back to Equation 7.17, it can be rewritten as,

$$\hat{\mathbf{P}} = \mathbf{P} + \frac{\sin\vartheta}{\vartheta}(\boldsymbol{\vartheta} \times \mathbf{P}) + \frac{1}{2}\frac{\sin^2(\vartheta/2)}{(\vartheta/2)^2}(\boldsymbol{\vartheta} \times (\boldsymbol{\vartheta} \times \mathbf{P})). \tag{7.19}$$

Thus, defining the auxiliary matrix

$$S = \begin{bmatrix} 0 & -\theta_z & \theta_y \\ \theta_z & 0 & -\theta_x \\ -\theta_y & \theta_x & 0 \end{bmatrix},$$

and taking into account that $\boldsymbol{\vartheta} \times \mathbf{P} = S\mathbf{P}$ and $\boldsymbol{\vartheta} \times (\boldsymbol{\vartheta} \times \mathbf{P}) = S^2\mathbf{P}$; Equation 7.19 can be re-expressed as,

$$\hat{\mathbf{P}} = \mathbf{P} + \frac{\sin\vartheta}{\vartheta} S\mathbf{P} + \frac{1}{2}\frac{\sin^2(\vartheta/2)}{(\vartheta/2)^2} S^2\mathbf{P} = T_{(\boldsymbol{\vartheta})}\,\mathbf{P}, \tag{7.20}$$

where $T_{(\boldsymbol{\vartheta})}$ is given by,

$$T_{(\boldsymbol{\vartheta})} = I_3 + \frac{\sin\vartheta}{\vartheta} S + \frac{1}{2}\frac{\sin^2(\vartheta/2)}{(\vartheta/2)^2} S^2.$$

Taking up again the shell formulation, vectors ${}^{t+\Delta t}\mathbf{V}_n$ and ${}^{t}\mathbf{V}_n$ appearing in Equation 7.16 can be associated with vectors $\hat{\mathbf{P}}$ and $\mathbf{P}$ respectively. Therefore,

$${}^{t+\Delta t}\mathbf{V}_n = T_{(\boldsymbol{\vartheta})}\,{}^{t}\mathbf{V}_n, \tag{7.21}$$

but also

$$\mathbf{V}_n = {}^{t+\Delta t}\mathbf{V}_n - {}^{t}\mathbf{V}_n = \hat{\mathbf{P}} - \mathbf{P} = T_{(\boldsymbol{\vartheta})}\,{}^{t}\mathbf{V}_n - {}^{t}\mathbf{V}_n = {}^{t}\mathbf{V}_n(T_{(\boldsymbol{\vartheta})} - I_3)$$

$$\mathbf{V}_n = {}^{t}\mathbf{V}_n\Big(\frac{\sin\vartheta}{\vartheta} S + \frac{1}{2}\frac{\sin^2(\vartheta/2)}{(\vartheta/2)^2} S^2\Big). \tag{7.22}$$

In this shell formulation it is assumed that no rotations about vector $\mathbf{V}_n$ take place. **Although this rotations do exist, they are usually too small to be considered**. In other words, only rotations about vectors ${}^{t}\mathbf{V}_1$ and ${}^{t}\mathbf{V}_2$, which are orthogonal to ${}^{t}\mathbf{V}_n$ are considered. *"Let α_k and β_k be the rotations of the director vector $\mathbf{V}_n^k$ about vectors ${}^{t}\mathbf{V}_1^k$ and ${}^{t}\mathbf{V}_2^k$ in the configuration at time t"*(Bat96). Remember that vector $\boldsymbol{\vartheta}_k$ can be considered as a rotation vector only for small rotations α_k and β_k. Including this assumption into the current shell formulation, a small strain but a large displacement scenario will be achieved.

ϑ_k represents the magnitude of $\boldsymbol{\vartheta}_k$ and, therefore, it can be calculated as,

$$\vartheta_k = (\alpha_k^2 + \beta_k^2)^{\frac{1}{2}}.$$

Consequently,

$$S_k = \begin{bmatrix} 0 & 0 & \beta_k \\ 0 & 0 & -\alpha_k \\ -\beta_k & \alpha_k & 0 \end{bmatrix},$$

and because small angles α_k and β_k are considered,

$$T_{(\boldsymbol{\vartheta}_k)} = I_3 + S_k + \frac{1}{2}S_k^2 \qquad \text{due to} \qquad \sin\vartheta_k \approx \vartheta_k.$$

Hence,

$$\mathbf{V}_n^k = {}^t\mathbf{V}_n^k\Big(S_k + \frac{1}{2}S_k^2\Big)$$
$$\mathbf{V}_n^k = -{}^t\mathbf{V}_2^k\,\alpha_k + {}^t\mathbf{V}_1^k\,\beta_k - \frac{1}{2}(\alpha_k^2 + \beta_k^2){}^t\mathbf{V}_n^k.$$

In this way, the displacements described by Equation 7.16 can be re-expressed as,

$$u_i = \sum_{k=1}^{4} h_{k(r,s)}\,u_i^k + \sum_{k=1}^{4} \frac{t}{2}a_k h_{k(r,s)}\Big[- {}^tV_{2i}^k\,\alpha_k + {}^tV_{1i}^k\,\beta_k - \frac{1}{2}(\alpha_k^2 + \beta_k^2){}^tV_{ni}^k\Big].$$

The non-linear term in the previous equation was neglected due to the fact that small rotations for the angles α_k and β_k are being considered. Hence,

$$u_i = \sum_{k=1}^{4} h_{k(r,s)}\,u_i^k + \sum_{k=1}^{4} \frac{t}{2}a_k h_{k(r,s)}\Big[- {}^tV_{2i}^k\,\alpha_k + {}^tV_{1i}^k\,\beta_k\Big]. \tag{7.23}$$

Once the degrees o freedom u_k, α_k, and β_k are somehow obtained, vector ${}^{t+\Delta t}\mathbf{V}_n^k$ can be calculated via Equation 7.21. An incremental TL finite Element formulation will be used to get the values of the dofs u_k, α_k, and β_k.

7.3.1 Total Lagrangian Formulation

In a TL formulation, the virtual work principle in a Curvilinear reference system can be written as,

$$\int_{{}^0V} {}_0^{t+\Delta t}\widetilde{S}^{\,ij}\,\delta\,{}_0^{t+\Delta t}\widetilde{\epsilon}_{ij}\,d\,{}^0V = {}^{t+\Delta t}R,$$

where

$$ {}^{t+\Delta t}_{0}\widetilde{S}^{ij} = {}^{t}_{0}\widetilde{S}^{ij} + {}_{0}\widetilde{S}^{ij}, \qquad {}^{t+\Delta t}_{0}\widetilde{\epsilon}^{ij} = {}^{t}_{0}\widetilde{\epsilon}^{ij} + {}_{0}\widetilde{\epsilon}^{ij}, \qquad {}_{0}\widetilde{\epsilon}^{ij} = {}_{0}\widetilde{e}_{ij} + {}_{0}\widetilde{\eta}_{ij}. $$

In the same way, the linearised principle of virtual work is

$$ \int_{{}_0V} {}^{t}_{0}\widetilde{C}^{ijrs}\, {}_{0}\widetilde{e}_{rs}\, \delta_0\widetilde{e}_{ij}\, d\,{}^0V + \int_{{}_0V} {}^{t}_{0}\widetilde{S}_{ij}\, \delta_0\widetilde{\eta}_{ij}\, d\,{}^0V = {}^{t+\Delta t}R - \int_{{}_0V} {}^{t}_{0}\widetilde{S}_{ij}\, \delta_0\widetilde{e}_{ij}; \quad (7.24) $$

such that,

$$ {}^{t}_{0}\widetilde{S}^{ij} = {}^{t}_{0}\widetilde{C}^{ijrs}\, {}^{t}_{0}\widetilde{\epsilon}_{rs}. $$

Similarly as it was stated in Equation 7.4, the covariant component of the Green-Lagrange strain tensor taking place at time $t+\Delta t$ but measured at time 0 can be written as,

$$ {}^{t+\Delta t}_{0}\widetilde{\epsilon}_{ij} = \frac{1}{2}\Big({}^{t+\Delta t}\mathbf{g}_i \cdot {}^{t+\Delta t}\mathbf{g}_j - {}^{0}\mathbf{g}_i \cdot {}^{0}\mathbf{g}_j\Big); $$

where,

$$ {}^{0}\mathbf{g}_i = \frac{\partial\, {}^{0}\mathbf{x}}{\partial\, r^i} = \frac{\partial\, {}^{0}x_m}{\partial\, r^i} = {}^{0}g_{mi} $$

and

$$ {}^{t+\Delta t}\mathbf{g}_i = \frac{\partial({}^{t}\mathbf{x} + \mathbf{u})}{\partial\, r^i} = \frac{\partial({}^{t}x_m + u_m)}{\partial\, r^i} = {}^{t+\Delta t}g_{mi}. $$

Note that $r^i = r^1, r^2, r^3$ represents the convected natural system such that $r^1 = r$, $r^2 = s$, and $r^3 = t$.

The Green-Lagrange strain tensor is therefore,

$$ \begin{aligned}
{}^{t+\Delta t}_{0}\widetilde{\epsilon}_{ij} &= \frac{1}{2}\Big[\Big(\frac{\partial^t\mathbf{x}}{\partial r^i} + \frac{\partial\mathbf{u}}{\partial r^i}\Big)\cdot\Big(\frac{\partial^t\mathbf{x}}{\partial r^j} + \frac{\partial\mathbf{u}}{\partial r^j}\Big) - \frac{\partial^0\mathbf{x}}{\partial r^i}\frac{\partial^0\mathbf{x}}{\partial r^j}\Big] \\
{}^{t+\Delta t}_{0}\widetilde{\epsilon}_{ij} &= \frac{1}{2}\Big[{}^{t}\mathbf{g}_i \cdot {}^{t}\mathbf{g}_j + {}^{t}\mathbf{g}_i\frac{\partial\mathbf{u}}{\partial r^j} + \frac{\partial\mathbf{u}}{\partial r^i}{}^{t}\mathbf{g}_j + \frac{\partial\mathbf{u}}{\partial r^i}\frac{\partial\mathbf{u}}{\partial r^j} - {}^{0}\mathbf{g}_i \cdot {}^{0}\mathbf{g}_j\Big] \\
{}^{t+\Delta t}_{0}\widetilde{\epsilon}_{ij} &= \underbrace{\frac{1}{2}\Big[{}^{t}\mathbf{g}_i \cdot {}^{t}\mathbf{g}_j - {}^{0}\mathbf{g}_i \cdot {}^{0}\mathbf{g}_j\Big]}_{{}^{t}_{0}\widetilde{\epsilon}_{ij}} + \underbrace{\frac{1}{2}\Big[{}^{t}\mathbf{g}_i\frac{\partial\mathbf{u}}{\partial r^j} + \frac{\partial\mathbf{u}}{\partial r^i}{}^{t}\mathbf{g}_j\Big]}_{{}_{0}\widetilde{e}_{ij}} + \underbrace{\frac{1}{2}\Big[\frac{\partial\mathbf{u}}{\partial r^i}\frac{\partial\mathbf{u}}{\partial r^j}\Big]}_{{}_{0}\widetilde{\eta}_{ij}};
\end{aligned} $$

in this way,

$$ {}_0\widetilde{e}_{ij} = \frac{1}{2}\Big[{}^t\mathbf{g}_i \frac{\partial \mathbf{u}}{\partial r^j} + \frac{\partial \mathbf{u}}{\partial r^i} {}^t\mathbf{g}_j \Big] \tag{7.25} $$

$$ {}_0\widetilde{e}_{ij} = \frac{1}{2}\Big[\frac{\partial ({}^0\mathbf{x} + {}^t\mathbf{u})}{\partial\, r^i} \frac{\partial \mathbf{u}}{\partial r^j} + \frac{\partial \mathbf{u}}{\partial r^i} \frac{\partial ({}^0\mathbf{x} + {}^t\mathbf{u})}{\partial\, r^j} \Big] $$

$$ {}_0\widetilde{e}_{ij} = \frac{1}{2}\Big[\frac{\partial {}^0\mathbf{x}}{\partial\, r^i} \frac{\partial \mathbf{u}}{\partial r^j} + \frac{\partial \mathbf{u}}{\partial r^i} \frac{\partial {}^0\mathbf{x}}{\partial\, r^j} + \underbrace{\frac{\partial {}^t\mathbf{u}}{\partial\, r^i} \frac{\partial \mathbf{u}}{\partial r^j} + \frac{\partial \mathbf{u}}{\partial r^i} \frac{\partial {}^t\mathbf{u}}{\partial\, r^j}}_{\text{initial displacement effect}} \Big] \tag{7.26} $$

$$ {}_0\widetilde{\eta}_{ij} = \frac{1}{2}\Big[\frac{\partial \mathbf{u}}{\partial r^i} \frac{\partial \mathbf{u}}{\partial r^j} \Big]. \tag{7.27} $$

The equations above can be directly used to quantify the strain terms appearing in the linearised principle of virtual work, see Equation 7.24.

A general expression for ${}_0\widetilde{e}_{ij}$

A vector containing all the degrees of freedom of the element is defined as,

$$ \hat{\mathbf{u}}^T = \begin{bmatrix} \dots & u_1^k & u_2^k & u_3^k & \alpha_k & \beta_k & \dots \end{bmatrix} \qquad \text{with} \qquad k = 1, 2, 3, 4. $$

There are 5 dofs at each node of the shell element; therefore, vector $\hat{\mathbf{u}}$ contains a total of 20 degrees of freedom.

${}_0\widetilde{e}_{ij}$ will be written as the product of a matrix B_L and the vector $\hat{\mathbf{u}}$; such that,

$$ \begin{bmatrix} {}_0\widetilde{e}_{11} \\ {}_0\widetilde{e}_{22} \\ {}_0\widetilde{e}_{33} \\ 2\,{}_0\widetilde{e}_{12} \\ 2\,{}_0\widetilde{e}_{13} \\ 2\,{}_0\widetilde{e}_{23} \end{bmatrix} = \begin{bmatrix} {}^t_0B_{L11} \\ {}^t_0B_{L22} \\ {}^t_0B_{L33} \\ {}^t_0B_{L12} \\ {}^t_0B_{L13} \\ {}^t_0B_{L23} \end{bmatrix} \hat{\mathbf{u}}, \tag{7.28} $$

where ${}^t_0B_{Lij}$ are matrices of size 1×20. In order to get those matrices, Equation 7.25 can be used; that is,

$$ {}_0\widetilde{e}_{ii} = \frac{1}{2}\Big[{}^t\mathbf{g}_i \frac{\partial \mathbf{u}}{\partial r^i} + \frac{\partial \mathbf{u}}{\partial r^i} {}^t\mathbf{g}_i \Big] = \frac{\partial \mathbf{u}}{\partial r^i} {}^t\mathbf{g}_i = \frac{\partial u_m}{\partial r^i} {}^t g_{mi}. $$

Using Equation 7.23, the above expression can be rewritten as,

$$ {}_0\widetilde{e}_{ii} = \sum_{k=1}^{4} h_{k,i}\, u_m^k\, {}^t g_{mi} + \sum_{k=1}^{4} \frac{t}{2} a_k h_{k,i} \Big[-({}^tV_{2m}^k\, {}^t g_{mi})\, \alpha_k + ({}^tV_{1m}^k\, {}^t g_{mi})\, \beta_k \Big], \tag{7.29} $$

where $h_{k,i} = \frac{\partial h_{(r,s)}}{\partial r^i}$.

Equation 7.29 can be particularised as,

$$
\begin{aligned}
{}_0\widetilde{e}_{11} &= \sum_{k=1}^{4} h_{k,1}\, u_m^k\, {}^t g_{m1} + \sum_{k=1}^{4} \frac{t}{2} a_k h_{k,1} \Big[-({}^t V_{2m}^k\, {}^t g_{m1})\,\alpha_k + ({}^t V_{1m}^k\, {}^t g_{m1})\,\beta_k \Big] \\
&= \sum_{k=1}^{4} h_{k,1}(u_1^k\, {}^t g_{11} + u_2^k\, {}^t g_{21} + u_3^k\, {}^t g_{31}) + \sum_{k=1}^{4} \frac{t}{2} a_k h_{k,1} \Big[-\alpha_k({}^t V_{21}^k\, {}^t g_{11} + \\
&\qquad {}^t V_{22}^k\, {}^t g_{21} + {}^t V_{23}^k\, {}^t g_{31}) + \beta_k({}^t V_{11}^k\, {}^t g_{11} + {}^t V_{12}^k\, {}^t g_{21}{}^t + V_{13}^k\, {}^t g_{31})\beta_k \Big]
\end{aligned}
$$

$$
\begin{aligned}
{}_0\widetilde{e}_{22} &= \sum_{k=1}^{4} h_{k,2}\, u_m^k\, {}^t g_{m2} + \sum_{k=1}^{4} \frac{t}{2} a_k h_{k,2} \Big[-({}^t V_{2m}^k\, {}^t g_{m2})\,\alpha_k + ({}^t V_{1m}^k\, {}^t g_{m2})\,\beta_k \Big] \\
&= \sum_{k=1}^{4} h_{k,2}(u_1^k\, {}^t g_{12} + u_2^k\, {}^t g_{22} + u_3^k\, {}^t g_{32}) + \sum_{k=1}^{4} \frac{t}{2} a_k h_{k,2} \Big[-\alpha_k({}^t V_{21}^k\, {}^t g_{12} + \\
&\qquad {}^t V_{22}^k\, {}^t g_{22} + {}^t V_{23}^k\, {}^t g_{32}) + \beta_k({}^t V_{11}^k\, {}^t g_{12} + {}^t V_{12}^k\, {}^t g_{22}{}^t + V_{13}^k\, {}^t g_{32})\beta_k \Big]
\end{aligned}
$$

$$
\begin{aligned}
{}_0\widetilde{e}_{33} &= \sum_{k=1}^{4} \frac{1}{2} a_k h_k \Big[-({}^t V_{2m}^k\, {}^t g_{m3})\,\alpha_k + ({}^t V_{1m}^k\, {}^t g_{m3})\,\beta_k \Big] \\
&= \sum_{k=1}^{4} \frac{1}{2} a_k h_k \Big[-\alpha_k({}^t V_{21}^k\, {}^t g_{13} + {}^t V_{22}^k\, {}^t g_{23} + {}^t V_{23}^k\, {}^t g_{33}) + \\
&\qquad \beta_k({}^t V_{11}^k\, {}^t g_{13} + {}^t V_{12}^k\, {}^t g_{23}{}^t + V_{13}^k\, {}^t g_{33})\beta_k \Big].
\end{aligned}
$$

These expressions can also be written in matrix form as,

$$
\begin{aligned}
{}_0\widetilde{e}_{11} &= \underbrace{h_{k,1} \Big[\ldots \quad {}^t g_{11} \quad {}^t g_{21} \quad {}^t g_{31} \quad -\tfrac{t}{2} a_k({}^t V_{2m}^k\, {}^t g_{m1}) \quad \tfrac{t}{2} a_k({}^t V_{1m}^k\, {}^t g_{m1}) \quad \ldots \Big]}_{{}_0^t B_{L11}} \hat{\mathbf{u}} \\
{}_0\widetilde{e}_{22} &= \underbrace{h_{k,2} \Big[\ldots \quad {}^t g_{12} \quad {}^t g_{22} \quad {}^t g_{32} \quad -\tfrac{t}{2} a_k({}^t V_{2m}^k\, {}^t g_{m2}) \quad \tfrac{t}{2} a_k({}^t V_{1m}^k\, {}^t g_{m2}) \quad \ldots \Big]}_{{}_0^t B_{L22}} \hat{\mathbf{u}} \\
{}_0\widetilde{e}_{33} &= \underbrace{h_k \Big[\ldots \quad 0 \quad 0 \quad 0 \quad -\tfrac{1}{2} a_k({}^t V_{2m}^k\, {}^t g_{m3}) \quad \tfrac{1}{2} a_k({}^t V_{1m}^k\, {}^t g_{m3}) \quad \ldots \Big]}_{{}_0^t B_{L33}} \hat{\mathbf{u}}
\end{aligned}
$$

with $k = 1, 2, 3, 4$. In this way, matrices ${}_0^t B_{L11}$, ${}_0^t B_{L22}$, and ${}_0^t B_{L33}$ have been obtained.

In accordance with Equation 7.25, the bending strain ${}_0\widetilde{e}_{12}$ is given by,

$$ {}_0\widetilde{e}_{12} = \frac{1}{2}\Big[{}^t\mathbf{g}_1 \frac{\partial \mathbf{u}}{\partial r^2} + \frac{\partial \mathbf{u}}{\partial r^1} {}^t\mathbf{g}_2 \Big] = \frac{1}{2}\Big[{}^t g_{m1} \frac{\partial u_m}{\partial r^2} + \frac{\partial u_m}{\partial r^1} {}^t g_{m2} \Big]. $$

Using again Equation 7.23, the the terms $\frac{\partial u_m}{\partial r^1}$ and $\frac{\partial u_m}{\partial r^2}$ can be computed as,

$$ \frac{\partial u_m}{\partial r^1} = \sum_{k=1}^{4} h_{k,1}\, u_m^k + \sum_{k=1}^{4} \frac{t}{2} a_k h_{k,1} \Big(- {}^tV_{2m}^k\, \alpha_k + {}^tV_{1m}^k \beta_k \Big) $$

$$ \frac{\partial u_m}{\partial r^2} = \sum_{k=1}^{4} h_{k,2}\, u_m^k + \sum_{k=1}^{4} \frac{t}{2} a_k h_{k,2} \Big(- {}^tV_{2m}^k\, \alpha_k + {}^tV_{1m}^k \beta_k \Big); $$

therefore,

$$ 2\, {}_0\widetilde{e}_{12} = \underbrace{\begin{bmatrix} \dots & h_{k,2}\, {}^tg_{11} + & h_{k,2}\, {}^tg_{21} + & h_{k,2}\, {}^tg_{31} + & \textcircled{1} & \textcircled{2} & \dots \\ & h_{k,1}\, {}^tg_{12} & h_{k,1}\, {}^tg_{22} & h_{k,1}\, {}^tg_{32} & & & \end{bmatrix}}_{{}^t_0B_{L12}} \hat{\mathbf{u}} $$

where

$$ \textcircled{1} = -\frac{t}{2} a_k \Big[h_{k,2} \, ({}^tV_{2m}^k\, {}^tg_{m1}^k) + h_{k,1} \, ({}^tV_{2m}^k\, {}^tg_{m2}) \Big] $$

$$ \textcircled{2} = \frac{t}{2} a_k \Big[h_{k,2} \, ({}^tV_{1m}^k\, {}^tg_{m1}^k) + h_{k,1} \, ({}^tV_{1m}^k\, {}^tg_{m2}) \Big]. $$

As it was said at the beginning of this section the shear strains ${}_0^{t+\Delta t}\widetilde{\epsilon}_{13}$ and ${}_0^{t+\Delta t}\widetilde{\epsilon}_{23}$ are going to be interpolated via Equations 7.12 and 7.13. However, if a closer look is taken to section 3.3, as a result of the linearisation process applied to the principle of virtual work, the final equation obtained (see Equation 7.24) only contains the incremental linear and the non-linear strain terms $\delta_0\widetilde{e}_{ij}$ and $\delta_0\widetilde{\eta}_{ij}$. Consequently, these shear strains will be interpolated as:

$$ {}_0\widetilde{e}_{13} = \frac{1}{2}(1+s)\, {}_0\widetilde{e}_{13}^A + \frac{1}{2}(1-s)\, {}_0\widetilde{e}_{13}^C \tag{7.30} $$

$$ {}_0\widetilde{e}_{23} = \frac{1}{2}(1+r)\, {}_0\widetilde{e}_{23}^D + \frac{1}{2}(1-r)\, {}_0\widetilde{e}_{23}^B \tag{7.31} $$

$$ {}_0\widetilde{\eta}_{13} = \frac{1}{2}(1+s)\, {}_0\widetilde{\eta}_{13}^A + \frac{1}{2}(1-s)\, {}_0\widetilde{\eta}_{13}^C \tag{7.32} $$

$$ {}_0\widetilde{\eta}_{23} = \frac{1}{2}(1+r)\, {}_0\widetilde{\eta}_{23}^D + \frac{1}{2}(1-r)\, {}_0\widetilde{\eta}_{23}^B. \tag{7.33} $$

In order to use Equations 7.30 and 7.31, it is necessary to find expressions to compute ${}_0\widetilde{e}^A_{13}$, ${}_0\widetilde{e}^C_{13}$, ${}_0\widetilde{e}^D_{23}$, and ${}_0\widetilde{e}^B_{23}$. According to Equation 7.25 the strain ${}_0\widetilde{e}^A_{13}$ can be computed as,

$$
\begin{aligned}
{}_0\widetilde{e}^A_{13} &= \frac{1}{2}\Big[{}^t\mathbf{g}_1\frac{\partial \mathbf{u}}{\partial r^3} + \frac{\partial \mathbf{u}}{\partial r^1}{}^t\mathbf{g}_3\Big]\Big|^A = \frac{1}{2}\Big[{}^t g_{m1}\frac{\partial u_m}{\partial r^3} + \frac{\partial u_m}{\partial r^1}\,{}^t g_{m3}\Big]\Big|^A \\
&= \frac{1}{2}\Big[{}^t\mathbf{g}^A_1\frac{\partial \mathbf{u}}{\partial r^3}\Big|^A + \frac{\partial \mathbf{u}}{\partial r^1}\Big|^A{}^t\mathbf{g}^A_3\Big] = \frac{1}{2}\Big[{}^t g^A_{m1}\frac{\partial u_m}{\partial r^3}\Big|^A + \frac{\partial u_m}{\partial r^1}\Big|^A{}^t g^A_{m3}\Big].
\end{aligned}
$$

Using Equation 7.23 and taking into account that the natural coordinates of point A are $r=0$, $s=1$, and $t=0$, the the terms $\frac{\partial u_m}{\partial r^3}\Big|^A$ and $\frac{\partial u_m}{\partial r^1}\Big|^A$ in the above expression can be computed as,

$$
\begin{aligned}
\frac{\partial u_m}{\partial r^3}\Big|^A &= \sum_{k=1}^{4}\frac{a_k h_k}{2}\Big(-{}^tV^k_{2m}\,\alpha_k + {}^tV^k_{1m}\beta_k\Big)\Big|^A = \sum_{k=1}^{4}\frac{a_k h^A_k}{2}\Big(-{}^tV^k_{2m}\,\alpha_k + {}^tV^k_{1m}\beta_k\Big) \\
\frac{\partial u_m}{\partial r^1}\Big|^A &= \sum_{k=1}^{4} h_{k,1}\,u^k_m\Big|^A + \sum_{k=1}^{4}\frac{t}{2}a_k h_{k,1}\Big(-{}^tV^k_{2m}\,\alpha_k + {}^tV^k_{1m}\beta_k\Big)\Big|^A = \sum_{k=1}^{4} h^A_{k,1}\,u^k_m;
\end{aligned}
$$

hence,

$$
2\,{}_0\widetilde{e}^A_{13} = \sum_{k=1}^{4}\frac{a_k h^A_k}{2}\Big[-\alpha_k({}^tV^k_{2m}\,{}^t g^A_{m1}) + \beta_k({}^tV^k_{1m}\,{}^t g^A_{m1})\Big] + \sum_{k=1}^{4} h^A_{k,1}\,(u^k_m\,{}^t g^A_{m3}).
$$

In matrix form it can be written as

$$
2\,{}_0\widetilde{e}^A_{13} = \underbrace{\Big[\ldots \quad h^A_{k,1}\,{}^t g^A_{13} \quad h^A_{k,1}\,{}^t g^A_{23} \quad h^A_{k,1}\,{}^t g^A_{33} \quad -\tfrac{a_k h^A_k}{2}({}^tV^k_{2m}\,{}^t g^A_{m1}) \quad \tfrac{a_k h^A_k}{2}({}^tV^k_{1m}\,{}^t g^A_{m1}) \quad \ldots\Big]}_{{}^t_0B_{L13A}}\hat{\mathbf{u}},
$$

and using the same strategy,

$$
2\,{}_0\widetilde{e}^C_{13} = \underbrace{\Big[\ldots \quad h^C_{k,1}\,{}^t g^C_{13} \quad h^C_{k,1}\,{}^t g^C_{23} \quad h^C_{k,1}\,{}^t g^C_{33} \quad -\tfrac{a_k h^C_k}{2}({}^tV^k_{2m}\,{}^t g^C_{m1}) \quad \tfrac{a_k h^C_k}{2}({}^tV^k_{1m}\,{}^t g^C_{m1}) \quad \ldots\Big]}_{{}^t_0B_{L13C}}\hat{\mathbf{u}}.
$$

With the above results, matrix ${}^t_0B_{L13}$ can be easily computed as

$$
\begin{aligned}
2\,{}_0\widetilde{e}_{13} &= \frac{1}{2}\Big[(1+s)\,2\,{}_0\widetilde{e}^A_{13} + (1-s)\,2\,{}_0\widetilde{e}^C_{13}\Big] \\
&= \underbrace{\frac{1}{2}\Big[(1+s)\,{}^t_0B_{L13A} + (1-s)\,{}^t_0B_{L13C}\Big]}_{{}^t_0B_{L13}}\hat{\mathbf{u}}.
\end{aligned}
$$

Following exactly the same strategy, the shear strain ${}_0\widetilde{e}_{23}$ can be computed, the final expressions obtained are:

$$2\,{}_0\widetilde{e}^D_{23} = \underbrace{\left[\ldots \quad h^D_{k,2}\,{}^t g^D_{13} \quad h^D_{k,2}\,{}^t g^D_{23} \quad h^D_{k,2}\,{}^t g^D_{33} \quad -\tfrac{a_k h^D_k}{2}({}^t V^k_{2m}\,{}^t g^D_{m2}) \quad \tfrac{a_k h^D_k}{2}({}^t V^k_{1m}\,{}^t g^D_{m2}) \quad \ldots\right]}_{{}^t_0 B_{L23D}} \hat{\mathbf{u}}$$

$$2\,{}_0\widetilde{e}^B_{23} = \underbrace{\left[\ldots \quad h^B_{k,2}\,{}^t g^B_{13} \quad h^B_{k,2}\,{}^t g^B_{23} \quad h^B_{k,2}\,{}^t g^B_{33} \quad -\tfrac{a_k h^B_k}{2}({}^t V^k_{2m}\,{}^t g^B_{m2}) \quad \tfrac{a_k h^B_k}{2}({}^t V^k_{1m}\,{}^t g^B_{m2}) \quad \ldots\right]}_{{}^t_0 B_{L23B}} \hat{\mathbf{u}},$$

and using the above results, matrix ${}^t_0 B_{L23}$ can be obtained as

$$\begin{aligned} 2\,{}_0\widetilde{e}_{23} &= \frac{1}{2}\Big[(1+r)\,2\,{}_0\widetilde{e}^D_{23} + (1-r)\,2\,{}_0\widetilde{e}^B_{13}\Big] \\ &= \underbrace{\frac{1}{2}\Big[(1+r)\,{}^t_0 B_{L23D} + (1-r)\,{}^t_0 B_{L23B}\Big]}_{{}^t_0 B_{L23}} \hat{\mathbf{u}}. \end{aligned}$$

Once all matrices ${}^t_0 B_{Lij}$ have been computed, matrix B_L can be assembled as shown in Equation 7.28.

A general expression for $\delta_0\widetilde{\eta}_{ij}$

Looking back at the linearised principle of virtual work (see Equation 7.24), the incremental non-linear strain $\delta_0\widetilde{\eta}_{ij}$ makes part of the term $\int_{{}_0V} {}^t_0\widetilde{S}_{ij}\,\delta_0\widetilde{\eta}_{ij}\,d\,{}^0V$. According to what it was explained in section 3.3, this term can be expressed as the product of a non-linear incremental stiffness matrix ${}^t_0 K_{NL}$ and vector $\hat{\mathbf{u}}$. That is,

$$\int_{{}_0V} {}^t_0\widetilde{S}^{ij}\,\delta_0\widetilde{\eta}_{ij}\,d\,{}^0V = \delta\hat{\mathbf{u}}^T \underbrace{\Big(\int_{{}_0V} {}^t_0 B^T_{NL}\,{}^t_0 S\,{}^t_0 B_{NL}\,d\,{}^0V\Big)}_{K_{NL}} \hat{\mathbf{u}}.$$

However, due to the fact that the non-linear incremental shear strains ${}_0\widetilde{\eta}_{13}$ and ${}_0\widetilde{\eta}_{23}$ have to be interpolated via Equations 7.32 and 7.33, obtaining a matrix B_{NL} becomes quite difficult. Therefore, matrix expressions for every single

non-linear strain ${}_0\widetilde{\eta}_{ij}$ will be found such that,

$$\int_{{}_0V} {}^t_0\widetilde{S}^{ij}\,\delta_0\widetilde{\eta}_{ij}\,d\,{}^0V = \int_{{}_0V} \Big({}^t_0\widetilde{S}^{11}\,\delta_0\widetilde{\eta}_{11} + {}^t_0\widetilde{S}^{22}\,\delta_0\widetilde{\eta}_{22} + {}^t_0\widetilde{S}^{33}\,\delta_0\widetilde{\eta}_{33} + 2\,{}^t_0\widetilde{S}^{12}\,\delta_0\widetilde{\eta}_{12} + 2\,{}^t_0\widetilde{S}^{13}\,\delta_0\widetilde{\eta}_{13} + 2\,{}^t_0\widetilde{S}^{23}\,\delta_0\widetilde{\eta}_{23}\Big)d\,{}^0V. \tag{7.34}$$

In accordance with Equation 7.27, the first variation of the incremental non-linear strain is given by,

$$\delta_0\widetilde{\eta}_{ij} = \frac{1}{2}\Big[\frac{\partial u_m}{\partial r^i}\delta\Big(\frac{\partial u_m}{\partial r^j}\Big) + \delta\Big(\frac{\partial u_m}{\partial r^i}\Big)\frac{\partial u_m}{\partial r^j}\Big]. \tag{7.35}$$

Thus, the first variation of the bending strains are

$$\delta_0\widetilde{\eta}_{11} = \frac{\partial u_m}{\partial r^1}\delta\Big(\frac{\partial u_m}{\partial r^1}\Big) \qquad \delta_0\widetilde{\eta}_{22} = \frac{\partial u_m}{\partial r^2}\delta\Big(\frac{\partial u_m}{\partial r^2}\Big) \qquad \delta_0\widetilde{\eta}_{33} = \frac{\partial u_m}{\partial r^3}\delta\Big(\frac{\partial u_m}{\partial r^3}\Big)$$

$$2\,\delta_0\widetilde{\eta}_{12} = \frac{\partial u_m}{\partial r^1}\delta\Big(\frac{\partial u_m}{\partial r^2}\Big) + \delta\Big(\frac{\partial u_m}{\partial r^1}\Big)\frac{\partial u_m}{\partial r^2}.$$

Using Equation 7.23, terms $\frac{\partial u_m}{\partial r^1}$ and $\delta(\frac{\partial u_m}{\partial r^1})$ can be directly obtained. That is,

$$\begin{aligned}
\frac{\partial u_m}{\partial r^1} &= \sum_{k=1}^{4} h_{k,1}\,u^k_m + \sum_{k=1}^{4}\frac{t}{2}a_k h_{k,1}\Big(-{}^tV^k_{2m}\,\alpha_k + {}^tV^k_{1m}\beta_k\Big) \\
&= \underbrace{h_{k,1}\Big[\ldots \quad 1 \quad 1 \quad 1 \quad -\tfrac{t}{2}a_k\,{}^tV^k_{2m} \quad \tfrac{t}{2}a_k\,{}^tV^k_{1m} \quad \ldots\Big]}_{H_{,1k}}\hat{\mathbf{u}} \\
\delta\Big(\frac{\partial u_m}{\partial r^1}\Big) &= \sum_{p=1}^{4} h_{p,1}\,\delta u^p_m + \sum_{p=1}^{4}\frac{t}{2}a_p h_{p,1}\Big(-{}^tV^p_{2m}\,\delta\alpha_p + {}^tV^p_{1m}\delta\beta_p\Big) \\
&= \underbrace{h_{p,1}\Big[\ldots \quad 1 \quad 1 \quad 1 \quad -\tfrac{t}{2}a_p\,{}^tV^p_{2m} \quad \tfrac{t}{2}a_p\,{}^tV^p_{1m} \quad \ldots\Big]}_{H_{,1p}}\delta\hat{\mathbf{u}};
\end{aligned}$$

therefore,

$${}^t_0\widetilde{S}^{11}\delta_0\widetilde{\eta}_{11} = \delta\hat{\mathbf{u}}^T\Big\{{}^t_0\widetilde{S}^{11}\Big[H^T_{,1p}\,H_{,1k}\Big]\Big\}\hat{\mathbf{u}}. \tag{7.36}$$

In the same way

$${}^t_0\widetilde{S}^{22}\delta_0\widetilde{\eta}_{22} = \delta\hat{\mathbf{u}}^T\Big\{{}^t_0\widetilde{S}^{22}\Big[H^T_{,2p}\,H_{,2k}\Big]\Big\}\hat{\mathbf{u}} \tag{7.37}$$

$${}^t_0\widetilde{S}^{33}\delta_0\widetilde{\eta}_{33} = \delta\hat{\mathbf{u}}^T\Big\{{}^t_0\widetilde{S}^{33}\Big[H^T_{,3p}\,H_{,3k}\Big]\Big\}\hat{\mathbf{u}} \tag{7.38}$$

$$2\,{}^t_0\widetilde{S}^{12}\delta_0\widetilde{\eta}_{12} = \delta\hat{\mathbf{u}}^T\Big\{{}^t_0\,\widetilde{S}^{12}\Big[H^T_{,2p}\,H_{,1k} + H^T_{,1p}\,H_{,2k}\Big]\Big\}\hat{\mathbf{u}}, \tag{7.39}$$

where

$$\frac{\partial u_m}{\partial r^2} = \underbrace{h_{k,2}\left[\ldots \quad 1 \quad 1 \quad 1 \quad -\tfrac{t}{2}a_k{}^tV_{2m}^k \quad \tfrac{t}{2}a_k{}^tV_{1m}^k \quad \ldots\right]}_{H_{,2k}}\hat{\mathbf{u}}$$

$$\delta\Big(\frac{\partial u_m}{\partial r^2}\Big) = \underbrace{h_{p,2}\left[\ldots \quad 1 \quad 1 \quad 1 \quad -\tfrac{t}{2}a_p{}^tV_{2m}^p \quad \tfrac{t}{2}a_p{}^tV_{1m}^p \quad \ldots\right]}_{H_{,2p}}\delta\hat{\mathbf{u}}$$

$$\frac{\partial u_m}{\partial r^3} = \underbrace{\frac{a_k h_k}{2}\left[\ldots \quad 0 \quad 0 \quad 0 \quad -{}^tV_{2m}^k \quad {}^tV_{1m}^k \quad \ldots\right]}_{H_{,3k}}\hat{\mathbf{u}}$$

$$\delta\Big(\frac{\partial u_m}{\partial r^3}\Big) = \underbrace{\frac{a_p h_p}{2}\left[\ldots \quad 0 \quad 0 \quad 0 \quad -{}^tV_{2m}^p \quad {}^tV_{1m}^p \quad \ldots\right]}_{H_{,3p}}\delta\hat{\mathbf{u}}.$$

On the other hand, the first variation of the incremental non-linear shear strains $\delta_0\widetilde{\eta}_{13}$ and $\delta_0\widetilde{\eta}_{23}$ are going to be calculated as stated by Equations 7.32 and 7.33. That is,

$$\delta_0\widetilde{\eta}_{13} = \frac{1}{2}(1+s)\,\delta_0\widetilde{\eta}_{13}^A + \frac{1}{2}(1-s)\,\delta_0\widetilde{\eta}_{13}^C$$
$$\delta_0\widetilde{\eta}_{23} = \frac{1}{2}(1+r)\,\delta_0\widetilde{\eta}_{23}^D + \frac{1}{2}(1-r)\,\delta_0\widetilde{\eta}_{23}^B,$$

such that

$$2\,\delta_0\widetilde{\eta}_{13}^A = \frac{\partial u_m}{\partial r^1}\Big|^A \delta\Big(\frac{\partial u_m}{\partial r^3}\Big)\Big|^A + \delta\Big(\frac{\partial u_m}{\partial r^1}\Big)\Big|^A \frac{\partial u_m}{\partial r^3}\Big|^A$$
$$2\,\delta_0\widetilde{\eta}_{13}^C = \frac{\partial u_m}{\partial r^1}\Big|^C \delta\Big(\frac{\partial u_m}{\partial r^3}\Big)\Big|^C + \delta\Big(\frac{\partial u_m}{\partial r^1}\Big)\Big|^C \frac{\partial u_m}{\partial r^3}\Big|^C$$
$$2\,\delta_0\widetilde{\eta}_{23}^D = \frac{\partial u_m}{\partial r^2}\Big|^D \delta\Big(\frac{\partial u_m}{\partial r^3}\Big)\Big|^D + \delta\Big(\frac{\partial u_m}{\partial r^2}\Big)\Big|^D \frac{\partial u_m}{\partial r^3}\Big|^D$$
$$2\,\delta_0\widetilde{\eta}_{23}^B = \frac{\partial u_m}{\partial r^2}\Big|^B \delta\Big(\frac{\partial u_m}{\partial r^3}\Big)\Big|^B + \delta\Big(\frac{\partial u_m}{\partial r^2}\Big)\Big|^B \frac{\partial u_m}{\partial r^3}\Big|^B.$$

Consistent with Equation 7.23 and taking into account that the natural coordinates of the points A, B, C, and D are $A(0,1,0)$, $B(-1,0,0)$, $C(0,-1,0)$, and $D(1,0,0)$; the terms appearing the the above equations can be calculated. e.g.

$$\frac{\partial u_m}{\partial r^1}\Big|^A = h_{k,1}^A\left[\ldots \quad 1 \quad 1 \quad 1 \quad -\tfrac{t}{2}a_k{}^tV_{2m}^k \quad \tfrac{t}{2}a_k{}^tV_{1m}^k \quad \ldots\right]\hat{\mathbf{u}}$$
$$= \underbrace{h_{k,1}^A\left[\ldots \quad 1 \quad 1 \quad 1 \quad 0 \quad 0 \quad \ldots\right]}_{H_{,1k}|^A}\hat{\mathbf{u}}$$

$$\left.\frac{\partial u_m}{\partial r^3}\right|^A = \underbrace{\frac{a_k h_k^A}{2}\left[\ldots \quad 0 \quad 0 \quad 0 \quad -{}^tV_{2m}^k \quad {}^tV_{1m}^k \quad \ldots\right]}_{H_{,3k}|^A}\hat{\mathbf{u}}$$

accordingly,

$$\begin{aligned}
2\,\delta_0\widetilde{\eta}_{13}^A &= \delta\hat{\mathbf{u}}^T\Big[H_{,3p}^T|^A H_{,1k}|^A + H_{,1p}^T|^A H_{,3k}|^A\Big]\hat{\mathbf{u}}\\
2\,\delta_0\widetilde{\eta}_{13}^C &= \delta\hat{\mathbf{u}}^T\Big[H_{,3p}^T|^C H_{,1k}|^C + H_{,1p}^T|^C H_{,3k}|^C\Big]\hat{\mathbf{u}}\\
2\,\delta_0\widetilde{\eta}_{23}^D &= \delta\hat{\mathbf{u}}^T\Big[H_{,3p}^T|^D H_{,2k}|^D + H_{,2p}^T|^D H_{,3k}|^D\Big]\hat{\mathbf{u}}\\
2\,\delta_0\widetilde{\eta}_{23}^B &= \delta\hat{\mathbf{u}}^T\Big[H_{,3p}^T|^B H_{,2k}|^B + H_{,2p}^T|^B H_{,3k}|^B\Big]\hat{\mathbf{u}}.
\end{aligned}$$

Therefore,

$$\begin{aligned}
2\,{}_0^t\widetilde{S}^{13}\delta_0\widetilde{\eta}_{13} = \delta\hat{\mathbf{u}}^T\Big\{&\frac{1}{2}(1+s)\,{}_0^t\widetilde{S}^{13}\Big[H_{,3p}^T|^A H_{,1k}|^A + H_{,1p}^T|^A H_{,3k}|^A\Big] +\\
&\frac{1}{2}(1-s)\,{}_0^t\widetilde{S}^{13}\Big[H_{,3p}^T|^C H_{,1k}|^C + H_{,1p}^T|^C H_{,3k}|^C\Big]\Big\}\hat{\mathbf{u}} \qquad (7.40)\\
2\,{}_0^t\widetilde{S}^{23}\delta_0\widetilde{\eta}_{23} = \delta\hat{\mathbf{u}}^T\Big\{&\frac{1}{2}(1+r)\,{}_0^t\widetilde{S}^{23}\Big[H_{,3p}^T|^D H_{,2k}|^D + H_{,2p}^T|^D H_{,3k}|^D\Big] +\\
&\frac{1}{2}(1-r)\,{}_0^t\widetilde{S}^{23}\Big[H_{,3p}^T|^B H_{,2k}|^B + H_{,2p}^T|^B H_{,3k}|^B\Big]\Big\}\hat{\mathbf{u}}. \qquad (7.41)
\end{aligned}$$

Now the term $\int_{{}^0V} {}_0^t\widetilde{S}_{ij}\,\delta_0\widetilde{\eta}_{ij}\,d\,{}^0V$ can be easily calculated by adding Equations 7.36, 7.37, 7.38, 7.39, 7.40, and 7.41, as it is stated by Equation 7.34.

7.4 Computer implementation

The 4-node mixed shell element explained in the previous section was implemented as a C++ program. Chapter 8 describes a controlled experiment that was done in order to validate the results; the deformations obtained in the experiment were measured with a 3–D laser scanner and compared with the numerical results. The User's Manual of the program can be consulted in Appendix D.

7.4.1 Examples

In addition to the simulations performed to validate the results, some other examples were accomplished. The Geometry file as well as the Properties file for these examples are inside the examples folder. Some of them are:

- Square plate: One side of a flat square plate with a hole in the middle was clamped, and therefore all the nodes belonging to this side were constrained in all their degrees of freedom. Vertical forces were applied to the opposite edge to the clamped side. The results obtained are shown in Figure 7.9a.

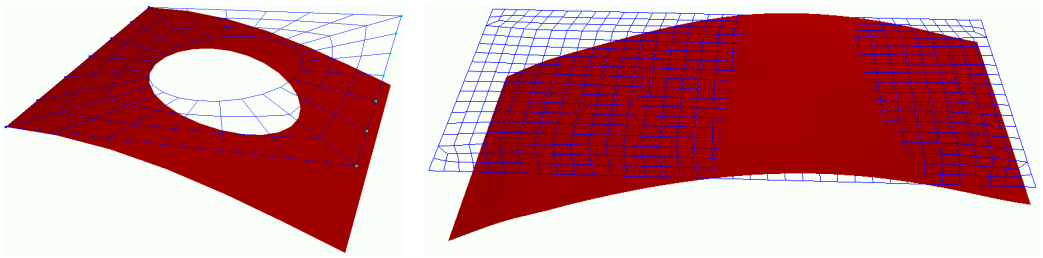

(a) Square plate with vertical forces applied on the edge

(b) Rectangular Plate with displacements boundary conditions

Figure 7.9: Some examples executed

Both, a linear and a non-linear simulation were run for this example. The final location of the plate predicted by the linear model was quite close to the non-linear. In the non-linear simulation the total amount of loading was split into two load-steps. The first load step converged after 7 iterations, while the second load step converged after 5 iterations.

- Flat plate: Only displacements boundary conditions were applied to a rectangular plate shown in Figure 7.9b. An amount of displacement along the y axis was given to the 4 corner nodes and to some inside nodes. Therefore, those nodes were constrained to displace a given amount along the y axis; but they were also free to move along the x and z axes. Only satisfactory results were achieved by the linear simulation.

- Arc structure: The structure chosen for this simulation is shown in Figure 7.10. The three nodes inside the circled area were constrained in all their degrees of freedom. By the other hand, nodes 3, 32, and 33 were allow to move freely along axis z. Therefore, these nodes were restricted to move in all its degrees of freedom except for the z axis. Besides, a force boundary conditions pointing in the direction of the $-z$ axis was applied to nodes 3, 32, and 33. Only satisfactory results were achieved by the linear simulation.

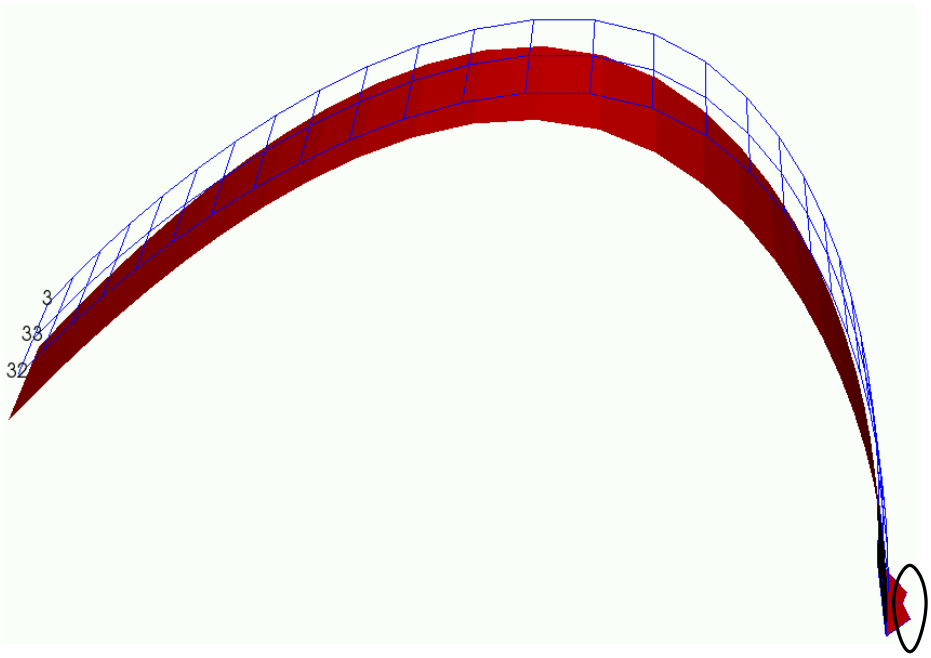

Figure 7.10: Arc structure with displacements + forces boundary conditions

Chapter 8

Validation Results

In order to verify the accuracy of the results obtained with the large deformation finite shell element model proposed herein, a validation experiment was designed.

8.1 Description of the Experiment

The experiment can be described as follows: A cantilever rectangular plate subject to a punctual force on its free end was chosen as the situation to be simulated, see Figure 8.1.

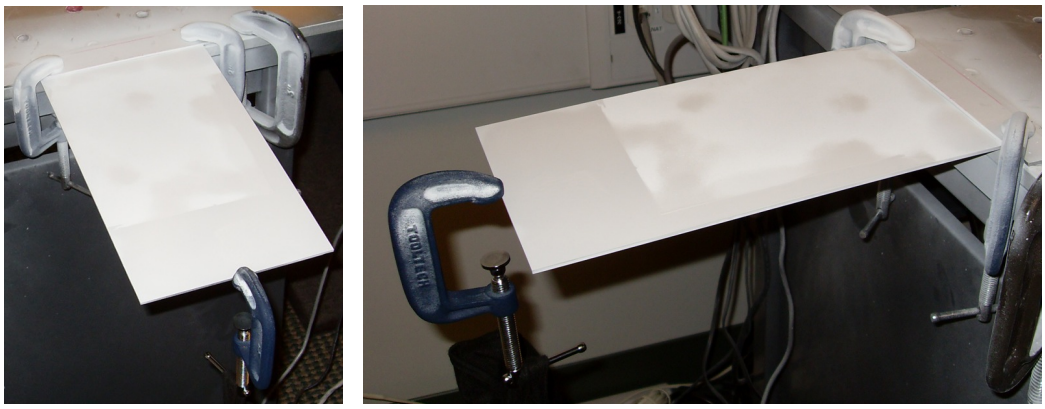

(a) (b)

Figure 8.1: Pictures of the experiment

This situation was chosen because the easy measuring of the boundary

conditions: The dimensions of the clamped region can be simply measured as well as the exact location and direction of the force to be applied.

A 300 mm × 150 mm steel plate with a thickness of 2.4 mm was fixed in one of its ends, see Figure 8.1. For that purpose, two screw clamps were placed over the region that was wanted to be fixed. To ensure that the clamping conditions were applied over a controlled area of the plate, a flat ruler-like element was placed in between the screw clamps and the plate in order to distribute the fixing conditions.

Then a quasi-punctual force was applied at the free end of the plate. The direction of this force coincides with the direction of the gravity vector because the force was applied in such a way that non-wished momentums could be introduced into the experiment. To achieve this situation a non-screwed clamp was hung at the free end of the cantilever, see Figure 8.2, and a bag containing a cylindrical object was attached to it. The total amount of weight was 3.538kg, this weight includes the screw clamp, the cylindrical part, and the bag.

Figure 8.2: Force applied

Before and after the application of the load, the geometry of the plate was acquired via a 3–D laser scanner. The scan of the deformed configuration represents the experimental data to be compared with the simulation results.

8.2 Obtaining the Geometry and the Properties Files

The scan data obtained for the non-deformed location was used to draw a CAD model of the plate at its initial location. This CAD drawing was exported into a meshing software with the intention of getting a quadrilateral mesh of the plate, see Figure 8.3. In order to get the information required by the Geometry file, once the quad-mesh was obtained, the following information was saved into a flat-text file:

- Cartesian coordinates of the nodes
- Indices of the elements
- A list of normal vectors associated to each node,

with this information the Geometry file was build. This file is also included with the source files delivered. It can be found inside the folder "Validation".

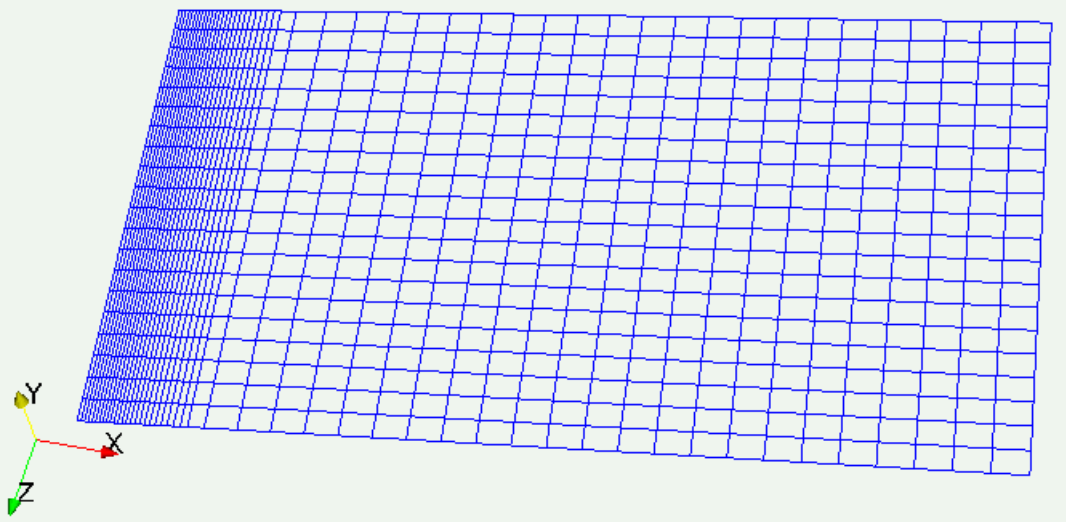

Figure 8.3: Meshed geometry

The mesh was built in such a way that the clamping region could be strictly controlled. With that aim, a good amount of nodes were located inside and on the edges of the region described by the ruler-like object. Figure 8.4 highlights these nodes in red color. All the red-highlighted nodes were constrained in all

their degrees of freedom, including displacements plus rotations. Because this information has to be included into the Properties file, the indices of the nodes belonging to the constrained area were saved in a flat-text file.

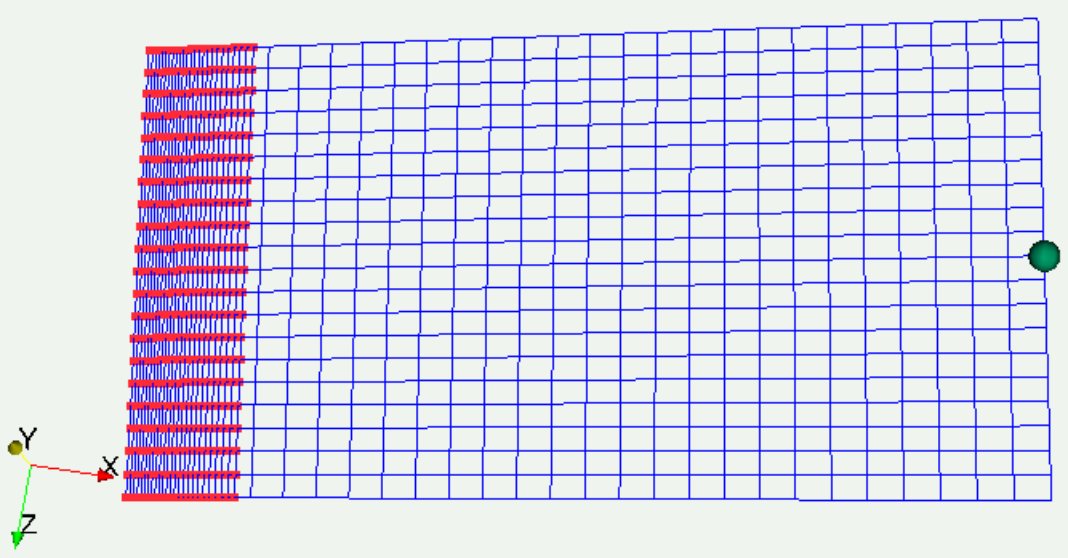

Figure 8.4: Forces + Displacements applied.

The location of the force was also strictly controlled by obligating the Quad-mesh to pass by the exact point of application. Figure 8.4 highlights this point with a green sphere. Because the direction of this force coincides with the gravity vector, a simple experiment to measure this direction was accomplished: A collar-like element was hung at one of its ends, and the other end was allowed to align with the gravity direction. The element was scanned and with the data obtained a director vector was deduced. This unitary vector was multiplied by the magnitude of the total amount of weight applied. The final result for the force vector was

$$\mathrm{F}_x = -38.4 \times 10^{-3}\,\mathrm{N} \qquad \mathrm{F}_y = -34707.8 \times 10^{-3}\,\mathrm{N} \qquad \mathrm{F}_z = 115.2 \times 10^{-3}\,\mathrm{N}. \tag{8.1}$$

As it can be seen, the biggest amount of force is applied in the y direction, which means that the y axis of the scanner is almost aligned with the gravity direction.

The Properties file also requires information about the material properties of the plate. The material has isotropic behaviour with a Young modulus of

130 Gpa, and a Poisson ratio of 0.33. The final Properties file which was built to run the simulation can be accessed inside the Validation folder.

8.3 Linear versus non-linear simulations

As the reader might know, either a linear or a non-the simulation can be carried out by the C++ program. Because the nature of the equations which rule this deformation process are highly non-linear, a non-linear simulation should be pursuited if the aim of getting accurate results is sought. However, this kind of simulations can carry out some serious problems such as:

- Convergence: The main reason why this problem occur is that the non-linear system of equations is solved via the Newton Raphson method. This method solves the problem iteratively, and at each iteration a linearisation of the system of equations made. Hence, an approximation to the final solution will be linearly reached at each iteration until a convergence criterion is satisfied. The problem is that sometimes the Newton Raphson method diverges. To try to avoid this problem several techniques can be applied. Some of them are: (i) split the total amount of force or displacement to be applied into smaller parts, (ii) change the density of the mesh, which means that the original geometry needs to be meshed either with more or less elements, and (iii) try to avoid element distortion. Although all these suggestions are carefully satisfied, in some cases of complex geometries the problem still does not converge. In those cases, some other techniques can be employed, but they belong more to the mathematical foundations of the method, and they are out of the scope of this study.

- Timing: If the problem converges, in most of the cases, it is still a long time consuming process. For example, when simulating very complicated geometries which are meshed with a big amount of elements, the final solution can arrive after several days of machine calculations. That is one of the main reasons why for inspection purposes non-linear solutions are not widely employed.

On the other hand, linear simulations are not as accurate as its counterpart, but they have the advantage of being fast and also do not have convergence problems. When dealing with inspection processes, an accurate prediction of the final location of the object is highly pursuited; however, it has been observed that a linear approximation is most of the times close enough to

the non-linear predicted final location of the object. For the reasons just mentioned, linear simulations are suggested for general inspection purposes.

8.4 Numerical Simulations

Two main simulations were carried out to validate the results. In both of them, linear approximations for the final solution were chosen. Nevertheless, before the simulation process began, a simply extra experiment was made. In this experiment the plate was double scanned on its initial non-deformed configuration. The cloud of points obtained for each scan was triangulated and the results were compared. Beforehand it was known that the precision of the scanner was 0.05 mm, however the intention of the experiment was to figure out how other sources of error could affect the results. These sources could be: scanning speed, reflection, and triangulation errors. When talking about triangulation errors, it is meant that even though the vertices of the triangles (which correspond to the points scanned) have a precision of 0.05 mm, the edges of the triangles are created entities whose error can be bigger than 0.05 mm. Because in this experiment two similar configurations were measured, it was known in advanced that the real error between them was zero, but after comparing the scanning results, this error was up to 0.2 mm.

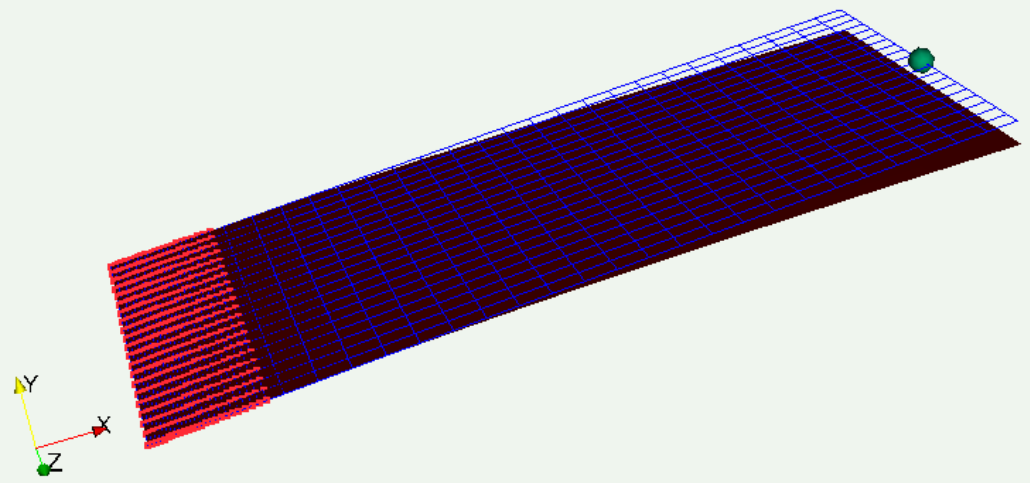

Figure 8.5: Results of the simulation

8.4.1 Cantilever with a single force on its free end

In the first simulation the force shown in Equation 8.1 was applied at the node highlighted with the green sphere, see Figure 8.4, and the clamping restrictions were located in the nodes highlighted with red. The deformed plate obtained is shown in Figure 8.5.

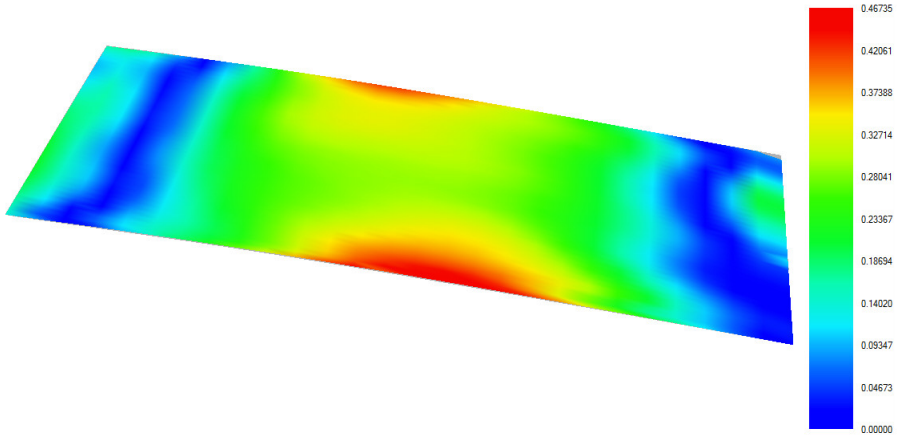

Figure 8.6: Comparison field between the simulation 1 and the scanned data.

The comparison between the scanned data and the simulation results are shown in Figure 8.6. The maximum error found is 0.467 mm, while the average error is 0.199 mm. These errors are not only caused by the simulation, they also include the errors discussed at the beginning of this section. Therefore, considering that other sources of error are up to an order of 0.20 mm, the maximum error of 0.467 mm can be considered as relatively close to the results expected.

8.4.2 Cantilever with displacement applied at its free end

In this simulation the punctual force described by Equation 8.1 was not considered; instead the free non-clamped corners of the plate were moved towards a displacement vector. These two vectors were calculated with the initial and the final locations of the corners, that is, the positions of the corners before and after deformation. These locations were obtained from the scanned data.

The comparison between the scanned data and the simulation results are shown in Figure 8.7. The maximum error found is 0.719 mm, while the average

error is 0.120 mm.

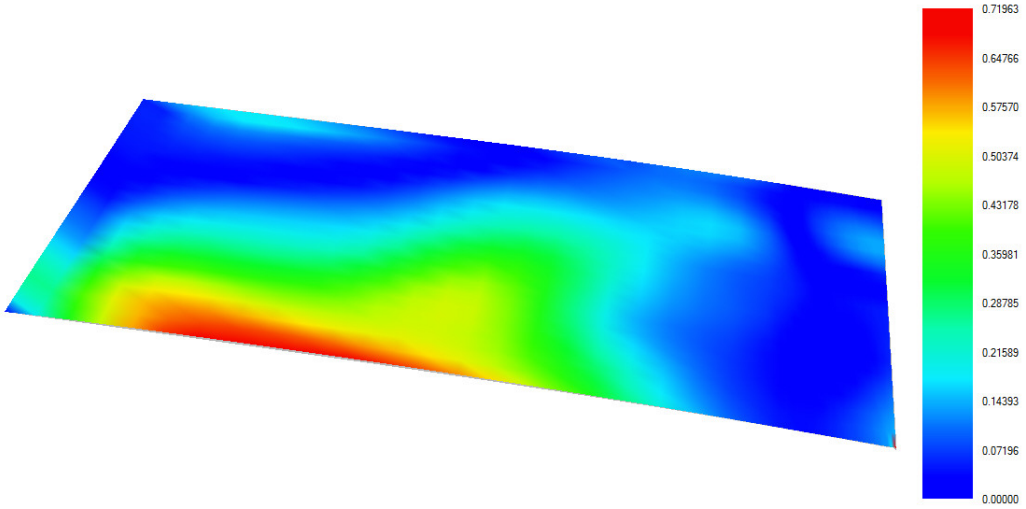

Figure 8.7: Comparison field between the simulation 2 and the scanned data.

Although the maximum error increased compared to the first simulation, the average error diminished considerably. As it can be seen in Figure 8.7, the field of comparison tends to be blue all over the surface except for a small region close to one edge of the plate.

Conclusions

The Finite Element equations for any kind of element can be proposed in any convenient reference system. It is clear that if an inconvenient reference system is chosen, some mathematical problems in the deduction process might be obtained, but eventually, because of the Frame Indifference Principle the same results must be achieved. The Frame Indifference Principle states that the frame of reference is only a mathematical artifice and it does not have any physical meaning. Therefore, it does not matter which frame of reference is chosen, the physical response of the structure analysed cannot be affected.

The principle of virtual displacements (Equation 1.2 deduced in section 1) is expressed in terms of the spatial coordinates (Eulerian formulation). In other words, it is applicable to the current deformed configuration of the object. For that reason, when using a Finite Element formulation, the principle has to be integrated over the deformed volume of the finite elements. However, in a small displacement scenario, the deformed configuration of the object lies too close to its original undeformed configuration. Consequently, the integration of the principle is performed over the original volume of the finite elements.

In some structural problems the small displacements hypothesis has to be abandoned. This occurs due to a more general formulation considering large displacements may represent a better approach to the real conditions of the problem which is intended to be solved. However, if a large displacement formulation is chosen, the principle of virtual displacements has to be rewritten in terms of stress and strain tensors which are invariant under rigid body motions. The problem is that usually those tensors involve nonlinear terms which make the principle of virtual displacements to be highly nonlinear. Therefore, a linearisation of the principle has to be achieved and an incremental solution method has to be used to obtain the solution the problem.

When dealing with elements that suffer from the shear locking phenomenon (this problem usually comes from a displacement based formulation), e.g. beams or shells, a mixed formulation represents a better approach to solve the problem. Otherwise, the element will exhibit a stiffer behaviour and the

displacements obtained will be smaller. However, it is also possible to get displacement based elements which present good predictive capabilities, the problem with these elements is that the polynomial of interpolation used for the displacements needs to satisfy continuity of the first derivative of the displacement between elements. For that reason the polynomials used are of very high order and the idea of using an iso parametric formulation has to be abandoned.

When studying shell elements, *"Although a rectangular system may be inscribed conveniently in certain bodies, deformation carries the straight lines and planes to curved lines and surfaces; rectangular coordinates are deformed into arbitrary Curvilinear coordinates"*(WT03). For that reason, somehow it is necessary to deal with Curvilinear coordinates.

A C++ Finite Element program for general quadrilateral shell elements has been implemented. A mixed Total Lagrangian model was used. The shell element is composed by four nodes (non-flat), and it accomplishes for geometric non-linear analysis. The element implemented is based on the article (DB84). In order to verify the accuracy of the results obtained with the large deformation finite shell element model, a validation experiment was designed. The deformation data obtained with the C++ program was pretty close to the deformation data measured in the experiment. With the validation experiment it was found that linear simulations are not as accurate as the nonlinears, but they have the advantage of being fast and also do not have convergence problems. When dealing with inspection processes, an accurate prediction of the final location of the object is highly pursuited; however, it has been observed that a linear approximation is most of the times close enough to the non-linear predicted final location of the object.

Future Work

A deeper and more complete study of the Newton Raphson method applied to the finite element method should be carried out. It might be important to solve some questions like: (i) Is the linearisation of the principle of virtual displacements affecting the convergence of iterative solution?, (ii) Are any of the assumptions made to linearise the this principle causing somehow an uncontrolled behaviour of the method?, and (iii) Do some finite element variables (as the mesh density or the element distortion) affect the iterative solution method? and in what degree do they do it?

The large displacement formulation discussed in this text has been deduced to support large displacements and large strains. However, the material constitutive relation used (Hook's law) applies to only small displacements; in consequence, a large displacements but small strain scenario has been achieved. It would be important to implement a large strain material behaviour. In this way, the range of engineering problems to be simulated would increase a lot, such as, hyper-elasticity and visco-elasticity. Indeed, large strain elastic-plastic behaviour could also be included.

Although the 4-node shell element seems to work well, it is necessary to have a quad-mesh of the geometry that is going to be simulated. This does not represent a big problem; but sometimes when meshing very complicated geometries, a triangular mesh could be generated in an easier way. Moreover, most of the commercial meshing softwares available have been designed for triangles. For that reason, implementing a triangular shell element under a large displacement hypothesis would represent an advantage in some cases.

Appendix A

Displacement and Deformation Gradient in a 3–D Cartesian coordinate system

Going back to the expression employed for the total differential of a vector function

$$u_i^* = u_i + \frac{\partial u_i}{\partial\, {}^t x_1} d\, {}^t x_1 + \frac{\partial u_i}{\partial\, {}^t x_2} d\, {}^t x_2 + \frac{\partial u_i}{\partial\, {}^t x_3} d\, {}^t x_3$$

$$u_i^* - u_i = \frac{\partial u_i}{{}_t x_j} d\, {}^t x_j,$$

and developing the above expression (in matrix notation) for the particular case of a 3–D Cartesian system, yields to

$$\begin{bmatrix} {}^{t+\Delta t}x + d\, {}^{t+\Delta t}x - ({}^t x + d\, {}^t x) \\ {}^{t+\Delta t}y + d\, {}^{t+\Delta t}y - ({}^t y + d\, {}^t y) \\ {}^{t+\Delta t}z + d\, {}^{t+\Delta t}z - ({}^t z + d\, {}^t z) \end{bmatrix} - \begin{bmatrix} {}^{t+\Delta t}x - {}^t x \\ {}^{t+\Delta t}y - {}^t y \\ {}^{t+\Delta t}z - {}^t z \end{bmatrix} = {}_t u_{i,j} \begin{bmatrix} d\, {}^t x \\ d\, {}^t y \\ d\, {}^t z \end{bmatrix}$$

$$\begin{bmatrix} d\, {}^{t+\Delta t}x - d\, {}^t x \\ d\, {}^{t+\Delta t}y - d\, {}^t y \\ d\, {}^{t+\Delta t}z - d\, {}^t z \end{bmatrix} = {}_t u_{i,j} \begin{bmatrix} d\, {}^t x \\ d\, {}^t y \\ d\, {}^t z \end{bmatrix}.$$

This means that

$$d\, u_i = {}_t u_{i,j}\, d\, {}^t x_j, \tag{A.1}$$

where ${}_t u_{i,j}$ is the displacement gradient which can be written as a 3×3 matrix; namely,

$${}_t u_{i,j} = \begin{bmatrix} \partial u/\partial\, {}^t x & \partial u/\partial\, {}^t y & \partial u/\partial\, {}^t z \\ \partial v/\partial\, {}^t x & \partial v/\partial\, {}^t y & \partial v/\partial\, {}^t z \\ \partial w/\partial\, {}^t x & \partial w/\partial\, {}^t y & \partial w/\partial\, {}^t z \end{bmatrix}.$$

Next, developing Expression A.1, and using the relations expressed in 4.5, yields to

$$\begin{bmatrix} d^{t+\Delta t}x - d^{t}x \\ d^{t+\Delta t}y - d^{t}y \\ d^{t+\Delta t}z - d^{t}z \end{bmatrix} = \begin{bmatrix} \frac{\partial u}{\partial^t x} d^{t}x + \frac{\partial u}{\partial^t y} d^{t}y + \frac{\partial u}{\partial^t z} d^{t}z \\ \frac{\partial v}{\partial^t x} d^{t}x + \frac{\partial v}{\partial^t y} d^{t}y + \frac{\partial v}{\partial^t z} d^{t}z \\ \frac{\partial w}{\partial^t x} d^{t}x + \frac{\partial w}{\partial^t y} d^{t}y + \frac{\partial w}{\partial^t z} d^{t}z \end{bmatrix}$$

$$\begin{bmatrix} d^{t+\Delta t}x - d^{t}x \\ d^{t+\Delta t}y - d^{t}y \\ d^{t+\Delta t}z - d^{t}z \end{bmatrix} = \begin{bmatrix} \frac{\partial ({}^{t+\Delta t}x - {}^{t}x)}{\partial^t x} d^{t}x + \frac{\partial ({}^{t+\Delta t}x - {}^{t}x)}{\partial^t y} d^{t}y + \frac{\partial ({}^{t+\Delta t}x - {}^{t}x)}{\partial^t z} d^{t}z \\ \frac{\partial ({}^{t+\Delta t}y - {}^{t}y)}{\partial^t x} d^{t}x + \frac{\partial ({}^{t+\Delta t}y - {}^{t}y)}{\partial^t y} d^{t}y + \frac{\partial ({}^{t+\Delta t}y - {}^{t}y)}{\partial^t z} d^{t}z \\ \frac{\partial ({}^{t+\Delta t}w - {}^{t}w)}{\partial^t x} d^{t}x + \frac{\partial ({}^{t+\Delta t}w - {}^{t}w)}{\partial^t y} d^{t}y + \frac{\partial ({}^{t+\Delta t}w - {}^{t}w)}{\partial^t z} d^{t}z \end{bmatrix}.$$

Finally, simplifying the above expression, where $\frac{\partial^t x_i}{\partial^t x_j} = 1$ if $i = j$, and $\frac{\partial^t x_i}{\partial^t x_j} = 0$ if $i \neq j$, the general expression to relate $d^{t+\Delta t}x_i$ with $d^{t}x_i$ via the deformation gradient ${}^{t+\Delta t}_{t}x_{ij}$ is obtained:

$$\begin{bmatrix} d^{t+\Delta t}x \\ d^{t+\Delta t}y \\ d^{t+\Delta t}z \end{bmatrix} = \begin{bmatrix} \frac{\partial^{t+\Delta t}x}{\partial^t x} & \frac{\partial^{t+\Delta t}x}{\partial^t y} & \frac{\partial^{t+\Delta t}x}{\partial^t z} \\ \frac{\partial^{t+\Delta t}y}{\partial^t x} & \frac{\partial^{t+\Delta t}y}{\partial^t y} & \frac{\partial^{t+\Delta t}y}{\partial^t z} \\ \frac{\partial^{t+\Delta t}z}{\partial^t x} & \frac{\partial^{t+\Delta t}z}{\partial^t y} & \frac{\partial^{t+\Delta t}z}{\partial^t z} \end{bmatrix} \begin{bmatrix} d^{t}x \\ d^{t}y \\ d^{t}z \end{bmatrix}$$

or in indicial notation

$$d^{t+\Delta t}x_i = {}^{t+\Delta t}_{t}x_{ij}\, d^{t}x_j \tag{A.2}$$

Appendix B

Evaluation of the Jacobian for a truss element in 2–D

Strictly talking, a bar is a 3–D element; however, it can be represented as a 1–D element. This strategy can be applied because some mechanical assumptions are accomplished. The most relevant are: (i) Strains and stresses can only be transmitted in the direction normal to its cross sectional area, and (ii) strains and stresses are considered as constant over its cross sectional area.

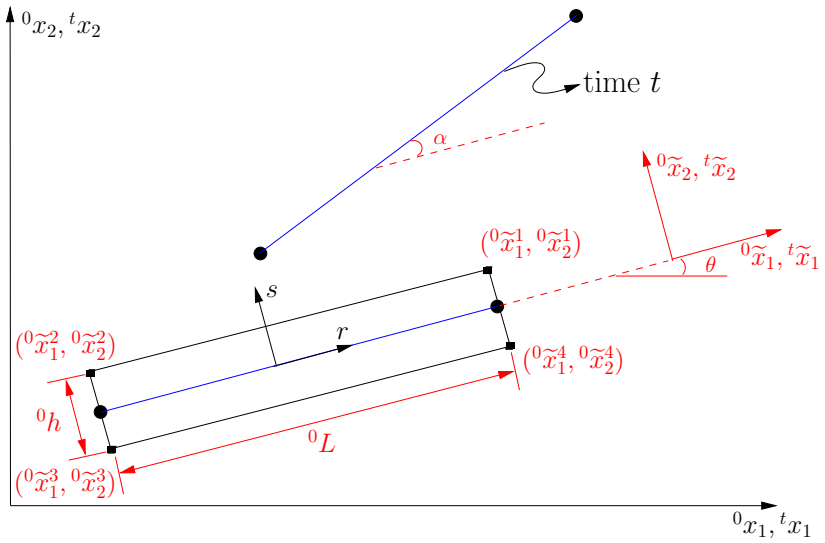

Figure B.1: Local coordinates of the truss element at time 0.

Therefore, it is entirely logic to pursue the evaluation of the Jacobian in

3–D. However, for the particular interest of this study, only an evaluation of the 2–D Jacobian is needed. In order to achieve this, equations relating the local coordinate system ${}^0\widetilde{x}_1 - {}^0\widetilde{x}_2$ with the natural convected coordinates r, s must be stated, see Figure B.1.

Because the original 3–D bar is simplified into a 1–D element, usually people tend to to find only a relation between ${}^0\widetilde{x}_1$ and r. Nevertheless, the 2–D Jacobian requires a complete relation between the local coordinates and the natural-convected coordinates. With that intention, the 2–D geometry of the bar can be interpolated in terms of the convected-natural coordinates as:

$$\begin{aligned} {}^0x_1 =& h_{1(r,s)}\,{}^t x_1^1 + h_{2(r,s)}\,{}^t x_1^2 + h_{3(r,s)}\,{}^t x_1^3 + h_{4(r,s)}\,{}^t x_1^4 \\ {}^0x_2 =& h_{1(r,s)}\,{}^t x_2^1 + h_{2(r,s)}\,{}^t x_2^2 + h_{3(r,s)}\,{}^t x_2^3 + h_{4(r,s)}\,{}^t x_2^4, \end{aligned}$$

where $h_{i(r,s)}$ are the interpolation functions, and are given by

$$h_{1(r,s)} = \frac{1}{4}(1+r)(1+s) \qquad h_{1,r} = \frac{1}{4}(1+s) \qquad h_{1,s} = \frac{1}{4}(1+r) \tag{B.1}$$

$$h_{2(r,s)} = \frac{1}{4}(1-r)(1+s) \qquad h_{2,r} = -\frac{1}{4}(1+s) \qquad h_{2,s} = \frac{1}{4}(1-r) \tag{B.2}$$

$$h_{3(r,s)} = \frac{1}{4}(1-r)(1-s) \qquad h_{3,r} = -\frac{1}{4}(1-s) \qquad h_{3,s} = -\frac{1}{4}(1-r) \tag{B.3}$$

$$h_{4(r,s)} = \frac{1}{4}(1+r)(1-s) \qquad h_{4,r} = \frac{1}{4}(1-s) \qquad h_{4,s} = -\frac{1}{4}(1+r). \tag{B.4}$$

Because de 2–D Jacobian is given by

$${}^0\widetilde{J} = \begin{bmatrix} \partial {}^0\widetilde{x}_1/\partial r & \partial {}^0\widetilde{x}_2/\partial r \\ \partial {}^0\widetilde{x}_1/\partial s & \partial {}^0\widetilde{x}_2/\partial s \end{bmatrix},$$

it is precise to evaluate all the derivatives of ${}^0\widetilde{x}_i$ with respect to r, s. That is,

$$\begin{aligned} \frac{\partial {}^0\widetilde{x}_1}{\partial r} &= h_{1,r}\,{}^0\widetilde{x}_1^1 + h_{2,r}\,{}^0\widetilde{x}_1^2 + h_{3,r}\,{}^0\widetilde{x}_1^3 + h_{4,r}\,{}^0\widetilde{x}_1^4 \\ &= \frac{1}{4}(1+s)\,{}^0\widetilde{x}_1^1 - \frac{1}{4}(1+s)\,{}^0\widetilde{x}_1^2 - \frac{1}{4}(1-s)\,{}^0\widetilde{x}_1^3 + \frac{1}{4}(1-s)\,{}^0\widetilde{x}_1^4 \\ &= \frac{{}^0L}{2}, \end{aligned}$$

$$\begin{aligned} \frac{\partial {}^0\widetilde{x}_2}{\partial r} &= h_{1,r}\,{}^0\widetilde{x}_2^1 + h_{2,r}\,{}^0\widetilde{x}_2^2 + h_{3,r}\,{}^0\widetilde{x}_2^3 + h_{4,r}\,{}^0\widetilde{x}_2^4 \\ &= \frac{1}{4}(1+s)\,{}^0\widetilde{x}_2^1 - \frac{1}{4}(1+s)\,{}^0\widetilde{x}_2^2 - \frac{1}{4}(1-s)\,{}^0\widetilde{x}_2^3 + \frac{1}{4}(1-s)\,{}^0\widetilde{x}_2^4 \\ &= 0, \end{aligned}$$

$$\begin{aligned}\frac{\partial^0\widetilde{x}_1}{\partial s} &= h_{1,s}{}^0\widetilde{x}_1^1 + h_{2,s}{}^0\widetilde{x}_1^2 + h_{3,s}{}^0\widetilde{x}_1^3 + h_{4,s}{}^0\widetilde{x}_1^4 \\ &= \frac{1}{4}(1+r)^0\widetilde{x}_1^1 + \frac{1}{4}(1-r)^0\widetilde{x}_1^2 - \frac{1}{4}(1-r)^0\widetilde{x}_1^3 - \frac{1}{4}(1+r)^0\widetilde{x}_1^4 \\ &= 0,\end{aligned}$$

$$\begin{aligned}\frac{\partial^0\widetilde{x}_2}{\partial s} &= h_{1,s}{}^0\widetilde{x}_2^1 + h_{2,s}{}^0\widetilde{x}_2^2 + h_{3,s}{}^0\widetilde{x}_2^3 + h_{4,s}{}^0\widetilde{x}_2^4 \\ &= \frac{1}{4}(1+r)^0\widetilde{x}_2^1 + \frac{1}{4}(1-r)^0\widetilde{x}_2^2 - \frac{1}{4}(1-r)^0\widetilde{x}_2^3 - \frac{1}{4}(1+r)^0\widetilde{x}_2^4 \\ &= \frac{{}^0h}{2}.\end{aligned}$$

The above expression have been found taking into account that (see Figure B.1),

$$\begin{aligned}{}^0\widetilde{x}_1^2 &= -({}^0\widetilde{x}_1^1 + {}^0L), \qquad {}^0\widetilde{x}_2^1 = {}^0\widetilde{x}_2^2 = \frac{h}{2} \\ {}^0\widetilde{x}_1^3 &= -({}^0\widetilde{x}_1^4 + {}^0L), \qquad {}^0\widetilde{x}_2^3 = {}^0\widetilde{x}_2^4 = -\frac{h}{2}.\end{aligned}$$

In this way, it has been shown that that the 2–D Jacobian ${}^0\widetilde{J} = \frac{\partial \widetilde{x}_i}{r_j}$ is

$${}^0\widetilde{J} = \begin{bmatrix} \frac{{}^0L}{2} & 0 \\ 0 & \frac{{}^0h}{2} \end{bmatrix}.$$

Appendix C

Calculation of matrices ${}^t_0K_L$, ${}^t_0K_{NL}$, and vector ${}^t_0\mathbf{F}$ for a truss element

"For the two node truss element shown in Figure C.1 develop the tangent stiffness matrix and force vector corresponding to the configuration at time t. Consider large displacement conditions".(Bat96)

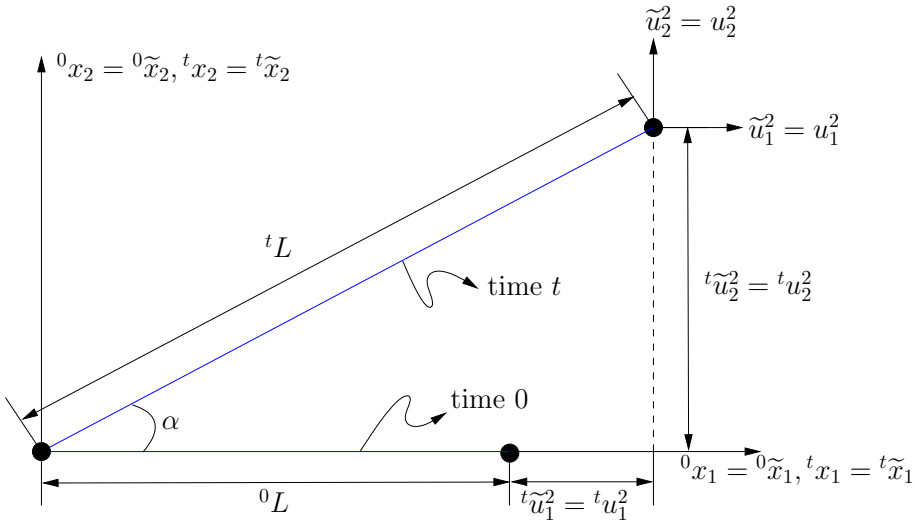

Figure C.1: Location of the element at times 0 and t. Figure taken from (Bat96, pag. 545)

It can be easily seen in the Figure above that the element at time 0 is aligned with the ${}^0x_1$ axis; therefore, plane ${}^0\widetilde{x}_1 - {}^0\widetilde{x}_2$ coincides with plane ${}^0x_1 - {}^0x_2$. In consequence, the displacement dofs also coincide. It means that ${}^t\widetilde{u}_i^k = {}^tu_i^k$ and $\widetilde{u}_i^k = u_i^k$. It is also possible to appreciate from Figure C.1 that:

1. ${}^t\widetilde{u}_1^1 = {}^tu_1^1 = 0$
2. ${}^t\widetilde{u}_2^1 = {}^tu_2^1 = 0$
3. $\theta = 0$
4. ${}^t\widetilde{u}_1^2 = {}^tu_1^2 = {}^tL\cos\alpha - {}^0L$
5. ${}^t\widetilde{u}_2^2 = {}^tu_2^2 = {}^tL\sin\alpha$.

Replacing these listed values into Equation 4.17, yields to

$$
\begin{aligned}
{}_0\widetilde{e_{11}} =& \underbrace{\frac{1}{{}^0L}\left[\begin{array}{cccc} \frac{{}^tu_1^1-{}^tu_1^2}{{}^0L} - \cos\theta & \frac{{}^tu_2^1-{}^tu_2^2}{{}^0L} - \sin\theta & \frac{{}^tu_1^2-{}^tu_1^1}{{}^0L} + \cos\theta & \frac{{}^tu_2^2-{}^tu_2^1}{{}^0L} + \sin\theta \end{array}\right]}_{{}^t_0B_L}\hat{\mathbf{u}} \\
=& \frac{1}{{}^0L}\left[\begin{array}{cccc} \frac{-({}^tL\cos\alpha-{}^0L)}{{}^0L} - 1 & \frac{-{}^tL\sin\alpha}{{}^0L} & \frac{{}^tL\cos\alpha-{}^0L}{{}^0L} + 1 & \frac{{}^tL\sin\alpha}{{}^0L} \end{array}\right]\hat{\mathbf{u}} \\
=& \frac{{}^tL}{{}^0L^2}\left[\begin{array}{cccc} -\cos\alpha & -\sin\alpha & \cos\alpha & \sin\alpha \end{array}\right]\hat{\mathbf{u}};
\end{aligned}
$$

therefore,

$${}^t_0B_L = \frac{{}^tL}{{}^0L^2}\left[\begin{array}{cccc} -\cos\alpha & -\sin\alpha & \cos\alpha & \sin\alpha \end{array}\right].$$

Because in this case ${}^t_0C_{ijrs}$ only accounts for ${}^t_0C_{1111}$, the linear incremental stiffness matrix ${}^t_0K_L$ can be computed as

$$
\begin{aligned}
{}^t_0K_L =& \int_{{}^0V} {}^t_0B_L^T\, {}^t_0C\, {}^t_0B_L\, d\,{}^0V \\
=& \int_{{}^0V} \frac{{}^tL}{{}^0L^2}\begin{bmatrix} -\cos\alpha \\ -\sin\alpha \\ \cos\alpha \\ \sin\alpha \end{bmatrix} {}^t_0C_{1111}\frac{{}^tL}{{}^0L^2}\left[\begin{array}{cccc} -\cos\alpha & -\sin\alpha & \cos\alpha & \sin\alpha \end{array}\right] d\,{}^0V.
\end{aligned}
$$

And assuming a constant cross-sectional area ${}^0A$,

$${}^t_0K_L = {}^t_0C_{1111}\frac{{}^tL^2}{{}^0L^3}\,{}^0A\begin{bmatrix} \cos^2\alpha & \cos\alpha\sin\alpha & -\cos^2\alpha & -\cos\alpha\sin\alpha \\ \cos\alpha\sin\alpha & \sin^2\alpha & -\cos\alpha\sin\alpha & -\sin^2\alpha \\ -\cos^2\alpha & -\cos\alpha\sin\alpha & \cos^2\alpha & \cos\alpha\sin\alpha \\ -\cos\alpha\sin\alpha & -\sin^2\alpha & \cos\alpha\sin\alpha & \sin^2\alpha \end{bmatrix}.$$

It is important to remark that this incremental linear stiffness matrix represents only an expression to be used in the particular case described herein. But in all the possibles 2–D cases, this matrix can be constructed following the same strategy.

It was shown already in chapter 3 that the non-linear incremental stiffness matrix ${}^t_0K_{NL}$ comes from writing in matrix form the term

$$\int_{{}^0V} {}^t_0S_{ij}\delta_0\eta_{ij}\, d\,{}^0V = \delta\hat{\mathbf{u}}^T \underbrace{\Big(\int_{{}^0V} {}^t_0B^T_{NL}\, {}^t_0S\, {}^t_0B_{NL}\, d\,{}^0V\Big)}_{{}^t_0K_{NL}} \hat{\mathbf{u}}.$$

Expression 4.19 quantifies the inner term $\delta_0\eta_{ij}$, that is

$$\delta_0\widetilde{\eta_{11}} = \delta\hat{\mathbf{u}}^T \frac{1}{{}^0L^2} \begin{bmatrix} 1 & 0 & -1 & 0 \\ 0 & 1 & 0 & -1 \\ -1 & 0 & 1 & 0 \\ 0 & -1 & 0 & 1 \end{bmatrix} \hat{\mathbf{u}}.$$

Moreover, ${}^t_0S_{ij}$ can be accomplished via Equation 4.21; however, ${}^t_0\epsilon_{11}$ has to be calculated. With that intention, Relation 4.20 is used:

$$\begin{aligned}
{}^t_0\widetilde{\epsilon_{11}} =& \frac{1}{{}^0L}\Big\{\Big[-{}^tu^1_1\cos\theta - {}^tu^1_2\sin\theta + {}^tu^2_1\cos\theta + {}^tu^2_2\sin\theta\Big] + \\
& \Big[\frac{({}^tu^1_1 - {}^tu^2_1)^tu^1_1}{2\,{}^0L} + \frac{({}^tu^1_2 - {}^tu^2_2)^tu^1_2}{2\,{}^0L} + \frac{({}^tu^2_1 - {}^tu^1_1)^tu^2_1}{2\,{}^0L} + \frac{({}^tu^2_2 - {}^tu^1_2)^tu^2_2}{2\,{}^0L}\Big]\Big\} \\
=& \frac{1}{{}^0L}\Big\{\Big[{}^tL\cos\alpha - {}^0L\Big] + \Big[\frac{({}^tL\cos\alpha - {}^0L)^2 + ({}^tL\sin\alpha)^2}{2{}^0L}\Big]\Big\} \\
=& \frac{1}{2}\Big[\Big(\frac{{}^tL}{{}^0L}\Big)^2 - 1\Big] \\
=& \frac{\Delta L}{{}^0L} + \frac{1}{2}\Big(\frac{\Delta L}{{}^0L}\Big)^2
\end{aligned}$$

where $\Delta L = {}^tL - {}^0L$. Consequently, ${}^t_0S_{11}$ is given by

$${}^t_0S_{11} = {}^t_0C_{1111}\Big[\frac{\Delta L}{{}^0L} + \frac{1}{2}\Big(\frac{\Delta L}{{}^0L}\Big)^2\Big], \tag{C.1}$$

and therefore, the final expression for the non-linear stiffness matrix can be obtained as:

$$\int_{{}^0V} {}^t_0S_{ij}\delta_0\eta_{ij}\, d\,{}^0V = \delta\hat{\mathbf{u}}^T \underbrace{{}^t_0S_{11}\frac{1}{{}^0L^2} \begin{bmatrix} 1 & 0 & -1 & 0 \\ 0 & 1 & 0 & -1 \\ -1 & 0 & 1 & 0 \\ 0 & -1 & 0 & 1 \end{bmatrix}}_{{}^t_0K_{NL}} \hat{\mathbf{u}} \tag{C.2}$$

where the value for ${}^t_0S_{11}$ can be calculated directly via Equation C.1.

In a similar way, an expression for vector ${}^t_0\mathbf{F}$ can be found, that is

$$\begin{aligned} {}^t_0\mathbf{F} &= \int_{{}_0V} {}^t_0B_L^T \, {}^t_0S \; d\,{}^0V \\ &= \int_{{}_0V} \frac{{}^tL}{{}^0L^2} \begin{bmatrix} -\cos\alpha \\ -\sin\alpha \\ \cos\alpha \\ \sin\alpha \end{bmatrix} {}^t_0S_{11} \; d\,{}^0V \\ &= {}^t_0S_{11} \frac{{}^tL}{{}^0L} \, {}^0A \begin{bmatrix} -\cos\alpha \\ -\sin\alpha \\ \cos\alpha \\ \sin\alpha \end{bmatrix}. \end{aligned} \tag{C.3}$$

Even though relations for ${}^t_0K_{NL}$ and ${}^t_0\mathbf{F}$ have been found already, they are not yet similar to the expressions provided by reference (Bat96). This happens because reference (Bat96) gives the results in terms of a variable ${}^tP$. This variable represents *"the current force carried in the truss element"*(Bat96). The problem is that ${}^tP$ is not a given value of the exercise being studied; however, it can be calculated as:

$${}^tP = {}^t_0S_{11} \frac{{}^tL}{{}^0L} \, {}^0A. \tag{C.4}$$

If this relation is included into expressions C.2 and C.3, then the same expression provided by reference (Bat96) will be obtained. Expression C.4 can be demonstrated using Equation 3.9, that written in matrix form is given by

$${}^t_0S = \frac{{}^0\rho}{{}^t\rho} \, {}^0_tX \, {}^t\tau \, {}^0_tX^T; \tag{C.5}$$

therefore, the inverse of the Displacement Gradient ${}^0_tX$ has to be found. If the Deformation Gradient ${}^t_0X$ is obtained, then its inverse can be easily computed. As it was mentioned in chapter 3, ${}^t_0X$ is given by

$${}^t_0X = \begin{bmatrix} \frac{\partial {}^tx_1}{\partial {}^0x_1} & \frac{\partial {}^tx_1}{\partial {}^0x_1} \\ \\ \frac{\partial {}^tx_1}{\partial {}^0x_1} & \frac{\partial {}^tx_1}{\partial {}^0x_1} \end{bmatrix},$$

and

$$\begin{aligned} \frac{\partial {}^tx_1}{\partial {}^0x_1} &= \frac{\partial {}^tx_1}{\partial r}\frac{\partial r}{\partial {}^0x_1} + \frac{\partial {}^tx_1}{\partial s}\frac{\partial s}{\partial {}^0x_1}, \qquad \frac{\partial {}^tx_1}{\partial {}^0x_2} = \frac{\partial {}^tx_1}{\partial r}\frac{\partial r}{\partial {}^0x_2} + \frac{\partial {}^tx_1}{\partial s}\frac{\partial s}{\partial {}^0x_2} \\ \frac{\partial {}^tx_2}{\partial {}^0x_1} &= \frac{\partial {}^tx_2}{\partial r}\frac{\partial r}{\partial {}^0x_1} + \frac{\partial {}^tx_2}{\partial s}\frac{\partial s}{\partial {}^0x_1}, \qquad \frac{\partial {}^tx_2}{\partial {}^0x_2} = \frac{\partial {}^tx_2}{\partial r}\frac{\partial r}{\partial {}^0x_2} + \frac{\partial {}^tx_2}{\partial s}\frac{\partial s}{\partial {}^0x_2}. \end{aligned}$$

If the Jacobian deduced in Appendix B is replaced into the above expressions, they reduce to

$$\frac{\partial^t x_1}{\partial^0 x_1} = \frac{\partial^t x_1}{\partial r}\frac{2}{{}^0L}, \qquad \frac{\partial^t x_1}{\partial^0 x_2} = \frac{\partial^t x_1}{\partial s}\frac{2}{{}^0h}$$
$$\frac{\partial^t x_2}{\partial^0 x_1} = \frac{\partial^t x_2}{\partial r}\frac{2}{{}^0L}, \qquad \frac{\partial^t x_2}{\partial^0 x_2} = \frac{\partial^t x_2}{\partial s}\frac{2}{{}^0h}.$$

Similarly as for the Jacobian, the geometry of the bar has to be interpolated in a 2–D scenario in order to get the fully 2–D Deformation Gradient. For this purpose the geometry of the object at time t can be interpolated in the same way as it was done with the Jacobian. That is,

$$\begin{aligned} {}^t x_1 =& h_{1(r,s)}\, {}^t x_1^1 + h_{2(r,s)}\, {}^t x_1^2 + h_{3(r,s)}\, {}^t x_1^3 + h_{4(r,s)}\, {}^t x_1^4 \\ {}^t x_2 =& h_{1(r,s)}\, {}^t x_2^1 + h_{2(r,s)}\, {}^t x_2^2 + h_{3(r,s)}\, {}^t x_2^3 + h_{4(r,s)}\, {}^t x_2^4, \end{aligned}$$

where $h_{i(r,s)}$ are the interpolation functions, see equations B.1 to B.4. From

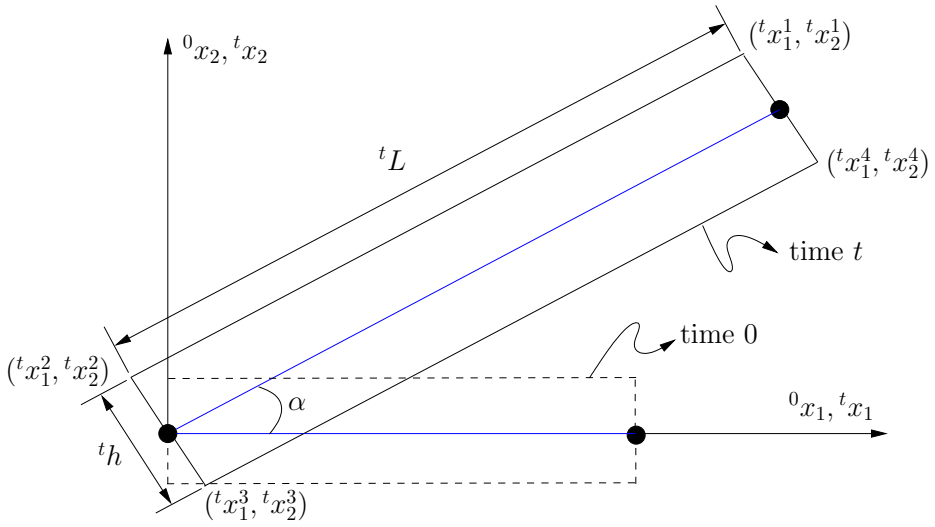

Figure C.2: Cartesian coordinates in configuration t.

Figure C.2, it is possible to deduce the following values:

$$
\begin{aligned}
{}^tx_1^1 &= {}^tL\cos\alpha - \frac{{}^th}{2}\sin\alpha & {}^tx_2^1 &= {}^tL\sin\alpha + \frac{{}^th}{2}\cos\alpha \\
{}^tx_1^2 &= -\frac{{}^th}{2}\sin\alpha & {}^tx_2^2 &= \frac{{}^th}{2}\cos\alpha \\
{}^tx_1^3 &= \frac{{}^th}{2}\sin\alpha & {}^tx_2^3 &= -\frac{{}^th}{2}\cos\alpha \\
{}^tx_1^4 &= {}^tL\cos\alpha + \frac{{}^th}{2}\sin\alpha & {}^tx_2^4 &= {}^tL\sin\alpha - \frac{{}^th}{2}\cos\alpha.
\end{aligned}
$$

In this way,

$$
\begin{aligned}
\frac{\partial^t x_1}{\partial^0 x_1} &= \left[\frac{\partial^t x_1}{\partial r}\right]\frac{2}{{}^0L} = \left[h_{1,r}\,{}^tx_1^1 + h_{2,r}\,{}^tx_1^2 + h_{3,r}\,{}^tx_1^3 + h_{4,r}\,{}^tx_1^4\right]\frac{2}{{}^0L} \\
&= \left[\frac{1}{4}(1+s)^tx_1^1 - \frac{1}{4}(1+s)^tx_1^2 - \frac{1}{4}(1-s)^0x_1^3 + \frac{1}{4}(1-s)^tx_1^4\right]\frac{2}{{}^0L} \\
&= \frac{{}^tL}{{}^0L}\cos\alpha
\end{aligned}
$$

$$
\begin{aligned}
\frac{\partial^t x_1}{\partial^0 x_2} &= \left[\frac{\partial^t x_1}{\partial s}\right]\frac{2}{{}^0h} = \left[h_{1,s}\,{}^tx_1^1 + h_{2,s}\,{}^tx_1^2 + h_{3,s}\,{}^tx_1^3 + h_{4,s}\,{}^tx_1^4\right]\frac{2}{{}^0h} \\
&= \left[\frac{1}{4}(1+r)^tx_1^1 + \frac{1}{4}(1-r)^tx_1^2 - \frac{1}{4}(1-r)^0x_1^3 - \frac{1}{4}(1+r)^tx_1^4\right]\frac{2}{{}^0h} \\
&= -\frac{{}^th}{{}^0h}\sin\alpha
\end{aligned}
$$

$$
\begin{aligned}
\frac{\partial^t x_2}{\partial^0 x_1} &= \left[\frac{\partial^t x_2}{\partial r}\right]\frac{2}{{}^0L} = \left[h_{1,r}\,{}^tx_2^1 + h_{2,r}\,{}^tx_2^2 + h_{3,r}\,{}^tx_2^3 + h_{4,r}\,{}^tx_2^4\right]\frac{2}{{}^0L} \\
&= \left[\frac{1}{4}(1+s)^tx_2^1 - \frac{1}{4}(1+s)^tx_2^2 - \frac{1}{4}(1-s)^0x_2^3 + \frac{1}{4}(1-s)^tx_2^4\right]\frac{2}{{}^0L} \\
&= \frac{{}^tL}{{}^0L}\sin\alpha
\end{aligned}
$$

$$
\begin{aligned}
\frac{\partial^t x_2}{\partial^0 x_2} &= \left[\frac{\partial^t x_2}{\partial s}\right]\frac{2}{{}^0h} = \left[h_{1,s}\,{}^tx_2^1 + h_{2,s}\,{}^tx_2^2 + h_{3,s}\,{}^tx_2^3 + h_{4,s}\,{}^tx_2^4\right]\frac{2}{{}^0h} \\
&= \left[\frac{1}{4}(1+r)^tx_2^1 + \frac{1}{4}(1-r)^tx_2^2 - \frac{1}{4}(1-r)^0x_2^3 - \frac{1}{4}(1+r)^tx_2^4\right]\frac{2}{{}^0h} \\
&= \frac{{}^th}{{}^0h}\cos\alpha.
\end{aligned}
$$

Finally, the Deformation Gradient ${}^{t}_{0}X$ and its inverse ${}^{0}_{t}X$ are given by

$$ {}^{t}_{0}X = \begin{bmatrix} \frac{{}^{t}L}{{}^{0}L}\cos\alpha & -\frac{{}^{t}h}{{}^{0}h}\sin\alpha \\ \\ \frac{{}^{t}L}{{}^{0}L}\sin\alpha & \frac{{}^{t}h}{{}^{0}h}\cos\alpha \end{bmatrix} \qquad [{}^{t}_{0}X]^{-1} = {}^{0}_{t}X = \begin{bmatrix} \frac{{}^{0}L}{{}^{t}L}\cos\alpha & \frac{{}^{0}L}{{}^{t}L}\sin\alpha \\ \\ -\frac{{}^{0}h}{{}^{t}h}\sin\alpha & \frac{{}^{0}h}{{}^{t}h}\cos\alpha \end{bmatrix}. \tag{C.6} $$

Before using Equation C.5, it is also necessary to find an expression for ${}^{t}\tau$. Because truss elements can only support loads along the axis normal to its cross-sectional area; hence, in configuration t, the Cauchy stress tensor measured in the local reference system ${}^{t}\widetilde{x}_1 - {}^{t}\widetilde{x}_2$ can be written in matrix form as

$$ {}^{t}\widetilde{\tau} = \begin{bmatrix} \frac{{}^{t}P}{{}^{t}A} & 0 \\ 0 & 0 \end{bmatrix}. $$

Nevertheless, in order to use Equation C.5, the components of the Cauchy stress tensor must be established in the global Cartesian system ${}^{t}x_1 - {}^{t}x_2$. This is,

$$ {}^{t}\tau = \begin{bmatrix} \cos\alpha & -\sin\alpha \\ \sin\alpha & \cos\alpha \end{bmatrix} \begin{bmatrix} \frac{{}^{t}P}{{}^{t}A} & 0 \\ 0 & 0 \end{bmatrix} \begin{bmatrix} \cos\alpha & \sin\alpha \\ -\sin\alpha & \cos\alpha \end{bmatrix}. \tag{C.7} $$

It is also important to remember that the mass m of the object remains constant at any time; it means that before, after, and while the deformation process is taking place, the mass of the object does not vary. Therefore,

$$ \begin{aligned} {}^{0}m &= {}^{t}m \\ {}^{0}\rho\,{}^{0}V &= {}^{t}\rho\,{}^{t}V \\ {}^{0}\rho\,{}^{0}A{}^{0}L &= {}^{t}\rho\,{}^{t}A{}^{t}L, \end{aligned} $$

hence

$$ \frac{{}^{0}\rho}{{}^{t}\rho} = \frac{{}^{t}A{}^{t}L}{{}^{0}A{}^{0}L}. \tag{C.8} $$

Expressions C.6, C.7, and C.8 can be directly replaced into C.5:

$$ \begin{aligned} {}^{t}_{0}S &= \frac{{}^{0}\rho}{{}^{t}\rho}\,{}^{0}_{t}X\,{}^{t}\tau\,{}^{0}_{t}X^{T} \\ &= \frac{{}^{t}A{}^{t}L}{{}^{0}A{}^{0}L} \begin{bmatrix} \frac{{}^{0}L}{{}^{t}L}\cos\alpha & \frac{{}^{0}L}{{}^{t}L}\sin\alpha \\ -\frac{{}^{0}h}{{}^{t}h}\sin\alpha & \frac{{}^{0}h}{{}^{t}h}\cos\alpha \end{bmatrix} {}^{t}\tau \begin{bmatrix} \frac{{}^{0}L}{{}^{t}L}\cos\alpha & -\frac{{}^{0}h}{{}^{t}h}\sin\alpha \\ \frac{{}^{0}L}{{}^{t}L}\sin\alpha & \frac{{}^{0}h}{{}^{t}h}\cos\alpha \end{bmatrix} \\ &= \frac{{}^{t}A{}^{t}L}{{}^{0}A{}^{0}L} \begin{bmatrix} \left(\frac{{}^{0}L}{{}^{t}L}\right)^{2}\frac{{}^{t}P}{{}^{t}A} & 0 \\ 0 & 0 \end{bmatrix}, \end{aligned} $$

for that reason

$$ {}^t_0S_{11} = {}^tP\frac{{}^0L}{{}^0A{}^tL} \Longrightarrow {}^tP = {}^t_0S_{11}\frac{{}^tL}{{}^0L}\,{}^0A. $$

Appendix D

User's Manual of the C++ Shell Program

A Finite Element software for general quadrilateral shell elements was implemented in C++. The shell element is composed by four nodes (non-flat), and it accomplishes for geometric non-linear analysis. The shell element implementation is based on the element presented in the article "A Continuum mechanics based four-node shell element for general non-linear analysis" published by Klaus-Jurgen Bathe. The equilibrium non-linear equations of the problem are solved iteratively via the Newton Raphson method.

This manual describes the basic requirements run a Finite Element Shell simulation using the code developed. The geometry of the object, its material properties, and the load (boundary) conditions are described using text files. The first part of this document describes the syntax of the files to accomplish a simulation. The Second part describes how to compile the source code.

D.1 Description of the input files

D.1.1 Geometry File

This file assumes that the CAD model of the object has been drawn already, see Figure D.1a, this process can be achieved in any commercial or non-commercial CAD software available.

Moreover, it is also assumed that the geometry has been appropriately meshed with Quads elements, see Figure D.1b. This also can be achieved with any available meshing software.

Frequently, in meshing softwares available, the numbering of the nodes

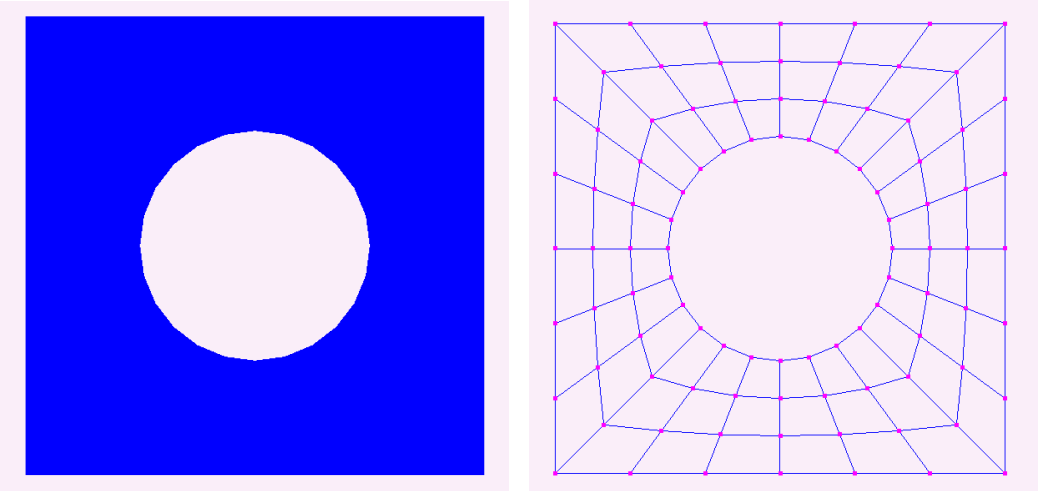

(a) CAD (b) Quad mesh

Figure D.1: Geometry of the object

obtained in the meshing process begins in "1". However, this Shell C++ program was designed to account for numbering of the nodes beginning in "0", see Figure D.2. Hence, in case that the numbering obtained begins in "1", it is precise to diminished 1 unity to each node number when indexing them to the flat-text geometry file.

Another important feature that has to be accounted for, is the normal vector associated to each node, see Figure D.3. The magnitude of these normal vectors has to be equal to 1, besides all of them must point either inside or outside of the domain. In general they can be obtained from the meshing software utilised; otherwise, a routine to calculate them can be easily implemented in any programming language (Matlab, C, C++, etc).

Each node of the domain also has a thickness value t associated to it, see Figure D.4. This value is measured along the normal vector associated to each node, in this way, the shell element accounts for variable thickness shell elements. **Therefore, the real object is represented in the simulation only by its middle surface, see Figure D.4, and the thickness of the object is given to the program as a list of external data values.**

Once all the geometry data has been obtained: (i) Cartesian coordinates of the mesh, (ii) normal vectors, (iii) list of thicknesses, and (iv) the indices of the elements (numbering beginning in "0"); the geometry file can be constructed as follows:

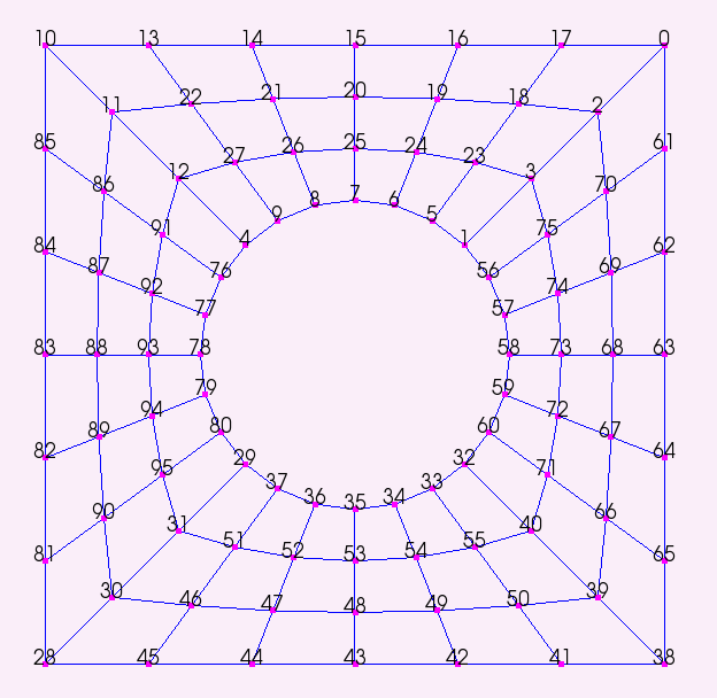

Figure D.2: Numbering of the nodes.

```
# flat-text file with the geometry information
# number of nodes
n
# <Coordinates>  <Normals>          <Thickness>
# <x y z>        <Nx Ny Nz>         <thick>
  x1  y1  z1     Nx1  Ny1  Nz1     t1
   .   .   .      .    .    .       .
   .   .   .      .    .    .       .
  xn  yn  zn     Nxn  Nyn  Nzn     tn
# Number of elements
E
# indices of the elements
ind1_e1  ind2_e1  ind3_e1  ind4_e1 #indices conforming element 1
   .        .         .        .
   .        .         .        .
ind1_eE  ind2_eE  ind3_eE  ind4_eE #indices conforming element E
```

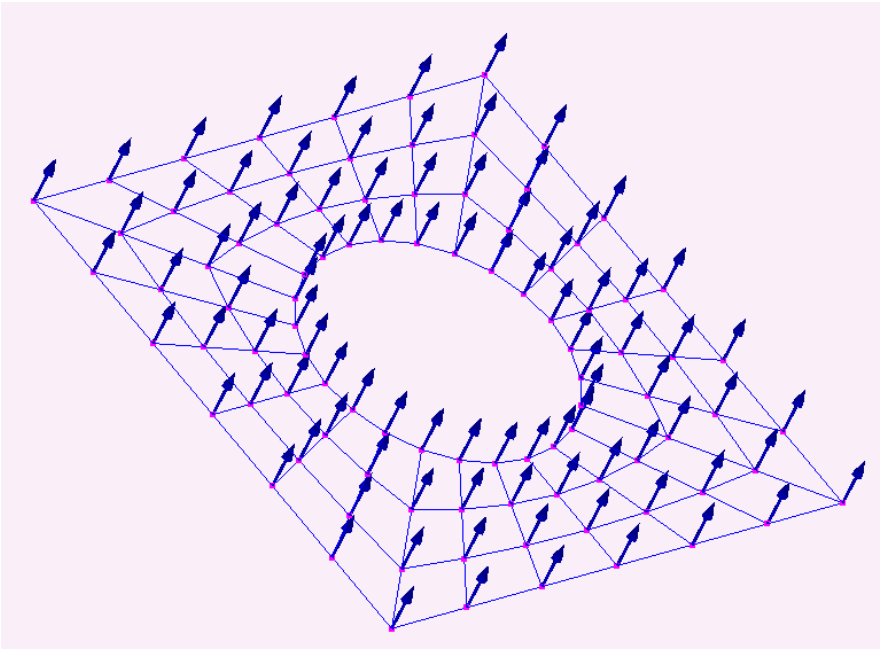

Figure D.3: Normals associated to the nodes of the geometry.

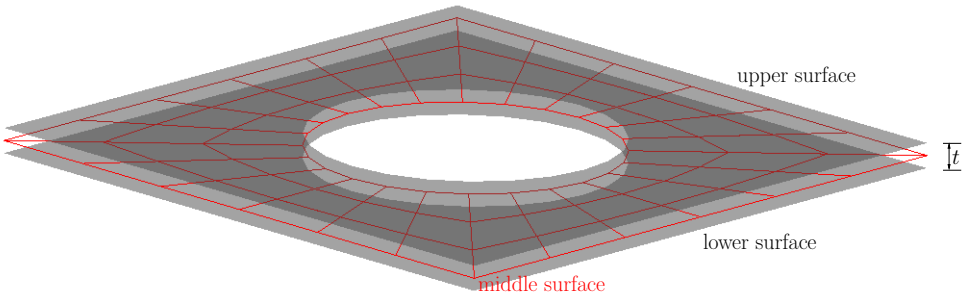

Figure D.4: Thickness of the shell element

where `n` is the total number of nodes, and `E` is the total amount of elements. If the symbol `#` is at the beginning of a line, it means that the rest of the line is considered as a comment; therefore, that information will not be used by the C++ program. It is important to make sure to follow strictly the order suggested herein to index the geometry information, otherwise fake or rubbish-like results can be obtained.

D.1.2 Properties File

This file contents the information of all the variables which do not have anything to do with the geometrical part. These variables must be provided in order to run the simulation appropriately. Those variables are:

Tolerances

Tolerance for zero value: Values inside the C++ program bellow this tolerance value are considered to be zero.

Tolerance for stop criterion: Because the final solution of the non-linear equations is achieved via a Newton Raphson iterative process, the final location of the object in general gets closer at each iteration. Therefore the amount of displacements of each node begins to decrease, as long as the process is converging. The stop criterion used to stop the Newton Raphson iterative process is achieved once the biggest displacement value obtained among the whole amount of nodes is less than the **tolerance for stop criterion**. If only a linear simulation is pursued, this tolerance value is not taken into consideration, but still some value has to be given within the properties file.

Number of Iterations

Maximum number of iterations per load step: This value accomplishes for the maximum number of iterations made by the Newton Raphson process. The iterative process will stop either if the stop criterion or if the maximum number of iterations is achieved.

Maximum number of iterations for the Preconditioned Conjugate Gradient linear solver: At each iteration within the Newton Raphson process, a set of linear equations has to be solved. This set of equations is solved via the Preconditioned Conjugate Gradient method, which is also an iterative method. In general if the system is well constrained, the set of equations will be non-singular, and a solution can be reached. The suggested maximum number of iterations can be calculated as: MxIt= $n * 15$, where n is the total amount of nodes within the simulation.

Material Properties

Young Elastic Modulus: The software was developed to handle linear elastic material behaviour. Therefore, appropriate Young Elastic Modulus must be indexed.

Poisson ratio: The Poisson ratio is also required to define the behaviour of the material

Shear Correction Factor: This factor is used to calculate adequately the shear strains and stresses, Reference (Bat96, pag. 399) gives a better explanation for this factor. In general the suggested value is $\frac{5}{6}$.

Boundary Conditions

The program implemented handles for both force and displacement boundary conditions. When carrying out a non-linear simulations, sometimes if the whole amount of force or displacement is applied at once, some converging problems can occur. Therefore, sometimes it is a good idea to split the total amount of force or displacement into smaller parts to ensure convergence. If a linear approximation is wanted, only one load step is required.

Forces + Moments: It is possible to apply punctual forces or moments to any node of the domain. The information required is: (i) Node number where the force/moment is going to be applied, (ii) degrees of freedom (dof) over which the force/moment is going to act, and (iii) value of the boundary condition. The dofs available are: $< 1 >$ forces along the x axis, $< 2 >$ forces along the y axis, $< 3 >$ forces along the z axis, $< 4 >$ moment along one of the axes orthogonal to the normal vector, and $< 5 >$ moment along the other axis orthogonal to the normal vector. There cannot be moments applied along the axis that points to the direction of the normal vector.

For example if a force pointing $-z$ axis is going to be applied to the object shown in Figure D.2, moreover, that force is wanted to be located at nodes 0 and 10 and its magnitude is 10 units of force, hence the statement to be used would be:

```
#<node number><DOF><value>
0  3 -10
10 3 -10
```

Displacements + Rotations: In order to constrain adequately the system, it is necessary to impose displacement boundary conditions. Any node can be constrained in any of the 5 dofs explained above. If a node is clamped, all its dofs must be constrained and the magnitude of the displacements and the rotations might be equal to zero. In the other hand, it is also possible to impose some displacements whose magnitude is different to zero; in this case the nodes where the impositions are applied will be moved towards the displacement vector an amount corresponding to magnitude of the vector.

For example if nodes 28 and 38 in Figure D.2 are clamped, the statement used would be:

```
#<node number><DOF><value>
28 1 0
28 2 0
28 3 0
28 4 0
28 5 0
38 1 0
38 2 0
38 3 0
38 4 0
38 5 0
```

The template designed to introduce all this information in the flat-text file of properties is: (this example is valid for the example shown in Figure D.2)

```
# flat-text file with the properties information
#TOLERANCES
#Tolerance for zero value
1e-15
#Tolerance for stop criterion
1e-5
#NUMBER OF ITERATIONS
#Maximum number of iterations per load step
40
#Maximum number of iterations for the PC Gradient linear solver
1440 # n = 96, MxIt = 96*15 = 1440
# MATERIAL PROPERTIES
# Elastic Module
2.1e6
```

```
#Poisson ratio
0.33
#Shear Correction Factor
0.83333333 #5/6 suggested
#BOUNDARY CONDITIONS
#Forces
#number of load-steps or displacement-steps to be applied
1
#number of forces or moments to be applied
2
#<node number><DOF><value>
0  3 -10
10 3 -10
#Displacements
#number of displacements to be applied
10
#<node number><DOF><value>
28 1 0
28 2 0
28 3 0
28 4 0
28 5 0
38 1 0
38 2 0
38 3 0
38 4 0
38 5 0
```

D.2 Compilation Process

In order to compile the C++ Shell program is necessary to have the following archives inside a folder:

- defs.h
- EntranceReader.cpp, EntranceReader.h
- Shell.cpp, Shell.h
- Geometry.cpp, Geometry.h

- Vector3D.cpp, Vector3D.h
- Node.cpp, Node.h
- functions.cpp, functions.h
- Point.cpp, Point.h
- SMatrix.cpp, SMatrix.h
- matx.cpp, matx.h
- vcr.h
- main.cpp

The program can be compiled either in Windows, Linux, or Mac OS X. operative systems. It was tested with the visual C++ compiler under windows and GNU gcc under Linux and Mac OS X. The next sections describe how to compile the code under this environments.

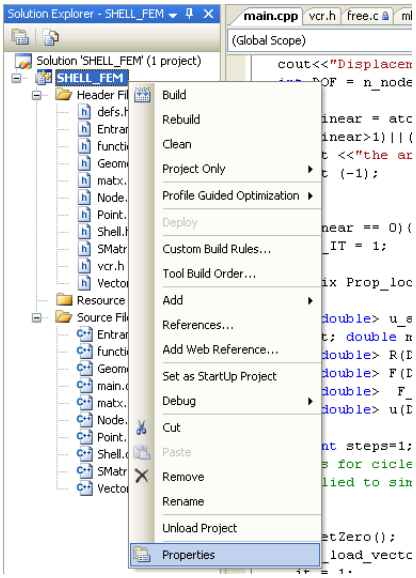

Figure D.5: Obtaining the properties window to specify the Command-line arguments in Visual C++.

D.2.1 Windows:

If this platform is chosen, then it is necessary to create a Visual C++ project and include all the files listed above. This Visual C++ Project is included with the source files but some information is provided here if the reader wants to create a new one from the source files

The file main.cpp contains the main sub-routine which is in charge of handling the whole simulation. In order to run the program it is necessary to specify three command-line arguments to the program. Those are:

1. A string with the full path where the Geometry file is stored.
2. A string with the full path where the Properties file is stored.
3. An integer number which could be 0 or 1. Zero (0) is used to carry out a linear simulation, while one (1) is used for a non-linear simulation.

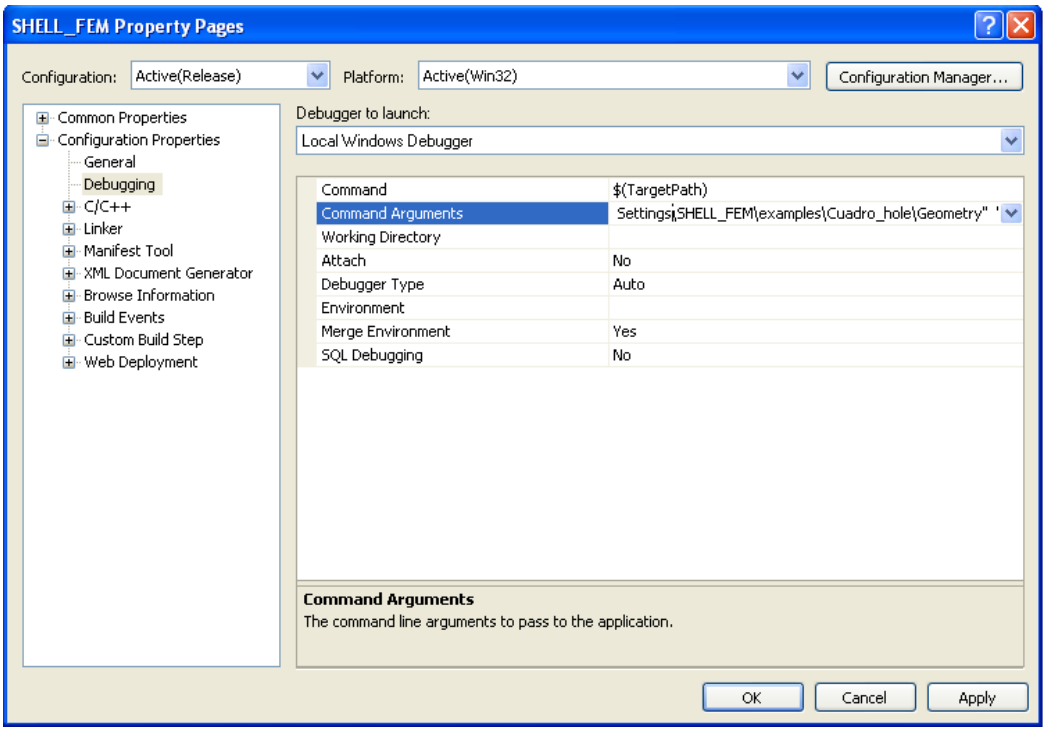

Figure D.6: Command-line arguments in Visual C++.

If the program is going to be run inside the visual C++ environment, it is also necessary to specify these arguments. An easy way to enter this arguments

is: Right click the mouse button over the C++ project name (written in bold text) located in the Solution Explorer window, see Figure D.5. In the sub-menu opened, click on the option "properties". Hence a "Property Pages" window is opened. Chose Debugging, and in the space set for the command arguments type: First, a string with the full path where the Geometry file is, followed by the path for indicating the location of the Properties file, and finally 0/1 integer. The path must be typed between quotation marks. See Figure D.6. Once this process is finished, the program can be compiled as normal. Just press the "Start Debugging" or the "Build" button.

D.2.2 Linux:

If this platform is chosen, also all the .h and .ccp files listed above must be included in a folder. There is also a file named "Makefile" which might be included. This file is Makefile description file that runs with the standard make or gnu make programs. In a shell terminal window, this makefile can be executed by only typing "make". Once the compilation process is finished, an executable file is created. This file can be executed from the shell and is also required to specify the command line arguments.

D.3 Result Files:

In the same folder where all the compilation process was made, it is necessary to create two new folders called: Results and VTK. In these folders all the results will be kept. Inside the Results folder the coordinates of the nodes plus the indices of the elements will be stored. The node coordinates will be stored both in the initial state and in the deformed state. Conversely, inside the VTK folder the geometry of the object both in the deformed and in the undeformed state are stored in "vtk" and in "wrl" format. files written in vtk format can be read in Paraview, which is a software designed for visualisation purposes. The wrl format can also be loaded in Paraview, however a bunch of other commercial softwares also handle this format.

Bibliography

[APK02] J.H. Argyris, M. Papadrakakis, and L. Karapitta. Elasto-plastic analysis of shells with the triangular element tric. *Computer Methods in Applied Mechanics and Engineering*, 191(33):3613–3636, June 2002.

[Arg82] John Argyris. An excursion into large rotations. *Computer Methods in Applied Mechanics and Engineering*, (32):85–155, 1982.

[Bat96] Klaus-Jurgen Bathe. *Finite Element Procedures*. Prentice-Hall, Inc., USA, 1996.

[BC99] A.P. Boresi and K.P. Chong. *Elasticity in Engineering Mechanics*. Wiley and Sons., USA, 2 edition, 1999.

[BF02] Richard L. Burden and J. Douglas Faires. *Numerical Analysis*. Thomson Learning, Mexico, 2002.

[BK62] P. J. Blatz and W. L. Ko. Application of finite elastic theory to the deformation of rubbery materials. *Transactions of the Society of Rheology*, VI:223–252, 1962.

[Cri01] M.A. Crisfield. *Non-linear Finite Element Analysis of Solids and Structures*. John Wiley and Sons, England, 2001.

[CS97] Francis A. Cozzarelli and Irving H. Shames. *Elastic and Inelastic Stress Analysis*. Taylor and Francis Group, 1997.

[CVP00] N. Chevaugeon, E. Verron, and B. Peseux. Finite element analysis of nonlinear transversely isotropic hyperelastic membranes for thermoforming applications. In *European congress on computational methods in applied sciences and egineering*, Barcelona, september 2000.

[DB84] Eduardo N. Dvorkin and Klaus-Jurgen Bathe. A continuum mechanics based four-node shell element for general non-linear analysis. *Engineering Computations*, 1:77–88, 1984.

[Fag92] M. J. Fagan. *Finite Element Analysis, Theory and Practice*. Longman Group UK Limited, Malaysia, 1992.

[Fel08] Carlos A. Felippa. Introduction to finite element methods. Course Notes, University of Colorado at Boulder, Department of Aerospace Engineering Sciences, 2008.

[FO74] F. Fardshisheh and E.T. Onat. Representation of elastoplastic behavior by means of state variables. In *Problems of plasticity: papers contributed to the international symposium on foundations of plasticity*, pages 89–115. Noordhoff, 1974.

[Gar01] Manuel Julio Garcia. *Lecture Notes in Advanced Numerical Analysis*. EAFIT University, Colombia, 2001.

[GGR06] M.J. Garcia, M.A. Gomez, and Oscar Ruiz. Spring-particle model for hyperelastic cloth. *sent to: DYNA*, 2006.

[GK07] Vijay K. Goyal and Rakesh K. Kapania. A shear-deformable beam element for the analysis of laminated composites. *Finite Elements in Analysis and Design*, 43(6-7):463–477, April 2007.

[GRL05] M.J. García, O. Ruiz, and C Lopez. Hyperelastic material modeling. Technical Report, Universidad EAFIT, 2005.

[Hod74] Philip G. Hodge. Computer solutions of plasticity problems. In *Problems of plasticity: papers contributed to the international symposium on foundations of plasticity*, pages 261–286. Noordhoff, 1974.

[Hop74] H.G. Hopkins. Mathematical methods in plasticity theory. In *Problems of plasticity: papers contributed to the international symposium on foundations of plasticity*, pages 235–260. Noordhoff, 1974.

[KB05] M. Kojic and Klaus-Jurgen Bathe. *Inelastic Analysis of Solids and Structures*. Springer, Germany, 2005.

[Kri95] C. S. Krishnamoorthy. *Finite Element Analysis: Theory and Programming*. McGraw-Hill, 1995.

[Lan86] Cornelius Lanczos. *The Variational Principles of Mechanics*. Dover Publictions, Inc., USA, 1986.

[Lev73] Enzo Levi. *Elementos de Mecánica del Medio Contínuo*. Limusa Wiley, Mexico, 1973.

[LG74] E.H. Lee and P. Germain. Elastic-plastic theory at finite strain. In *Problems of plasticity: papers contributed to the international symposium on foundations of plasticity*, pages 117–133. Noordhoff, 1974.

[Mal69] Lawrence E. Malvern. *Introduction to the mechanics of a continuous medium*. Prentice-Hall, Inc., USA, 1969.

[Man74] Jean Mandel. Director vectors and constitutive equations for plastic and visco-plastic media. In *Problems of plasticity: papers contributed to the international symposium on foundations of plasticity*, pages 135–143. Noordhoff, 1974.

[Moo40] M. Mooney. A theory of large elastic deformation. *Journal of Applied Physics*, 11:582–592, January 1940.

[Phi74] A. Phillips. Experimental plasticity. some thoughts on its present status and possible future trends. In *Problems of plasticity: papers contributed to the international symposium on foundations of plasticity*, pages 193–233. Noordhoff, 1974.

[SB87] Theodore Sussman and Klaus-Jurgen Bathe. A finite element formulation for nonlinear incompressible elastic and inelastic analysis. *Computers and Structures*, 26(1/2):357–409, 1987.

[SO85] J.C. Simo and M. Ortiz. A unified approach to finite deformation elastoplastic analysis based on the use of hyperelastic constitutive equations. *Computer Methods in Applied Mechanics and Engineering*, 49:221–245, june 1985.

[SS04] Hiroyuki Sugiyama and Ahmed A. Shabana. Application of plasticity theory and absolute nodal coordinate formulation to flexible multibody system dynamics. *Journal of Mechanical Design*, 126(3):478–487, may 2004.

[ST98] J.C. Simo and Hughes T.J.R. *Computational Inelasticity*. Springer, USA, 1998.

[TG07] Jose Rafael Toro Gomez. *Variational Problems and Finite Elements in Mechanical Engineering*. Ediciones Uniandes, Colombia, 2007.

[THMG04] Matthias Teschner, Bruno Heidelberger, Matthias Muller, and Markus Gross. A versatile and robust model for geometrically complex deformable solids. *Computer Graphics International*, pages 312–319, 2004.

[WT03] Gerald Wempner and Demosthenes Talaslidis. *Mechanics of Solids and Shells: Theories and Approximations*. CRC Press, USA, 2003.

[WTT95] Yi Wu, Daniel Thalmann, and Nadia Magnenat Thalmann. Deformable surfaces using physically-based particle system. In *Computer Graphics International*, 1995.

[XH97] Jian-Xue Xu and Norio Hasebe. The problem of an elastic-plastic beam dynamics and incomplete co-dimension two bifurcation. *International Journal of Non-Linear Mechanics*, 32:127–143, january 1997.

[Yeo93] O. H. Yeoh. Some forms of the strain energy function for rubber. *Rubber Chem. Technol.*, 66:754–771, 1993.

[ZT00] O.C. Zienkiewicz and R.L. Taylor. *Finite Element Method: The Basis*, volume 1. John and Wiley, USA, 2000.